Pre-Thrust Normal Faults and Post-Tectonic Micas in the Taconic Range of West-Central Vermont

Abstract of

a thesis presented to the Faculty

of the University at Albany, State University of New York

in partial fulfillment of the requirements

for the degree of

Master of Science

College of Sciences and Mathematics

Department of Earth and Atmospheric Sciences

Nicholas W. Hayman

1997

SUNY-ALBANY
UNIVERSITY LIBRARIES
ALBANY, NY 12222

Abstract

New geologic maps show that the Champlain Thrust System traces continuously between Shoreham and Benson, Vermont. The Champlain Thrust System consists of at least three internally imbricated thrust slices in continental shelf facies quartzites and carbonates. From north to south there is a structurally controlled thinning of the Champlain Thrust System, and a climbing in stratigraphic level by the thrusts. Within the Champlain Thrust System are a set of across-strike structures which create offsets in the thrusts and the surrounding lithic map unit boundaries. These structures function as lateral ramps in the thrust system geometry and bound thrust duplexes. Often there are changes in the stratigraphic level across these offsets which cannot be explained by the thrust geometry. These are interpreted to be to be pre-thrust normal faults, and a subsidiary (trench normal) set to the normal faults predicted by the model of Bradley and Kidd (1991), wherein normal faulting occurs in the continental crust in response to lithospheric flexure with the onset of collision. Trench parallel normal faults bounded grabens containing shales, and horsts of carbonate rocks. These horsts and grabens are now reflected in the thrust system's geometry. The Mettawee River Fault, an east-side-down normal fault, juxtaposes an intermixed belt of Middle Ordovician shelf facies shale and Pre-Cambrian continental rise facies slates and arenites, and Middle Ordovician flysch and melange, against the Champlain Thrust System. This structure could be late Taconic (orogenic) to post- Taconic in age, and have amounts of throw of tens to hundreds of meters. East of the Mettawee River Fault is the westernmost Taconic allochthon, the Sunset Lake Slice. This is a roughly north - south trending belt of green slates interspersed with lenses of continental rise facies quartzites. The Sunset Lake Slice is bound to the east by the Taconic Frontal Thrust, a late, out of sequence thrust which transports an eastern belt of intermixed Ordovician and Taconic shales and melange, as well as an eastern thrust belt of shelf facies carbonates and shales. This belt of carbonates and shales is lithologically identical to the rocks found in the

Champlain Thrust System but structurally dissimilar. The separation of these rocks from their facies equivalents in the Champlain Thrust System is suggested to be due to their topographically higher position on the paleo- continental shelf, the topography being largely (pre-thrust) normal fault controlled.

"Cross-micas" are observed mica grains from the slates at the Cedar Point Quarry, W. Castleton, Vt.. The Cedar Point cross-micas cross-cut the boundaries of a late crenulation cleavage which has the morphology of micro-kinks at the microscopic scale. This cross-cutting relationship suggests that these grains grew later than the deformation which produced the micro-kinks, and therefore later than the deformation which produced the slaty cleavage. If this is the case, then perhaps many, or all of the mica grains in the slate grew at this later time. The investigation to gain insight into the timing of the development of the cross-micas included producing a structural map and cross-section of the Cedar Point Quarry which may be useful for related future studies. Field based observations provide insight into the deformation history recorded at Cedar Point. The cross-micas, and the surrounding micro-structure of the slate are documented with photomicrographs. The observation that some micro-kinks are enriched with opaque minerals (oxides and sulfides), whereas other, adjacent, micro-kinks are enriched with phyllosilicates, is evidence that there was some amount of mass transfer, presumably due to solution processes, after the formation of the micro-kinks. Electron Microprobe data was attained from the slates in the hopes of confirming whether the cross-micas represent mica growth which was localized along the micro-kinks (and thus in the absence of a widespread metamorphic / mica growth event), or mica growth which was widespread throughout the slates. It was found that there are two groups of muscovite in the slate, a high K and a low K muscovite. There is also a group of interlayered muscovite and chlorite. There is no obvious relationship between structural setting, such as cross-micas, and the mineralogical variation, though with future work, such a relationship may be established.

Pre-Thrust Normal Faults and Post-Tectonic Micas in the Taconic Range of West-Central Vermont

A thesis presented to the Faculty

of the University at Albany, State University of New York

in partial fulfillment of the requirements

for the degree of

Master of Science

College of Sciences and Mathematics

Department of Earth and Atmospheric Sciences

Nicholas W. Hayman

1997

Acknowledgments

This work was given partial support from the Graduate Student Organization and the U.A. Benevolent Association. D.O.G.S. / D.E.A.S supplied personal financial support via a much enjoyed Teaching Assistantship position. Bill Kidd taught me how to map and how to do geology. I look forward to bringing the work discussed here to new levels, and thank Bill for the Taconic problems which are so mysterious and thought provoking. I have had the unique opportunity to be a student and colleague (if I may be so bold) of Win Means. He has taught me how to write and how to work (did I mention continuum mechanics, structural petrology, ...). He "gave" me what was an ideal problem for a master's student, or as Win likes to put it, for an "apprenticeship". Though I fumbled around a bit with the project itself, it has shaped my future direction as I head out to Washington State to work with Darrel Cowan on fault rocks. Greg Harper was great to talk with about minerals, scale, and holistic vs. reductionist approaches to science. His suggestions greatly improved this thesis. Thanks to John Delano, maybe some day we can all take one step in his direction and make this place actually work. This thesis could not have been brought to its multi-color format without the help of Brad Lindsley. Art Goldstein helped with sample prep. when I was in a bind, with words of enthusiasm and encouragement. Bill Blackburn at S.U.N.Y. Binghamton took a joy-ride across the micron scale slate landscape with me. Diane Paton helped out above and beyond. Frank Spear and various R.P.I. faculty and students have helped shape my views on water, rocks, and faults. Correspondence and conversation with Nick Ratcliffe, Don Fisher, Jean Crespi, and multitudes of others were informative and helpful. YoungDo Park and Ben Hanson provided inspiration and encouragement during the early, confused, phases of this work. Steffi Dannenman, Steffan Kosanke, Mike Edwards, Rich Messier, and Taohung Li have provided thought provoking conversation and been undeniable sources of positivity. Field partner and college buddy Andre Hamilton was a force. Field Campers provided outcrops and some great Vermont summers. J&W, J&J, J&M, and the beautiful Marianne Schat have always been there for a beer, some billiards, or a little mid-afternoon Silat. Thanks to my family, and to Dad, whose taking me out on the AT as a kid undoubtedly had something to do with me having spent the last few years looking for "Appalachians" those mythical creatures not far removed from Hephalumps.

Table of Contents

Abstract ii

Acknowledgments v

Table of Contents vi

List of Tables ix

List of Plates ix

List of Figures x

Chapter 1. Introduction

1.1. Geologic Context and Purpose of Study 1

1.2. Geographic Locations and Methods of Study 2

1.3. Overview 7

Chapter 2. Lithologic Units and Stratigraphy of the Lower Champlain Valley and Adjacent Regions

2.1. Introduction 9

2.2. Map Units 16

2.2.1. Tabulated definitions of map units 16

2.2.2. Problems identifying map units in the field 27

2.2.3. The lack of fossil data 30

2.3. Discussion 31

2.3.1. Stratigraphic Problems - Early to Middle Cambrian Rocks (?) 31

2.3.2. Stratigraphic Problems - The Carbonates 32

2.3.3. Stratigraphic Problems - Pelitic Rocks 35

2.3.4. Stratigraphic Problems - the Sunset Lake Region 36

2.4. Summary 37

Chapter 3. Structural Geology of the Lower Champlain Valley

3.1. Introduction 39

3.2. The Champlain Thrust System 42

3.2.1. The Regional Trace of the Champlain Thrust System 42

3.2.2. Local Duplexing Within the Champlain Thrust System 45

3.2.3. Changes in Thrust Orientation and Ramping of Thrusts 49

3.2.4. Across-Strike Offsets in the Champlain Thrust System 52

3.3. A Late Normal Fault and the Slate Belt 62

3.3.1. The Mettawee River Fault 62

3.3.2. The Sunset Lake Slice 63

3.3.3. The Taconic Thrusts: Structural Implications of the Hortonville - Taconic Black - Taconic Melange Lithologies 69

3.4. The Eastern Carbonate Belt 70

3.5. Summary and Discussion 74

Chapter 4. Introduction: Are There Post-Tectonic Micas in the Taconic Slates?

4.1. Post-Tectonic Micas and Their Implications 77

4.1.1. Absolute Dates for Deformation Events 80

4.1.2. Timing of Metamorphic vs. Deformation Events 81

4.1.3. Fabric Control on Mineral Growth 85

4.2. Cross - Micas at the Cedar Point Quarry 85

4.2.1. Regional Setting and Terminology 85

4.2.2. A Strategy for Investigation 90

Chapter 5. Field, Petrographic and Geochemical Observations of the Taconic Slates at the Cedar Point Quarry, W. Castleton, Vermont

5.1. Field Observations 91

5.1.1. General Information on the regional geology 91

5.1.2. Overview of the structures at Cedar Point 92

5.1.3. Locality Map, Field Data, and Projected Cross-section 97

5.1.4. Additional Observations 115

5.1.5. Discussion - Deformation History 119

5.2. Petrographic Observations 121

5.2.1. Mineralogy and Microstructure of the Cedar Point Slates. 121

5.2.2. Micro-Kink Geometries 122

5.2.3. Cross-Micas 126

5.2.4. Discussion - Products of Solution Processes 139

5.3. Geochemical Observation 141

5.3.1. Chemical Compositions of the Phyllosilicate Minerals 142

5.3.2. Backscatter S.E.M. Imagery 148

5.3.3. Discussion - K_2O and Na_2O 154

5.4. Discussion 159

Chapter 6. Conclusion 163

6.1. Geologic Maps of the Shoreham to Benson Region 163

6.2. Investigation of the Cedar Point Slates 166

References 169

Tables

Table 2-1) A tabulated account of map units, defining lithologic characteristics, associated structures, and approximate stratigraphic level 17

Table 5-1) Relative positions of Control Stations 105

Table 5-2) X,Y,Z (geographic) and X',Y',Z' (projected) Coordinates 108

Table 5-3) Geologic Data from Control Stations 111

Table 5-4) Pitch of S_0 and S_2 in Projected Cross-section 112

Table 5-5) Oxide Weight Percent - Electron Microprobe Analyses 144

Table 5-6) Cation Totals - Electron Microprobe Analyses 146

Plates

Plate I Geologic Map of the Shoreham - Whiting Region

Plate II Geologic Map of the Benson - Orwell Region

Plate III Structural Map of the Cedar Point Quarry

List of Figures

1.1) Generalized Geologic Map of Vermont (Doll et. al, 1961) 3

1.2a) Topographic Map of the Shoreham - Whiting Area 4

1.2b) Topographic Map of the Orwell - Benson Region 5

2.1) Stratigraphic Nomenclature of the Champlain Valley 10

2.2) Stratigraphic Nomenclature for the Taconic Sequence 11

2.3) Map Units and Stratigraphic Equivalents 12

2.4) Schematic of the Laurentian Passive Margin 14

2.5) Taconic Melange and Hortonville Shales (outcrop photos) 29

2.6) Sciota Limestone (outcrop photo) 34

3.1) Generalized Map Cross-Section of the Shoreham - Whiting Region 40

3.2) Generalized Map and Cross-Section of the Benson - Orwell Region 41

3.3) Geologic Map of Doll et. al. (1961) 43

3.4) The Pinnacle Duplex in Map and Cross-Section 46

3.5) A Classic Duplex Structure (schematic from Ramsay and Huber, 1987) 46

3.6) Map and Three Cross-Sections of the Shoreham Duplex 47

3.7a) Lens of shale beneath the Shoreham Thrust (outcrop photo and model of emplacement) 50

3.8) Ramp above the Ticonderoga Formation (outcrop photo) 51

3.9) Map View of the Lemon Fair River Fault 55

3.10) Map View of the Benson Landing Region 57

3.11) The Champlain Thrust - structural extension (outcrop photo) and a model of the development of the Benson Landing Region 58

3.12) Geologic Map of the Taconic Foredeep and Normal Faulting of the Continental Margin with the Onset of Collision and Lithospheric Flexure 61

3.13a) Cross-Section Across the Sunset Lake Slice from Doll et. al. (1961) 64

3.13b) The Hatch Hill Formation (outcrop photo) 64

3.14a) Multiple Cleavages and Quartzite Clasts in the Bull Formation (outcrop photo) 67

3.14b) Photomicrograph of Taconic Crenulation Cleavage 67

3.15) Folding in Slaty Cleavage (outcrop photo) 68

3.16) The Sudbury Thrust (outcrop photos) 72

3.17) Model of the development of the Felton Hill Thrust System 73

4.1) A Three Stage History of Mica Development in a Continental Margin Setting (cartoon) 78

4.2) A 1-dimensional Time - Deformation - Metamorphism Plot (cartoon) 79

4.3) Fabric Control on Mica Growth (cartoon) 75

4.4) Slaty Cleavage Formation (cartoon) 83

4.5) Cross-Micas at the Cedar Point Quarry (cartoon) 87

4.6) The Localized Growth Hypothesis vs. the widespread Growth Hypothesis (cartoon) 89

5.1) A Generalized Structural Map of the L. Bomoseen Area from Rowley (1983) 93

5.2) Cross-Section of the L. Bomoseen Area from Rowley (1983) 94

5.3a) A View to the North of the Cedar Mountain Syncline (outcrop photo) 95

5.3b) The Traces of a Conjugate Set of S_2 and the S_1 / S_2 intersection lineation (outcrop photo) 95

5.3c) S_1, S_2 and Veins on the Back Wall of the Cedar Point Quarry (outcrop photo) ... 95

5.4) The Contact Between the Brown's Pond Formation and the Middle Granville Slates (outcrop photos) 98

5.5) The Contact Between the Brown's Pond Formation and the Middle Granville Slates on the Back East Wall of the Cedar Point Quarry (outcrop photo) 99

5.6) Stereographic Projections of Structural Data from the Cedar Point Quarry 102

5.7) The Projected Cross- Section of the Cedar Point Quarry 103

5.8) The Coordinate Transformation Formula (cartoon) 104

5.9) Slickenlines on a Bedding Plane (outcrop photo) 117

5.10) Anastomosing Cleavage on the Lower East Wall of the Cedar Point Quarry (outcrop photo) 118

5.11) A Thin Section and Line Drawing from a Float Sample 123

5.12) A Thin Section and Line Drawing from Sample 45 124

5.13a) A Micro-Deposit of Opaque Minerals Oriented Parallel to S_1 and Deflected by S_2 125

5.13b) Opaque Minerals Preferentially Following a Foliation 125

5.13c) Opaque Enriched Micro-kink Pinches Out 125

5.14) Two Stage View of a Micro-Kink (photomicrograph) 127

5.15a) A Micro-Kink in a Thin Section from Station 41 (photomicrograph) 128

5.15b) S2 in the Brown's Pond Formation (photomicrograph)..... 128

5.16) Photomicrographs of cross-micas..... 129

5.17) Cross-Micas from L.E.C. (photomicrograph) 131

5.18) A Line Drawing of Figure 5.18 132

5.19) Photomicrograph and Line Drawing of Cross-Micas from L.E.G. 133

5.20) Photomicrograph and Line Drawing of Cross-Micas from 41 135

5.21a) Cross-Mica from station 45 (photomicrograph) 137

5.21b) Chlorite surrounding 001 mica (photomicrograph) 137

5.22a) Backscatter S.E.M. Image of a Micro-Kink from station 41 149

5.22b) Muscovite and Chlorite Interlayering at the Micron Scale 149

5.23) Line Drawing of Figure 5.24a 150

5.24) Backscatter S.E.M. Image and Line Drawing of a Micro-Kink from L.W.C 151

5.25) High Magnification Views of Figure 5.26 152

5.26a) Na_2O vs. K_2O for Muscovite Minerals 156

5.26b) Na_2O vs. K_2O for Muscovite Minerals 156

5.27a) Al_2O_3 vs. SiO_2 for Chlorite - Muscovite for all Analyses 158

5.27b) MgO vs. SiO_2 for Chlorite - Muscovite for all Analyses 158

5.28a) Analyses from L.W.C. 160

5.28b) Analyses from 41 160

Chapter 1. Introduction

1.1. Geologic Context and Purpose of Study

The bedrock geology of Vermont consists of diverse lithologies arranged in roughly north-south trending belts (**fig.1.1**). The history of study of Vermont geology is over a century old and involves natural philosophers and geologists whose names are legendary in the annals of the geologic sciences. By the 1950's Vermont had been well mapped and a working model for the accretion of western Vermont had been developed. This model was dominated by the concept that separate basins of sedimentary rocks and unlithified sediment had been uplifted, and incorporated into the Taconic Mountains during the Ordovician. Concurrent deformation of the rocks consisted of regional folding with overthrusts juxtaposing different sedimentary facies against one another, without large amounts of lateral transport (e.g., discussions in Zen, 1961; Bird, 1969; Rodgers, 1971).

Throughout the 1960's and 1970's further mapping, in conjunction with changes in thought concerning the role of faulting and plate tectonics in the development of mountain belts, lead to significant revisions of the previously accepted model for the accretion of western Vermont. To date, it is widely accepted that the emplacement of thrust sheets, each internally imbricated, was a consequence of the Taconic collisional event (Bird and Dewey, 1970; Rowley and Kidd, 1981; Stanley and Ratcliffe, 1985). Yet, much of Vermont has not been mapped since this change in thought and thus many of the older themes of regional folding of thick geosynclinal sedimentary sequences still remain in the literature and geologic maps, without correction. My mapping is part of a continued effort of University at Albany students to improve our understanding of the Ordovician Taconic Mountains and in particular, the Champlain and Taconic Thrust Systems which were integral to their development.

An understanding of fundamental geologic processes can also be attained from the study of Vermont. A transect of the region will bring a worker through a wide variety of lithological and structural settings (**fig.1.1**). One small section of such a transect, the

Lower Champlain Valley is one of the classic localities for studying the structural geology of slates (e.g. Dale, 1899).

The Taconic slates at the Cedar Point Quarry in W. Castleton, Vermont (**fig.1.1, 1.2b**) provide an excellent setting in which to study a foliation, slaty cleavage. This particular study was inspired by the observation of Prof. W.D. Means that some of the micas in a slaty cleavage orientation appear, in thin section, to cross-cut structures which formed later than the slaty cleavage. This lead to the suggestion that perhaps the minerals which define the slaty cleavage post-date the deformation which produced the slaty cleavage. If so, this greatly affects the interpretation of any isotopic dates which could be attained from these Taconic slates. This could then influence the interpretation of the relative timing of mineral growth and deformation from multiply deformed rocks world-wide. Furthermore, it could provide an excellent example of minerals growing into a foliation in the absence of active deformation. Such an example could be of importance to future experimental, theoretical, and field studies of foliation development.

1.2. Geographic Locations and Methods of Study

The Lower Champlain Valley of west-central Vermont is the valley between Lake Champlain and the present day Taconic and Green Mountains. The area of interest is bounded by the Shoreham - Benson area to the west, and the Whiting - Castleton areas to the east (**fig.1.1, 1.2a-b**). Generally, the higher topography is dominated by slate bedrock lithologies and the lower topography by carbonate bedrock lithologies. The entire region is intermittently covered by glacial till. The lowlands of the region are used for cattle grazing and apple orchards. Towards the highlands, the land use is dominated by residential and recreational areas surrounding "sustainable" lumber operations. In the slate belts, there are several active and inactive quarries. The hydrography of the region includes the Lemon Fair River, its tributary and distributary brooks, and adjacent swamp lands.

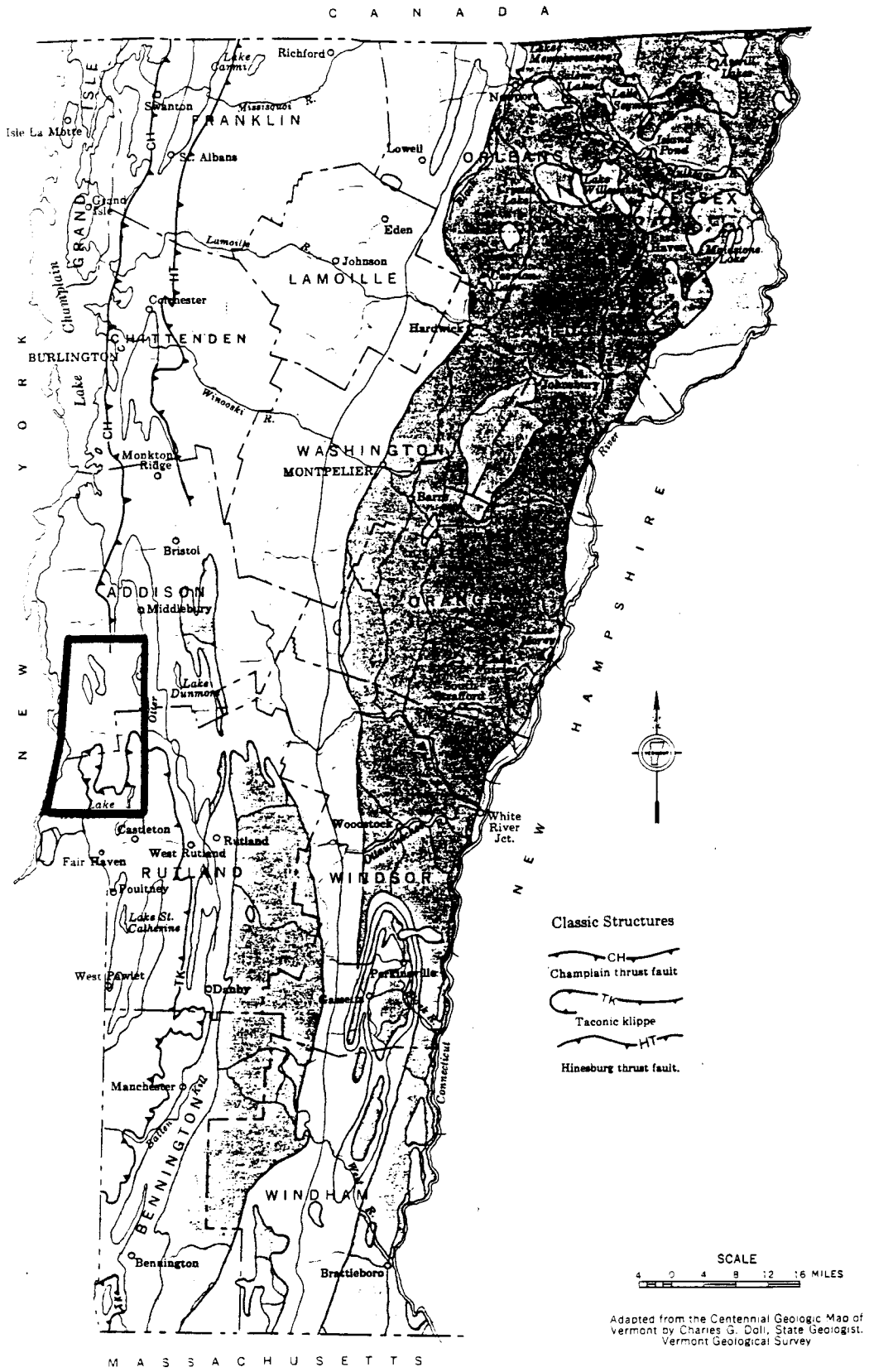

Figure 1.1) Generalized Geologic Map of Vermont - area of interest is outlined.

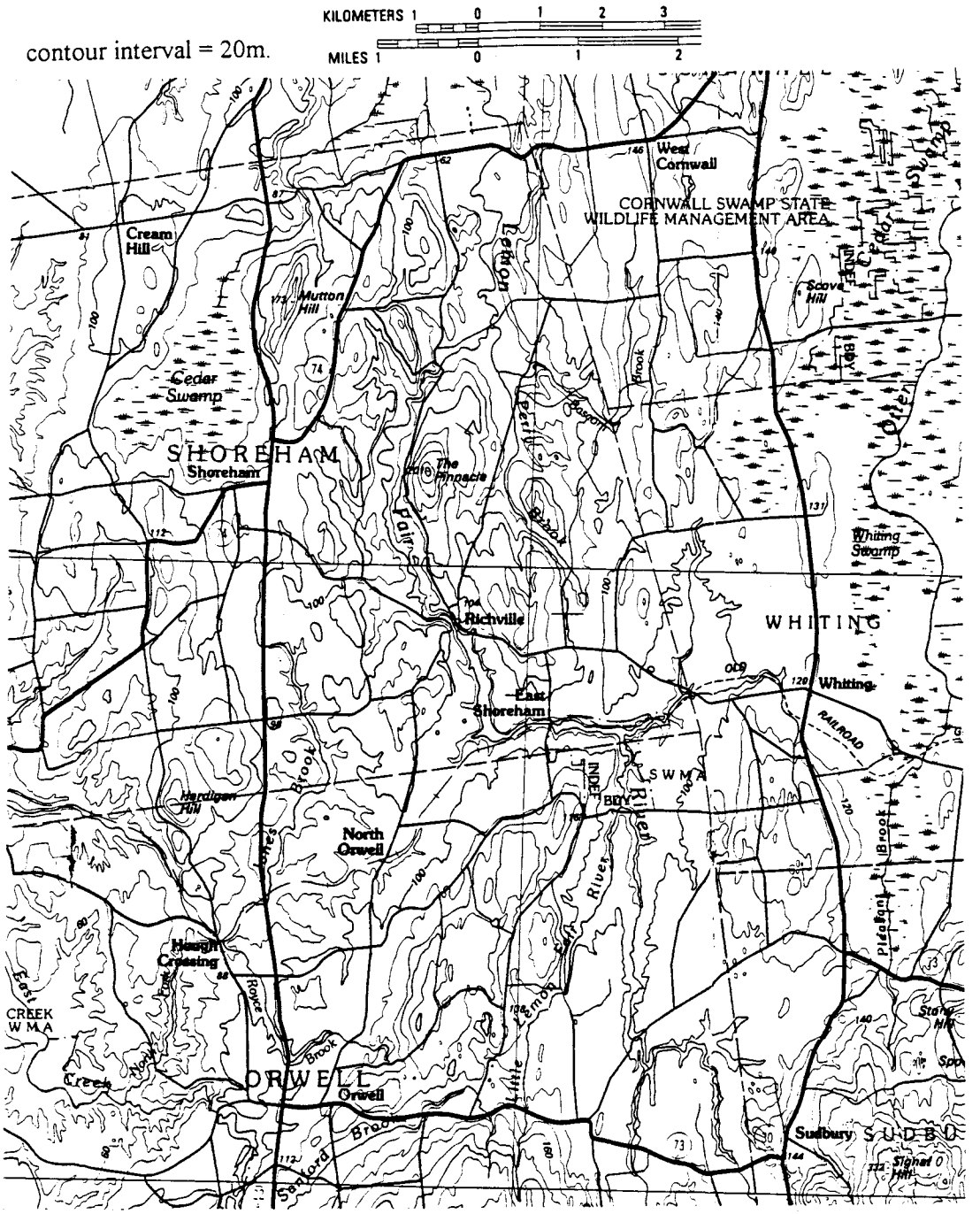

Figure 1.2a) Topographic Map of the Shoreham - Whiting region. The Lemon Fair River is the large river which runs from north to south through most of the region, but east to west immediately south of the Pinnacle. Delano Hill and Cutting Hill are the two hills east of the Pinnacle on the north and south sides of Perry Brook (respectively).

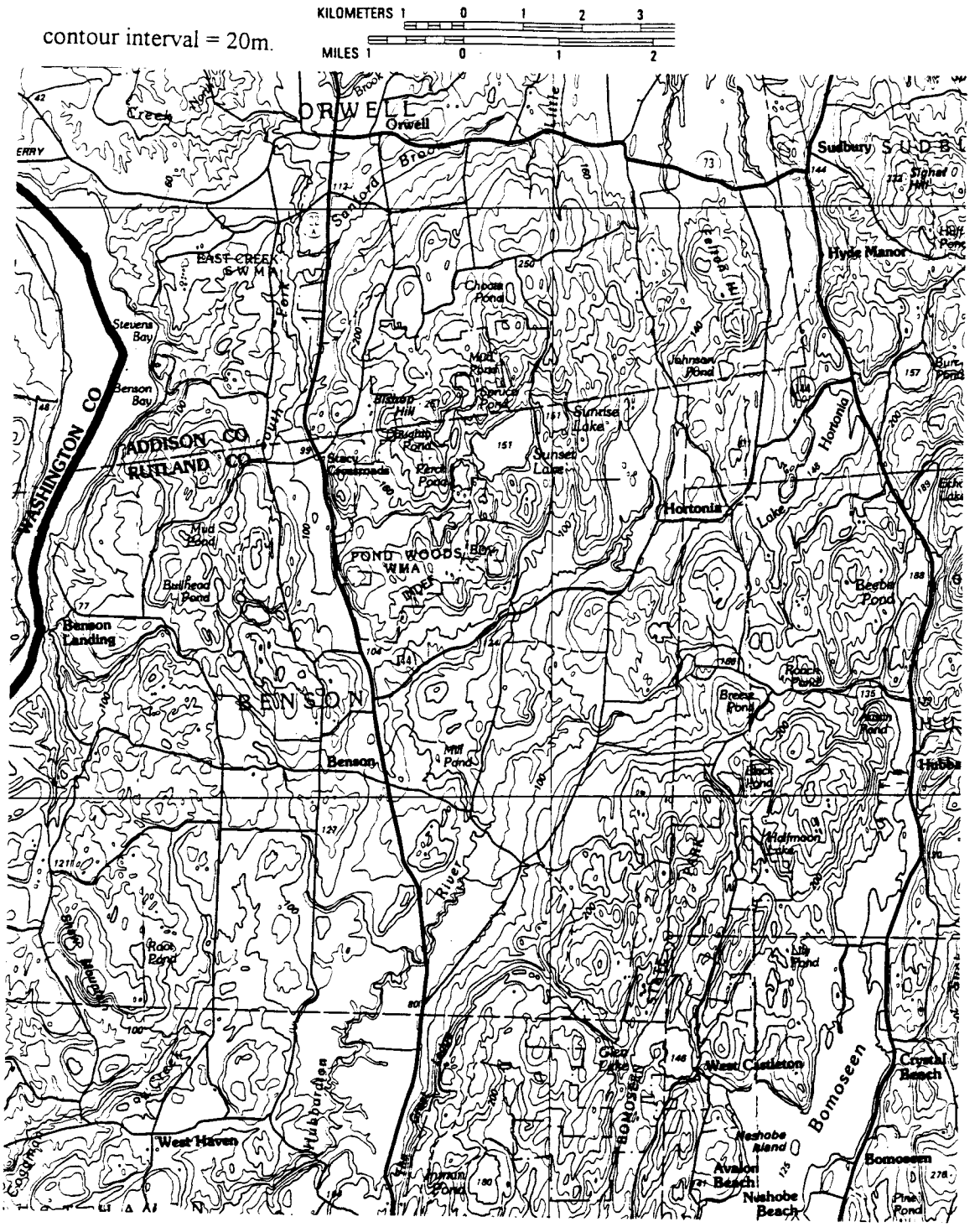

Figure 1.2b) Topographic Map of the Orwell - Benson region. Cedar Point Quarry is on the penninsula on the west side of L. Bomoseen.

This drainage system runs across areas with predominantly carbonate lithologies. In the slate belts there are fewer rivers, but there are several lakes including Sunrise and Sunset Lake, Lake Hortonia, Lake Bomoseen, and adjacent smaller lakes. The topographic map of **figure 1.2 a** and **b** should be used as a reference for any geographic locations mentioned in this thesis.

Outcrop mapping was conducted from August, 1994 to 1996 with a total field time of roughly 12 weeks. 1:12000 enlargements of 7.5′ U.S.G.S. topographic maps were used as base maps. Over the course of mapping several workers contributed to field mapping including W.S.F. Kidd, Andre Hamilton, and the members of the 1994 and 1996 field mapping course. In particular, J. Voght, J. Bamberger, C. Lajewski, and T. Crocker discovered outcrops and contributed ideas which became integral to the final maps. Some of the themes presented on the maps of J. Granducci (1995) and R. Eisenmann (field camp, 1992) were incorporated into the maps of this study. Compilation of the maps was done using AutoCad 10 and CorelDraw 3.5 on a DEC personal computer with a 486 processor. Drill core data was not studied and the data from high resolution seismic surveys of the Columbia Gas company is still proprietary.

Structural mapping of the Cedar Point Quarry locality was conducted over roughly three weeks in the summer of 1995 and included constructing a large scale basemap for the quarry (**Plate III**). The basemap and cross-section were created following the general method used by David Narahara during an undergraduate mapping project of Cedar Point conducted in 1980. Thin sections were prepared on standard wet saws and polishing wheels and studied using an optical microscope. Some thin sections were polished for microprobe analyses by Prof. A.Goldstein of Colgate University whose assistance was invaluable at a time when equipment for polishing in the University at Albany laboratory were temporarily lacking. Scanning Electron Microscope back-scatter imagery and analyses

of micro-chemistry were attained with the help of Bill Blackburn over two days at the JEOL 8900 electron microprobe laboratory at S.U.N.Y. Binghamton.

All illustrations and images presented in this thesis were done either on a 486 DEC PC or an Apple Macintosh with a Polaroid slide scanner or a Silverscan scanner. Drafting software used was developed by either Adobe, Deneba, Micrografix, or Corel. Word processing and spreadsheet applications used were by Microsoft, and stereoprojections were drafted using the program Stereonet, by Richard Allmendinger of Cornell University.

1.3. Overview

Chapter 2 and **Chapter 3** of this thesis discuss the stratigraphy and structural geology of the Lower Champlain Valley. Major splays of the Champlain Thrust System were traced through the region. This imbricate thrust belt is cut by a late normal fault which also traces through the region. The stratigraphic changes between imbricate thrust slices in the carbonate rocks provide the data necessary to contribute to a discussion of the development of the Cambrian through Ordovician passive margin. Evidence is presented which supports the idea that pre-thrust normal faults, developed during the onset of collision, contributed to the development of the Champlain Thrust System's geometry. Evidence is also reported to support the conclusion that the Taconic Frontal Thrust juxtaposed the eastern allochthonous thrust slices against the western thrust slices. A large belt of shelf facies carbonates and shales, lithologically correlative to those found in the Champlain Thrust System, is structurally above this thrust, but below the eastern allochthons. The separation of this belt of carbonates and shales from the Champlain Thrust System is proposed to be the result of relative changes in paleo-topography across the normal faulted continental shelf.

Chapters 4 and 5 present data and discussions concerning potential late mineral growth in the Taconic slates. This work leaves open the possibility that large amounts of

mineralogical changes were occurring within the allochthon either late in, or after the main phase of deformation. This has implications for the history of the Taconic orogeny as well as implications for more general studies of mountain belts and foliation development.

To my knowledge, this is some of the first evidence for pre-thrust normal faults exerting control on the further development of local fold and thrust belt geometry. Though the microstructural study of slates yielded less concrete results, the work presented here gives an excellent indication of how to further test the proposed hypotheses. Thus, this thesis served not only as an educational experience for myself, but may one day produce a paper which could be of interest to other workers.

2. Lithologic Units and Stratigraphy of the Lower Champlain Valley and Adjacent Regions

2.1. Introduction

The most useful data set for constructing a geologic map in an area such as the Champlain Valley, with diverse and often massive rock types, is the distribution of different rock types over a broad area. To conduct structural and stratigraphic analyses, it is desirable to provide a full stratigraphy and the thickness of each stratigraphic unit. This can be very difficult because of sparseness of outcrop, ambiguities in the lithologic criteria, and structural complexity.

The rocks were divided into map units based upon lithologic criteria, following the general framework of Granducci (1995) (see **section 2.2**). These function independently of any stratigraphy developed by previous workers (**fig.2.1, 2.2**). Nonetheless, this study identified the approximate stratigraphic level to which a map unit might correlate based upon lithologic criteria (**fig.2.3**) and found that a combination of the stratigraphy used by Fisher (1984), Zen (1961), and Jacobi (1977) was most applicable. Using map units as non-stratigraphic divisions is intended to eliminate prejudices when compiling the geologic maps and interpreting the geologic history of the region. The correlation to stratigraphic units increases the universality of this study and makes the relation to other worker's findings easier to understand. Correlation to stratigraphic units also aids in understanding age and paleogeographic relationships of the map units.

The earliest work in the Champlain Valley was solely concerned with the fossils found at particular horizons (e.g. Dana, 1877), almost exclusively in carbonate lithologies. The first stratigraphy developed for the region was that of Brainard and Seeley (1890), which drew largely upon paleontologic data. By the mid-twentieth century there had been many revisions to this stratigraphy and new stratigraphic names had been introduced (**fig.2.1, 2.2**). This era of study resulted in the stratigraphy of the Champlain Valley as presented on the *Centennial Geologic Map of Vermont* (Doll et. al., 1961). Though not all

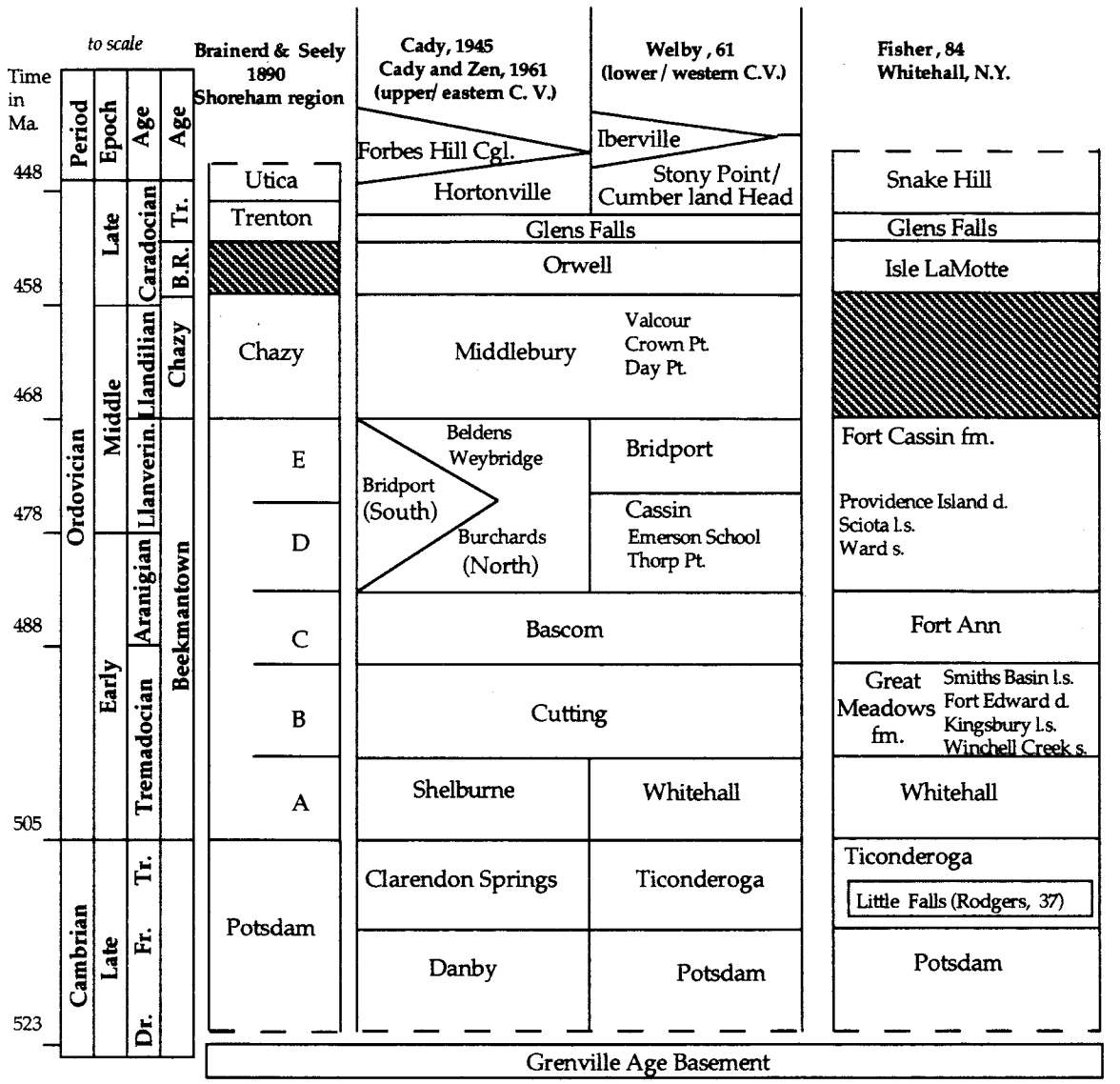

Fig. 2.1) Stratigraphic nomenclature of the Champlain Valley. Stratigraphic units are placed at their approximate age.

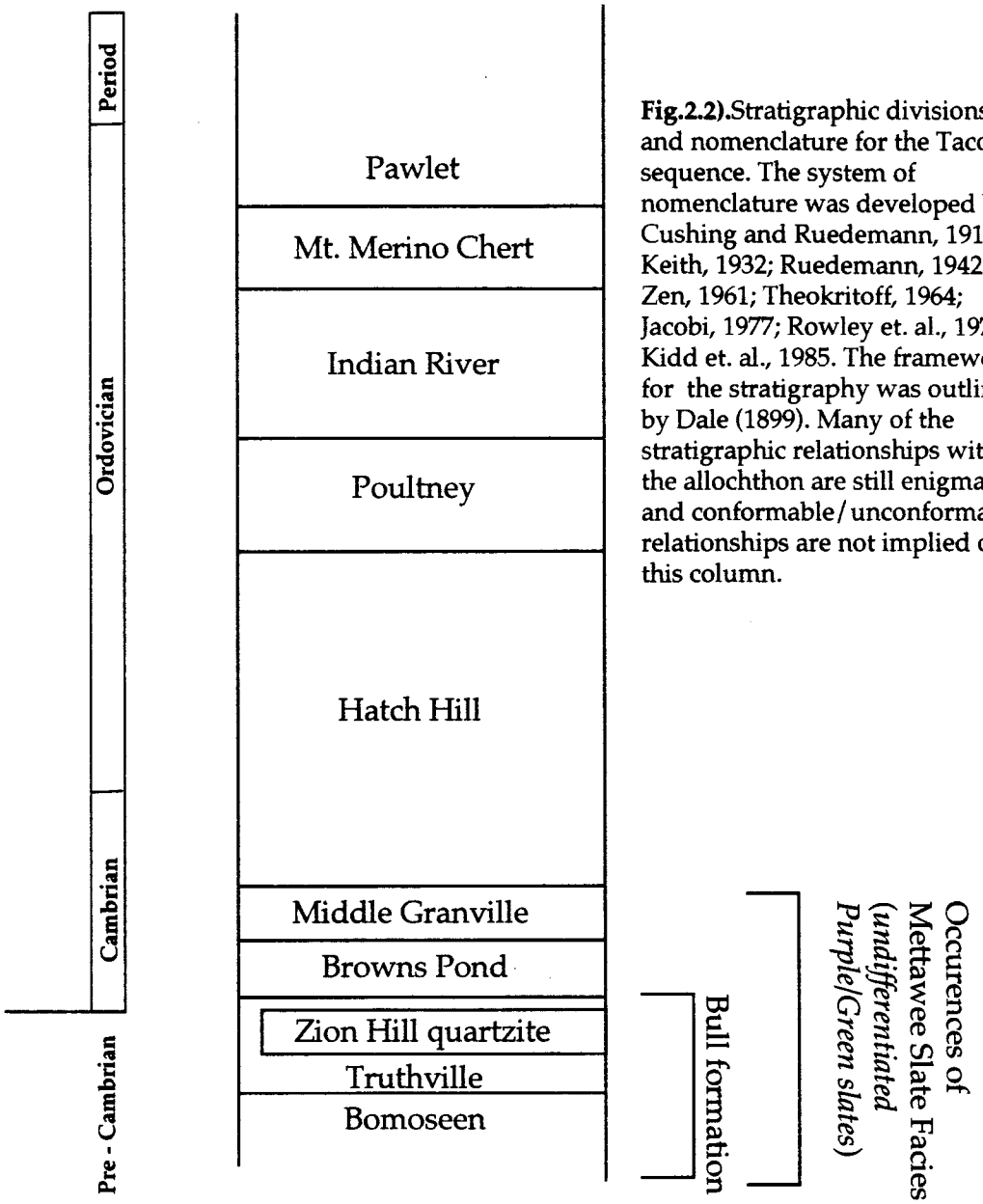

Fig.2.2). Stratigraphic divisions and nomenclature for the Taconic sequence. The system of nomenclature was developed by Cushing and Ruedemann, 1914; Keith, 1932; Ruedemann, 1942; Zen, 1961; Theokritoff, 1964; Jacobi, 1977; Rowley et. al., 1979; Kidd et. al., 1985. The framework for the stratigraphy was outlined by Dale (1899). Many of the stratigraphic relationships within the allochthon are still enigmatic, and conformable/unconformable relationships are not implied on this column.

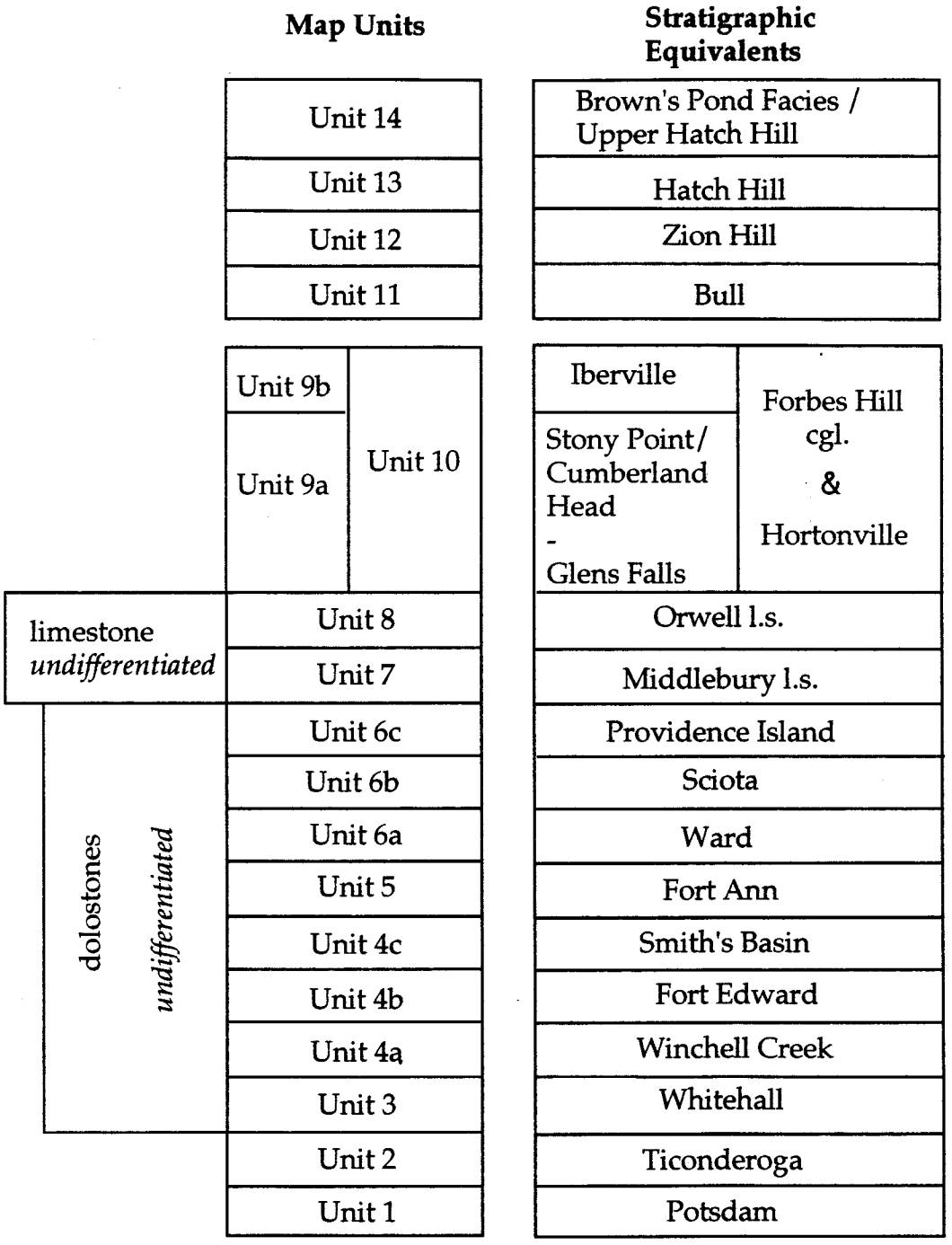

Fig.2.3) Map Units for the geologic maps (plates I and II) are shown on the left. Undifferentiated limestone and dolostone units were used when divisions between map units could not be made. No thickness or age is implied. Approximate lithologically correlative stratigraphic units are indicated on the right.

inclusive, a list of the most influential studies to contribute to this stratigraphy includes that of Cady (1945) as revised by Cady and Zen (1960), and the work of Welby (1961). The *Geologic Map of the Whitehall quadrangle* (Fisher, 1984) built upon and revised that system of Champlain Valley stratigraphy. The stratigraphy and stratigraphic nomenclature of the slate rocks (Taconic rocks) are largely known through the efforts of Dale (1899), Zen (1961), Jacobi (1977), Rowley (1983), Rowley et. al.(1979), and Kidd et. al. (1985) (**fig.2.2**).

Differences in stratigraphic nomenclature and interpretations of the stratigraphy are due to the change in rock types between regions of study (i.e. lateral variations in a particular stratigraphic horizon between map areas), differences in opinions regarding field observations, and differences in interpretations of the geologic structures in the region. When formulating a stratigraphy the worst confusion results from the combination of paleontologic, lithologic, and structural divisions. To avoid this confusion, this study developed map units based primarily upon lithologic criteria. Unfortunately, some criteria used for establishing lithic map units are the result of post-deposition processes, and therefore may not be uniform across a map unit, or may be present in more than one map unit (cleavage, veins, breccia, and quartz nodules, for example).

The sandstones and carbonates have been interpreted to be part of a continental shelf - passive margin facies (Rodgers, 1968) (**fig.2.4**). The rocks dominated by pelitic lithologies belong to a deeper water continental slope and rise facies. As early as 1909, Ruedemann suggested that the Taconic range consists of autochthonous (near-traveled or stationary) rocks and allochthonous (far-traveled) rocks. Later, E-An Zen recognized that the Taconic allochthon was emplaced as a series of discrete thrust slices (Zen, 1961). These two observations introduced an "Alpine" paradigm to the Taconics and set the stage for modern interpretations. The influence of plate tectonics on the interpretation of these rock types facilitated the placement of the Taconic range in the context of an arc-continent

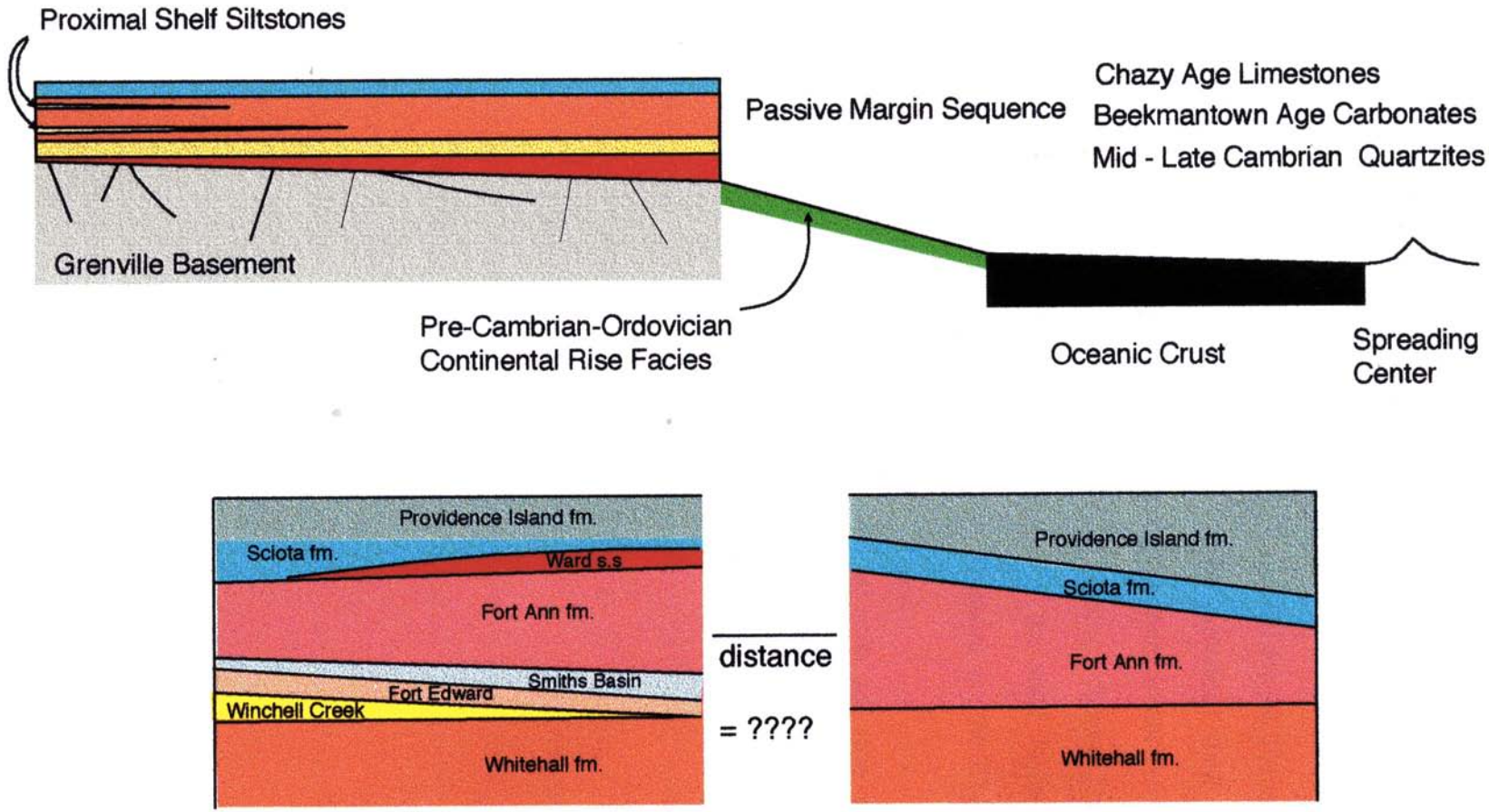

Fig.2.4) Schematic of the Cambrian sea off of the Laurentian passive margin. The lower illustrationis a schematic of stratigraphic relationships within the Beekmantown group at some unspecified distances on the proximal and distal shelf (left and right, respectively).

collision (or perhaps arcs- and / or microplate- continental collision) (Zen, 1967; Bird and Dewey, 1970; Rowley and Kidd, 1981; Rowley, 1983; Stanley and Ratcliffe, 1985; Delano et. al., 1990).

One consequence of the arc-continent collision model for the Taconics is the view that, prior to the onset of collision, the paleo-North American shelf deepened and deposition of shales and flysch type sediment ensued. The result is that the youngest, deep-water, sedimentary facies also represent a "shelf-drowning" facies. The most recent tectonic model proposed for these rocks is that even the shelf facies / proximal / "autochthonous" rocks have been transported great distances on the Champlain Thrust (Rowley, 1982).

This chapter presents a tabulated account of map units and then addresses some stratigraphic problems which bear on the map compilations and interpretations.

2.2 Map Units

2.2.1. Tabulated definitions of map units

Table 2-1 is a synopsis of the major lithologic units and their characteristics as defined by this study. Any terms used to describe grain size or bedding thickness follow the commonly used terminology recommended by Greensmith (1989). The fields of **Table 2-1** are as folows:

- **Map Unit** is the lithic map unit described by the criteria in the following 9 fields. The division of map units follows the general format of Granducci (1995), though these map units sometimes differ from that study.
- **Rock Type** is the most general rock type for the map unit.
- **Color** is the shade or color of the rock as found in the field.
- **Grain Size** is based upon silt, sand and pebble sizes with fine, medium and coarse being the basic subdivisions. Phi units were not measured.
- **Bedding Thickness** is separated into "thin", , "medium", and "thick". "Massive" indicates that bedding indicators are only rarely observed.
- **Mineralogy** is essentially an indicator of carbonate vs. silica mineralogy and the approximate percentage. It is noted where there is a significant oxide or clay component.
- **Sedimentary Structures** are those structures which are interpreted to be due to sedimentary processes rather than tectonic processes.
- **Tectonic Structures** are those structures interpreted to be due to deformation or solution processes related to mountain building activity.
- **Notes** are those observations regarding stratigraphic relationships or other important information.
- **Stratigraphic Nomenclature** is a lithologic correlation of map units to previous stratigraphic divisions (**fig.2.3**)

Table 2-1. A tabulated account of map units, defining lithologic characteristics, associated structures, and approximate stratigraphic level.

Map Unit	1
Rock Type	quartzite
Color	light gray to tan with occasional red-brown horizons
Grain Size	medium sand
Bedding Thickness	thin bedded (cm. scale), with meter spacing of joints along bedding planes
Mineralogy	>90% quartz (well rounded) <10% opaque minerals dolomitic horizons pelitic horizons
Sedimentary Structures	graded bedding (fining upwards) cross-bedding and wavy bedding thin syn-sedimentary normal faults (slumps) sole marks against pelitic horizons localized deposits filled with dolomitic sand and well rounded quartz pebbles.
Tectonic Structures	folding
Notes	interpreted to be the base of this stratigraphic section
Stratigraphic Nomenclature	Potsdam (Emmons, 1838)

Map Unit	2
Rock Type	arenitic dolostone, dolomitic arenite
Color	gray, weathers to yellow, orange
Grain Size	medium sand in a finer grained matrix
Bedding Thickness	thick to massive beds with thin arenitic beds
Mineralogy	≅50% quartz (sub-angular) in a dolomitic matrix arenitic and hematite rich horizons
Sedimentary Structures	arenitic horizons exhibit cross-bedding and wavy bedding
Tectonic Structures	jointing
Notes	The contact against unit 1 is gradational over a 4 - 5 m. contact. There is an apparent transition from a quartz grain supported matrix to a carbonate matrix. The arenitic beds weather to a red-brown detritus.
Stratigraphic Nomenclature	Ticonderoga Formation (Rodgers, 1955)

Table 2-1. A tabulated account of map units, defining lithologic characteristics, associated structures, and approximate stratigraphic level.

Map Unit	3
Rock Type	dolostone
Color	gray to light gray
Grain Size	coarse sand sized (depending upon degree of recrystallization)
Bedding Thickness	massive
Mineralogy	100% dolomitic carbonate material
Sedimentary Structures	none identified
Tectonic Structures	veins and fractures, particularly a conjugate joint set
Notes	The contact with unit 2 is defined by the disappearance of quartz grains. Unit 3 is interpreted to have lithified mostly from a carbonate mud. It has a "sparry" or "sugary" texture.
Stratigraphic Nomenclature	Whitehall (Rodgers, 1937)

Map Unit	4a
Rock Type	dolomitic siltstone, dolomitic sandstone
Color	blue gray, gray orange silt and sand layers
Grain Size	coarse silt, fine sand, medium sand
Bedding Thickness	thin (cm. scale) siltstone and sandstone beds, medium dolostone beds
Mineralogy	quartz and carbonates of varying degree depending upon horizon
Sedimentary Structures	well defined cross-bedding wavy orange sand beds worm borings (*Scolithus*)
Tectonic Structures	none identified
Notes	The stratigraphy of Fisher (1984) places the Winchell Creek over the Whitehall dolostone and underneath the Kingsbury limestone member. The Kingsbury limestone is not present in the region.
Stratigraphic Nomenclature	Winchell Creek Siltstone member (Fisher, 1984) Cutting (Cady, 1945)

Table 2-1. A tabulated account of map units, defining lithologic characteristics, associated structures, and approximate stratigraphic level.

Map Unit	4b
Rock Type	dolostone
Color	white, weathers to tan or yellow
Grain Size	medium to coarse sand
Bedding Thickness	massive
Mineralogy	carbonate chert horizons and nodules
Sedimentary Structures	none identified
Tectonic Structures	jointing
Notes	The Fort Edward Dolostone is only found in the Benson region. It is interesting to note that the Cutting Formation was named after Cutting Hill in the Shoreham township (Cady, 1945). In fact, there are no lithologies on Cutting Hill which fit the description of the Cutting Formation (Rodgers, 1969).
Stratigraphic Nomenclature	Fort Edward dolostone member (Fisher, 1984) Cutting (Cady, 1945)

Map Unit	4c
Rock Type	limestone
Color	white to light gray
Grain Size	micritic to silt
Bedding Thickness	massive
Mineralogy	carbonate + dolomitic component
Sedimentary Structures	none observed
Tectonic Structures	none observed
Notes	The Smiths Basin limestone is only found in the flat lying strata on Doughty Hill, usually in the river valleys.
Stratigraphic Nomenclature	Smith's Basin Limestone (Fisher, 1984) Cutting (Cady, 1945)

Table 2-1. A tabulated account of map units, defining lithologic characteristics, associated structures, and approximate stratigraphic level.

Map Unit	5
Rock Type	dolostone
Color	Dark gray
Grain Size	varies ; fine to coarse sand
Bedding Thickness	massive
Mineralogy	carbonate calcite, quartz and chert filled nodules and veins
Sedimentary Structures	wavy layering / laminations
Tectonic Structures	orthogonal joint sets, one of which may be perpendicular to bedding
Notes	In regions where unit 4a, 4b, and 4c are not present, it is very difficult to determine where the contact between unit 3 and unit 5 is located.
Stratigraphic Nomenclature	Fort Ann dolostone (Flower, 1964) Lower Bascom / Upper Cutting formation (?) (Cady, 1945)

Map Unit	6a
Rock Type	dolomitic siltstone
Color	gray to black with light brown laminations
Grain Size	fine to coarse silt
Bedding Thickness	thin
Mineralogy	quartz silt horizons in carbonate (dolomitic) matrix
Sedimentary Structures	cross-bedding
Tectonic Structures	none identified
Notes	The Ward siltstone is present only in the western thrust slices of the study area, associated with the Providence Island dolostone.
Stratigraphic Nomenclature	Ward Silstone (Fisher, 1977) Fort Cassin formation (Whitfield, 1890, Fisher, 1984))

Table 2-1. A tabulated account of map units, defining lithologic characteristics, associated structures, and approximate stratigraphic level.

Map Unit	6b
Rock Type	limestone
Color	light blue-gray
Grain Size	micritic
Bedding Thickness	massive with fossiliferous and dolomitic horizons as bedding indicators
Mineralogy	100% carbonate minerals
Sedimentary Structures	dolomitic reticulations stand out prominently on weathered surface
Tectonic Structures	veining, stylolitic horizons and incipient cleavages (?) suggest solution ("pressure solution") processes may have occurred
Notes	Unit 6b is remarkably similar to unit 7. An intact stratigraphic contact with unit 6a, unit 5 or unit 6c has not been observed.
Stratigraphic Nomenclature	Fort Cassin formation (Whitfield, 1890 ; Fisher, 1984) Sciota limestone (Fisher, 1977)

Map Unit	6c
Rock Type	dolostone
Color	dark gray, weathers to tan
Grain Size	fine sand to coarse silt
Bedding Thickness	massive
Mineralogy	carbonate (dolomitic) calcite, quartz and chert filled nodules and veins
Sedimentary Structures	none identified
Tectonic Structures	heavily fractured / brecciated, thin calcite veins
Notes	There is a remarkable resemblance between unit 6c and unit 5. An intact stratigraphic contact with unit 6b and unit 7 has not been observed.
Stratigraphic Nomenclature	Providence Island (Ulrich, 38) Bridport member of the Chipman formation (Cady, 1945; Cady and Zen, 1960) Fort Cassin formation (Whitfield, 1890; Fisher, 1984)

Table 2-1. A tabulated account of map units, defining lithologic characteristics, associated structures, and approximate stratigraphic level.

Map Unit	7
Rock Type	limestone
Color	light blue-gray to gray
Grain Size	micritic
Bedding Thickness	massive, with fossiliferous and dolomitic horizons as bedding indicators
Mineralogy	100% carbonate material
Sedimentary Structures	dolomitic reticulations stand out prominently on weathered surface
Tectonic Structures	veining, stylolitic horizons and incipient cleavages suggest solution ("pressure solution") processes have occurred
Notes	Unit 7 is remarkably similar to unit 6b. An intact stratigraphic contact between unit 7 and unit 6c has not been observed.
Stratigraphic Nomenclature	Middlebury Limestone (Cady, 1945) Chazy Age Limestone (Brainard and Seely, 1890)

Map Unit	8
Rock Type	limestone
Color	dark gray
Grain Size	fine silt
Bedding Thickness	thin to medium , though these could be cleavage planes
Mineralogy	100% carbonate material, though microscopy could reveal a significant pelitic component
Sedimentary Structures	none identified
Tectonic Structures	a well defined cleavage, rock can be mylonitic
Notes	The well defined cleavage could be the expression of higher strain, or it could be the result of a greater pelitic component than is found in unit 7. It is difficult to differentiate unit 8 from unit 7.
Stratigraphic Nomenclature	Orwell Limestone (Cady, 1945) Isle LaMotte Limestone (Emmons, 1838; Fisher 1984) Black River Age Limestone (Cady and Zen, 1960)

Table 2-1. A tabulated account of map units, defining lithologic characteristics, associated structures, and approximate stratigraphic level.

Map Unit	9a
Rock Type	calcareous shale
Color	light gray to dark gray; black and brown layers
Grain Size	fine silt to mud
Bedding Thickness	varies from thin to medium
Mineralogy	carbonate and phyllosilicate with minor quartz
Sedimentary Structures	alternating layers of black calcareous shale and brown arenitic shale layers (transitional to the Iberville - map unit 9b)
Tectonic Structures	outcrop and hand - sample scale folding with associated axial planar cleavage
Notes	The Stony Point and the Cumberland Head are essentially equivalent. The name Cumberland Head has been used to describe this calcareous shale to the north (e.g. Fisher, 1968). Because there is no uniquely identifiable Glens Falls limestone in the region, the Glens Falls has been included in the map units 9a and 8.
Stratigraphic Nomenclature	Uppermost Glens Falls Limestone (Ruedemann, 1912; Cady, 1945) Cumberland Head formation (Doll et. al., 1961) Stony Point Shale (Welby, 1961)

Map Unit	9b
Rock Type	non-calcareous shale, local greywacke
Color	black / dark gray
Grain Size	fine silt to mud, local arenite
Bedding Thickness	thin
Mineralogy	phyllosilicates, some dolomite, quartz
Sedimentary Structures	interlayering of arenites and shales graded bedding within arenitic portions
Tectonic Structures	a well defined slaty cleavage
Notes	Unit 9b has only been found in isolated lenses which may be a reflection of its deposition. The red/brown dolomitic silt horizons interlayered with black shales are included with map unit 9a, though this likely represents a transition from Stony Point/Cumberland Head to Iberville (the transitional stratigraphic unit of Welby (1961)).
Stratigraphic Nomenclature	Iberville Shale (Welby, 1961)

Table 2-1. A tabulated account of map units, defining lithologic characteristics, associated structures, and approximate stratigraphic level.

Map Unit	10a
Rock Type	slate
Color	black; weathers to a brown rust
Grain Size	fine silt to mud
Bedding Thickness	thin bedded, though few bedding indicators exist
Mineralogy	silica minerals (quartz and phyllosilicates), lenticular nodules of limestone
Sedimentary Structures	none observed
Tectonic Structures	at least one dominant cleavage, outcrop scale folds
Notes	One fossil locality has been found. It is often impossible to differentiate between unit 10a, b, and c.
Stratigraphic Nomenclature	Hortonville Shale (Keith, 1932) Trenton Age Shale (Cady and Zen, 1960)

Map Unit	10b
Rock Type	melange
Color	silver to dark gray
Grain Size	mud to fine silt
Bedding Thickness	none identified
Mineralogy	phyllosilicate, quartz, cobbles of limestone and quartzite
Sedimentary Structures	none recognized
Tectonic Structures	veining, cleavage, multi-phase folding, vein orientations,
Notes	The Forbes Hill Conglomerate is not a conglomerate, nor is it found on Forbes Hill. This unit is a tectonized melange zone.
Stratigraphic Nomenclature	Taconic Melange (Zen, 1961) Forbes Hill Conglomerate (Zen, 1961)

Table 2-1. A tabulated account of map units, defining lithologic characteristics, associated structures, and approximate stratigraphic level.

Map Unit	10c
Rock Type	slate
Color	black to gray
Grain Size	fine silt to mud
Bedding Thickness	few indicators are present; lenticular sections exist, parallel to the slaty cleavage
Mineralogy	phyllosilicates and minor quartz, some quartzite nodules
Sedimentary Structures	none observed
Tectonic Structures	several orientations of well defined cleavage planes, folds at all scales
Notes	This unit may be equivalent to some portion of the Brown's Pond and / or Hatch Hill formation of Rowley et. al. (1979) or to a flysch facies allochthonous formation which is not well defined to date (by stratigraphic studies).
Stratigraphic Nomenclature	Taconic Black (informal)

Map Unit	11
Rock Type	slate
Color	silver to green
Grain Size	fine silt to mud
Bedding Thickness	thin, where indicators are present
Mineralogy	phyllosilicate and minor quartz, local quartzite beds
Sedimentary Structures	lenses of quartzites, potential slump structures
Tectonic Structures	several well defined sets of slaty cleavage, folding at all scales, transposed layering
Notes	This unit is only present in the Sunset Lake region and in the northeastern region of the area on Scove Hill.
Stratigraphic Nomenclature	Bull Formation (Swinnerton, 1922; Zen, 1961)

Table 2-1. A tabulated account of map units, defining lithologic characteristics, associated structures, and approximate stratigraphic level.

Map Unit	12
Rock Type	quartzite
Color	dark gray; weathers to white; occasional red/brown sections
Grain Size	medium sand sized
Bedding Thickness	thin to medium
Mineralogy	quartz, local dolomite, phyllitic cement, minor opaques.
Sedimentary Structures	none observed
Tectonic Structures	none observed
Notes	Zion Hill quartzite is the general term for "Taconic", Pre-Cambrian quartzites.
Stratigraphic Nomenclature	Zion Hill Quartzite (facies) (Zen, 1961)

Map Unit	13
Rock Type	shale / slate interbedded with dolomitic arenite
Color	"sooty" black; red-brown interbeds
Grain Size	fine silt to mud; sand and silt sized in red-brown sections
Bedding Thickness	medium
Mineralogy	phyllosilicate, quartz, dolomite
Sedimentary Structures	interbedding of arenite and shale
Tectonic Structures	outcrop scale folding
Notes	The West Castleton Formation of Zen (1961) was originally used to describe this unit as well as several other lithologies. The more concise nomenclature, the Hatch Hill Formation of Rowley et. al. (1979) is used by this study.
Stratigraphic Nomenclature	Hatch Hill (Theokritoff,1964)

Table 2-1. A tabulated account of map units, defining lithologic characteristics, associated structures, and approximate stratigraphic level.

Map Unit	14
Rock Type	Calcareous shale and wacke
Color	gray to black
Grain Size	mud
Bedding Thickness	thin to thick
Mineralogy	carbonate, quartz, phyllosilicate
Sedimentary Structures	bedding
Tectonic Structures	map scale folding
Notes	May or may not be Browns Pond formation.
Stratigraphic Nomenclature	Browns Pond (facies) (Jacobi, 77) or upper Hatch Hill Formation (Rowley et. al., 1979)

2.2.2. Problems identifying map units in the field

Map units 1 (Potsdam) and 2 (Ticonderoga) are readily identified map units, as they are a predominantly quartzite lithology. Units 1 and 2 are easily distinguished from one another, and the contact between the two is marked by the dolomitic mineralogy of unit 2. The contact between units 2 and 3 (Whitehall) is gradational over a few meters and is characterized by a change from a quartz supported matrix to a dolomite supported matrix.

It is difficult to differentiate the dolomitic units that lack bedding, sedimentary structures, arenitic horizons, or pelitic horizons. Differences in color can be used to differentiate map units. Units 6c (Providence Island) and 5 (Fort Ann) have a tendency to weather to tan while unit 3 (Whitehall) is gray and unit 4b (Fort Edward) weathers to white. In the field, however, these color changes are subtle and often unreliable characteristics. Lenses of chert, calcite and quartz veins, fractures, and cleavage planes often help in determining the map unit to which a rock belongs. These characteristics may all be the product of post-deposition, and even post-tectonic, deformation or chemical processes. It follows that these characteristics are not always uniform, or present, throughout entire map units and may be present across the contact between two map units

(especially across a fault contact). With the exception of contrasting silt, sand or calcareous horizons, the difficulty in distinguishing dolomitic units applies to the entire section. In some instances on the geologic maps (**Plates I and II**), rather than try to differentiate unit 3 (Whitehall), 4b (Fort Edward), 5 (Fort Ann) and 6c (Providence Island), the dolostones were mapped as undifferentiated. Those recognizable units 4a (Winchell Creek siltstone), 4c (Smith's Basin limestone), 6a (Ward siltstone), and 6b (Sciota limestone)were mapped as individual map units, even where surrounding units could not be differentiated.

The differences between units 7 (Middlebury) and 8 (Orwell) are subtle. While unit 8 is darker and more pelitic than unit 7, the main criterion for differentiating between the two is a strong cleavage in unit 8. However, cleavage is a structural property and may be a reflection of local changes in the mineralogy and grain size of the rock, rather than a change in rock type that is consistent over a broad area. Thus, where the map unit was uncertain, or where outcrop was poor, these limestones are mapped as undifferentiated. It should be noted that there was no map unit which corresponded directly to the stratigraphic unit called the Glens Falls limestone. Any possible localities of this stratigraphic unit would be either in belts mapped as unit 8, undifferentiated limestone, or in the base of unit 9a.

Units 9a (Cumberland Head) and 9b (Iberville) are readily identified as they respectively constitute the calcareous and non-calcareous shales west of the Champlain Thrust. Furthermore, unit 9a is the only calcareous shale in the region. Outcrops of unit 9b have a dolomitic siltstone interlayered with a non-calcareous shale. Welby (1961) proposed a third stratigraphic unit for this lithology, a transitional unit between Cumberland Head and Iberville. This lithology was mapped as unit 9b (Iberville) in this study.

In the slate belt, it is often very difficult to distinguish between units 10a (Ordovician age Hortonville slate), 10b (Taconic melange), and 10c (Pre-Cambrian age Taconic black slates) (**fig.2.5**). Unit 10c has a very well defined cleavage, whereas units 10a and 10b have a weaker cleavage which tends to have a less consistent orientation and is

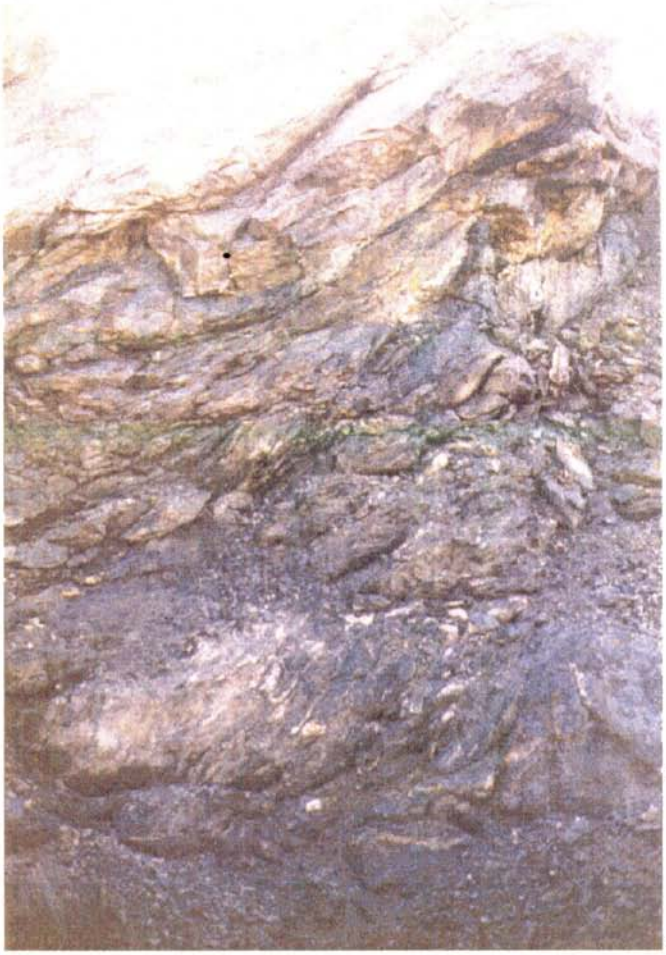

Fig.2.5) Taconic Melange (top) from a quarry near US route 22A, northwest of Sunset Lake, and Hortonville shale (bottom) from an outcrop southwest of Whiting. These are the two middle Ordovician black shales. Though both are well cleaved, the melange is associated with localized strain such as occurs along the Taconic Frontal Thrust. The Taconic Black (not shown) has a more pervasive and well defined cleavage than the Hortonville and does not have the rust weathering commonly found in the Hortonville.

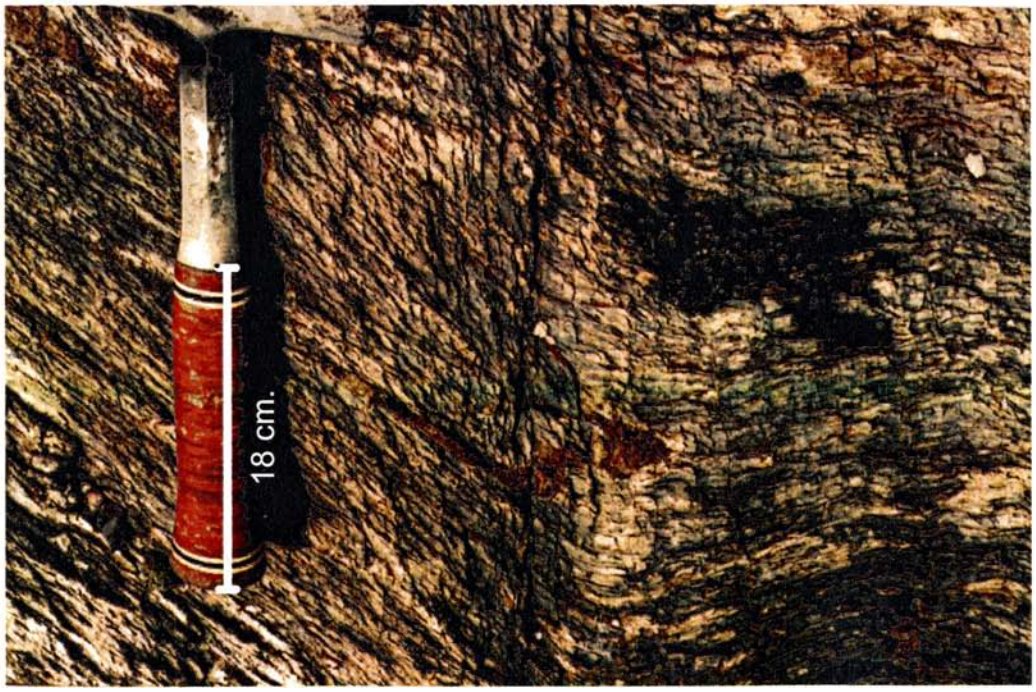

a good deal more fissile. Unit 10c (Taconic black) also has large nodules of vein quartz, whereas units 10a (Hortonville) and b (melange) have rare, lenticular sections of limestone. Unit 10a weathers to a rusty brown color. Unfortunately, outcrops rarely expose these diagnostic criteria. Unit 10b (melange) has distinguishing characteristics typical of a melange with exotic clasts of limestone and vein quartz. In the absence of limestone clasts or thick veins, unit 10b can be distinguished by a lenticular cleavage (or phacoidal cleavage). This last criterion, however, requires a qualitative assessment of the cleavage of the pelite. Units 10b and 10c do not trace continuously through the map area. While some of this may be due to poor outcrop, in the case of unit 10c the reason is likely because the distribution of the map unit is related to a fault zone and the unit is either covered by the hanging wall or is not present at all. Despite the ambiguities inherent to distinguishing these map units, they represent different ages, and different depositional and tectonic environments. Naming the units 10a, 10b, and 10c, as well as tracing contacts between the three in dashed lines (on the geologic maps) is intended to underscore their similarity. Within the Taconic-type slate rocks, the best distinguishing criteria is color. Unit 11 is a silver-green slate, whereas unit 10 is a black slate.

2.2.3. The Lack of Fossil Data

This study found only limited fossil data. One locality of heavily fragmented fossils was found on the side of the Pinnacle in a belt that is mapped as unit 6b (Sciota). A brachiopod locality was found in unit 11 (Hortonville) on Felton Hill, though the species was not identified. *Scolithus* worm borings were identified in several localities, the best less than 1 mile southwest of Benson Landing, in the lowermost portion of unit 4a (Winchell Creek) which runs roughly along the 200′ contour line. Stromatolitic algal mat material was found in some portions of unit 2 (Ticonderoga). Unit 7 (Middlebury / Chazy Age) formation is the only stratigraphic unit with truly plentiful fossils. Most of the

dolomite sequence is unfossiliferous, presumably because of dolomitization. It should be noted that conodonts could be plentiful and extremely useful in dating the rocks of the dolomite and limestone section (D.W.Fisher, person. commun., 1997), though this study did not attempt to do so.

2.3. Discussion

Discussions of the relationship of map units with one another are considered in the following sections titled **Stratigraphic Problems**. Correlating a map unit with a stratigraphic unit is a problem unto itself that involves an understanding of previous workers' observations. The division of map units roughly corresponds to Fisher's Whitehall map (1984) (**fig.2.1, 2.2**) and this local stratigraphic nomenclature will be used for further discussions in this thesis.

2.3.1. Stratigraphic Problems - Early to Middle Cambrian Rocks (?)

There is a thick section of early to middle Cambrian rocks that is mapped in regions to the north and east (Hermann, 1992; Hashke, 1994; Mehrtens and Dorsey, 1987). The stratigraphy is the following: the basal Cheshire quartzite (Emerson, 1892), the Dunham dolomite (Clarke, 1934), the Monkton quartzite (Keith, 1932) and the Winooski dolomite (Hitchcock et. al., 1861). These rock units are reported to have unique lithologic characteristics which distinguish them from the rock units found in the map area of this study. While there is a report of a slice of Winooski in the Shoreham township (Washington, 92), this study did not identify it. The Cheshire and Monkton quartzite were not identified either, and the major belts of quartzites in the region are considered equivalents of the Potsdam formation. Indeed, one of the major points of evidence for the degree of stratigraphic imbrication, and the trace of the Champlain Thrust System through

the map area is the repetition of the Potsdam formation through the Shoreham area (Hayman, Kidd, and Granducci, 1996).

The presence and / or absence of a lower Cambrian shelf facies is important to consider when interpreting the depositional environments of the basal quartzite unit of this study's succession of map units, making calculations of stratigraphic thickness of section in the map area, or drafting palinspastic reconstructions. South of Benson, near West Haven, the Potsdam rests unfaulted upon the Grenville basement of the eastern Adirondacks (Steinhardt, 1983). Thus, truly autochthonous sections of the shelf sequence, such as in the southernmost portions of the Benson region, can be inferred to contain the Potsdam quartzite as the basal unit, and any early Cambrian sequence is absent. To the north, towards Shoreham, there is no evidence for the presence of the early to middle Cambrian shelf sequence below the Potsdam quartzite. It is likely that the Potsdam remains the basal quartzite in these areas.

2.3.2. Stratigraphic Problems - The Carbonates

The stratigraphic column described here (**fig.2.1, 2.2**), includes several limestone horizons within the dolomitic horizons. There are lime-rich horizons found within formations that are mostly dolostones. These are local characteristics and of little concern for a large scale classification of map units. There are two sections of limestone found which can be traced intermittently throughout the mapped region. These units were mapped as units 4c and 6c. Unit 4c is equivalent to the Smiths Basin limestone and is a relatively thin limestone unit within the lower dolostone sequence. Unit 6c, however, is a relatively thick unit and is equivalent to the Sciota limestone. Up-section of the Sciota is the Providence Island dolostone or map unit 6c. The Sciota is, in some localities, lithologically identical to the Middlebury limestone. In other studies (e.g. Fisher, 1984), the Sciota has been mapped using fossil data to separate it from the Middlebury. In addition, the base of

the Middlebury is reported to have distinguishing characteristics such as a siltstone horizon (D.W. Fisher, person. commun., 1997) and a distinctive sequence of members such as the Crown Point. Unfortunately, traceable sections of these members were not found in the study area. The Providence Island dolostone has never been verified to exist in a truly autochthonous section and is always found proximal to a thrust fault. Thus, the belt of Sciota and Providence Island found throughout the map area may be a belt of Middlebury limestone with a slice of other dolostones thrust on top of it. If this is the case, then this would affect any calculations of thickness of the stratigraphic column, interpretations of the structure, and amount of displacement along thrust faults through the region. Indeed, it calls into question the nature of the lower contact of the limestone column (the contact between the Providence Island dolostone and the Middlebury limestone). However, the best exposure of the Sciota in this area, on the west side of the Pinnacle, reveals at least one thick dolomite bed that changes in thickness along strike (**fig.2.6**) whereas the Middlebury is entirely without a dolomitic component, with the exception of faint dolomitic reticulations on bedding planes. Thus, it is entirely possible that the Sciota exists as a distinct stratigraphic unit.

If the Providence Island, in this map area, is a structurally isolated stratigraphic unit, then it follows that it has a more distal shelf origin than the other dolostone units. Evidence for this is the observation that thick sections of Providence Island dolostone are only found above demonstrable thrust faults. A locality where there is the possibility of an intact contact between the Providence Island and an underlying unit is in the above described Delano Hill section. Here the Providence Island is very thin and the Winchell Creek and other siltstones absent. In fact, thin units such as the Winchell Creek and the Smiths Basin Limestone are never found in sections with Providence Island, Sciota or Ward. In the Benson region, the Providence Island is associated with the Ward siltstone but not with the Winchell Creek. Based upon the Geologic map (**Plate I and II**), and

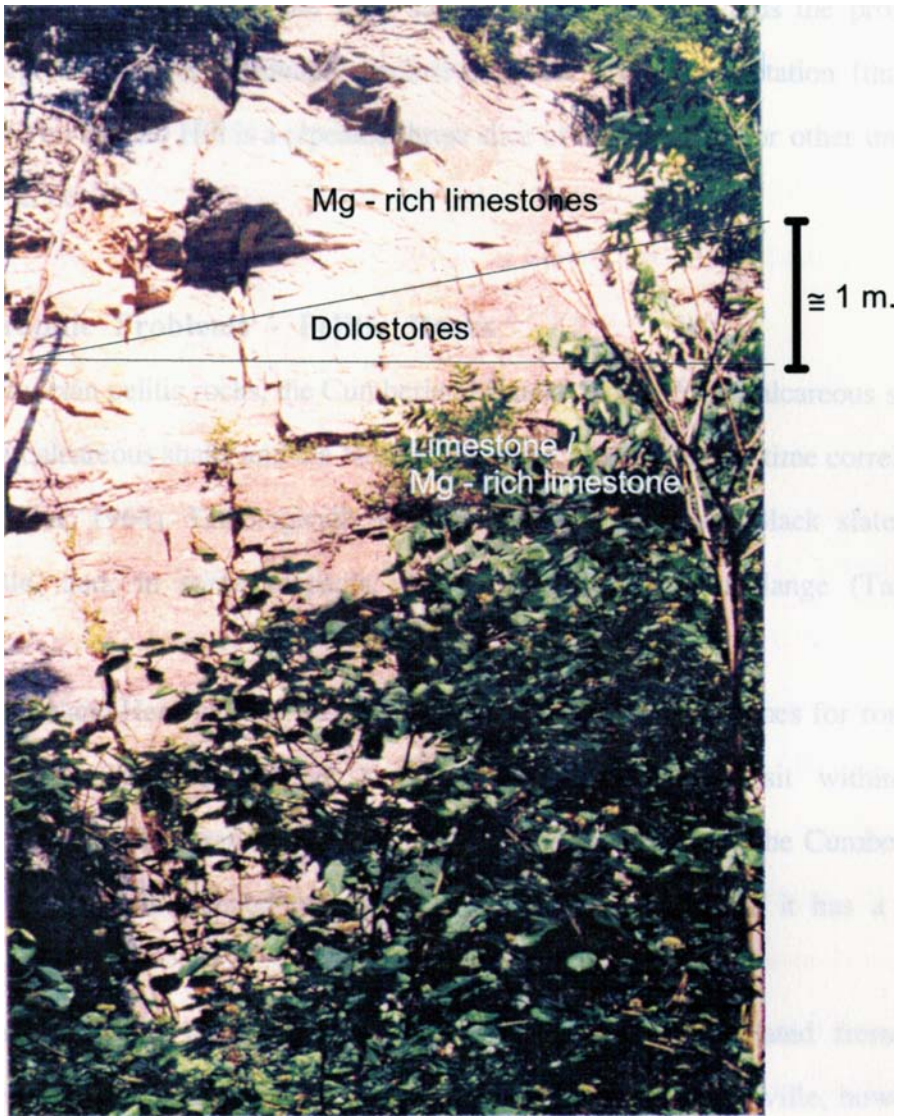

Fig. 2.6) An outcrop of Sciota limestone on the east side of the Pinnacle. Sciota limestone can be identical to the Middlebury limestone. This outcrop, however, has a thick bed of dolostone which pinches to out the north (left). A great deal of the calcareous section also has a dolomitic component. This outcrop is not far up-section of the floor thrust of the Pinnacle Duplex.

these relationships, this study proposes that the Providence Island is of a distal shelf origin where it constitutes the majority of the shelf sequence, and thins towards the proximal shelf. This interpretation is not mutually exclusive of the prior interpretation (that the Providence Island on Delano Hill is a repeated thrust slice of Fort Ann and/or other units in the Delano Hill section).

2.3.3. Stratigraphic Problems - Pelitic Rocks

The Ordovician pelitic rocks, the Cumberland Head / Stony Point calcareous shale, the Iberville non-calcareous shale, and the Hortonville shale, are all roughly time correlative (Welby, 1961; Zen, 1964). Lithologically correlative are the Taconic Black slate, the Hortonville shale, and, in some respects, the medial Ordovician melange (Taconic Melange).

The Cumberland Head and the Stony Point are the stratigraphic names for roughly equivalent lithologies. The Iberville is a noncalcareous flysch deposit within the Cumberland Head basin. The transitional zone of Welby (1961) between the Cumberland Head and the Iberville was mapped here as map unit 9b (Iberville), as it has a non-calcareous component.

The Hortonville and the Cumberland Head are readily differentiated from one another by the carbonate component of the Cumberland Head. The Hortonville, however, has traditionally been a "garbage can" term for all of the Ordovician non-calcareous shales east of the shelf carbonates. As was discussed in **section 2.2.2**, the belt of Hortonville likely contains large amounts of Taconic, Cambrian and / or Ordovician, black slates. Thus, the most significant boundary in the entire map area, the boundary between the Ordovician rocks (or Champlain structural group) and pre- to early Cambrian rocks (or Taconic structural group), is the least well defined. This will be discussed further in

Chapter 3, and is discussed extensively in Zen (1961), Rowley (1983), Jacobi (1977), and Bierbrauer (1990).

Fortunately, the boundary between the black and green slates is well defined. This boundary marks the change between the Hortonville / Taconic black slates, and the Bull formation (Zen, 61). The Bull formation has an internal stratigraphy described by Jacobi (1977), Aparisi (1984), and Rowley et.al. (1979). In the Sunset Lake area, there were only two map units defined and the stratigraphy of Jacobi (1977) was not applied.

2.3.4. Stratigraphic Problems - the Sunset Lake Region

In the northernmost section of the Sunset Lake area, there is an isolated belt of Hatch Hill formation. The Hatch Hill is an interlayered black shale / slate and orange weathered dolomitic sandstone of a continental rise facies. South of this belt are two outcrops of a calcareous, dark gray shale. This map unit would correlate lithologically to the Brown's Pond formation of Jacobi (1977). The formation name Brown's Pond implies a stratigraphic unit downsection of the Hatch Hill. This map unit can also be correlated to a limestone member within the Hatch Hill formation, just below the contact with the Poultney formation (up-section) (Rowley et. al., 1979). Thus, applying a formation name to this belt of calcareous shale / limestone is a structural problem. If the stratigraphic sequence in the Sunset Lake Slice is inverted then the calcareous unit can be correlated to the Brown's Pond formation (see **Chapter 3**). If the sequence is intact, then the calcareous unit can be correlated to the upper Hatch Hill formation.

Within the Bull formation in the Sunset Lake area, there are several quartzite horizons. These are considered to belong to the Zion Hill quartzite facies, a general name for all pre- Cambrian quartzites. It is entirely possible that the individual belts of quartzite are repeated sections across thrust faults. Alternatively, each belt of quartzite could be

separate horizons. Pre- Cambrian and Cambrian quartzite members are described in Dale (1899), Zen (1961), Rowley (1983), and Rowley et. al. (1979).

2.4. Summary

This geologic mapping of the Lower Champlain Valley provided map units for different lithologies through the area. These are correlated lithologically to stratigraphic units described by Fisher (1984) and Zen (1961) and other Taconic workers. Due to the uncertainties involved with the stratigraphic column, this study did not attempt to systematically calculate stratigraphic thicknesses nor did it attempt a palinspastic reconstruction of rock types. A schematic paleo-reconstruction of the shelf sequence is offered (**fig.2.4**) to show approximate paleo-geographic locations of the stratigraphic units.

This study identified no early Cambrian shelf dolostone - clastic section and has interpreted the Potsdam quartzite to be the basal shelf unit in the area mapped. The Winchell Creek, Fort Edward, and Smiths Basin limestones were only found in western slices and the autochthonous section and therefore are inferred to be only of proximal shelf origin. It is proposed that the Providence Island dolostone is a distal shelf facies rock and that the Ward Siltstone is associated with the Providence Island.

Another observation supports a different origin for the Providence Island, in some instances. The location of the Providence Island above major thrust faults suggests that the Providence Island may be an equivalent of another dolostone unit, repeated across a thrust. This implies that the Sciota is a section of Middlebury limestone, rather than a separate stratigraphic unit. The maps of this study do not incorporate these themes, though they are acknowledged as a possibility.

Two limestone units were identified, the Middlebury and the Orwell formations, though they could not always be differentiated. There was no separate Glens Falls

limestone identified by this study. The Cumberland Head / Stony Point formation is mapped as more extensive than in previous efforts (e.g. Welby, 1961), with the Iberville Shale mapped as isolated lenses.

The black slates consist of three map and stratigraphic units. These are the Ordovician Hortonville Shale, the higher grade Taconic Black Slate, and the tectonized Taconic Melange. They could not be differentiated in all cases. The Allochthonous sections of the map area are mapped as Bull Formation, a green slate. Within this belt are several discontinuous quartzite horizons which are referred to as the Zion Hill quartzite facies. Hatch Hill arenites and Brown's Pond facies formation calcareous shales were also mapped.

This study was conducted within the framework set forth by Bird and Dewey (1971), Rowley and Kidd (1981), Bradley and Kidd (1991). Collectively, this means studying the Taconic range as an ancient collisional belt with syn-collisional shale and flysch deposition upon an earlier passive margin sequence. Large amounts of transport along an imbricate thrust belt are also a part of this framework and are discussed in **Chapter 3**.

3. The Structural Geology of the Lower Champlain Valley

3.1. Introduction

The three major structures in the Lower Champlain Valley region are the Champlain Thrust, the Mettawee River normal fault, and the Taconic Thrusts. These structures trace the boundaries of the major sedimentary facies, the Cambrian - Ordovician shelf facies quartzite and carbonates, the middle Ordovician basin facies shale and flysch, and the late Pre-Cambrian to Cambrian continental rise shales and greywackes. The Champlain thrusts and the Taconic thrusts lie on two different structural levels and are brought to close proximity to one another by the post-thrust, east-side down, Mettawee River Fault (**fig. 3.1, 3.2**).

Within the shelf sequence rocks, east of the Champlain Thrust, are three major thrust faults which carry three thrust slices. Collectively, the faults may be referred to as the Champlain Thrust System. (**fig.3.1, 3.2**). Within thrust slices are minor thrust faults, thrust duplexes and thrust related folds.

East of the Mettawee River Fault, in the Taconic structural domain, are several thrusts. The Sunset Lake Thrust and the Taconic Basal Thrust transport continental rise facies rocks. The Sudbury Thrust, which transports dolostones, and the here named *Felton Hill Thrust System* which transports limestones and shales, are in the valley between the Sunset Lake Slice and the Giddings Brook Slice.

Throughout the entire mapped region, roughly east-west trending, across-strike offsets of the thrusts and surrounding map unit boundaries can be found. Some of these have only minor displacement on them, function as lateral ramps for thrusts, or are the sites of thrust duplexes. Others have abrupt changes in map units across them. In these instances there is not an adequate lateral or vertical displacement in the thrust fault responsible for lateral transport to account for the stratigraphic change. These offsets are thus interpreted to be pre-thrust structures and, furthermore, are suggested to be normal faults. This chapter is

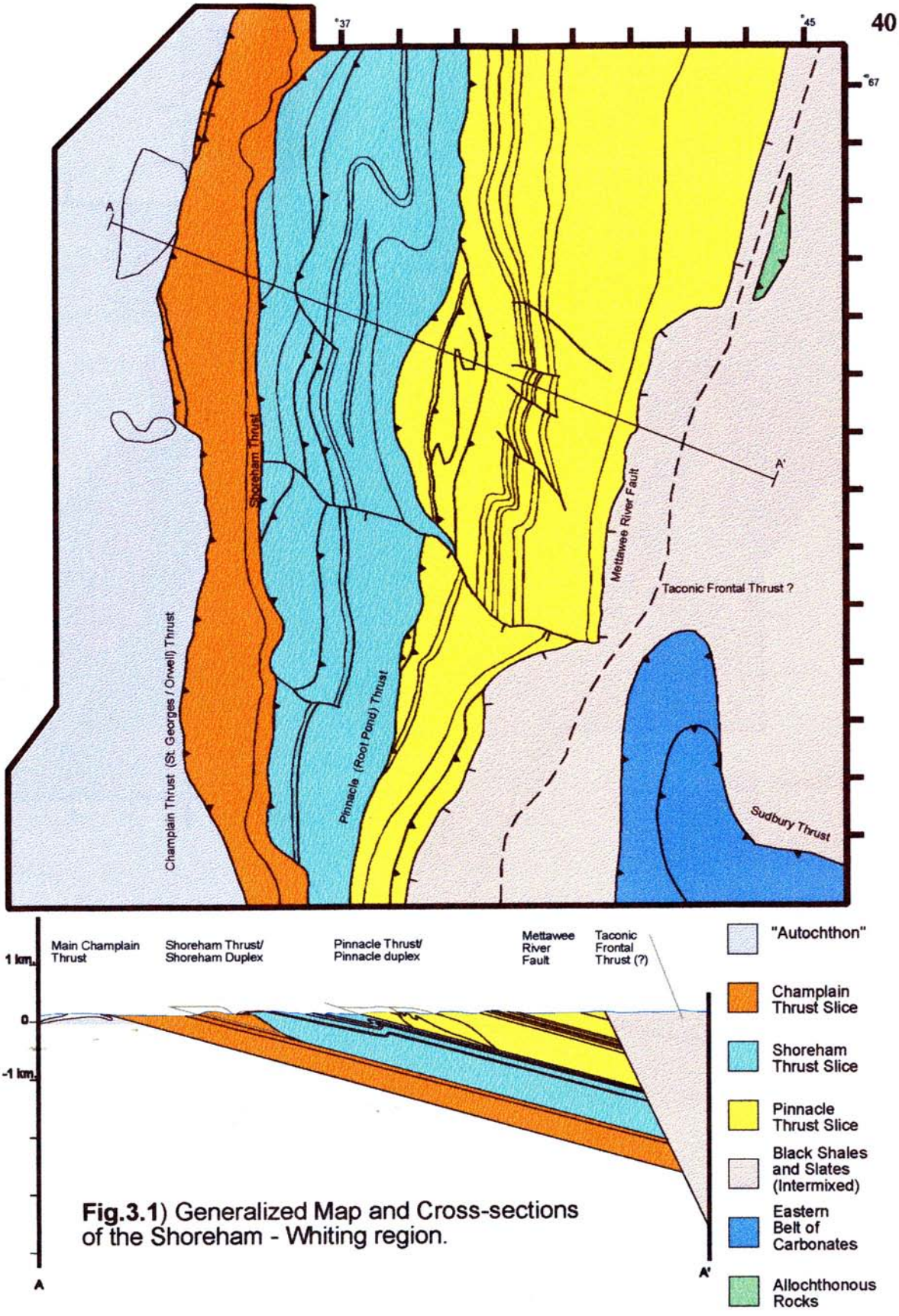

Fig.3.1) Generalized Map and Cross-sections of the Shoreham - Whiting region.

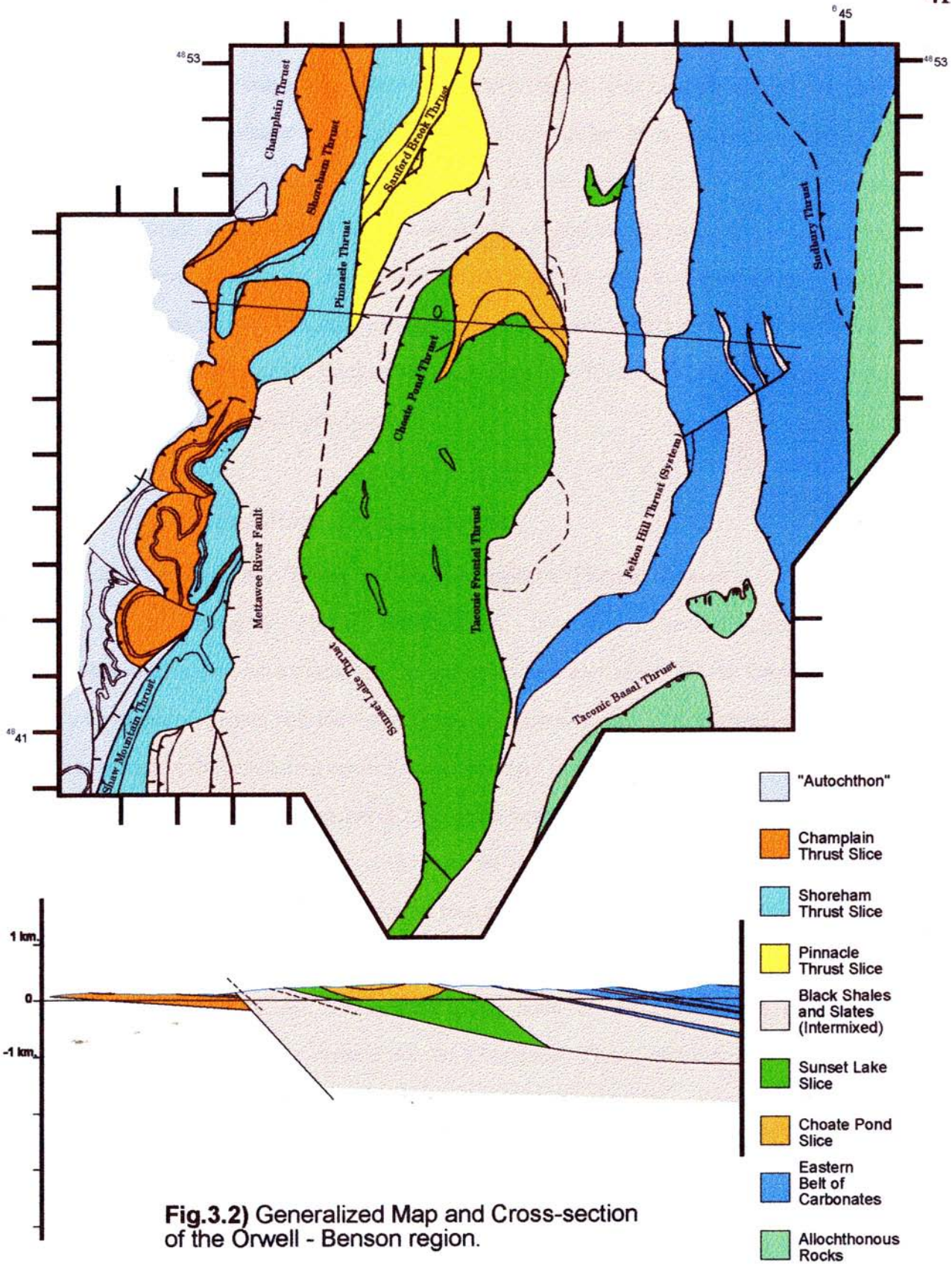

Fig.3.2) Generalized Map and Cross-section of the Orwell - Benson region.

partly focused on evidence supporting this interpretation. This chapter also shows how the interpretations presented on these geologic maps differ from previous efforts. Some attention is paid to trying to determine the relative age of structures. Cross-sections, geologic maps of local areas, and photographs of noteworthy outcrops and samples are used to clarify discussions and provide evidence for the favored interpretations. All of the cross-sections used by this study are not balanced as there is virtually no data on tip lines of faults, and the stratigraphic thicknesses and variation in thicknesses of transported units are not known with adequate precision.

3.2. The Champlain Thrust System

3.2.1. The Regional Trace of the Champlain Thrust System

The Champlain Thrust, *sensu stricto*, as exposed in Burlington and traced southward, is the contact between the quartzites and carbonates of the Champlain Valley stratigraphic sequence and the basin facies calcareous shales. The Champlain Thrust was recognized in the nineteenth century by Sir William Logan, but Rowley (1982) was the first to suggest that large displacements (an upper limit of 120 km.) occurred upon it. Until recently, the Champlain Thrust could only be traced from Burlington to the Middlebury region, at which point it was interpreted to either "tip-out" to zero displacement, or for the trace of the fault on the surface to trend to the west or east, though there was no control as to where (Coney et. al., 1972) (**fig.3.3**). Kidd et. al. (1995) first discussed the Champlain Thrust in the context of the Champlain Thrust System as extending from Vermont through the upper Hudson River region. A thrust system is a suite of thrust faults, as opposed to a single overthrust, which are collectively responsible for the bulk of the displacement. This study was able to trace the Champlain Thrust, and the Champlain Thrust System, from Shoreham to Benson where it was previously unrecognized.

In the region between Shoreham and Benson the Champlain Thrust System consists

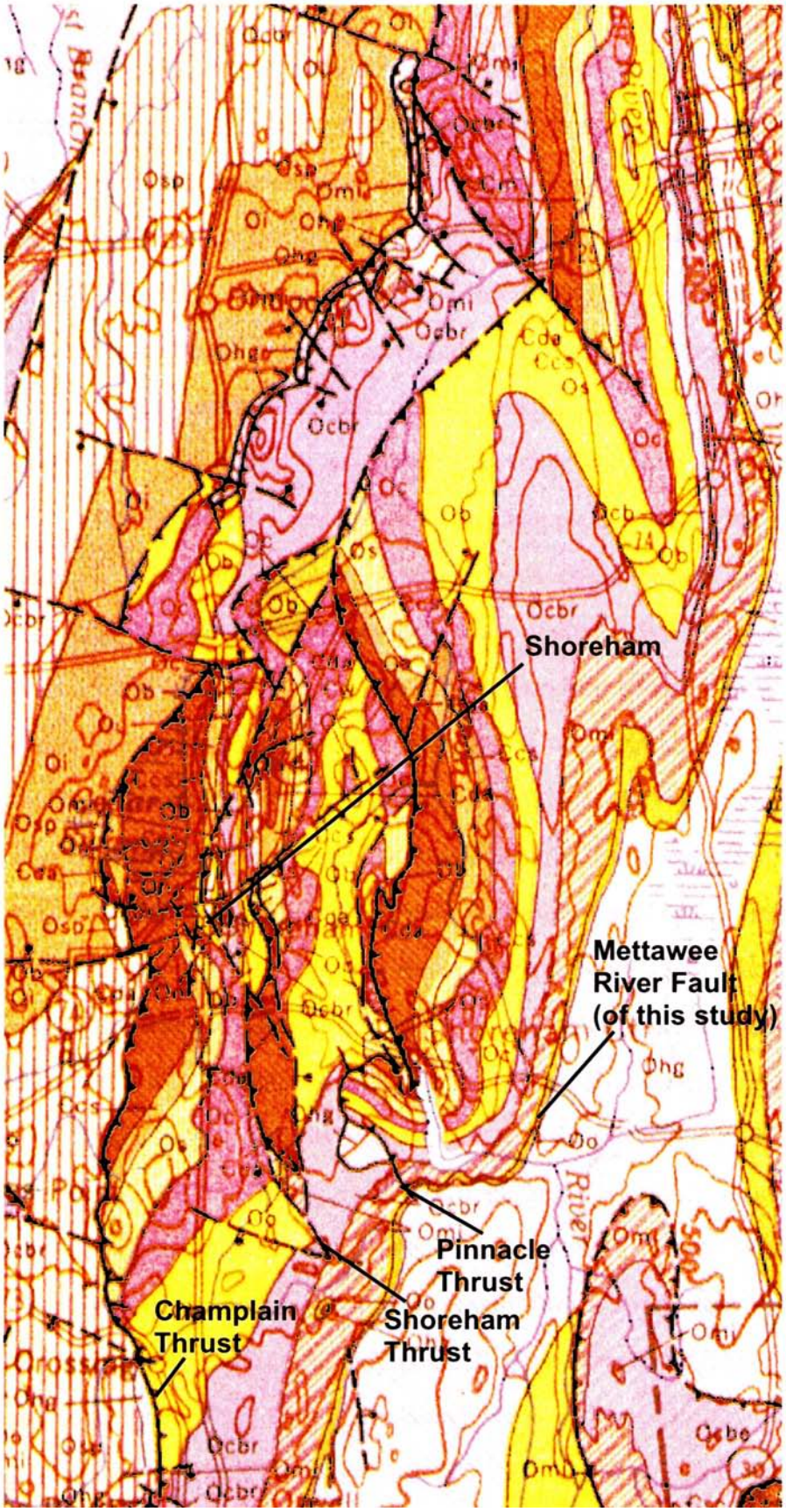

Fig.3.3) The Centennial Geologic Map of Doll et. al. (1961), showing the region between Bridport and Orwell. Most of the map units do not correspond to the map units used in this study. The three thrusts in the Shoreham region (labeled), roughly correspond to the three major thrusts of the Champlain Thrust System. However, it has been uncertain where the trace of the Champlain Thrust continues, south of this region. Note that the Mettawee River Fault (labeled) is here interpreted to be an intact stratigraphic contact between Ohg (Hortonville) and Ogo (Orwell).

of three continuous thrusts. These faults had been previously recognized around Shoreham (Brainard and Seeley, 1890; Doll et. al., 1961; Washington, 1992) (**fig.3.3**) though for the most part they were considered local structural complications and not mapped as part of a regional thrust belt. Notable exceptions to this are the assertion of Keith (1932) that the lower Champlain Valley was a fold and thrust belt and Washington's (1992) recognition that these structures likely projected into the Middlebury region and the hinge of the "Middlebury Synclinorium", the common interpretation for the large scale structure of the Lower Champlain Valley (Cady, 1945; Doll et. al., 1961).

The larger, individual thrusts of the Champlain Thrust System have been previously named. The *St. Georges Thrust* (Coney, 72), which can be seen adjacent to the Champlain Thrust on the **Centennial Geologic Map** of Doll (1961) (**fig.3.3**), correlates to the *Main Champlain Thrust* of this region. The *Shoreham Thrust* is adjacent to the Champlain Thrust and has been previously recognized in the Shoreham area, but never previously traced southward. The *Pinnacle Thrust* (Washington, 1985) is the easternmost thrust in the Shoreham - Whiting region and may correlate to the *Root Pond Thrust* (Granducci, 1995) southeast of Benson. There is a thrust in the town of Orwell, here named the *Sanford Brook Thrust*, east of the Pinnacle thrust which does not trace to the north or south as it is cut by the Mettawee River Fault. It is unclear whether this fault is a splay of the Pinnacle Thrust or if it is a separate thrust which continues elsewhere, perhaps to the north in the belt of Middlebury and Orwell limestones, near Delano Hill. The *Shaw Mountain Thrust* (Granducci, 1995), transports dolostones from high in the Beekmantown group stratigraphic section (Providence Island formation, for example). Thus, the Shaw Mountain Thrust is roughly equivalent to the Shoreham Thrust, and is considered the southern trace of Shoreham Thrust in this study (**fig.3.2**). However, south of Wilcox Hill, and into the map area of Granducci (1995), the Shaw Mountain Thrust is structurally equivalent to the

Champlain Thrust because it is the basal thrust of the tectonically transported carbonates, in that area (also see **section 3.2.4**).

From north to south there is an overall thinning of the entire thrust package. This occurs despite the overall north to south flattening of thrusts and surrounding map units. The mechanisms for this are duplexing within major thrust slices thereby thickening the structural section in the north, convergence of thrusts towards the south, thrusts climbing in stratigraphic section towards the south, and abrupt changes in stratigraphic level across across-strike offsets. These are now considered in order.

3.2.2. Local Duplexing Within The Champlain Thrust System

The thrust and fold belt of the Champlain Thrust System is very thick in the region east of Shoreham. Apparent thickening in map view occurs because the Mettawee River Fault is farther to the east in this region than to the south (**fig.3.1, 3.2**). The true thickness of the northern section is also anomalously thick relative to the south as there is a large amount of duplicating of map units within duplex structures, internal to the major thrust slices. The two largest duplex structures are the Pinnacle and the Shoreham duplexes.

The Pinnacle duplex (Washington, 1985), located on the Pinnacle in the valley between Shoreham and Whiting, involves three thrusts which are interpreted to merge at depth (**fig.3.4**). The Pinnacle Thrust, which here transports a slice of Sciota limestone and Providence Island dolostone, is the floor to the duplex structure. The next thrust to the east transports a horse of Potsdam quartzite. The easternmost thrust transports the entire shelf sequence as a roof to the duplex. Thus, the entire structure is a bit different from the classic duplex structure of consistently repeated stratigraphic units along several horses (**fig.3.5**). Rather, the Potsdam quartzite is duplicated in a single horse, which is internally folded. The lowest horse is not a repeated stratigraphic unit, but is instead a portion of

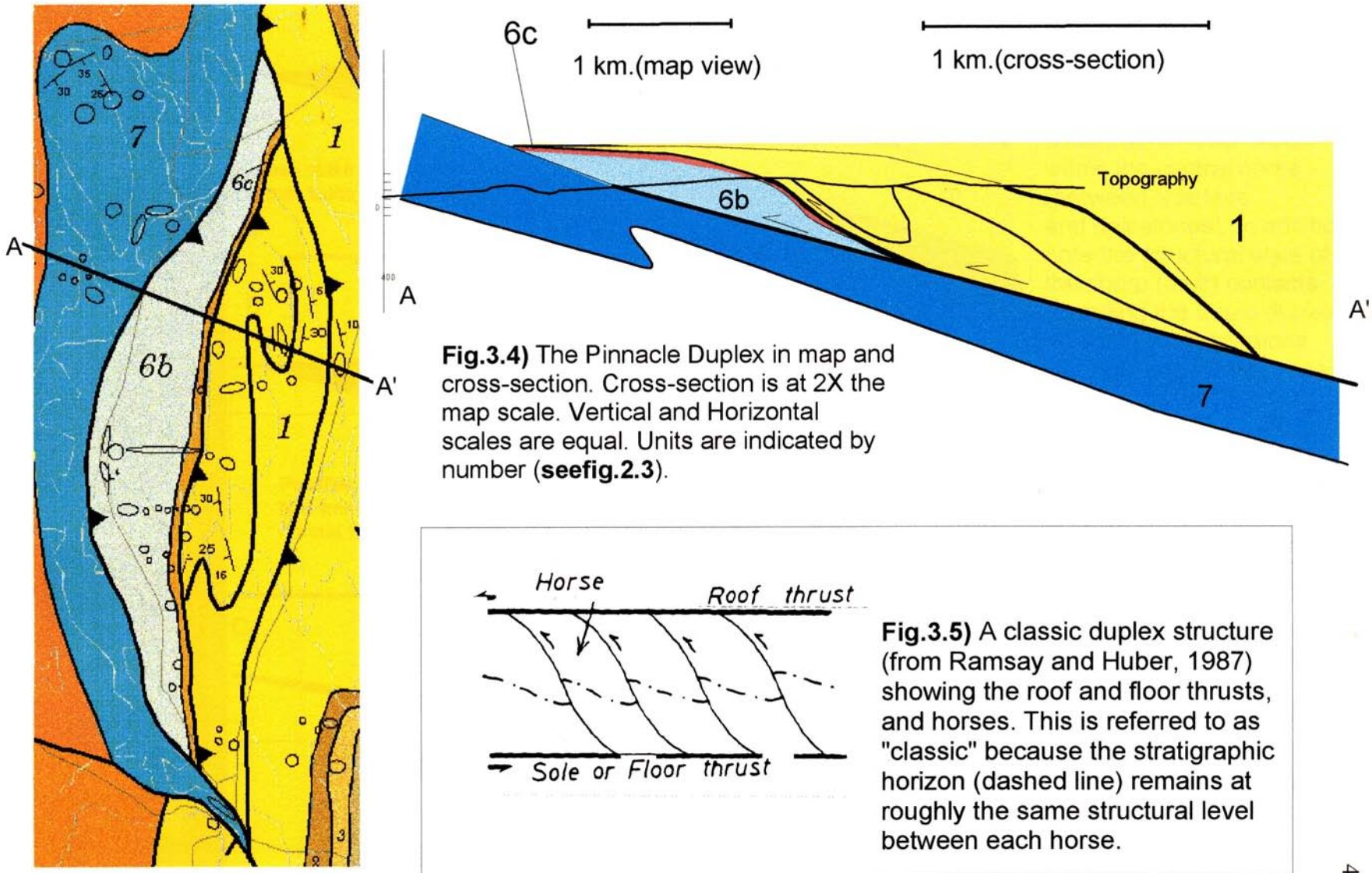

Fig.3.4) The Pinnacle Duplex in map and cross-section. Cross-section is at 2X the map scale. Vertical and Horizontal scales are equal. Units are indicated by number (**seefig.2.3**).

Fig.3.5) A classic duplex structure (from Ramsay and Huber, 1987) showing the roof and floor thrusts, and horses. This is referred to as "classic" because the stratigraphic horizon (dashed line) remains at roughly the same structural level between each horse.

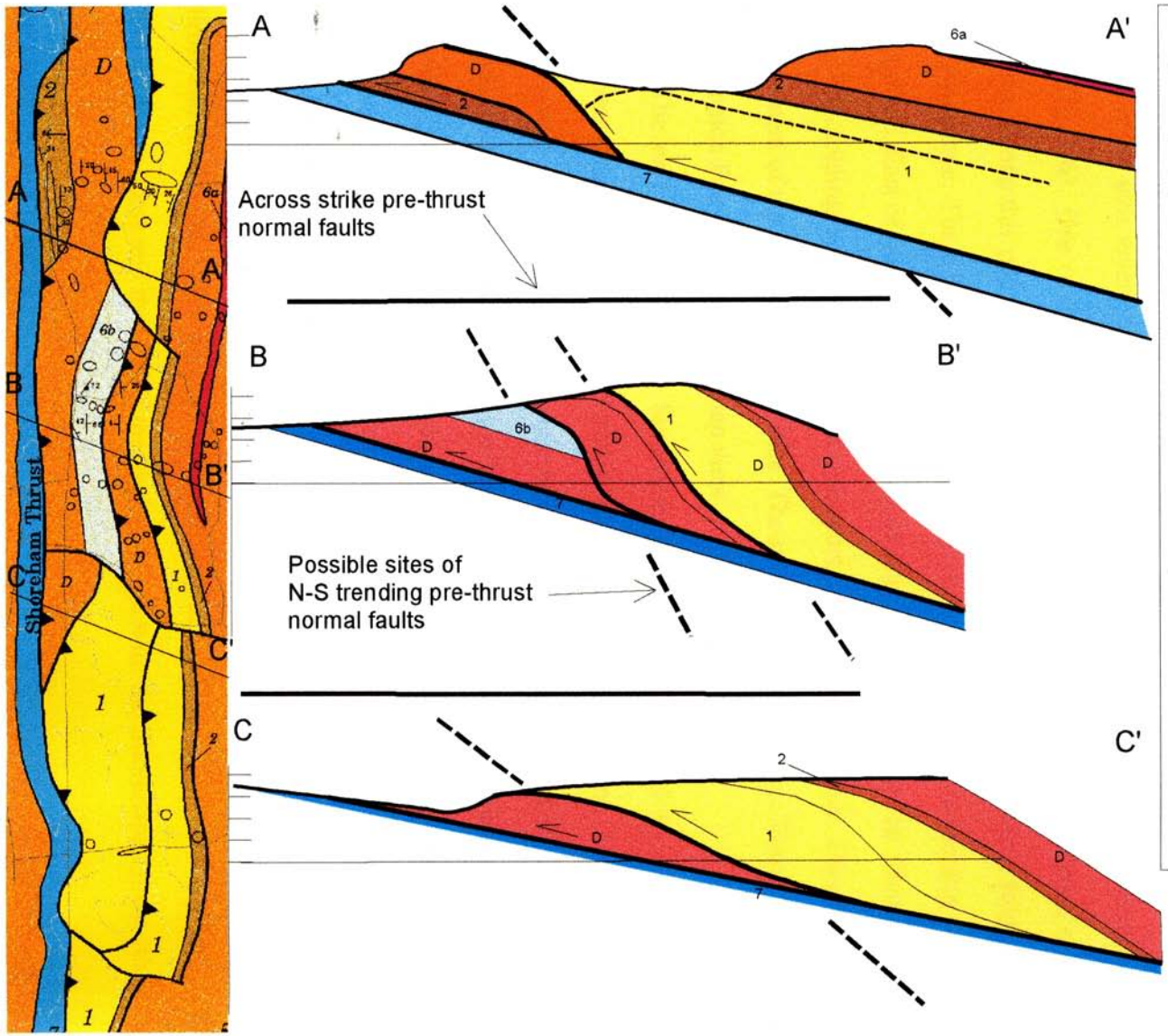

Fig.3.6) Map and three cross-sections of the Shoreham Duplex. Abrupt changes in stratigraphic level occurs within the central horse (between quartzite and dolostones). In addition, note the structural style of the sharp (fault) contacts bounding the thrust duplexes. These two observations suggest that the east-west striking normal faults bounding the duplexes are of a pre-thrust origin. Potential north-south striking pre-thrust normal faults are indicated by dashed lines. The ramps in the duplex structure may have nucleated upon these and/or they are concealed below the thrust sheets. See **fig.2.3** for key to map units

stratigraphic units from higher in the stratigraphic section. In map view, the thrusts of the Pinnacle duplex merge on the surface to the north and south. The Lemon Fair River Fault, an east-west striking normal fault to the south, likely played a key role in the geometric evolution of the Pinnacle Duplex (**section 3.2.4**).

The Shoreham Duplex is found in the Shoreham township. The Shoreham Thrust, which regionally transports either the Potsdam quartzite or the lowermost dolostone sections, splits into several splays around Shoreham. These are interpreted to converge at depth (**fig.3.6**). One of these splays continues to the north towards Bridport, out of the Map area. Along this portion of the splay the Potsdam Quartzite dips west, folded against the thrust plane. The dolostone section in the foot wall dips east, steepening against the thrust plane. East of this is a broad syncline / anticline fold pair within the Shoreham thrust slice. The folding is either related to transport along the Shoreham Thrust, or to the emplacement of the Pinnacle Thrust Slice. The splays of the Shoreham Thrust merge south of the Lemon Fair River Fault, in map view.

The eastern splay of the Shoreham Thrust ramps up and to the east on the southeastern margin of Mutton Hill, functioning as a roof to the duplex. South of the ramp is the northern half of the duplex. Here two horses of dolostone and Sciota limestone lie between the floor thrust (the Shoreham Thrust) and the roof thrust (the eastern splay). As the Sciota limestone and the undifferentiated dolostone are similar in stratigraphic level, this repetition is more akin to a classic duplex structure than the Pinnacle thrust. South of the Lemon Fair River, however, the thrust at the base of the horses transports Potsdam Quartzite rather than dolostone. Here, the repetition is between the hanging wall of the roof thrust and the horses, rather than the hanging wall of the floor thrust and the horses. In map view, the horse and the roof of the duplex merge with the Shoreham Thrust (the floor thrust) to the south.

There are other, more local duplex structures throughout the area. Many of the exposures of thrusts have large amounts of shale in the footwall (**fig.3.7**). Lenses of Hortonville and Iberville shales found at localities along the Pinnacle and Shoreham Thrusts, and the large lenses of limestones found along the Champlain Thrust, all could be interpreted as small horses preserved in local and minor duplexes. It is difficult to say how extensive these lenses are due to a lack of outcrop. There are a variety of possibilities as to how these lenses might have been transported with the hanging wall (roof). One such proposal is that there was an irregularity (such as a fault scarp) in the pre-thrust shelf surface, from which blocks of Hortonville, Iberville and upper limestone facies rocks were "plucked" and preserved in duplexes (**fig.3.7**).

3.2.3. Changes in Thrust Orientation and Ramping of Thrusts

Another mechanism for thinning of the Champlain Thrust System thrust slices consists of changes in the stratigraphic level of the thrusts. Changes in the dip of the thrusts relative to the map units does not cause thinning of a thrust slice. If anything, a general flattening of thrusts to the south (**fig.3.1, 3.2**) should lead to a widening, and thickening, of the total thickness in map view. Rather, a change in the strike of a thrust relative to the strike of map unit boundaries would result in a change in stratigraphic level of a thrust. In turn, lateral ramps (structures which offset thrusts, and across which thrusts change stratigraphic level) would result in abrupt changes in structural level.

South of the Lemon Fair River Fault, the strike of the Pinnacle Thrust is oblique to the strike of the map units. The overall effect is that the thrust climbs in stratigraphic level. Thus, near Orwell, the Pinnacle Thrust is transporting dolostones rather than quartzites.

The Shoreham Thrust exhibits similar behavior within the Shoreham Duplex where the Ticonderoga sandstone and overlying dolostones take a southwest strike. To the north there is a change in the orientation of the Ticonderoga sandstone (**fig.3.8**) which is

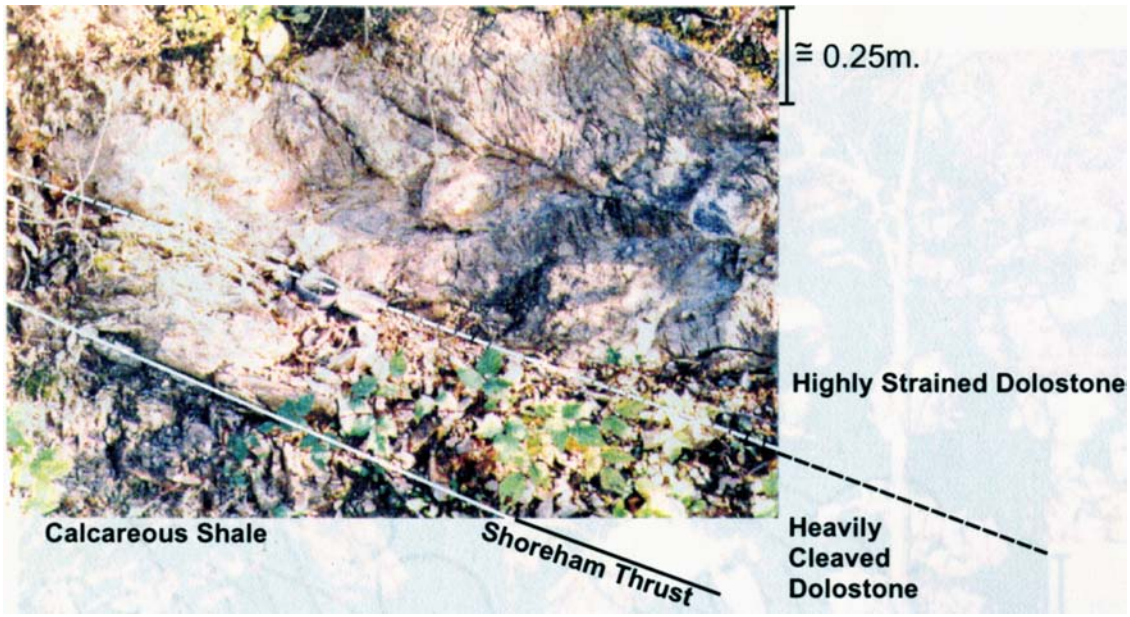

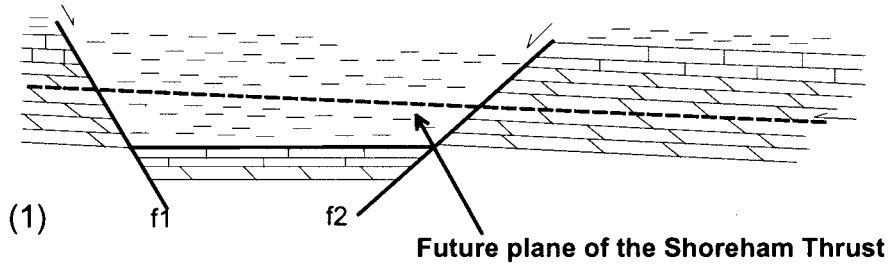

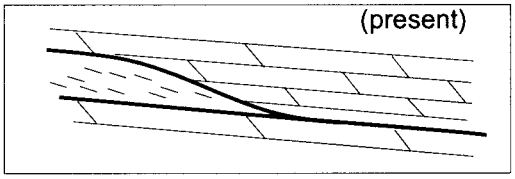

Fig.3.7) One possible history of the incorporation of shale into the base of thrust slices, as exhibited in outcrop along the Shoreham Thrust, southwest of Orwell (top). Normal faulting along the continental shelf, prior to tectonic transport, creates small graben filled with shale (1). As the thrusts propagate, and intersect the graben bounding normal faults (2), they split and form small duplex structures. Another possible interpretation, not shown here, is that there is an out of sequence thrust immediately below the Shoreham Thrust bringing the shales up from under the Champlain Thrust.

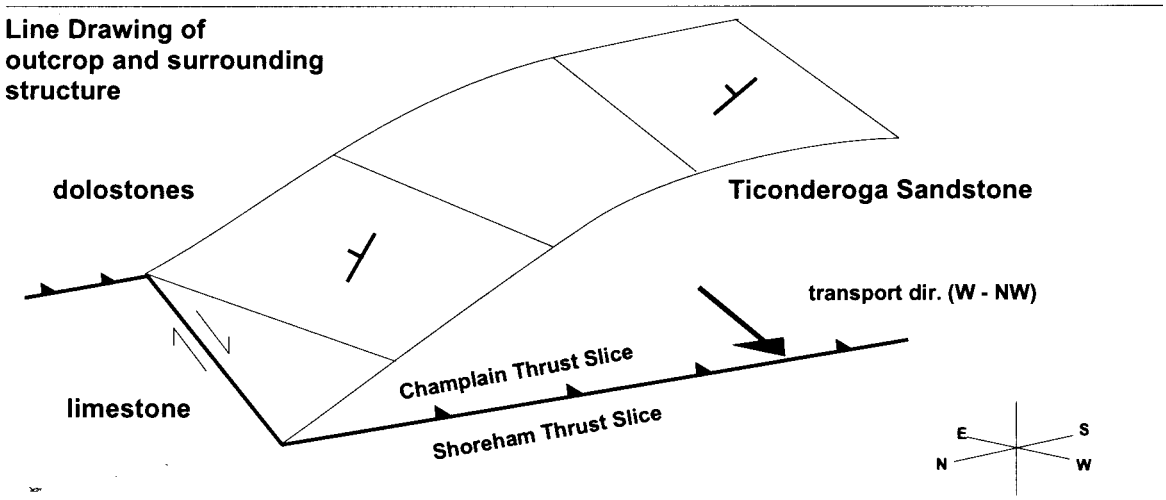

Fig.3.8) This outcrop is on route 22A, on the west side of Mutton Hill, north of which the Shoreham Thrust transports Beekmantown Age dolostones. South of this outcrop, the thrust transports the Ticonderoga sandstone, shown in the photo. At this outcrop, the Ticonderoga is folded with bedding deflected from a steep dip to to the northeast, to a shallow dip to the east. This outcrop is roughly where the Shoreham Thrust ramps up and over the Ticonderoga formation. Thus the folding is related to, and functions as, a lateral ramp in the Shoreham Thrust.

effectively a lateral ramp in the Shoreham Thrust, and leads to the Shoreham Thrust climbing in section to the north. To the south, near Orwell, the Shoreham Thrust abruptly changes structural level along a classic lateral ramp. South of this ramp, the Shoreham Thrust transports dolostones over limestones. Thus, south of Orwell, all of the thrusts transport dolostones, and the entire Potsdam quartzite and lower dolostone units are excised from the section. In conjunction with the encroachment of the Mettawee River Fault on Lake Champlain, these lateral ramps lead to an elimination of the entire eastern shelf sequence in map view (**Plate I and II**).

Another example of a lateral ramp in the Champlain Thrust System is on the Champlain Thrust. Between Benson and Orwell the Champlain Thrust is fairly flat at an elevation of 200 feet above sea level. In the region of Benson bay, however, the Champlain Thrust climbs 100 feet and then drops 100 feet. There does not appear to be a discrete structure related to these changes in elevation, though the fairly uniform topography could be concealing the lateral ramps responsible.

3.2.4. Across-Strike Offsets in the Champlain Thrust System

The final structures in this discussion of thinning of the total thrust package from north to south are across-strike offsets in the thrust faults and surrounding map unit boundaries. These alone do not change the map pattern significantly. Along the group of ridges which include Delano and Cutting Hill, northwest of Whiting, are several offsets which have no significant impact on the overall map pattern. From north to south these three faults provide a map view left-lateral, right lateral, and left lateral displacement, respectively. I originally interpreted these to be either post-thrust (and post-orogenic) strike-slip or normal faults. Welby (1961) also proposed that similar offsets in the Champlain Thrust were a set graben structures initiated during a post-Taconic phase of deformation. The alternative to these hypotheses is that the across-strike structures were

syn-thrust offsets (tear faults) which never evolved to the point of lateral ramps, and lack significant changes in stratigraphic level across them.

In contrast to a syn- or post- tectonic origin for the across-strike offsets, I propose that all of the across-strike structures in the map area are part of a set of faults that were initiated during the onset of the Taconic collision and prior to thrust faulting. Occasionally lateral ramps were nucleated on these. Other offsets never evolved to this point, and remained minor tear fault structures in the thrust geometry. Some of these offsets did not affect the thrust geometry but did cause abrupt changes in the stratigraphic level.

A striking example of a major facies change across an across-strike offset occurs in the Taconic section and not in the Champlain System. Across route 22A, south of Sunset Lake, there is a change between continental rise facies slates and upper shelf facies limestones. The adjacent thrust faults have no offset across the contact. Thus, the contact must originate on a pre-thrust generation of structure. With emplacement by the Sunset Lake thrust, the relationship between the limestones and slates was preserved (**Plate II**, southernmost portion).

The Lemon Fair River Fault is a normal fault between the Shoreham and Whiting areas. This fault is the most obvious discontinuity in the Champlain Thrust System in this region. It is across this fault that the map units immediately east of the Pinnacle Thrust slice change from a roughly north - south strike to a northeast - southwest strike, oblique to the Pinnacle Thrust. This change in the strike of the bedrock does not occur elsewhere along the entire length of the Lemon Fair River Fault, but it does affect the Pinnacle Thrust Slice along the length of the Pinnacle Thrust. These observations support the hypothesis that there is some change in the overall thrust geometry due to a pre-thrust Lemon Fair River Fault. The alternative is that the origin of the change in strike orientation was an effect of drag on the Lemon Fair River Fault after thrusting. Such drag would create a more local

(from north to south) change in strike orientation which would be more pervasive (from east to west) along the entire length of the Lemon Fair River Fault.

A more profound change across the Lemon Fair River Fault is that the belt of Middlebury limestone on the west side of the Pinnacle, below the Pinnacle Duplex, is absent immediately south of the Lemon Fair River. The Pinnacle Thrust is displaced to the west by .5 km. in map view. The map unit boundaries around the Middlebury limestone have not undergone the same amounts of displacement. In addition, the Shoreham Thrust Slice section has a consistent sense, though half the amount, of displacement as the Pinnacle Thrust Slice section, across the Lemon Fair River Fault. Thus, there is a change in stratigraphic level across the Lemon Fair River Fault without adequate lateral or vertical displacement in the thrust (**fig.3.4, 3.9**). The only way to explain this is that a pre-thrust structure created a separate basin of limestone within the middle shelf dolostones.

A similar situation arises across the Lemon Fair River Fault on the southern margin of the Shoreham Duplex. The easternmost splay of the Shoreham Thrust carries Potsdam Quartzite and ramps up-section near Shoreham. It then drops back down across the Lemon Fair River. The result is that the central splay carries a slice of dolostone in Shoreham, but a slice of Potsdam quartzite south of the Lemon Fair River Fault. There must be a pre-thrust structure bringing the horse of dolostones to what is otherwise the level of the Potsdam Quartzites (**fig.3.6**).

Perhaps the best example of an across-strike offset across which there is an abrupt change in stratigraphic level, independent of lateral ramping or thrust duplexing, is on the Champlain Thrust. North of Doughty Hill (where the Addison / Rutland county line cuts due southeast of Benson Bay), below the flat lying, middle dolostone section, the Champlain Thrust sits above the Cumberland Head, basin facies calcareous shales. Across the northernmost left lateral offset in map unit boundaries, the Champlain Thrust goes from juxtaposing shelf facies dolostones over basin facies calcareous shales, to juxtaposing shelf

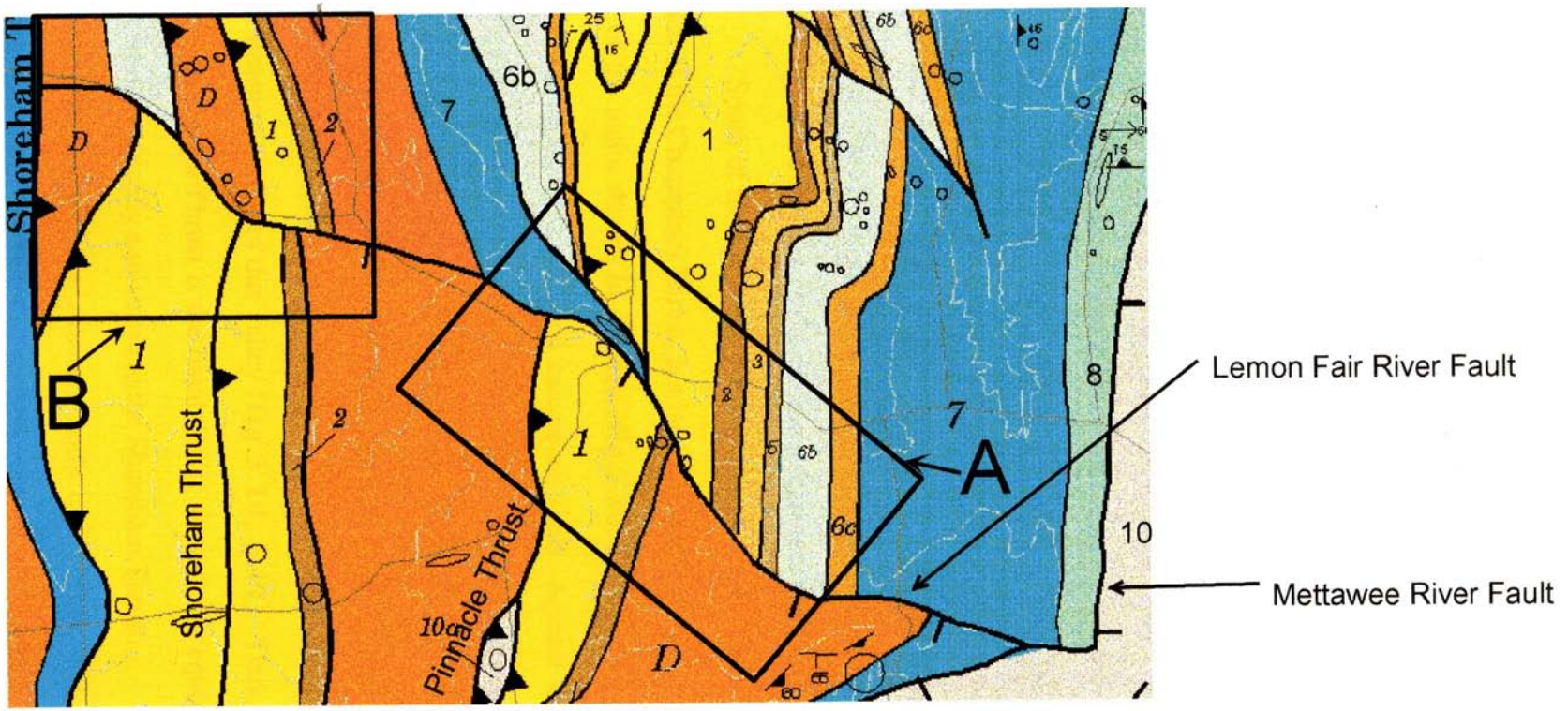

Fig.3.9) Region A shows a section of the Lemon Fair River Fault where there is an apparent offset in map units of 0.5 km.. Region B has apparent offsets of less than 0.25 km.. In addition, the map units in region B have a south-west strike on the hanging wall of the Lemon Fair River Fault and a north-south strike on the foot wall. This does not occur elsewhere in the region. Abrupt changes in stratigraphic level, inconsistent with the change in structural level of the transporting thrust faults, can be seen in both regions A and B. Altogether, these observations suggest a pre-thrust origin for the Lemon Fair River Fault. Clearly slip on the fault continued during transport and emplacement as well. See **fig.2.3** for a key to the map units.

facies dolostones over shelf facies dolostones (**fig.3.10, 3.11**). The best explanation for this abrupt change in the level of the Champlain Thrust is with a pre-thrust structure. North of this structure is the belt Cumberland Head shale, and south of it is autochthonous dolostones. With the emplacement of the Champlain Thrust package, this relationship is preserved on Doughty Hill. An alternative explanation is that this is a duplex structure in which the floor thrust is cut and obscured by the shore of Lake Champlain and a normal fault parallel to Lake Champlain (exposed north of Stony Point). However, the flatness of the map units is an observation which strongly conflicts with such an interpretation. Furthermore, south of the Lighthouse (normal) Fault, the western shelf sequence rests, unfaulted, upon the basement rock (see the trace of this belt from the area of Granducci (1995) to the area of Steinhardt (1983)). The region around Doughty Hill is where the Champlain Thrust climbs section and a truly autochthonous shelf sequence remains to the west. I propose that one of the dominant mechanisms for this is a pre-thrust normal fault.

South of the flat lying dolostones of Doughty Hill, and south of the southernmost trace of the Champlain Thrust, is a large normal fault which functions as a lateral ramp for all of the major thrusts in the area (**fig.3.10, 3.11**). This fault bounds a narrow valley with a bedrock of the basinal calcareous shale. Against the southern escarpment of this valley is the Shaw Mountain Thrust which juxtaposes upper dolostones (Providence Island formation, for example) against the autochthon. The Shaw Mountain Thrust becomes the Shoreham Thrust across this lateral ramp / normal fault. The Champlain Thrust is last exposed in a thin layer immediately below the Shaw Mountain / Shoreham Thrust in the northeastern corner of this valley (**fig.3.10, 3.11**). Thus, south of the normal fault, the Shaw Mountain Thrust is the basal thrust, structurally equivalent to the Champlain Thrust but stratigraphically equivalent to the Shoreham Thrust.

The across-strike structure north of Doughty Hill, across which the Champlain Thrust climbs in stratigraphic section, and the normal fault to the south, across which the

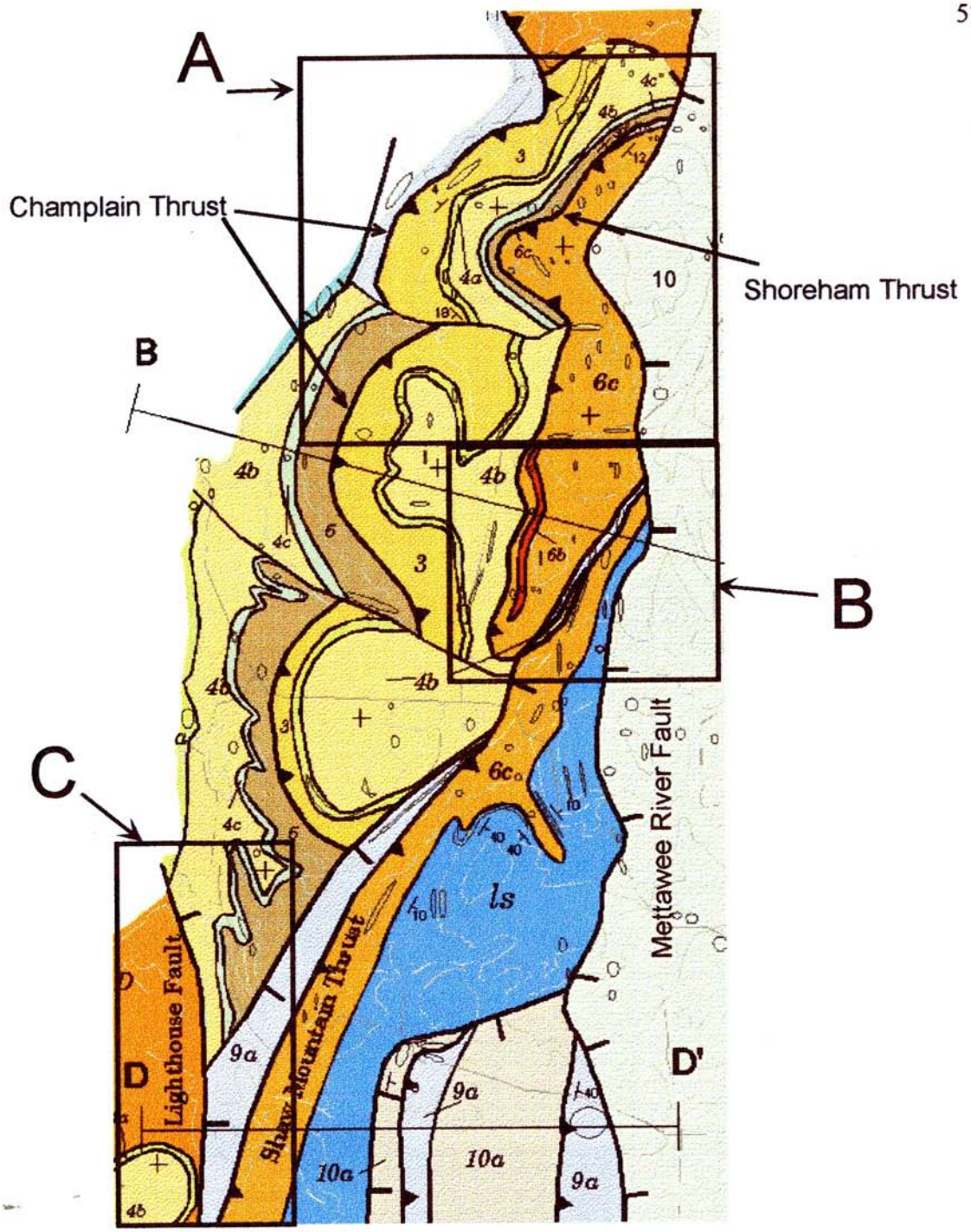

Fig.3.10) In region A the Champlain Thrust is cut by a normal fault which sends it upsection, above the Fort Ann dolostone. By region C, the dolostones rest unfaulted upon the basement. This is due to the pre-thrust origin of these normal faults, creating such abrupt changes in the stratigraphic level. Region B is where a northeast trending normal fault / lateral ramp bounds a narrow belt of Cumberland Head shale, above which the Shoreham Thrust is offset, and becomes the Shaw Mountain Thrust to the south. See **fig.2.3** for a key to the map units.

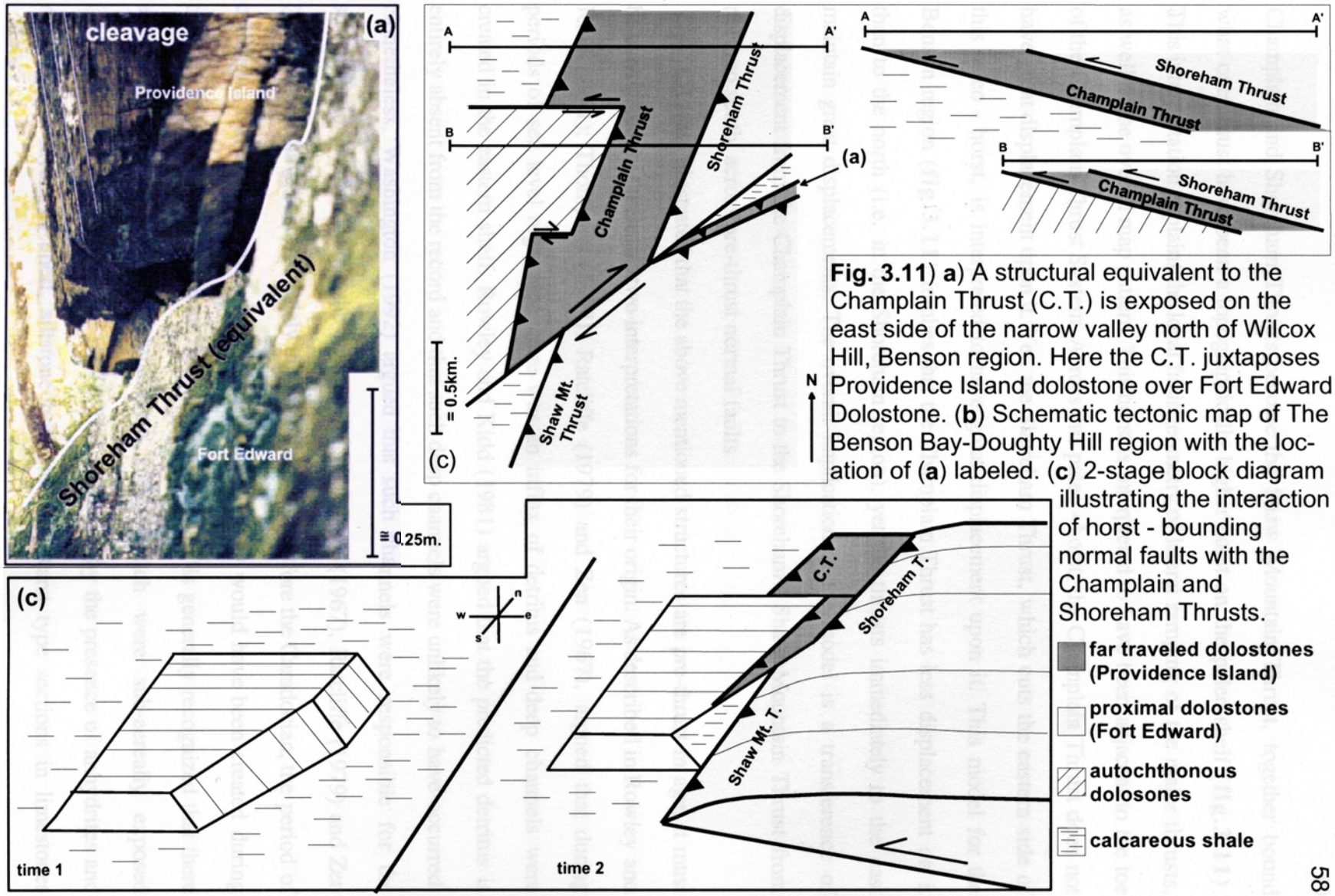

Fig. 3.11) **a**) A structural equivalent to the Champlain Thrust (C.T.) is exposed on the east side of the narrow valley north of Wilcox Hill, Benson region. Here the C.T. juxtaposes Providence Island dolostone over Fort Edward Dolostone. (**b**) Schematic tectonic map of The Benson Bay-Doughty Hill region with the location of (**a**) labeled. (**c**) 2-stage block diagram illustrating the interaction of horst - bounding normal faults with the Champlain and Shoreham Thrusts.

Champlain and Shoreham Thrusts become the Shaw Mountain Thrust, together bound what once must have been a topographically higher horst on the paleo-shelf (**fig.3.11**). This interpretation explains the local fault geometry of lateral ramping of the major thrusts, as well as the overall map pattern. This horst is interpreted to have been adjacent to the toe of the Champlain Thrust System. Across this paleo - horst, the Champlain Thrust does not have great displacement upon it. Yet, the Shoreham Thrust, which cuts the eastern side of this paleo - horst, is interpreted to have great displacement upon it. This model for the Benson region (**fig.3.11**) implies that the Champlain Thrust has less displacement on it than to the north (i.e. in the Shoreham region), yet the thrusts immediately to the east maintain great displacements. The overall implication of the model is a transference of displacement from the Champlain Thrust to the Shoreham / Shaw Mountain Thrust from north to south, across pre-thrust normal faults.

Having illustrated that the above mentioned structures are pre-thrust in age, it must be considered that there are two interpretations for their origin. As described in Rowley and Kidd (1981); Thompson (1967), Ratcliffe (1979) and Zen (1967), argued that during periods of sea level regression there was an influx of detritus and deep channels were created in the eastern shelf. Rowley and Kidd (1981) argued that the predicted detritus is entirely absent from the record and that such deep channels were unlikely to have occurred. Nonetheless, Washington (1992) argued that such channels were responsible for the structures in question. While the channels of Thompson (1967), Ratcliffe (1979) and Zen (1967) would have occurred solely in Llandillian time (before the Caradocian, the period of collision), the channels proposed by Washington (1992) would have been created during onlap - offlap periods throughout Beekmantown time. It is generally recognized that there are many horizons in the Beekmantown group which were sub-aereally exposed (D.W.Fisher, person. commun., 1997). This is shown by the presence of anhydrites and related thick layers of chert, siltstone horizons, and karst type sections in limestones

(Friedman, 1996). However, siltstones are located only in the western slices, and pinch out laterally. Chert horizons are discontinuous and thin and no major deposits of anhydrites or evaporites have been recognized. There is no sign of pre-thrust detritus and the only syn-sedimentary normal faults are in the quartzite lithologies and have small amounts of throw. The onlap - offlap cycles proposed as major facies control in Black River - to - Trenton Age limestones in the Highgate area (Mehrtens and Dorsey, 1987) do not seem to be present in the lower stratigraphic sections. The candidates for the boundaries of such cycles are the thrust faults on which this study is based. Furthermore, it would be unreasonable to argue that formation of deep channels occurred on the continental shelf during these periods of relative environmental quiescence as shown by generally micritic lithologies. Thus, there is no independent evidence for channels of depths equivalent to stratigraphic formations, in the paleo-shelf before emplacement of the thrust sheets.

The best argument for the normal faults and lateral ramps having nucleated on pre-thrust normal faults is contextual. Bradley and Kusky (1986) and Bradley and Kidd (1991) demonstrated that many similar contacts in the Mohawk Valley (the autochthonous inner shelf) formed as pre-collisional normal faults (**fig.3.12**). With analyses of present day Timor trough and the thrust belt in the Arkoma basin (southern Appalachians - Ouchitas), they showed that these likely formed via flexural bulging of the lithosphere with the onset of collision. They predicted that these faults would be found on the distal as well on the proximal continental shelf (**fig.3.12b**). They did not predict that pre-thrust normal faults would exert such a basic structural control on the fold and thrust belt geometry above the basal thrust(s).

A flexural bulge mechanism for normal faulting would predict that these structures would be north-south striking (trench parallel) and not east-west striking (trench normal). In the Taconic autochthon of the Mohawk Valley, however, there is evidence for a subsidiary set of east-west (trench normal) normal faults (W.S.F. Kidd, person. commun.,

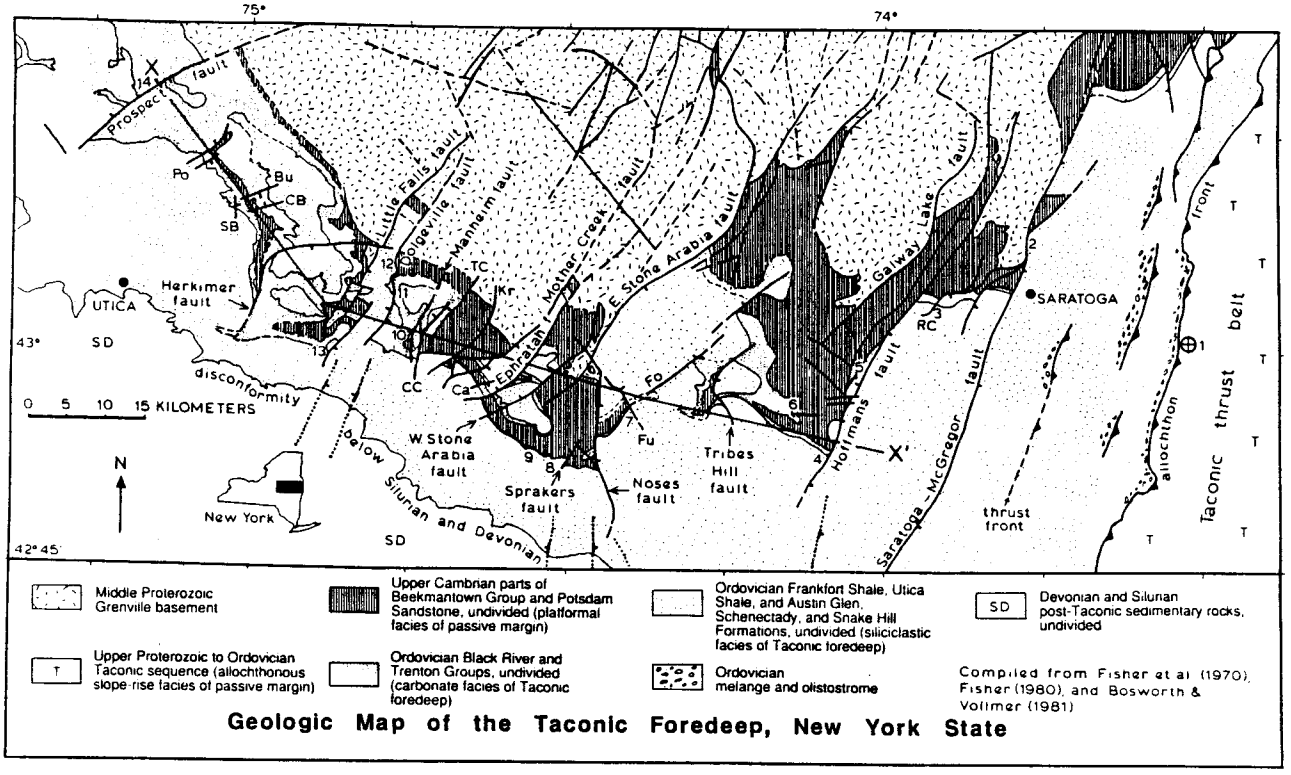

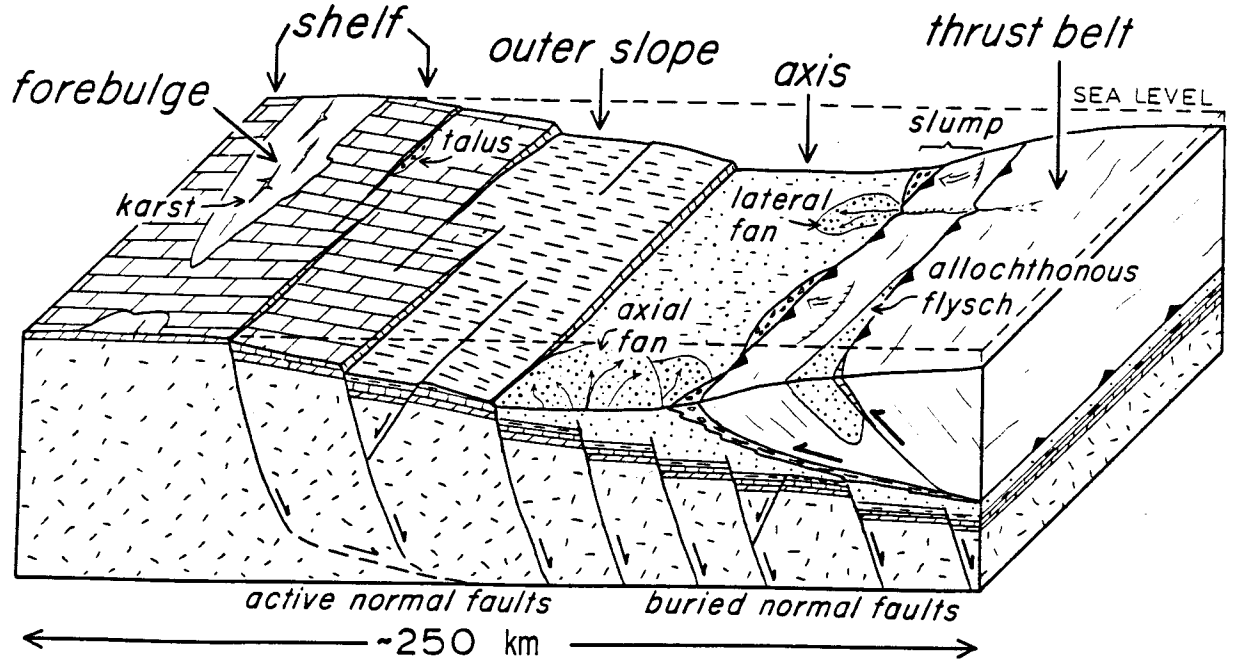

Fig. 3.12) (**a**) (top) Geologic Map of the Taconic Foredeep showing the trace of normal faults across the Mohawk Valley. Note that there are two sets of faults, short faults in a northwest-southeast orientation, and the more dominant northeast-southwest trending faults.
(**b**) (bottom) The model of Bradley and Kidd (1991) for normal faulting along the continental shelf in response to lithospheric flexure.
Both (**a**) and (**b**) are from Bradley and Kidd (1991).

1997; **fig.3.12a**). This study proposes that above the basal thrust (the Champlain Thrust), these normal faults became lateral ramps, and the sites of abrupt changes in stratigraphic levels by thrusts. As the thrusts in the Champlain Thrust System were west vergent (modern geographic coordinates), the major set of trench parallel normal faults were either concealed below the thrusts or, as implied by this study, became ramps in the thrust faults.

East of the Sunset Lake Slice, which is a preserved klippe of tectonically transported continental rise facies material, is another belt of east dipping carbonate rocks. A stratigraphic section representing the very top of the Providence Island formation through the Hortonville shale is preserved. These rocks lithologically correlate to the stratigraphic sections found in the upper shelf sequence (upper Beekmantown - Trenton Age), and were likely deposited on a shelf continuous with the rocks preserved to the west. The following question remains: was there some syn-Hortonville, pre-thrust structure that is responsible for this belt of shales and carbonates having been emplaced this far east of the Champlain Thrust System?.

3.3. A Late Normal Fault and the Slate Belt

3.3.1. The Mettawee River Fault

One of the most important structures for defining the map pattern of the area is the east-side-down normal Mettawee River Fault. This structure juxtaposes a belt of intermixed shales and slates, and overlying thrust slices, against the carbonates in the Champlain Thrust System. Previously this contact was interpreted as a stratigraphically intact contact (**fig.3.3**) (Doll et. al., 1961). There is no locality in this study's map area where the Mettawee River Fault is exposed. It is exposed in the West Haven-Whitehall area (Granducci, 1995) and has been mapped through the Whitehall quadrangle (Fisher, 1984). This structure traces through the entire map area (**fig.3.1, 3.2**) and is inferred to continue

through the Middlebury region (the hinge of the "Middlebury Synclinorium") and to the map area of Hashke (1994) in the Highgate Springs region of northern Vermont.

Near West-Haven, the Mettawee River Fault has a fairly high angle (Granducci, 1995). Near Benson, it seems to follow the topography fairly closely and dips around 50 degrees to the east. It then crosses the Lemon Fair River and maintains the same strike. It likely steepens towards the Whiting area, where it strikes parallel to the sides of the valley.

There is no control for the timing of the Mettawee River Fault other than that it is of a post-thrust age. This is best shown in the region just south of the Orwell township where it cuts the Shoreham Thrust. South of this the Shoreham Thrust reappears. This cutting of thrusts is common southward as well, towards the area mapped by Granducci (1995) where the Mettawee River Fault splits and several other late normal faults appear (**fig.3.10**). One complicated aspect to this normal fault geometry is that there is a lateral ramp, striking northeast - southwest, which is likely of the pre-thrust generation of faults (see **section 3.2.4**). This lateral ramp should not be confused with post-thrust normal faults found at this locality.

3.3.2. The Sunset Lake Slice

The Sunset Lake Slice is a Taconic klippe. It was previously interpreted as a broad synclinal structure (**fig.3.13a**) and part of a suite of nappe structures making up the five Taconic klippe of Zen (1967). I have interpreted the Sunset Lake Slice to be a largely north-south striking structure, bounded to the east by the Taconic Frontal Thrust and bounded to the west by the Sunset Lake Thrust. Within the Sunset Lake Slice is an additional east-west striking thrust slice, here named the *Choate Pond Slice*, consisting largely of Hatch Hill Formation (**fig.3.2**). There may be several other thrusts which this study did not identify. The Sunset Lake Slice has received less attention by other workers than its eastern counterparts such as the Giddings Brook Thrust Slice. In part, this is due to lack of

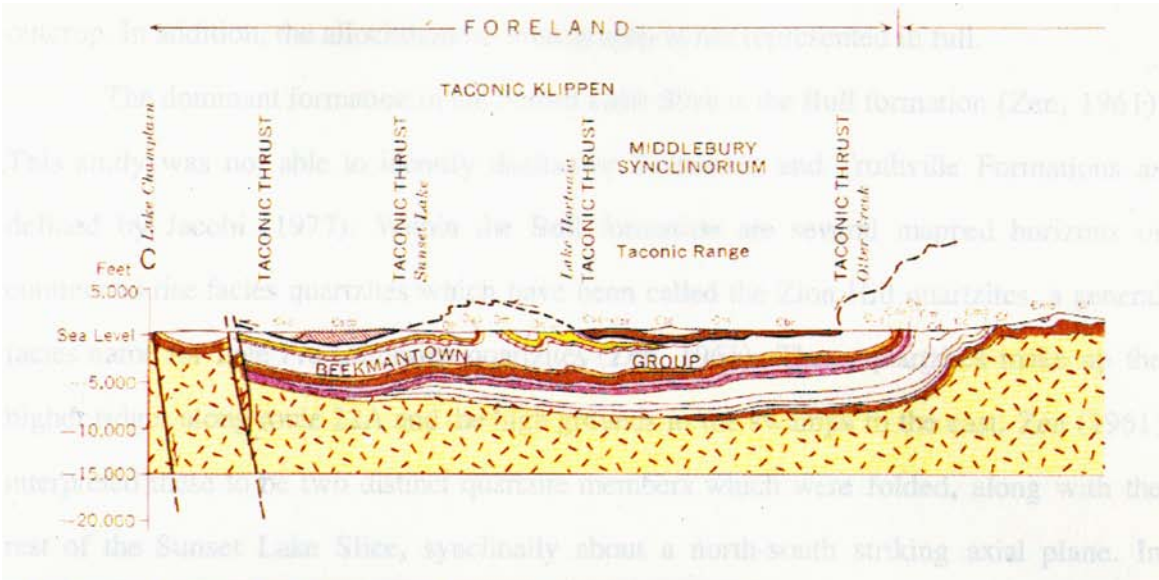

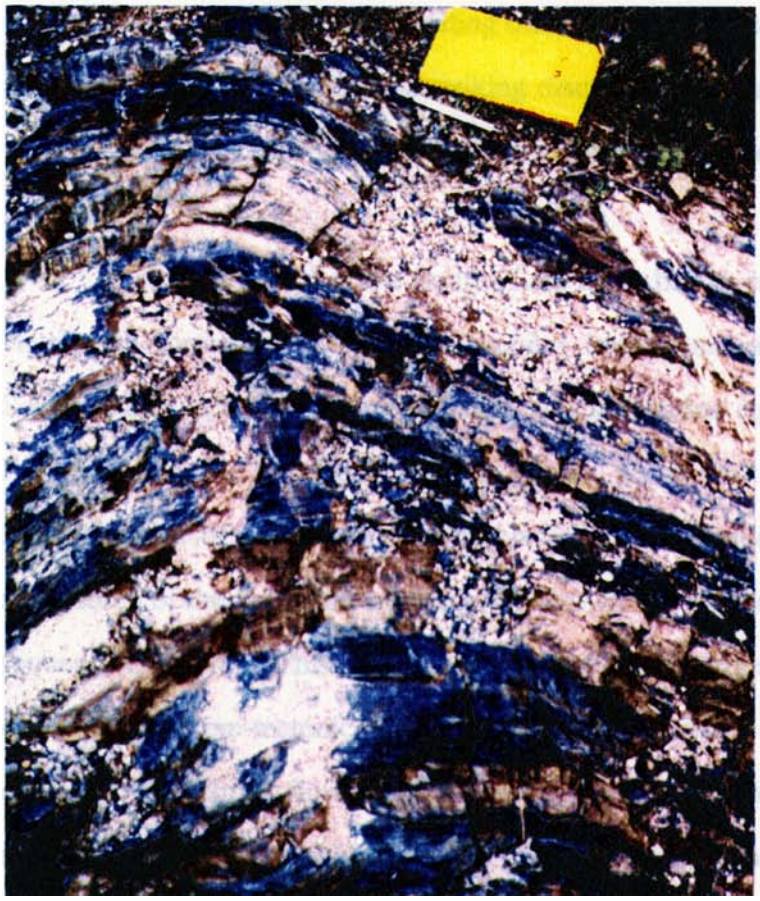

Fig.3.13a) (above) The cross-section from Doll et. al. (1961) presents an interpretation of the Lower Champlain Valley with the Sunset Lake Slice preserved as a synclinally folded nappe within the Middlebury Synclinorium. The interpretation from Doll et.al. (1961) is in contrast to the view presented in this study that the major structures in the region are east dipping thrusts. This includes the Sunset Lake Slice which is a Thrust Slice, but not a nappe structure.

Fig.3.13b) The Hatch Hill formation (found southeast of Orwell) is folded about a north-south striking axial plane. This type of observation supports an interpretation that the Sunset Lake Slice is a folded nappe structure. However, this study suggests that the Hatch Hill belongs to a seperate thrust slice within the surrounding Sunset Lake Slice.

outcrop. In addition, the allochthonous stratigraphy is not represented in full.

The dominant formation in the Sunset Lake Slice is the Bull formation (Zen, 1961). This study was not able to identify distinctive Bomoseen and Truthville Formations as defined by Jacobi (1977). Within the Bull formation are several mapped horizons of continental rise facies quartzites which have been called the Zion Hill quartzites, a general facies name for Late Pre-Cambrian quartzites (Zen, 1961). These quartzites make up the higher ridges along route 22A and the high grounds in the swamps to the east. Zen (1961) interpreted these to be two distinct quartzite members which were folded, along with the rest of the Sunset Lake Slice, synclinally about a north-south striking axial plane. In contrast, based upon observed bedding orientations and outcrop distribution, the quartzites are interpreted to be north-south striking discontinuous lenses in this study. Though they were not mapped as such, it is possible that these are repeated quartzite units across one or more thrusts.

The northern end of the Sunset Lake Slice has an east-west striking thrust slice of Hatch Hill formation of dolomitic arenites interlayered with black shale (**fig.3.13b**). South of this belt is a calcareous shale which is either equivalent to the Brown's Pond Formation or the uppermost section of the Hatch Hill Formation. This uncertainty highlights one of the outstanding problems in the Taconic allochthon. If the calcareous shale south of the dolomitic arenite is the Brown's Pond Formation, then the stratigraphic sequence is inverted. This could have occurred during deposition along the continental rise or during some pre-tectonic "disturbance" (i.e. the Brown's Pond Formation may represent diachronous debris flows surrounding Hatch Hill deposition). Alternatively, the stratigraphic sequence could have been inverted during tectonic transport. The interpretation of the Sunset Lake Slice by Zen (1967) was that it represented a nappe structure. If this is true, then such an inversion of the stratigraphy via thrust related folding might be expected.Either of these hypotheses is not disproved by the mapping of this study.

A hypothesis is preferred in this study wherein the Hatch Hill Thrust Slice is cut by the Sunset Lake Fault and that the Bull formation south of this slice has a north-south strike. This suggests that the Hatch Hill slice is a discrete thrust slice. It may have been detached and transported prior to the Sunset Lake Slice, and amalgamated and deformed within the Sunset Lake Slice during transport along the Sunset Lake Thrust. Thus, the calcareous shale represents either Brown's Pond Formation or upper Hatch Hill Formation depending upon whether the thrust related fold of the slice is a syncline or anticline. Based solely upon conjecture, it is suggested that the unit in question represents upper Hatch Hill Formation and that the overall structure of the Choate Pond Slice is a syncline.

There is a host of outcrop scale structures in the Sunset Lake Slice which are not completely addressed in this study. The Bull formation exhibits at least two cleavages (**fig3.14a**), a crenulation cleavage axial planar to a late generation of folding (**fig.3.15**), extensive transposed layering (indicated by tightly folded quartz veins oriented parallel to layering) and potentially, pre- or syn- tectonic sedimentary structures, some of which may be related to debris flow / slump structures commonly associated with continental rise facies deposition.

The only structure I discuss here is the cleavage axial planar to the late generation folding. In outcrop, on slaty cleavage surfaces, this structure is an apparent north-south trending intersection lineation, much the same as the common crenulation cleavage / slaty cleavage intersection lineation is throughout the Taconics of Vermont. Indeed, this may be the same structure which is discussed at length in **Chapters 4-5** of this thesis. Chan and Crespi (1997) associate this late cleavage with a late thrust located near the Green Mountain Front. Rowley (1983) suggested that this structure may be related to the final emplacement of the Champlain Thrust (proposed by him to be the final deformation episode in the Taconic event). Regardless, if these are the same structure (which is not verified) this implies that there was a deformation event which affected all of the central Vermont Taconic

Figure .3.14a) An outcrop of Bull formation (Taconic Green Slate) from just south of Perch Pond with two sets of cleavage and lenses of quartzite.

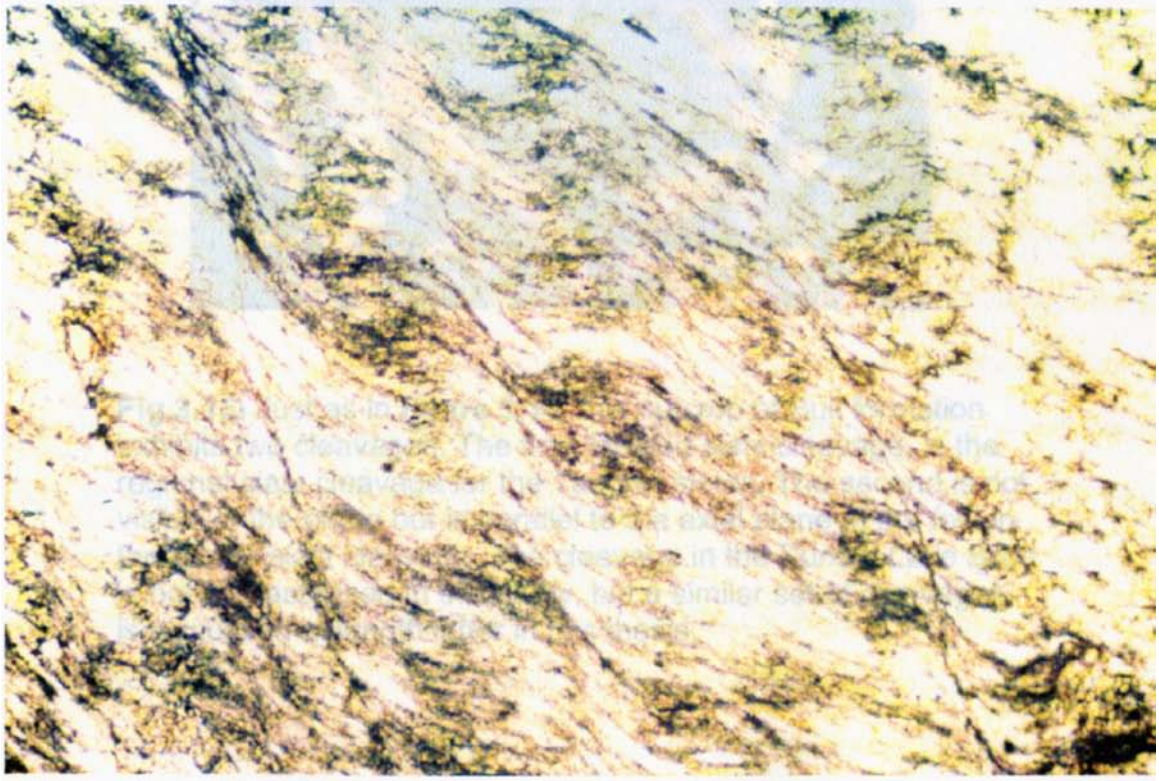

Figure 3.15b) Photomicrograph of the Taconic - wide late crenulation cleavage from route 4, east of route 22A (courtesy of Jean Crespi).

Fig.3.15) Just as in **figure 3.14**, this outcrop of Bull formation exhibits two cleavages. The first, labeled slaty cleavage, is the regional slaty cleavage for the Taconic slates. The second is not visible in the photo but is parallel to the axial plane of the fold in the earlier slaty cleavage. The cleavage in the Sunset Lake Slice is not characterized in this study, but a similar set of cleavages is discussed at length latter in this thesis.

klippe with the same principal directions of finite strain. In other words, in the Sunset Lake Slice there is a D2 folding about a N-S striking axial plane, in the Giddings Brook slice there is a D2 crenulation without large scale folding (**fig.3.14b**) (in addition to larger scale folding) and as one approaches the Green Mountain Front, there is a D2 metamorphic fabric developed, all possibly produced by the same deformation event. This model is contingent upon the assumption that all of the late, north-south trending crenulation cleavages resulted from the same late Taconian deformation.

3.3.3. The Taconic Thrusts: Structural Implications of the Hortonville - Taconic Black - Taconic Melange Lithologies

The Sunset Lake Thrust and the Taconic Frontal Thrust are well defined by the so called Black-Green boundary, where black slates are juxtaposed against green slates. Zen (1961) recognized the Sunset Lake Thrust and later recognized that the Sunset Lake Slice was a discrete thrust slice and not part of the Giddings Brook Slice (Zen, 1967). If the Sunset Lake Slice is a separate slice, than its eastern boundary cannot be the folded (early) Giddings Brook Thrust as mapped by Zen (1961) (roughly equivalent to the Taconic Basal Thrust of Rowley (1983)). The belt of limestones and shales to the east also require a Thrust upon which they were transported. I propose that the western boundary of the Sunset Lake Slice is the Sunset Lake Thrust as previously proposed, but that the eastern boundary is the Taconic Frontal Thrust (1983), an out-of sequence thrust which traces from the south near route 4, and likely continues north into the Shoreham-Whiting area. Furthermore, this thrust transports structurally higher thrusts carrying carbonates and shales, along with the more distal allochthon (i.e. the Taconic Basal Thrust).

Bosworth (1980), Rowley (1983), Bierbrauer (1990), and Kidd (unpublished) have all mapped the Vermont Taconics such that the Taconic Basal Thrust is an early, folded thrust. In addition, the Taconic Frontal Thrust, a late, out of sequence thrust,

extends along the western Taconic margin, associated with a melange zone, the Taconic melange (or the Forbes Hill conglomerate of Zen (1961)). The Taconic melange, as described in **Chapter 2**, is a non-calcareous shale - a highly deformed rock with lenticular cleavage, intense veining, and exotic clasts of flysch, Taconic derived rocks, and rare limestones. It is related to the Taconic flysch in that it is an Ordovician rock with roughly coeval deposition to early stages of thrusting, yet it is a shale facies similar to the Hortonville. Complicating matters in the greater Orwell region is that within the belt of Hortonville shale are lenses of slightly higher grade, multiply deformed slates which are almost certainly the Taconic black slates as discussed by Zen (1961). Melange is associated with these as well. Thus, it is difficult to say from the melange zones alone whether the Taconic Frontal Thrust lies to the east or to the west of the Sunset Lake Slice.

I propose that the Taconic black slate to the west is associated with a separate melange zone. An individual thrust for the transport of this belt of melange has not been identified, though it is possible that the trace of the fault is in the now eroded hanging wall of the Mettawee River Fault. The Taconic Frontal Thrust, on the other hand, is proposed to be the eastern margin of the Sunset Lake slice, and its trace to be defined by the discontinuous belts of Taconic melange found to the north and immediately below the Taconic Frontal Thrust. The deflection in the strikes of both slate- and carbonate - bearing thrusts immediately above the Taconic Frontal Thrust is further evidence for its existence. What is not clear is how the separate small klippen of Bull formation (which may be erosional remnants of the Giddings Brook Slice) found on Scove Hill and just south of Whiting are related to the Taconic Frontal Thrust.

3.4. The Eastern Carbonate Thrust Belt

Zen (1972) interpreted the Sudbury slice to be a discrete thrust slice of par-autochthonous dolostones. The proposal that the Sudbury Slice was a nappe structure with

the west limb overturned was always considered a possible (Zen, 1961) if not likely (Voight, 1965) interpretation. Though no younging indicators were found, evidence from this study suggest that the Sudbury Slice consists of two thrust slices, one of limestone (transported over Hortonville shale) and one of dolostone (transported over limestone) (**fig.3.16**). The thrust belt in the area surrounding the Sudbury Thrust Slice is here named *the Felton Hill Thrust System* (**fig.3.2**), and includes the Sudbury Thrust and overhanging dolostones.

Related to the reinterpretation of the Sudbury Thrust is the reinterpretation of the Sunset Lake Slice described in **section 3.3**. With the recognition that the Sunset Lake Slice is not a synclinally folded thrust nappe there needs to be an explanation for the eastern belt of carbonates. The previous section suggests that a late thrust, the Taconic Frontal Thrust, transported the thrust slices and shale units found to the east of the Sunset Lake Slice. Therefore, as the Sunset Lake Slice is structurally above any carbonate slices, it follows that the Taconic Frontal Thrust must have cut through the Sunset Lake Slice (**fig.3.2; 3.17**) bringing these carbonates to a higher structural level. Therefore, it is possible that the Felton Hill Thrust System was initially part of the Champlain Thrust System. Alternatively, these may have been a part of a separate fault bounded horst on the distal shelf which was transported either later than, or earlier than the Champlain Thrust System. The latter is more likely, especially if one abides by the model that thrusts become younger towards the foreland (Rowley and Kidd, 1981; Stanley and Ratcliffe, 1985). Regardless, this eastern belt of middle Ordovician carbonates and shales may represent a "topographic" high in the Ordovician shelf which was cut by the Taconic Frontal Thrust (**fig.3.17**). This topography would have been controlled by normal faults, activated in response to lithospheric flexure (Bradley and Kidd, 1991) (**fig.3.12**).

The changing thickness of the Hortonville throughout Vermont may be an indicator of several Hortonville basins. There are places where the Hortonville rests unfaulted upon

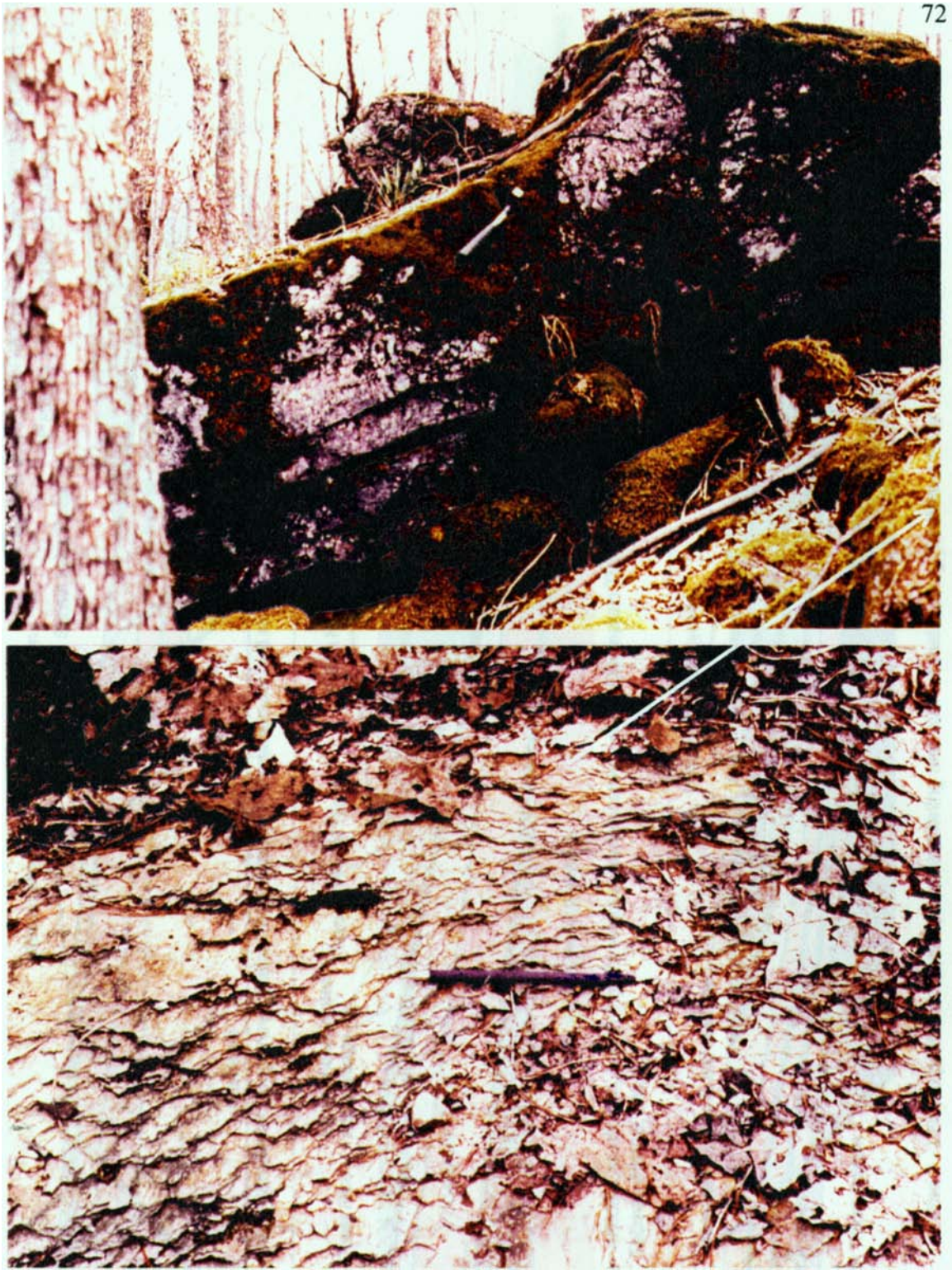

Fig.3.16) The Sudbury Thrust (outcrops found southwest of Whiting) juxtaposes broadly folded dolostones (top) above well cleaved limestones (bottom). The deformation is partial evidence of the thrust contact. This is one of the carbonate bearing thrusts east of (above) the Taconic Frontal Thrust.

Figure 3.17) Schematic of the development of the Felton Hill Thrust System

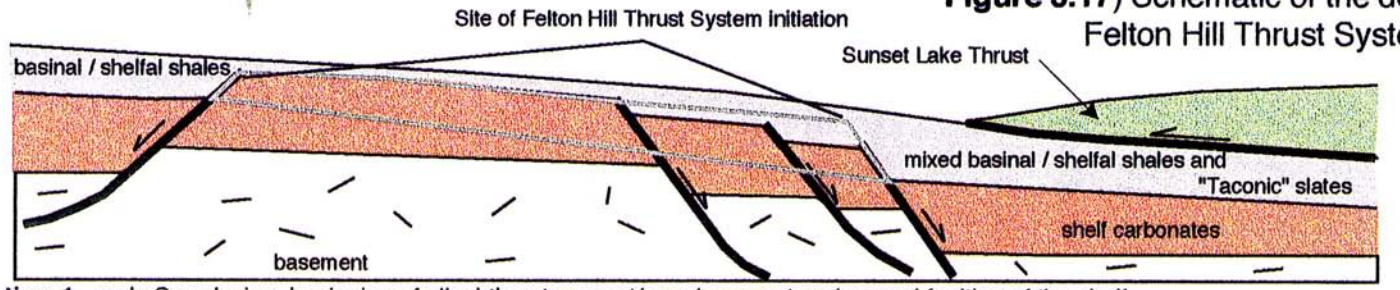

time 1 - early Caradocian, beginning of allochthon transport/ emplacement and normal faulting of the shelf

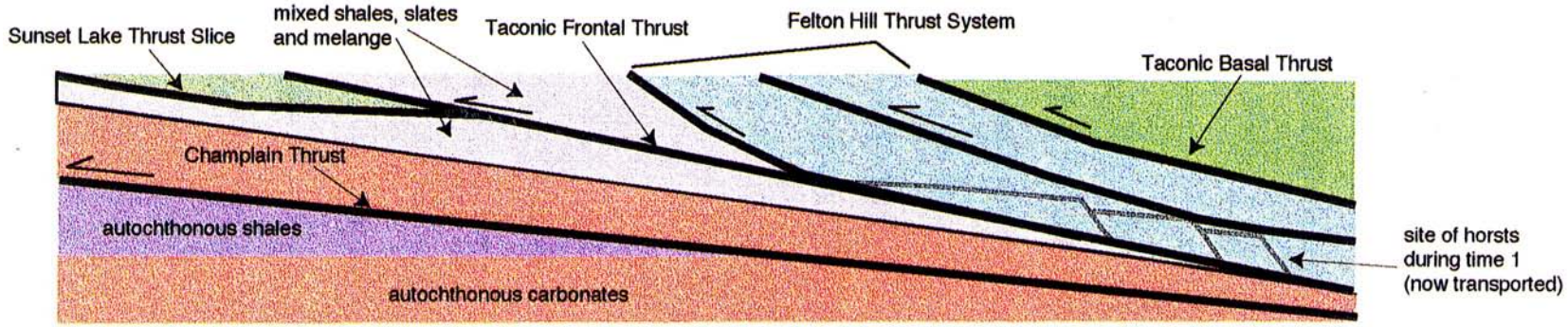

time 2 - middle Caradocian, beginning of transport / emplacement of the Champlain Thrust System, Felton Hill Thrust System, and Taconic Frontal Thrust

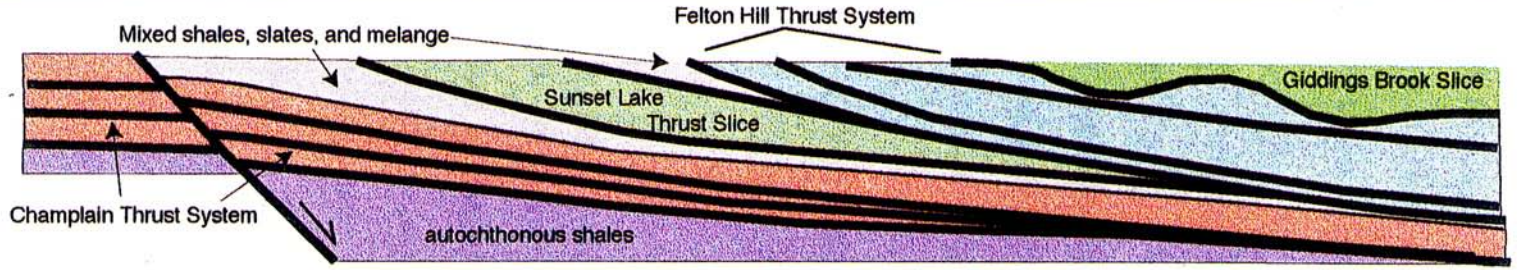

time 3 - Late, to post- Caradocian, final shortening and later normal faulting (Mettawee River Fault)

dolostone units (W.S.F. Kidd, person.commun., 1997). Such information suggests that in some regions the Hortonville was deposited into deep basins, while in others it was thinly deposited before later incorporation into Taconic Thrust sheets. In this map area, the Hortonville not only changes in thickness (admittedly, a large reason for this are changes in strike of the Mettawee River Fault) but also is associated with Taconic slates both below and above the Taconic Frontal Thrust. I therefore suggest that the eastern carbonate bearing thrusts are not part of the Champlain Thrust System, but rather represent imbricates in Taconic style thrust sheets transporting shelf facies rocks. This is consistent with the findings of Zen (1972). These carbonates existed as horsts along the normal faulted continental shelf of the early Caradocian (or more generally, the time of lithospheric flexure and associated block faulting of the continental crust) (Bradley and Kusky, 1985). Due to their structurally higher position, these rocks were incorporated into the Taconic thrusts and not the Champlain Thrust System.

3.5. Summary and Discussion

The Lower Champlain Valley is a structurally complicated region containing the far traveled Champlain (within shelf) thrusts and Taconic (distal shelf and continental rise) thrusts (Rowley, 1982). These thrust "systems" are separated by the post-thrust, east-side down Mettawee River Fault. Prior to this mapping the splays of the Champlain Thrust System had not been recognized south of Orwell. In addition, the Mettawee River Fault was not recognized in this particular region by previous workers. Thus, this study, in conjunction with several others (Washington, 1992; Hermann, 1992; Kidd et.al., 1995; Hashke, 1994; Granducci, 1995; Steinhardt, 1993), reinforces the view that the bedrock geology of the Lower Champlain Valley is one of a thin-skinned fold and thrust belt, with thrust faults being the dominant structure.

Thinning of the Champlain thrust belt occurs from North to South, independent of the changes in orientation of the Mettawee River Fault. This is due to repetition of stratigraphic units across thrust duplexes in the north, and ramping of thrusts up-section towards the south. A set of pre-thrust normal faults are largely responsible for the regional and local thrust geometry. These faults are a set of faults subsidiary to the northeast - southwest trending faults predicted by the flexural bulge model of Bradley and Kidd (1991). Evidence for pre-thrust normal faults is in part from abrupt stratigraphic changes within thrust slices which cannot be explained by syn- or post- thrusting events. To this author's knowledge, there are no previously reported examples of pre-thrust normal faults exerting such basic structural control within thrust belts.

The Sunset Lake Slice is one of the Taconic klippe of Zen (1961,1967). Within the Sunset Lake Slice is a thrust slice, the Choate Pond Slice, of Hatch Hill formation which is proposed to have been transported prior to transport upon the Sunset Lake Thrust. However, there is an alternative explanation that the entire Sunset Lake Slice has been stratigraphically inverted. Such an explanation is consistent with the observation that other Taconic allochthons also have sections of Hatch Hill - level stratigraphic units which have a similar map pattern of an intermittently traceable section of Hatch Hill arenite and adjacent calcareous shale (Bierbrauer, 1991; W.S.F. Kidd, person. commun., 1997). This inversion may be related to a nappe - like emplacement such as proposed by Zen (1961), or it could be related to further shortening associated with the emplacement of the Taconic Frontal Thrust. Alternatively, the inversion of stratigraphic sequence could be related to the depositional, or pre-transport, high energy environment of the continental rise. The evidence from this study favors the initial proposal that the Hatch Hill is preserved in a discrete thrust slice (without extensive stratigraphic inversion) as south of the belt of Hatch Hill formation, internal to the Sunset Lake Slice, is a large north-south striking belt of Bull formation.

The Taconic Frontal Thrust is the eastern boundary of the Sunset Lake Slice and is defined by discontinuous belts of Taconic melange. This thrust transports a large belt of mixed Hortonville and Taconic shale and slate and an eastern thrust slices, collectively termed the Felton Hill Thrust System, of carbonate rocks. The location of the Ordovician shales and carbonates east, and structurally higher than, the Pre- to early Cambrian continental rise facies rocks suggests that the Taconic Frontal Thrust cuts the Sunset Lake Slice in the subsurface. The eastern thrust slices of carbonates and shales were initially preserved as horsts along the normal faulted shelf with faulting being of the same generation as the onset of collision, lithospheric flexure, and deposition of the Hortonville shale and Taconic melange. The faults reponsible for creating the Felton Hill Thrust System had more throw on them than the faults responsible for creating the horsts and grabens along the western shelf (such as the Dougty Hill region). This is consistent with the findings of Bradley and Kusky (1985) that the amount of throw on syn-collisional normal faults decreases towards the foreland. With the initiation of thrust faulting along the upper shelf, and ensuing transport, these topographic (bathymetric - ?) highs (paleo-topography) were clipped off and transported. What is somewhat ambiguous is how the timing of this event (the initiation and transport of the Taconic Frontal Thrust) can post-date the emplacement of the Sunset Lake Slice. Clearly more work is needed before an in depth understanding of the timing and nature of these events is attained. Barring the availability of seismic and borehole data, a good place to begin attaining such an understanding would be by separating the Ordovician shales and slates in the areas adjacent to the allochthon with more detail than was provided by this study (i.e. via an illite crystallinity study).

Chapter 4. Introduction: Are There Post-Tectonic Micas in the Taconic Slates?

4.1. Post-Tectonic Micas and Their Implications

In the Taconic slates at the Cedar Point Quarry, W. Castleton, Vt., there is a late crenulation cleavage which has the morphology of micro-kinks at the microscopic scale. Prof. W.D.Means (person. commun., 1994) observed that some grains of mica (cross-micas) cut across the micro-kink band boundaries without being deflected from the main slaty cleavage orientation. This cross-cutting relationship lead to the suggestion that these grains of mica may represent mineral growth after the formation of the micro-kinks and therefore after the formation of the slaty cleavage. If this is the case, then perhaps many, or all of the micas which define the slaty cleavage are younger than the deformation which produced the slaty cleavage; the micas may be "mimetic" (Knopf and Ingerson, 1938) and post-tectonic. This is in sharp contrast to the usual assumption that micas which are parallel to the slaty cleavage are older than, or the same age as the deformation which produced the slaty cleavage. Though the proposal that there are post-tectonic micas may seem unlikely, it is important to consider because:

a) any isotopic ages of the mineral grains would have to be interpreted as placing a lower limit on ages of deformation, as opposed to placing an upper limit on ages of deformation (i.e. ages would be "youngest" ages as opposed to "oldest" ages) (**fig.4.1**).

b) it is possible that the ages of metamorphic vs. deformation events in a metamorphic belt may be quite far apart, rather than overlapping (as is usually proposed) (**fig.4.2**).

c) there was an influence on (or a mechanism for) the preferred direction of mineral growth by the pre-existing fabric (**fig.4.3**).

There is no new data reported in this section which *directly* addresses these implications (**a - c**). Rather, isotopic dating of rocks, the relationship of mineral growth to slaty cleavage, and the mechanisms of mineral growth are discussed hypothetically to

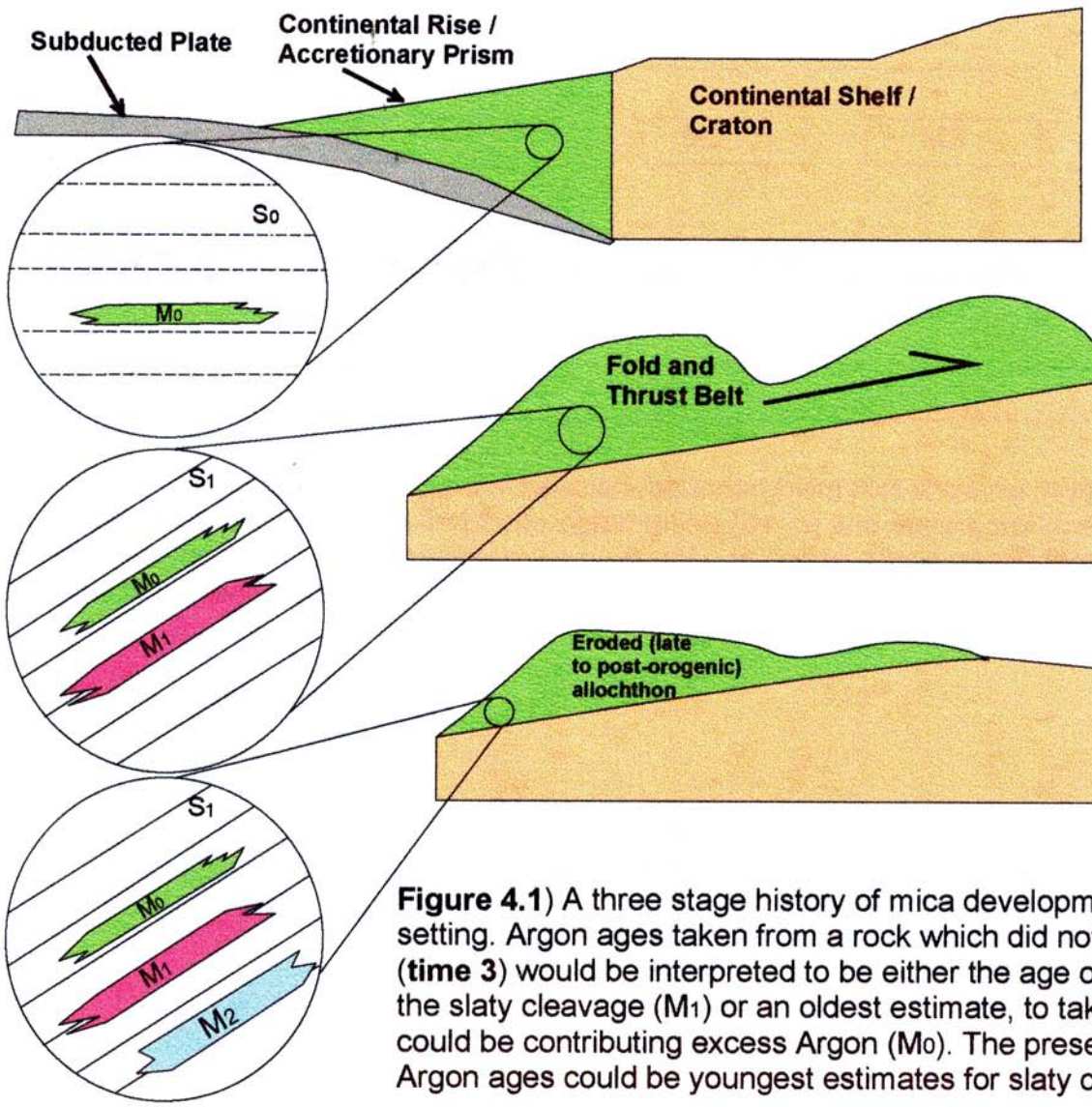

Time 1) Detrital grains and pre-tectonic metamorphic grains (M_0) in a sedimentary fabric (S_0). The tectonic setting is that of an accretionary prism prior to collision.

Time2) With the transport of the accretionary prism along a thrust fault, a slaty cleavage is formed (S_1). The M_0 grains are rotated into the S_1 orientation and new metamorphic grains (M_1) grow into that orientation.

Time 3) At some later time new grains (M_2) grow into the slaty cleavage orientation.

Figure 4.1) A three stage history of mica development in an active continental margin setting. Argon ages taken from a rock which did not have the third stage of mica growth (**time 3**) would be interpreted to be either the age of the deformation which produced the slaty cleavage (M_1) or an oldest estimate, to take into account earlier grains which could be contributing excess Argon (M_0). The presence of M_2 grains would mean that Argon ages could be youngest estimates for slaty cleavage development.

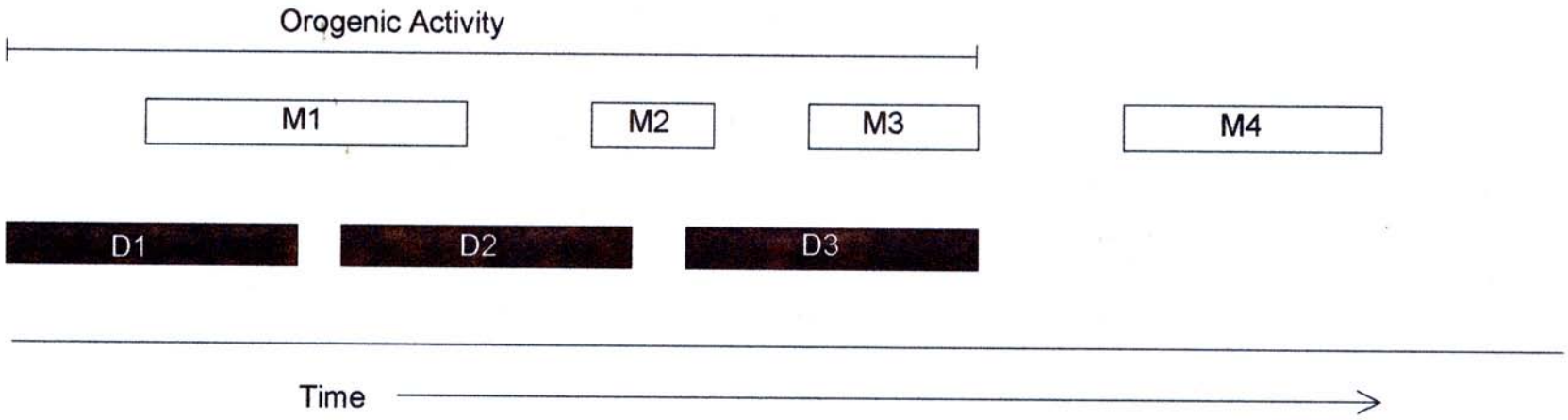

Figure 4.2) A 1-dimensional time-deformation-metamorphism plot showing three discontinuous deformation events and four metamorphic events. The first three deformation (D_{1-3}) and metamorphic events (M_{1-3})span the period of orogenic activity. The last metamorphic event (M_4) is during a time period that is absent of any deformation and after the final stages of orogenisis.

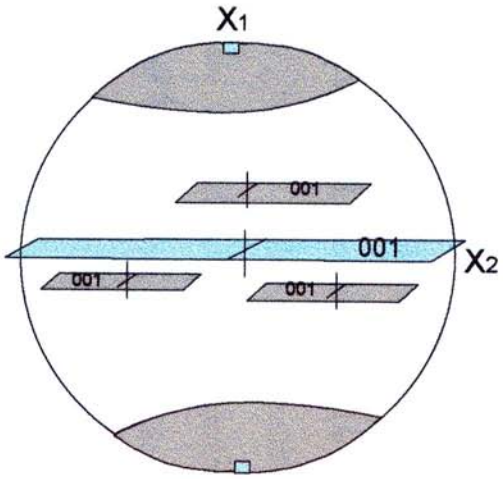

Figure 4.3) M_1 - M_3 minerals with a mica habit (in grey) shown with M_4 minerals with a mica habit (in blue). The view of the grains is oblique to the 001 face and is superposed on a cartoon streographic projection with the poles to 001 plotted. All of the poles to 001 plot within a few degrees of X_1. M_1 - M_3 grains grew during active deformation. What is the mechanism which could cause the post-tectonic M_4 grain to grow into this orientation?

provide a context for the study of slaty cleavage, and the observation of cross-micas.

4.1.1. "Absolute" Dates for Deformation Events

A research tool used by geologists who study mountain belts is to use a parent-daughter isotope system preserved in a given mineral grain to attain an "absolute", isotopic, numerical age for that mineral grain. Technology has become advanced to the point where the $^{40}Ar/^{39}Ar$ system in fine grained, clay mineral rich samples can be measured with certainty (Dong et. al., 1995). Interpreting any ages attained, however, remains a challenge.

The earliest isotopic dates for the Taconic Range came from low grade, fine grained phyllitic rocks (Harper, 1968), using the K-Ar system on whole rock samples. These ages, though acquired using now out-of-date technology and decay constraints, correlate to other isotopic ages for the Caradocian (460 - 445 Ma.), the graptolite - defined time of Taconic collision (broadly speaking). The Argon ages would be interpreted to represent an oldest estimate for the main phase of Taconic deformation, to take into account any parent radioactive K that was not completely degassed during the associated prograde metamorphic event (e.g., if there was a contribution of Argon from a detrital mica component). Alternatively, the ages would be interpreted to represent crystallization ages of the micas in the slate and, indirectly, the age of the main phase of Taconic deformation. However, the ages could represent cooling ages, the time at which any micas in the slate cooled below the closure temperature for the K-Ar system. Cooling ages would be interpreted to be slightly younger than the main phase of deformation (after prograde metamorphism). This latter interpretation for Argon ages acquired from Taconic slates is supported by the peak temperatures for Taconic metamorphism, inferred from the Conodont Alteration Index obtained from rocks nearby (Harris et. al., 1978).

All of the above discussed interpretations of the geologic history of the Taconic slates, and the relative timing of Argon entrapment, have the same result: an isotopic age from cleaved slates in the Taconics, or any similar mountain belt in the world, would classically be interpreted to represent an age within the broadest limits of the timing of orogenic activity (**fig. 4.1, 4.2**) (barring information which suggested otherwise). If there was "wide-spread" mica growth event after the development of slaty cleavage, either due to a re-heating event, or in the absence of high temperatures, the resulting interpretation of the age is the same; the ages attained from the Taconic slates would be youngest possible ages for deformation, or greatly underestimate deformation.

A possible example of late mineral growth providing ages which underestimate the age of deformation involves the Martinsburg slate, at the heart of the flysch terrain preserved at the Lehigh Gap, Pennsylvania. The age of the deformation which produced the slaty cleavage in the Martinsburg is historically controversial (Hess, 1955; Drake et. al., 1960; Epstein and Epstein, 1969). The deformation could have been due to the Alleghenian event, the last collisional event to affect the eastern margin of Laurentia, or the Taconic event. Recently attained Argon ages of micas defining the slaty cleavage are of Alleghenian age (Wintsch and Kunk, 1992). However, there may be a post-deformation generation of micas in the Martinsburg which are yielding Argon ages that underestimate the age of slaty cleavage development (J. Gilotti, person. commun. to W.D. Means, 1995). If this is the case, then the age of slaty cleavage formation in the Martinsburg could be Taconian though Argon ages of the micas defining the slaty cleavage yield an Alleghenian age.

4.1.2. Timing of Metamorphic vs. Deformation Events

Metamorphic events, in the narrow sense, are those events which cause a change in the mineral composition of the rock. The tectonic events which can cause metamorphism, such as the Taconic orogeny, also cause a great deal of deformation. One of the records of

deformation is the fabric developed during the tectonic event. Yet, fabric can also be the expression of metamorphic event. This dichotomy is the center of one of the classic geologic controversies.

Fabric refers to any repeated geometric element in a rock such as a foliation. A foliation, such as slaty cleavage, is a family of planes which are prevalent through a rock. Slaty cleavage is defined by the alignment of elongate minerals within the rock. In his paper, *On the Development of Slaty Cleavage*, Sorby (1856) argued that in a given rock with randomly distributed and elongate grains, after flattening of the rock the vast majority of the grains would be aligned within 20 degrees of the slaty cleavage direction. Prior to Sorby's work the proposed mechanism for slaty cleavage development was that of mineral growth of grains into the slaty cleavage orientation (Sedgewick, 1835) (**fig.4.4**).

Considering the dominant mechanism for slaty cleavage development was a problem addressed from the 1960's on, primarily concerning the previously mentioned Martinsburg slates at the Delaware Water Gap, Pa. (Maxwell, 1962; Epstein and Epstein, 1969; Holleywell and Tullis, 1974; Beutner, 1978). In general, slaty cleavage is found to roughly span the Y and X axes of the finite strain ellipsoid as determined from strain indicators such as reduction spots (Wood, 1974; Williams (1976) discusses an opposing view) (**fig.4.4**). The X-Y plane is thought to represent the plane normal to the maximum shortening directions. The problem exists that if grains grew via a metamorphic process into the cleavage orientation, then how was there such a consistent relationship to axes determined by a deformation process such as flattening? How are stress, strain and mineral growth related?

In 1978, Knipe and White at the University of Leeds began to publish detailed transmission electron microscopy (T.E.M.) images of slates at the sub-micron scale (White and Knipe, 1978; Knipe, 1981). Recrystallized and neocrystallized grains were interpreted to have fewer dislocations and sub-grain boundaries than rotated grains of an earlier

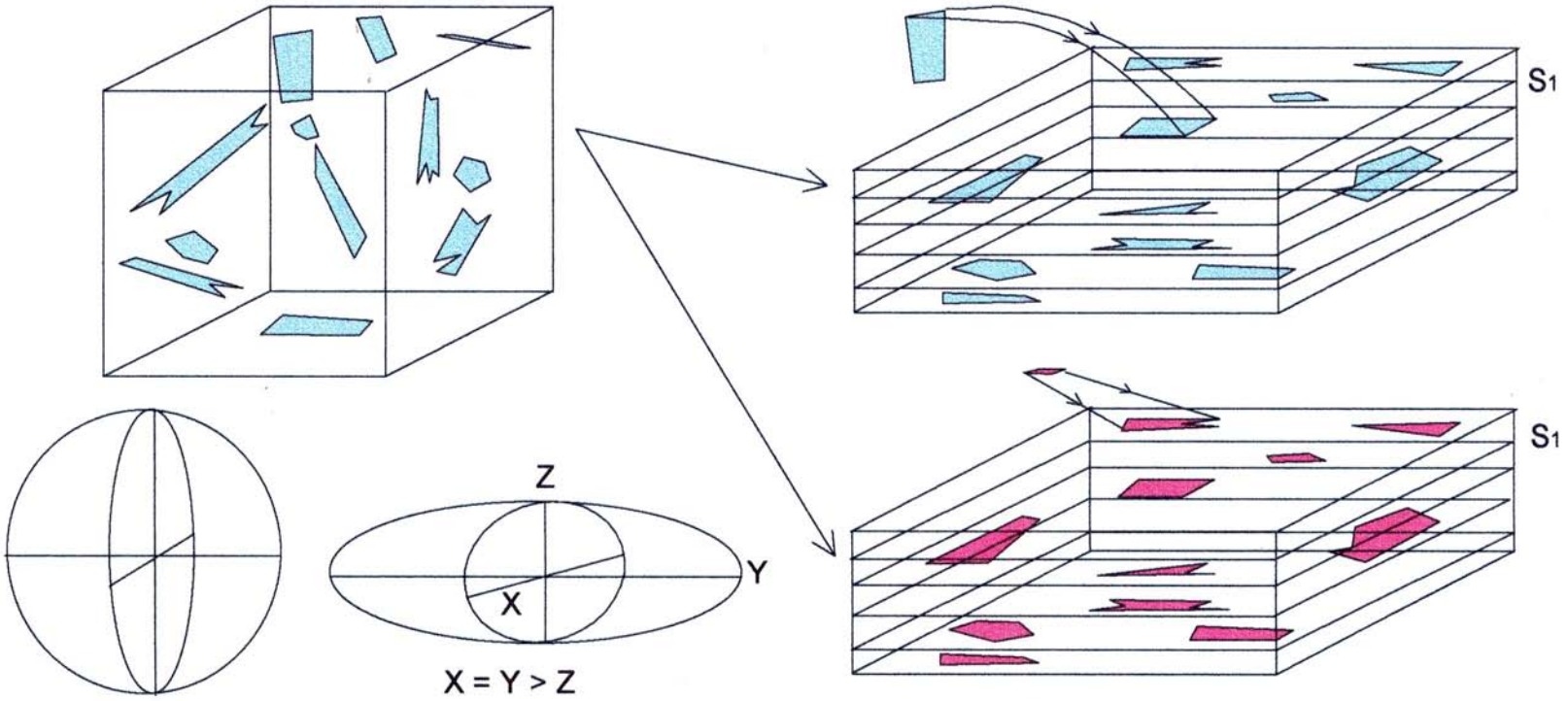

Figure 4.4) During slaty cleavage formation, do mineral grains become aligned via rotation (top right) (Sorby, 1854) or growth (bottom right) (Sedgewick, 1835)?
This figure implies that slaty cleavage develops normal to the direction of maximum shortening, However, the questions remain:
Why would minerals grow into the slaty cleavage orientation, an orientation seemingly defined by strain?
What is the relationship between *active* deformation processes and mineral growth?

generation of growth (i.e. detrital grains). The outcome of their work was the revelation that slates had a group of phyllosilicates which grew into a slaty cleavage orientation, and a group of phyllosilicates which rotated into that orientation. Beyond this, there is still little understanding of how interdependent, or independent, mineral growth ("chemical processes") and strain ("physical processes") are during slaty cleavage development.

The study of Knipe and White (White and Knipe, 1978; Knipe, 1981) in conjunction with other studies (e.g. Holleywell and Tullis, 1976; Ishi, 1988; Ho et. al., 1995) show that, in the presence of active deformation (i.e. folding), an assortment of intergranular and intragranular processes occur at different stages of the deformation / metamorphic history to aid in the development of slaty cleavage. Rotation of grains occurs to satisfy the grain-scale geometric requirements of the strain the rock undergoes during deformation. Meanwhile, dissolution and reprecipitation occur as transport mechanisms. Nucleation and growth of minerals occur to form new minerals. Processes such as recovery and recrystallization occur to change pre-existing minerals into new minerals which are free of internal strain and potentially are of a different phase. These processes act in response to energy requirements internal to the system. An example of this would be the "need" of a mineral grain to decrease the amount of lattice dislocations and thereby reduce strain energy. Another example would be the "need" of a solution to precipitate new mineral material, which then grows into a single mineral grain to meet surface (and other general thermodynamic) energy requirements of the system.

It is obvious why active deformation could produce rotation of grains during slaty cleavage formation. It is much more mysterious as to why active deformation would control directions of mineral growth. Furthermore, if active deformation does not produce mineral growth, how might it contribute to it? If it could be verified that there was post-tectonic growth in a low grade slate, where phyllosilicate grains grew into the slaty cleavage orientation after deformation had ceased, than there would be a perfect example of

mineral growth via a mechanism that was completely independent of active deformation (**fig4.1 - 4.4**). This could then serve as a natural example for future experimental, theoretical, and natural investigations.

4.4. Fabric Control on Mineral Growth

If there are mimetic, post-tectonic micas in the Cedar Point Slates, then there must have been some process aiding mineral growth which was dependent on the fabric of the rock. Any mineral growth controlling / contributing process could have been dependent on the foliation orientation for the orientation of the concurrent growth. Many of these reasons have likely never been explored by previous workers. Furthermore, there may be some previously unrecognized growth process which is dependent upon a pre-existing foliation.

4.2. Cross-Micas at the Cedar Point Quarry

4.2.1. Regional Setting and Terminology

The Cedar Point Quarry sits on the west side of Lake Bomoseen, W. Castleton, Vt., and is one of the classic localities within the fold and thrust belt of the Taconic allochthon. It was first studied by T.N. Dale (1899) who was also, incidentally, the first to study the Lehigh Gap outcrop in Pennsylvania (Dale et. al., 1914). The Cedar Point Quarry provided roofing slates for the surrounding area in the late 19th and early 20th century. Though the slate has a well defined cleavage, a crenulation cleavage and a lineation on slaty cleavage surfaces decreased the economic value of the slate. For this reason, the quarry closed in the first half of this century.

The quarry yields excellent exposure of a recumbent syncline. The slaty cleavage is axial planar to the fold. The crenulation cleavage is at high angles to the slaty cleavage and has the morphology of micro-kinks at the microscopic scale. The observation of importance

is that some of the micas which define the slaty cleavage cross-cut the micro-kink band boundaries without leaving the main foliation orientation (**fig. 4.5**).

Initially these micas were referred to as "transverse micas" as they lie transverse to the micro-kink band boundaries without being deformed. Later, they were termed "cross-micas" to include them with a general type of mica with 001 plane normal to the surface within which they lie (Turner and Weiss, 1963). While the cross-micas in this study are not strictly speaking the classic cross-micas, the term is applicable in that the cross-cutting portion of the micas of this study have 001 planes at a high angle to the preferred orientation of the micas within micro-kinks.

The interpretation of the observation at Cedar Point is that cross-micas cross-cut a structure produced by a late, Taconic-wide deformation event. This structure is discussed at some length in the context of the regional geology of the Taconics in **chapter 3** and again in **Chapter 5**. Cross-micas are classic evidence for mica growth which post-dates the surrounding deformation / metamorphism produced fabric (Turner and Weiss, 1963). In this case, the mica growth post-dates the latest deformation and potentially post-dates the entire phase of Taconic deformation. In either case, the micas post-date the deformation which produced the slaty cleavage.

There are several alternative interpretations of the Cedar Point cross-micas all of which are mutually exclusive of the above proposed interpretation but none of which are mutually exclusive of the main hypothesis of mimetic, post-tectonic micas. These are:

a) The interpretation of a cross cutting relationship of the cross-micas and the micro-kink band boundaries is based upon idealized micro-kink and foliation geometries. Perhaps the cross-cutting relationship is an "artifact of view". Potential reasons for this could be irregular micro-kink band boundaries or changes in the amount of rotation to have occurred along a particular micro-kink.

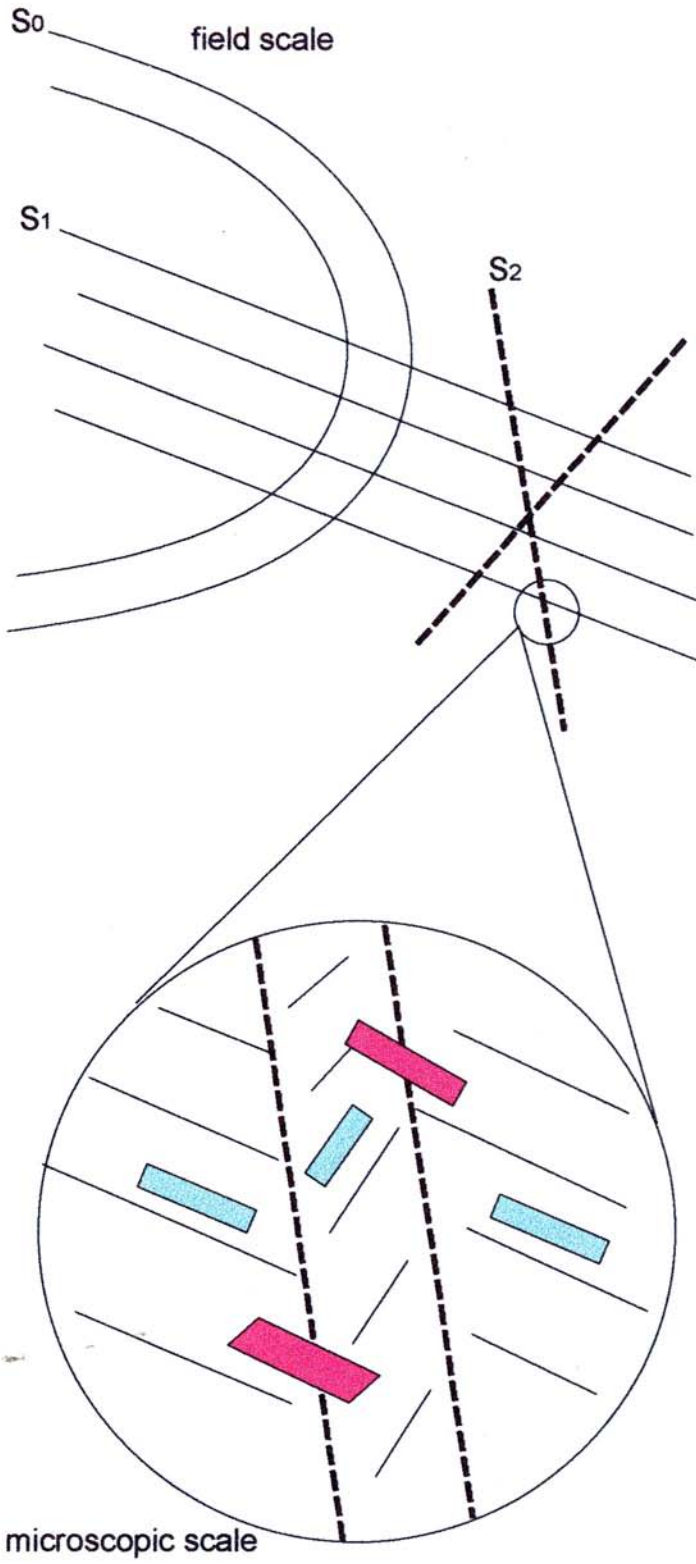

Figure 4.5) Cartoon of the observation of cross-micas at the Cedar Point Quarry. The Cedar Point Quarry yields exposure of a fold in the bedding (S_0) of the Taconic slates. A slaty cleavage (S_1) is axial planar to the fold. At a high angle to the axial planar cleavage is a crenulation cleavage (S_2). At the microscopic scale (bottom) this crenulation has the morphology of micro-kink bands (generally of the reverse type following the classification scheme of Dewey (1965)) within which grains are rotated from the slaty cleavage orientation. Some grains (in red) are observed to cross the micro-kink band boundaries without leaving the main slaty cleavage orientation. This cross-cutting relationship suggests that the cross-micas grew at some later time than the deformation which produced the micro-kinks. If these grains grew later than the micro-kink producing deformation event, then perhaps other (in blue), or even all (lines) of the grains in the slate grew later than this deformation event.

b) The cross-micas were oblique to the slaty cleavage prior to the deformation which produced the micro-kinks. With the rotation of grains within the micro-kink, these grains were rotated into the slaty cleavage orientation thereby producing the cross-cutting relationship.

c) There was late growth, but the growth was localized along the micro-kink band boundary. This could be referred to as the "localized growth hypothesis" as opposed to the "widespread growth hypothesis" in which most, or all of the micas in the slaty cleavage orientation post-date the slaty cleavage producing deformation (**fig.4.6**).

Situation (**a**) can be shown to be right or wrong via detailed petrographic work. It is an interesting problem that the technique of analysis can be integral to the interpretation supplied for the observation. Situation (**a**) is discussed again both in the presentation of petrographic work and general discussions.

Situation (**b**) is perhaps the most difficult to verify. If the cross-micas result from the same rotation as the rotated micas, then there will be no discernible difference between the micas in the kinked orientation, the slaty cleavage orientation and the cross-mica orientation. This is because their present-day geometry resulted from the same deformation and growth history. However, if there was a widespread growth event, minerals in all three orientations may be the result of post-tectonic growth and the cross-micas represent grains which, for some reason, grew in an oblique orientation to the others. Thus, a survey of the mineralogy of the slate would yield identical results for both situation (**b**) and the widespread growth hypothesis.

Situation (**c**) is verifiable. If the cross-micas represent localized growth along the micro-kink band boundaries, then there should be a discernible chemical difference between the two sides of the micro-kink band boundaries.

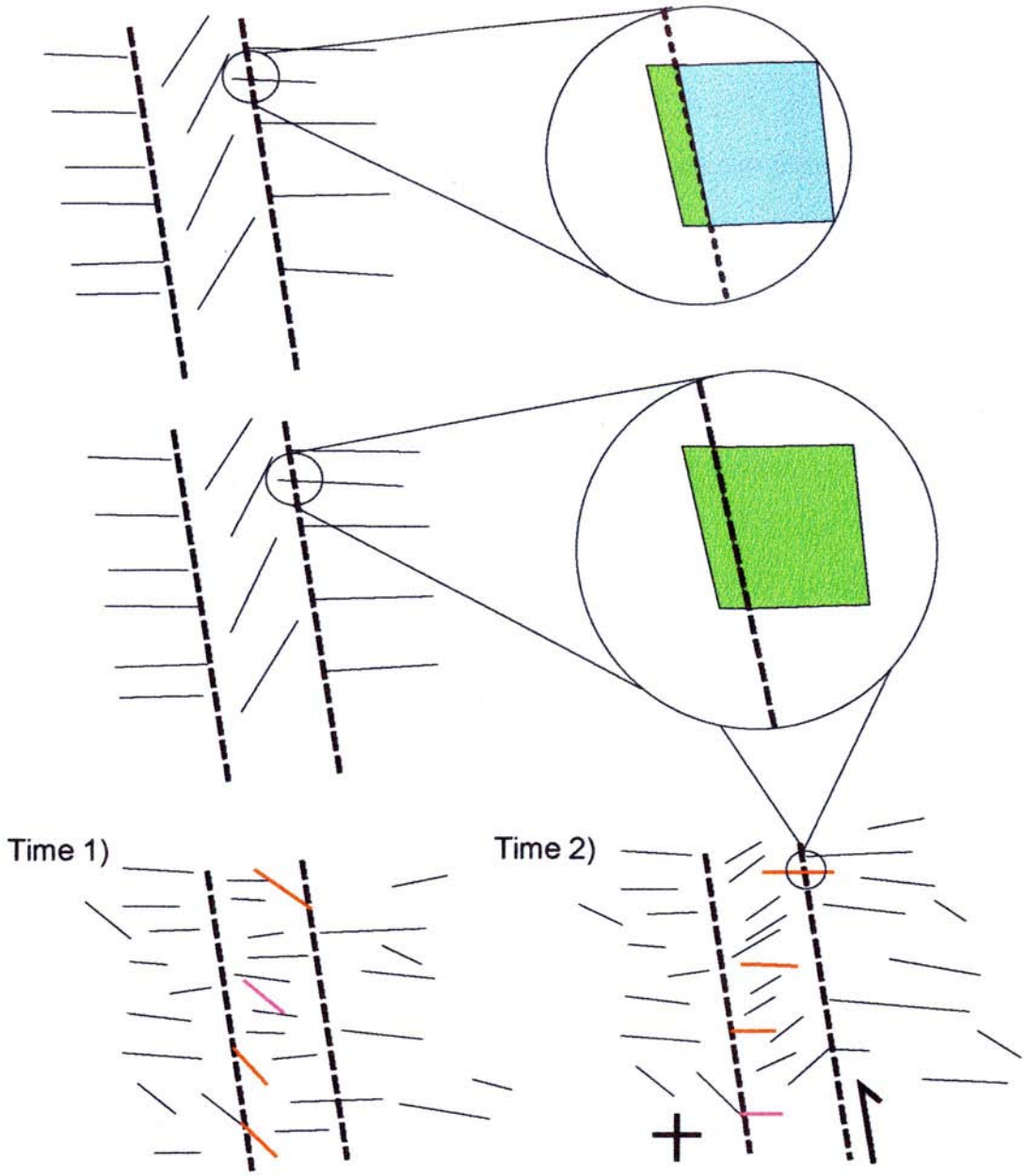

Figure 4.6) The localized growth hypothesis (top) is an alternate to the wide-spread growth hypothesis (middle). If the cross-mica has a discernable difference (optically or chemically) between one side of the micro-kink band boundary and the other (top), then the observation of cross-micas does not support the widespread growth hypothesis. If the two sides are the same, then the hypothesis of a widespread late growth event remains open for further study. However, the cross-micas predicted by the widespread growth hypothesis would be identical to those produced via the two stage deformation history presented in the lower illustration. In this situation, the micas which were initially at a high angle to the slaty cleavage were rotated into the slaty cleavage orientation by the same deformation which produced the micro-kinks, and thus are idential on both sides of the micro-kink band boundary.

4.2.2. A Strategy for Investigation

To investigate properly the hypothesis that there are post-tectonic micas defining the slaty cleavage in the Cedar Point slates would likely involve an intensive survey of the entire mica population in the slate. With this research beginning without a previously existing database, this is beyond the scope of this worker's efforts. Perhaps a future study can document the Cedar Point slates with a variety of techniques such as whole-rock X-ray diffraction, electron microprobe data, S.E.M. back-scatter imagery, and even T.E.M. data. This study provides field scale observations and maps of Cedar Point, petrographic analyses from an optical microscope, and some reconnaissance electron microprobe data and backscatter Scanning Electron Microscope (S.E.M.) imagery.

The Cedar Point cross-micas are the best evidence for post-tectonic growth in the Taconic slates. As the micro-kinks are identifiable on a variety of scales, this study will provide an analysis of the micro-kinks and the cross-micas. If the cross-micas represent an artifact of view or localized growth, this will become apparent. However, to confirm the post-tectonic origin of the cross-micas cannot be done with the techniques used by this study as other origins for the cross-micas may be possible.

It should be stated (and is previously implied) that even though the observation of the cross-micas inspired the hypothesis of a widespread post-tectonic growth event, it is not predicted by it. If the cross-micas grew as a result of a foliation controlled growth event, then why didn't they follow the preferred orientation within the micro-kinks or overprint the micro-kinks altogether?

Chapter 5. Field, Petrographic, and Geochemical Observations of the Taconic Slates at the Cedar Point Quarry, W. Castleton, Vermont

5.1. Field Observations

The problem described in **Chapter 4** concerns the relationships of several geologic structures. This section describes the geologic context of these structures at the Cedar Point Quarry. It then presents the results from detailed structural mapping of the Cedar Point Quarry. Lastly, it discusses the implications of the field scale observations.

5.1.1. General information on the regional geology

The slate at the Cedar Point Quarry was given a stratigraphic formation name "Cambrian Roofing Slate" by T.N. Dale (1899) who also defined an extensive stratigraphy using letter and number codes to designate particular stratigraphic horizons. Zen (1961) mapped the Cedar Point slates as the Mettawee slate formation. Later, Jacobi and Rowley (Rowley et. al., 1979; Kidd et. al., 1984) recognized that the Mettawee slate was a formation name applied to all purple and green slates in the Vermont Taconic allochthon, regardless of stratigraphic level. For this reason Jacobi (1977) proposed the formation name "Middle Granville" for the slate formation exposed at the Cedar Point Quarry. The heterogeneous assemblage of quartz arenites and calcareous shales and slates which make up the eastern escarpment of the Cedar Point Quarry was given the formation name the "Brown's Pond" (Rowley et. al., 1979; Kidd et. al., 1984). This nomenclature differentiates between the two lithologies at Cedar Point and thus will be used in this locality study. The name Mettawee Slate is still used by other workers to describe the slates at Cedar Point (e.g. Goldstein, 1996).

The rocks at Cedar Point are of Early Cambrian Age and were deposited in a continental rise environment off the Laurentian Passive Margin (Bird and Dewey, 1970; Rowley and Kidd, 1981). With the Taconic collisional event in the middle Ordovician, the

suite of continental shelf and rise facies rocks were emplaced on the continent as a series of thrust slices (Zen, 1961, 1967; Rowley and Kidd, 1981; Stanley and Ratcliffe, 1985). The westernmost Taconic thrust slice (as opposed to Champlain thrust slice), the Sunset Lake Slice, is preserved to the northwest of the Cedar Point Quarry. The rocks at the Cedar Point Quarry belong to the Giddings Brook Thrust Slice (above the Taconic Basal Thrust). To the east is the Bird Mountain Thrust Slice which makes up the highest present day topography of the preserved allochthons. The Mud Brook Thrust, a thrust which runs through Glen Lake - within the Giddings Brook Slice (**fig.5.1**), and the Taconic Frontal Thrust are later thrusts than the other Taconic thrusts (Rowley, 1983). The Taconic Frontal Thrust juxtaposes the major Taconic thrust slices, along with Ordovician shelf facies carbonates, shale, and flysch against the Sunset Lake Slice (**fig.5.1, 5.2**; **Plate II**; **Chapter 3**).

The structure exposed at the quarry, the Cedar Mountain Syncline, is the easternmost fold above the Mud Brook Thrust. There is another significant thrust fault (potentially of the same age as the Taconic Frontal Thrust) which runs along the east side of Lake Bomoseen (W.S.F. Kidd, person. commun., 1997) (**fig.5.1, 5.2**). Across this thrust, to the northeast, is a fold in the axial planes of folds which are presumably of the same generation as the Cedar Mountain Syncline. The axial plane of this later generation of folds is about a roughly north-south striking axial plane (Aparisi, 1984; Goldstein, person. commun., 1995). Thus, there are at least two generations of regional faulting and folding apparent at the map scale.

5.1.2. Overview of the Structures at Cedar Point

The Cedar Point Quarry yields excellent exposure of the Cedar Mountain Syncline (**fig.5.3**). Bright purple and green horizons in the otherwise dark purple rock are due to the change between an oxidized and reduced state of the iron in iron-rich phases within the

Figure 5.1) A generalized structural map from Rowley (1983). The Taconic Frontal Thrust (T.F.T) is the basal thrust and transports the Giddings Brook Thrust Slice. The Bird Mountain Thrust Slice is several kilometers to the east. The Cedar Mountain Syncline is the easternmost fold above the Mud Brook Thrust. There is likely a thrust on the east side of L. Bomoseen. To the northeast of L. Bomoseen the generation of folds shown here are themselves folded by a later deformation event.

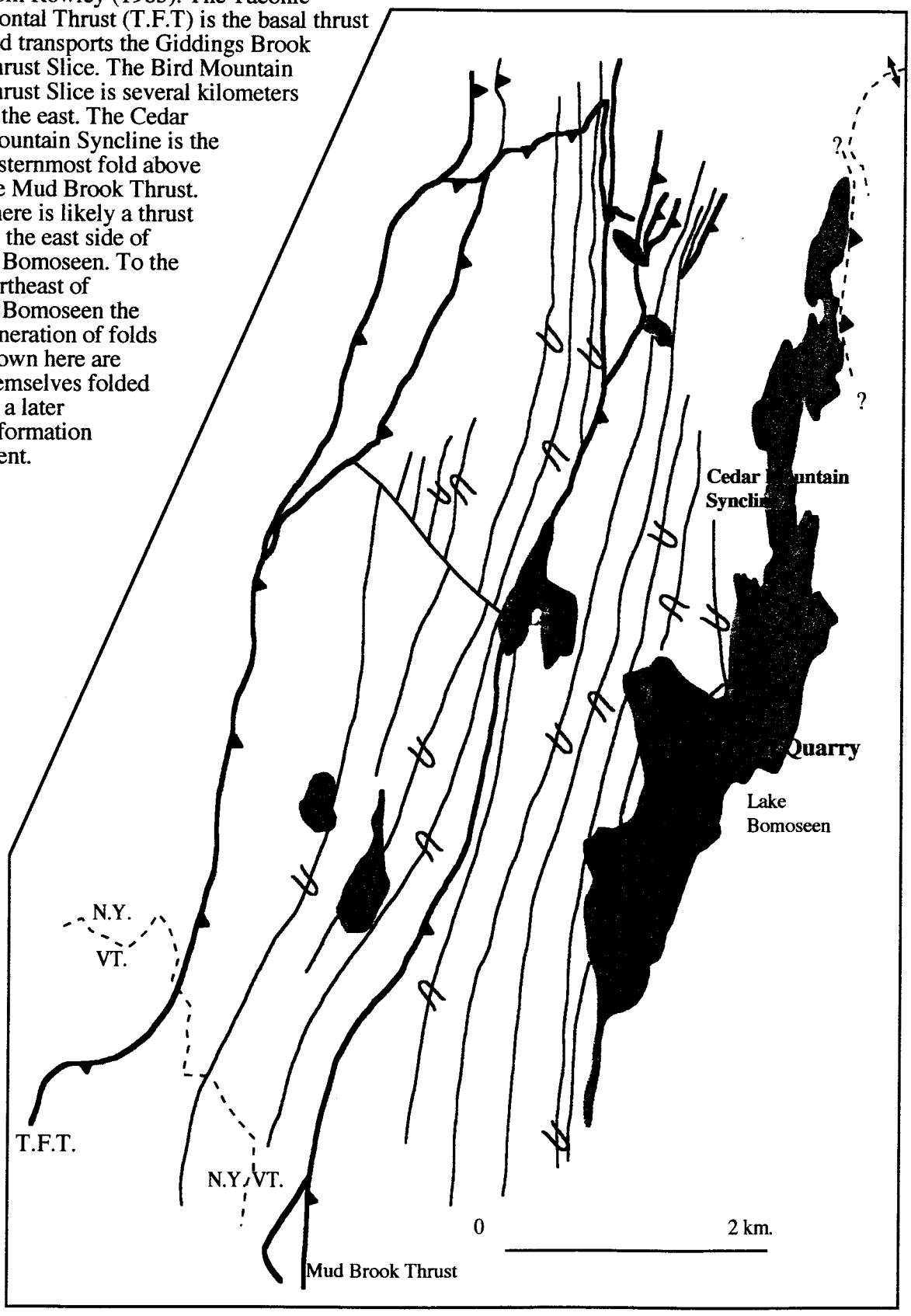

Figure 5.2) Cross-section of the L. Bomoseen area from Rowley (1983). The Cedar Point Quarry (C.P.Q.) is to the far right. Note how the Taconic Frontal Thrust (T.F.T.) is the latest thrust through the area.

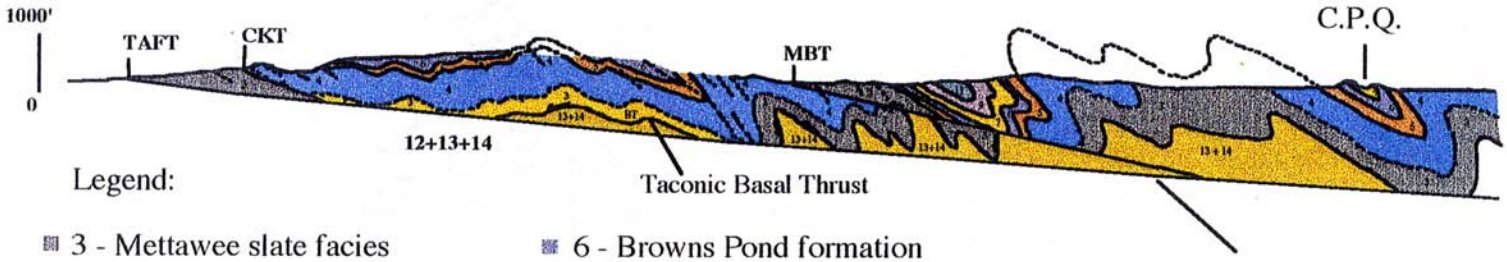

Legend:

- 3 - Mettawee slate facies
- 4 - Bomoseen member
- 5 - Truthville formation
- 6 - Browns Pond formation
- 7 - Mid - Granville formation
- 9 - Hatch Hill formation
- 11 - combined Poultney and Hatch Hill formations
- 13 + 14 - Forbes Hill and Hortonville slates and melange

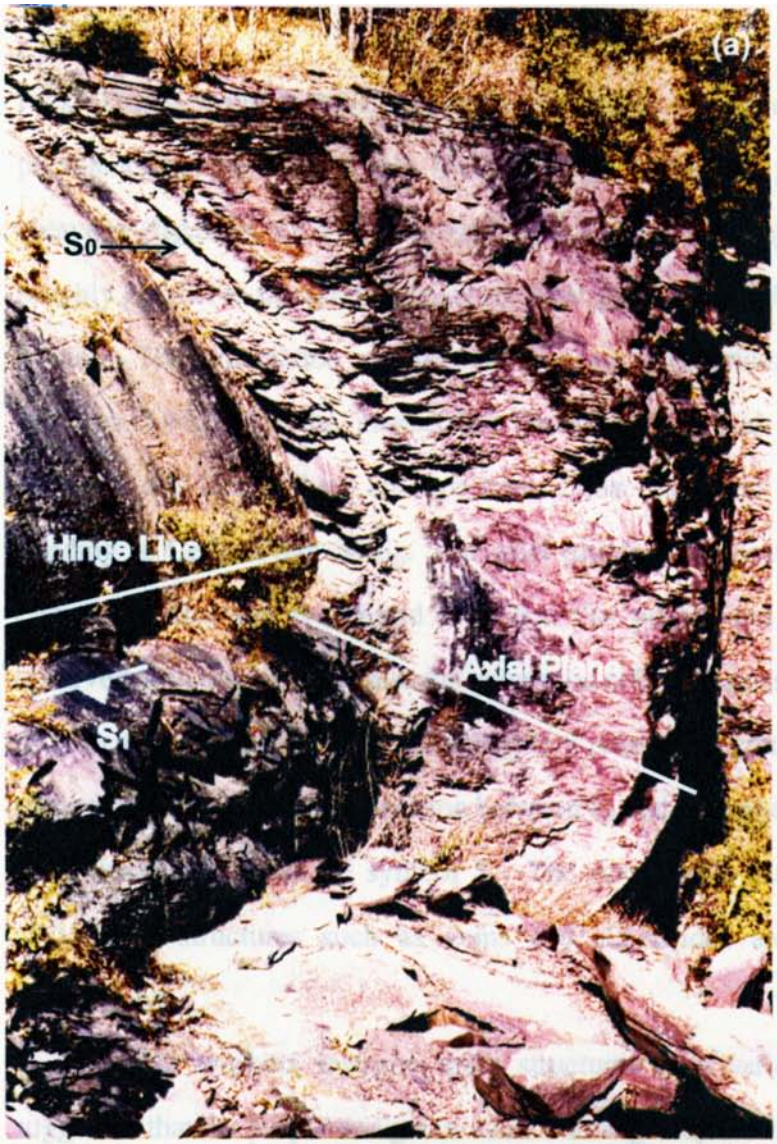

Figure 5.3) **a**) A view to the north of the Cedar Mountain Syncline. The joint face yielding the cross-sectional view of the fold is at station 55 on the quarry map (**Plate III**). (**b**) Trace of a conjugate set of S_2 and S_1 / S_2 intersection lineation near station 26. Lens cap (for scale) rests on S_1 surface. (**c**) Trace of S_2 at a high angle to S_1, between stations 41 and 42. Quarter in the center of the photo is for scale. There are S_1 parallel veins of granular quartz barely visible in the photo in the dark purple slate.

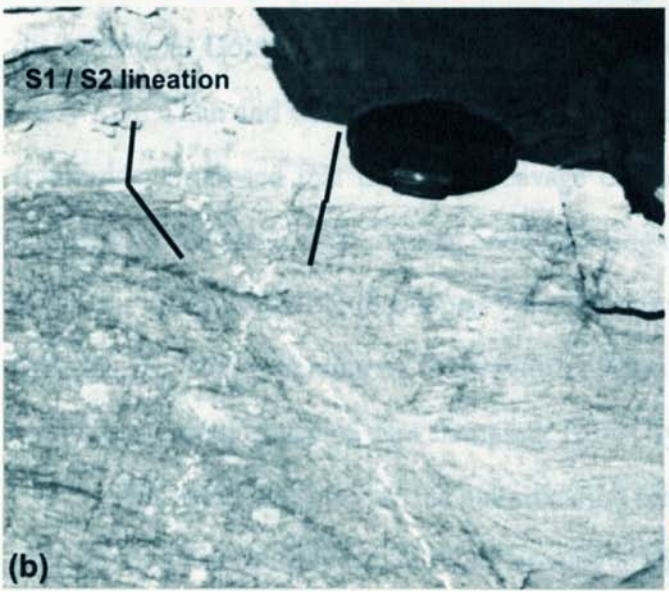

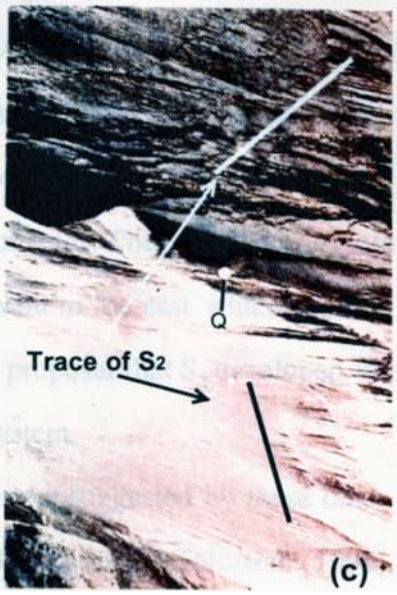

rock. This layering is folded about an axial plane. A well defined axial planar cleavage is prevalent throughout the quarry. At a high angle to the axial planar cleavage is a crenulation cleavage (**fig.5.3b, c**). This cleavage often occurs as a conjugate set, one set of which is roughly parallel to the axial plane of the later generation of folds discussed in the previous section. The crenulation cleavage creates an intersection lineation (**fig.5.3b**) on S_1 surfaces. Ordinarily, the intersection lineation creates an anastomosing network on S_1 surfaces, and locally there are two intersection lineations. This study refers to the color banding at Cedar Point as S_0. The axial planar slaty cleavage is referred to as S_1. The crenulation cleavage is referred to as S_2. The purple and green banding is the earliest observed structure and, because the coloration reflects a compositional variation originating prior to tectonic transport, S_0 (bedding) is a reasonable symbol to apply to it. There is no recognized structure of a generation between S_0 and the axial planar cleavage, and thus the slaty cleavage is given the symbol S_1. The same holds true for the crenulation cleavage (S_2). Other structures such as veins and slikensides are discussed in the following discussions.

Other workers interpret these structures in a variety of ways. Rowley (1983) suggested that the purple and green color banding may be different than the actual horizon of deposition. Goldstein (1996) recognized a cleavage which developed earlier than this study's S_1. Chan and Crespi (1997), based upon analyses of fibrous overgrowths on pyrite framboids, proposed that the slaty cleavage developed after the initial stage of folding, during a second stage of shortening and tightening of folds. They go on to propose that the S_2 of this study (their S_3) developed via a thrust event to the east which created a fourth foliation, S_4. This is in contrast to Rowley's (1983) proposal that S_2 developed in response to the final emplacement of the Champlain Thrust System.

This study does not use the classification scheme suggested by these other workers (i.e. S_0 - S_4). This is because the S_0 of Rowley (1983), the S_1 of Goldstein (1996), and the

S_4 of Chan and Crespi (1997) were not observed in this study. It is important to note that there is evidence for multiple deformation events, not dissimilar to those that would produce additional foliations. As previously mentioned, one set of S_2, of this study, is axial planar to late folds of S_1, throughout the Taconic slates. The deformation which produced this late folding, and S_2, could have been induced by either the Taconic Frontal Thrust's generation of deformation, thrust events towards the Green Mountain Front, or the latest stages of the Champlain Thrust System's evolution. However, which event produced S_2 is a matter of conjecture until further study demonstrates how the various foliations are genetically related to the various generations of faulting.

5.1.3. Locality Map, Field Data, and Projected Cross-Section

Sampling and mapping was done with a 50′ tape measure, a Brunton compass, and a 5.25′ high leveling rod. Control stations were placed using Mason's nails and Duct Tape to flag the stations, with the origin for the coordinate system placed at an arbitrary position towards the center of the southern end of the quarry map (**plate III**). The nails fastened to the quarry wall should have a long lifetime, barring someone removing them. Some of the stations flagged in the soil for location control may not have as long a lifetime. Stations on the lower east wall of the quarry were given the labels *L.E.* followed by sequential lettering (i.e. *L.E.A.*, *L.E.B.* etc...). Stations on the lower west wall of the quarry were given the labels *L.W.* followed by sequential lettering (i.e. *L.W.A.* , *L.W.B.* etc...). The other stations were labeled numerically (i.e. *1, 2, 3*...), with some stations against the quarry walls given a number - letter combination for a label (i.e. *15a, 15b* ...). This labeling system allowed me to differentiate between stations in the lower west, lower east, and upper quarry walls as well as to record observations at precise locations without departing from the primary sequential numbering system around the perimeter of the quarry. For

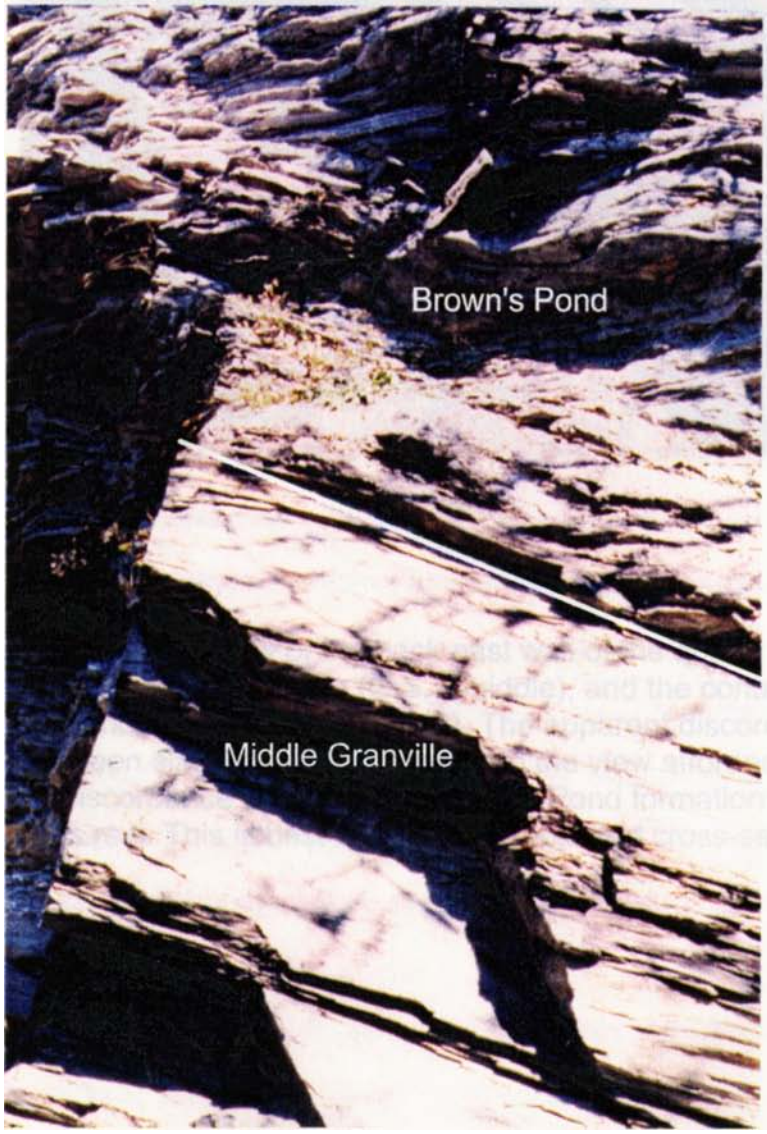

Fig.5.4) The contact between the Brown's Pond formation and the Middle Granville slate (bottom left) is above a large section of green slate. The layering in the Brown's Pond is, in many instances, internally folded (top - B) and occasionally slump structures (top -A) are preserved. These structures have the characteristics of a pre-lithification origin.

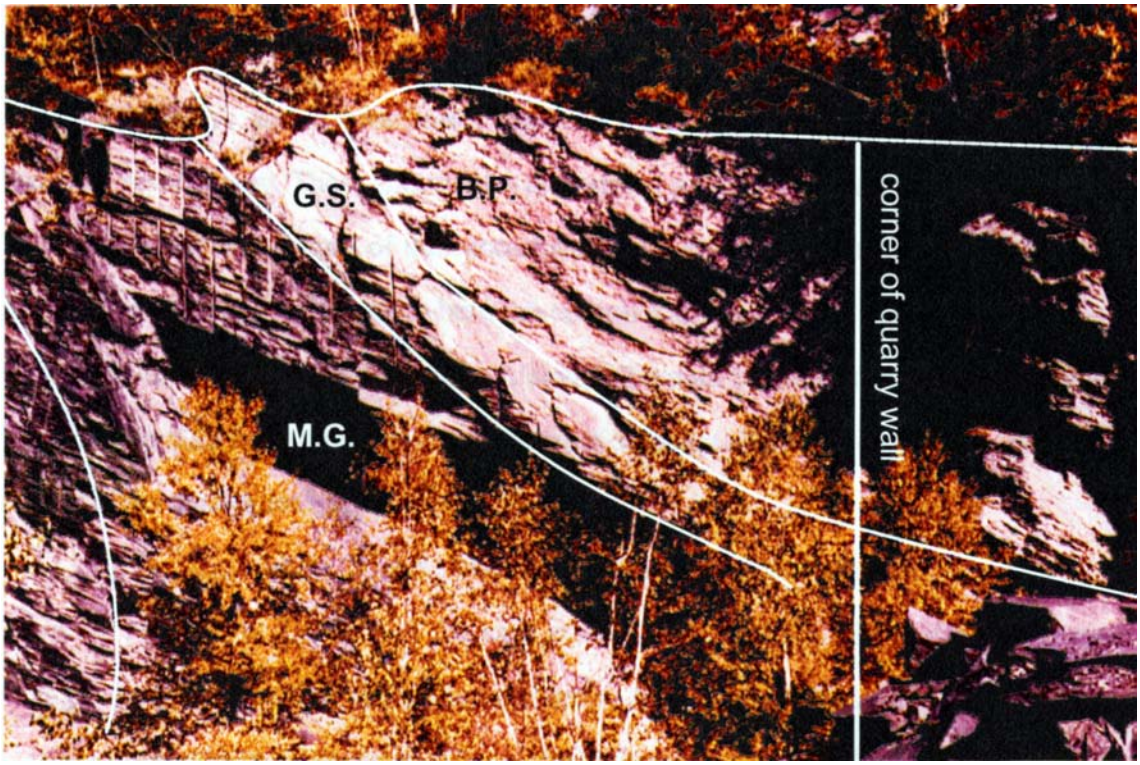

Fig 5.5) A view of the back east wall of the quarry with the fold (at left), the thick green slate (G.S.) (middle), and the contact with the Brown's Pond formation (B.P.) (right). The apparent discordance between the green slate and the fold is due to the view afforded by the quarry. The discordance between the Brown's Pond formation and the fold, however, is real. This is best seen on the projected cross-section (**fig.5.7**).

example, observations were made immediately south of *station 15* at a latter date than the initial mapping and, rather than change the numbering system, the label *15a* was used.

The quarry map (**plate III**) should be used both as a field reference and reference for samples and observations presented in this study. Control stations are plotted as a $1m^2$ box which represents the maximum uncertainty of location at a given station. The positive ends of the X, Y, and Z coordinates represent east, north, and upwards in the vertical direction, respectively. These coordinates are printed as text adjacent to the station. **Table 5-1** reports relative positions of the control stations. Horizontal Distance (in feet), Change in Elevation (in feet), and Azimuth between control stations are tabulated incrementally. For example, if one was standing at *station 1*, *station 2* would be 29.03 feet in the 010 azimuth direction and 5.25 feet above the ground level of *station 1*. **Table 5-2** reports absolute X, Y, and Z coordinates for each control station.

S_0, S_1, S_2, and the S_1 / S_2 intersection lineation were measured where possible. These are reported in **Table 5-3** for each control station, along with notes which report geologic features other than the major structures. Any measurements of a conjugate set of S_2 is also reported in these notes. The geologic data is plotted on the quarry map both as text and as stereographic projections. The plots are assigned to the control station by a tie-line. Some measurements were omitted from the quarry map for the sake of clarity.

Plotted on the quarry map is the contact between the Middle Granville and the Brown's Pond formations. The lithologic contact between the two formations is above a thick layer of green slate (**fig. 5.4, 5.5**). An estimation of the top of the quarry is drawn in a dashed line around the perimeter of the map. The trend and plunge of the fold axis (in this case, roughly equal to the hinge line orientation) is drawn as an arrow in the center of the map.

The geologic data was compiled on four stereographic projections (**fig.5.6**). The poles to S_0 plot around a great circle on the projection (a girdle distribution), with each

point having varying amounts of deviation from the best fit great circle. This indicates that the fold is roughly, but not perfectly, cylindrical. The fold axis orientation was calculated as the pole to the defined great circle. The poles to S_1 planes plot on the stereoprojection with tight grouping. This indicates that S_1 remains in a constant orientation throughout the quarry. Poles to S_2 define two fields of the stereoprojection. One of the fields is defined by tightly grouped poles to a set of S_2 planes which are steeply east dipping. The second field is defined by a more loosely grouped set of poles to a set of S_2 planes which are west dipping. The west dipping set has a shallower dip than the east dipping set.

To properly visualize the fold geometry, a cross-section was constructed, projected normal to the fold axis orientation (**fig.5.7**). The cross-section plane is thus represented by the great circle defined by the poles to bedding (**fig.5.6**). The projection was created by taking the geographic X, Y, and Z coordinates of stations shown on the quarry map, and multiplying them by a 3 X 3 matrix thereby calculating a new X′, Y′, and Z′ coordinate for each control station. The components of the matrix are equal to the cosines of the angles between all combinations of the primary X, Y, and Z axes of geographical space and the X′, Y′, and Z′ axes of the fold space (**fig.5.6, 5.8**). The plane of the cross-section spans the X′ and Z′ directions. Geologic data, and the trace of the fold, was plotted on the cross-section as the pitch of the intersection line of the planar structure of interest and the cross-section plane. The results of the projection of coordinate data is reported in **Table 5-4** and the projection of geologic data is reported in **Table 5-5**. A representative S_1 measurement was projected, rather than the total set, as S_1 has a consistent orientation throughout the quarry.

The cross-section shows all of the individual stations, though for the sake of clarity only those stations with geologic data are labeled. The cross-section includes an estimation of the trace of the contact between the Mid-Granville and the Brown's Pond formations.

Figure 5.6) Stereographic Projections of structural data from the Cedar Point Quarry (see text for details).

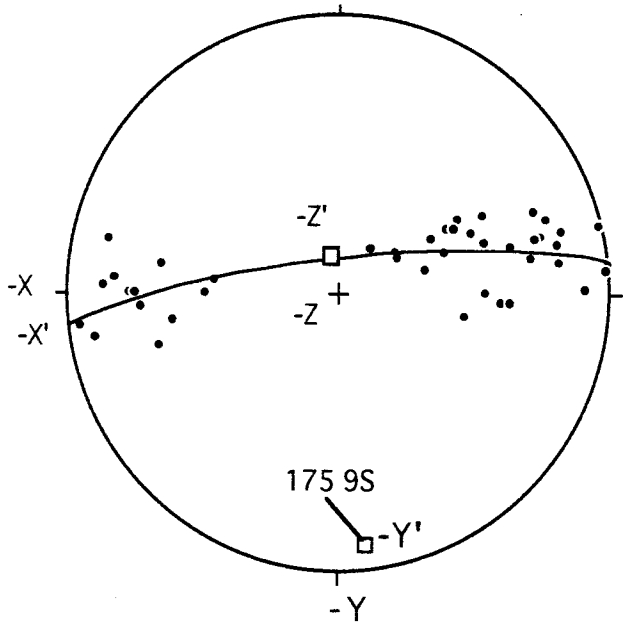

a) poles to S_0, geographic axes, and projected axes.

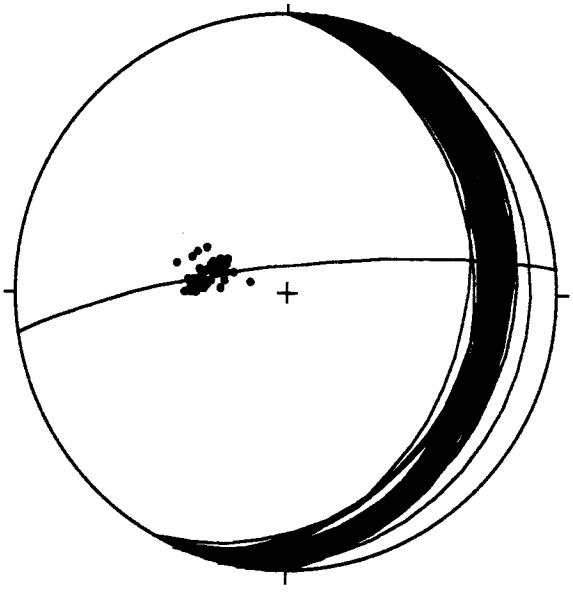

b) S_1 great circles and poles to planes.

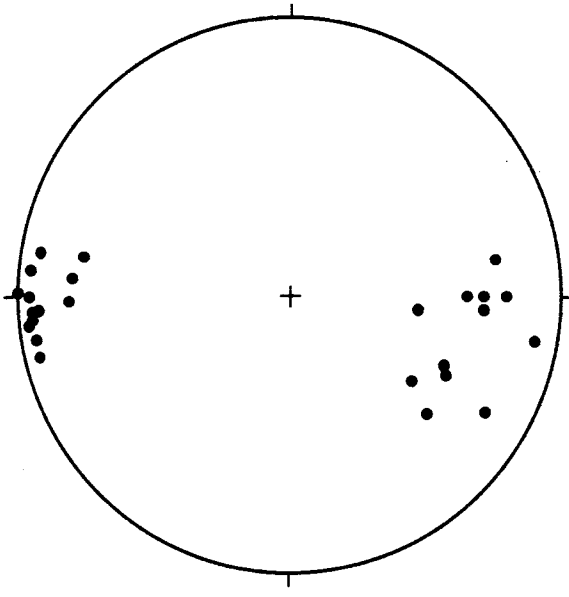

c) Poles to S_2

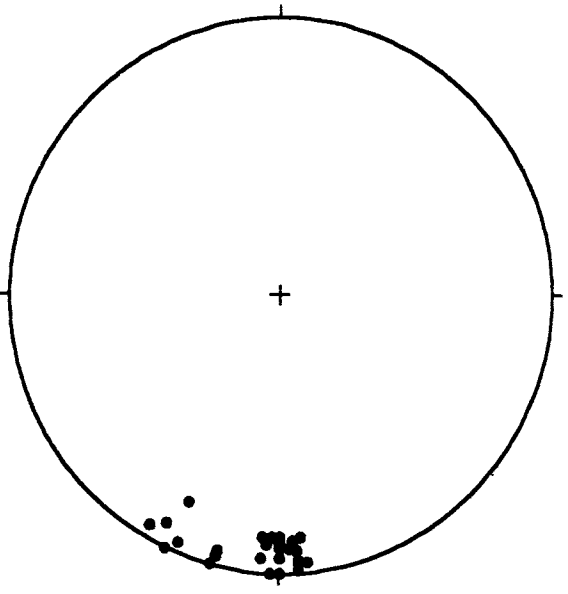

d) S_1 / S_2 intersection lineation

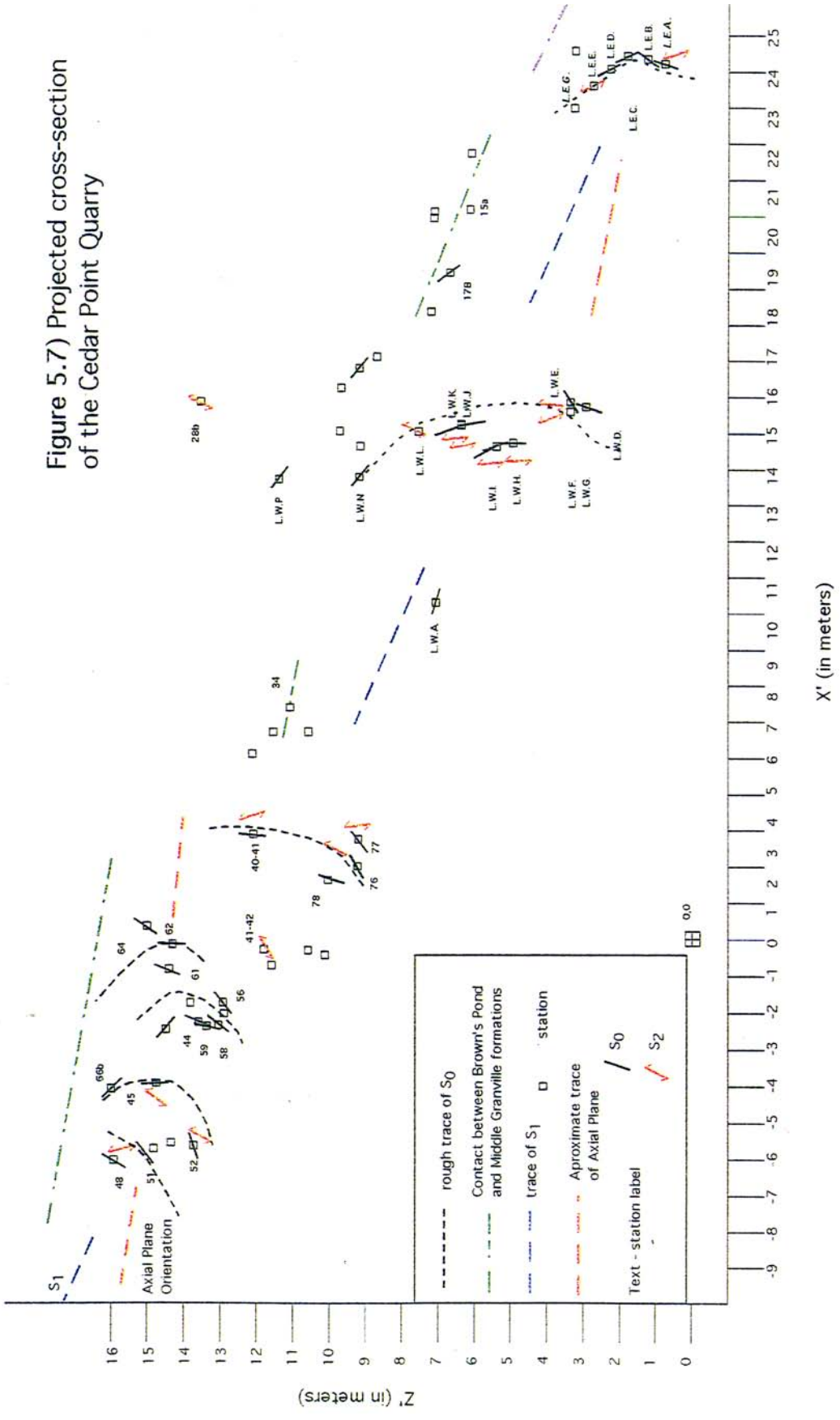
Figure 5.7) Projected cross-section of the Cedar Point Quarry
Z' (in meters)
X' (in meters)
S1
Axial Plane Orientation
rough trace of S0
Contact between Brown's Pond and Middle Granville formations
trace of S1
station
Aproximate trace of Axial Plane
Text - station label
S0
S2
0,0
L.W.A
L.W.P
L.W.N
L.W.L
L.W.K
L.W.J
L.W.I
L.W.H
L.W.E
L.W.F
L.W.G
L.W.D
L.E.G
L.E.E
L.E.D
L.E.C
L.E.B
L.E.A

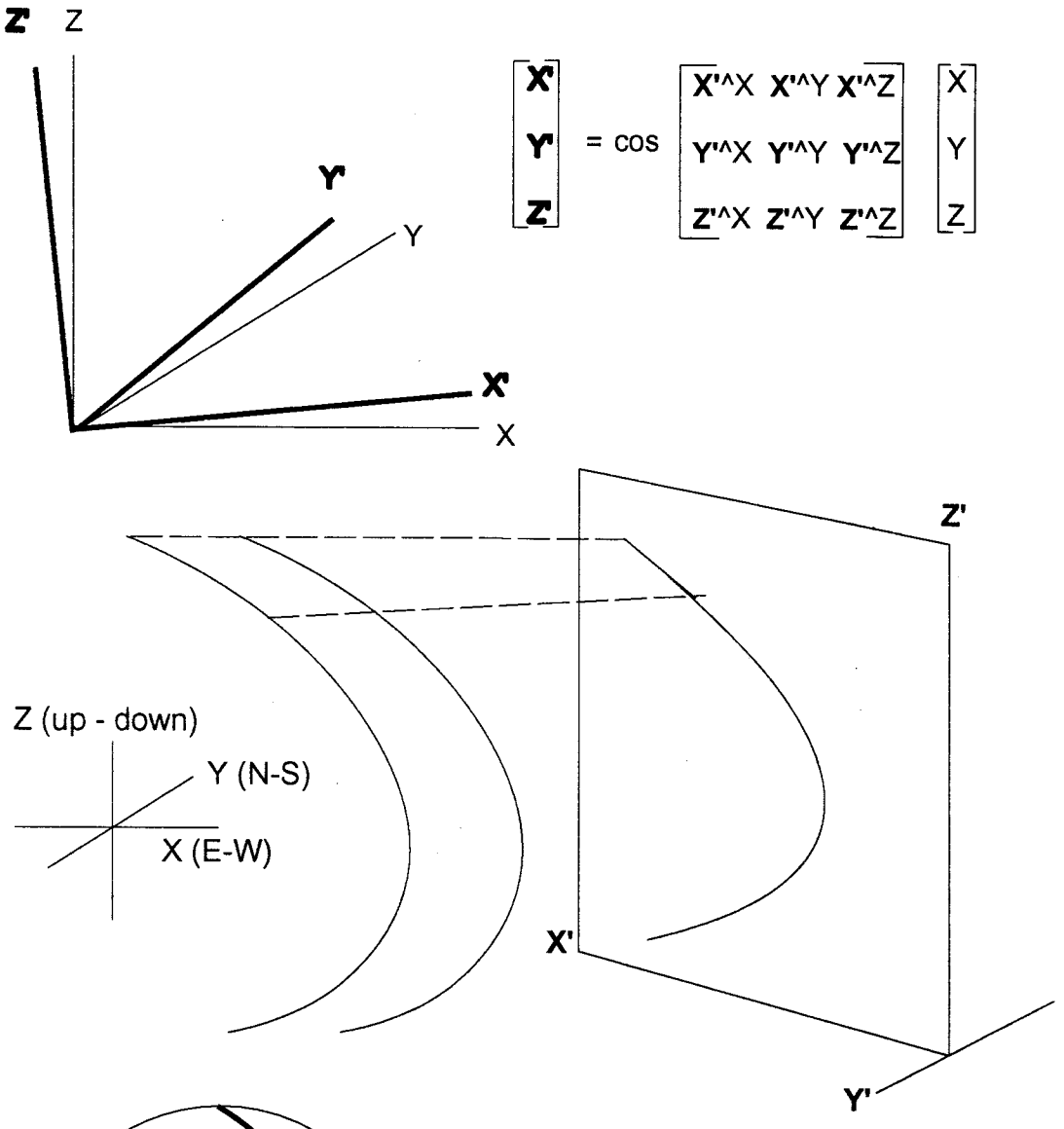

$$\begin{bmatrix} X' \\ Y' \\ Z' \end{bmatrix} = \cos \begin{bmatrix} X'\hat{}X & X'\hat{}Y & X'\hat{}Z \\ Y'\hat{}X & Y'\hat{}Y & Y'\hat{}Z \\ Z'\hat{}X & Z'\hat{}Y & Z'\hat{}Z \end{bmatrix} \begin{bmatrix} X \\ Y \\ Z \end{bmatrix}$$

Figure 5.8) The "coordinate transformation formula" is outlined above. To change X,Y,Z coordinates to a new X',Y',Z' coordinate system (bold), the old coordinates are multiplied by the cosine matrix. Thus, new X',Y', Z' coordinates are found (bold). To project geologic data into this new coordinate system (where Y' is parallel to the hinge line), the pitch of the intersection lineation of the cross-section plane and the geologic structure of interest is plotted.

Table 5-1) Relative positions of Control Stations

Station	Azimuth	Height (ft.)	Distance (ft.)	Last Station / Notes
1				midpoint of entry
2	10	5.25	29.03	1/ stations
3	13	5.25	17.92	2 / go up the
4	8	5.25	16.04	3/ west side
5	6	5.25	15.11	4 /of the trail
6	10	5.25	16.96	5/ incrementally
7	15	5.25	16.43	6
8	20	5.25	16.43	7
9	25	5.25	16.17	8
10	356	5.25	18.22	9
11	357	5.25	18.6	10
12	10	5.25	19.47	11
13	15	5.25	31.9	nail @ base of tree
14	322	-0.917	48.07	note vert. ht.
15	344	5.25	39.07	14
16	20	5.25	33.55	15
17	325	5.25	43.94	16
18	7	5.25	36.37	17
19	306	5.25	14.23	18
20	12	5.25	14.89	19
21	280	5.25	18	20
22	10	5.25	21.28	21
23	20	5.25	15.11	22
24	295	5.25	13.92	23
25	30	5.25	21.84	24
26	47	5.25	7.52	25
27	80	5.75	7.14	on outcrop
28	8	20.36	32.58	climbing outcrop
29	306	18.08	33.99	**23
30	341	0	33.67	heading west
31	347	0	30.375	towards "trail"
32	333	-15.67	18.67	31
33	343	0	32.29	32
T	320	6.6	9.42	
34	6	3.25	7.31	33
35	348	-5.79	23.21	34
36	3	3.77	15.12	35
37	11	6.74	8.32	36
38	335	6.1	12.51	37
39	270	-1.81	14.72	38
40	292	0.69	9.9	39
41	306	-5.79	15.1	40
42	284	1.52	21.72	41
43	285	8.86	21.93	42

Table 5-1) Relative positions of Control Stations

Station	Azimuth	Height (ft)	Distance (ft)	Last Station / Notes
44	290	7.44	1.45	43
45	283	14.46	17.24	44
46	285	7.1	15.22	45
47	268	1.35	15.42	46
48	43	3.41	11.9	47
49	186	-6.57	24.51	48
T	120	-1.93	3.21	
50	178	-3.27	3.89	49
51	170	-5.01	6.65	50
52	194	-6.71	6.48	51
53	133	-9.09	23.69	52
54	144	1.3	18.53	53
55	165	0	23.5	54
T	170	0	13.25	
56	195	0.4	2.51	55
57	240	1.02	8.27	56
58	180	5.98	8.23	57
59	165	2.76	15.63	58
60	164	3.45	13.83	59
T	160	1	3.74	
61	171	2.12	13.36	60
T	161	0	12.29	
62	168	-0.75	7.13	61
63	176	4.48	17.95	62
64	172	3.32	9.65	63
65	269	-5.06	26.05	64
66	204	13.05	73.98	65
67	131	-14.7	21.8	66
68	145	-10.73	10.73	67
69	123	-10.97	11.76	68
70	178	-9.27	11.05	69
71	160	-10.69	10.32	70
72	200	-5.06	5.43	71
T	180	-4.82	4.82	
73	200	-1.22	3.99	72
74	160	-2.92	16.53	73
75	132	0	15.5	74
76	135	0	9.25	75
77	154	0	15.5	76
78	199	8.73	55.14	77
L.W.A	275	36.75	143.11	9
L.W.B	300	52.7	78.14	4
L.W.C.	265	28.36	66.81	3
L.W.D	260	30.28	71.34	2

Table 5-1) Relative positions of Control Stations

Station	Azimuth	Height (ft)	Distance (ft)	Last Station / Notes
L.W.E	10	4.66	21.93	L.W.D
L.W.F	349	0	9.83	L.W.E
L.W.G	350	10.99	11.39	L.W.C
L.W.H	315	7.24	16.25	L.W.G
L.W.I	354	5	5.5	L.W.H
L.W.J	53	10.79	8.76	L.W.I
L.W.K	7.3	0	10.12	L.W.J
L.W.L	0	12.76	21.21	L.W.K
L.W.M	274	17.34	13.54	L.W.L/ on pipe
L.W.N	150	0	15.75	L.W.M
L.W.O	260	11.73	13.98	L.W.N
L.W.P	180	12.37	33.99	L.W.N
L.E.A	69	4.67	35.95	3
L.E.B	20	5.25	6.04	L.E.A
L.E.C	22	5.25	3.4	L.E.B
L.E.D	74	5.25	30.38	5
L.E.E	174	5.25	8.71	L.E.D
L.E.F	357	5.25	20.59	L.E.D
L.E.G.	74	5.25	20.33	7
L.E.H.	85	5.25	10.79	8
M.E.A	90	5.25	19.82	14
M.E.B	110	5.25	5.24	M.E.A
M.E.C	25	5.25	8.51	13
15A	87	5.25	22.95	15
15B	0	5.25	0	15a
16A	105	5.25	12.17	16
16B	0	5.25	0	16a
16C	180	0	18	16b
16D	355	0	11.67	16b
17A	111	0	23.25	17
17B	95	0	24.5	17
17C	45	5.25	27.93	17
18A	140	0	16.75	18
18B	120	5.25	12.35	18
20A	60	5.25	11.53	20
21A	70	5.25	26.48	21
22A	110	5.25	17.04	22

Table 5-2) (X,Y,Z) and (X′,Y′,Z′) Coordinates

Station	X (m)	Y (m)	Z (m)	X′(m)	Y′(m)	Z′(m)
1	69.48	0	0	21.07	0	-0.67
2	71.02	8.72	1.6	21.26	2.59	-0.19
3	72.24	14.04	3.2	21.46	4.15	0.29
4	72.92	18.88	4.8	21.51	5.57	0.77
5	73.41	23.46	6.4	21.51	6.91	1.26
6	74.3	28.55	8	21.62	8.4	1.74
7	75.6	33.39	9.6	21.86	9.82	2.21
8	77.31	38.1	11.2	22.23	11.2	2.69
9	79.4	42.57	12.8	22.72	12.5	3.16
10	79.01	48.11	14.41	22.42	14.13	3.65
11	78.71	53.77	16.01	22.15	15.79	4.15
12	79.74	59.62	17.61	22.28	17.52	4.63
13	82.26	69.01	19.21	22.74	20.31	5.1
14	73.24	80.56	18.93	19.64	23.82	5.11
15	69.96	92.01	20.53	18.28	27.24	5.64
16	73.45	101.62	22.13	19.03	30.11	6.1
17	65.77	112.59	23.73	16.35	33.38	6.67
18	67.12	123.6	25.33	16.41	36.67	7.16
19	63.61	126.15	26.93	15.27	37.39	7.68
20	64.56	130.59	28.53	15.41	38.69	8.16
21	59.15	131.54	30.13	13.74	38.92	8.7
22	60.28	137.93	31.73	13.88	40.81	9.18
23	61.86	142.26	33.33	14.22	42.07	9.65
24	58.01	144.05	34.93	13	42.56	10.18
25	61.34	149.82	36.53	13.83	44.26	10.64
26	63.02	151.38	38.14	14.28	44.68	11.11
27	65.16	151.76	39.89	14.92	44.74	11.62
28	66.54	161.6	46.1	15.03	47.53	13.5
29	53.47	148.35	38.85	11.49	43.74	11.41
30	50.13	158.06	38.85	10.16	46.69	11.46
31	48.05	167.09	38.85	9.25	49.42	11.48
32	45.46	172.16	34.07	8.3	51.11	10.07
33	42.59	181.57	34.07	7.13	53.97	10.1
34	40.97	185.99	37.07	6.5	55.21	11.03
35	39.5	192.91	35.31	5.83	57.37	10.52
36	39.74	197.52	36.46	5.76	58.73	10.87
37	40.22	200.01	38.51	5.82	59.42	11.49
38	38.61	203.46	40.37	5.22	60.4	12.07
39	34.12	203.46	39.82	3.86	60.42	11.95
40	31.32	204.59	40.03	2.98	60.76	12.04
41	27.6	207.3	38.26	1.76	61.63	11.54

Table 5-2) (X,Y,Z) and (X′,Y′,Z′) Coordinates

Station	X (m)	Y (m)	Z (m)	X'(m)	Y'(m)	Z'(m)
42	21.17	208.9	38.73	-0.24	62.1	11.75
43	14.72	210.63	41.43	-2.25	62.54	12.63
44	14.3	210.79	43.7	-2.38	62.52	13.33
45	9.18	211.97	48.1	-3.97	62.74	14.71
46	4.7	213.17	50.27	-5.37	63.03	15.41
47	0	213.01	50.68	-6.79	62.97	15.58
48	2.48	215.66	51.72	-6.12	63.74	15.88
49	1.7	208.23	49.72	-6.12	61.55	15.27
50	2.59	206.55	48.13	-5.8	61.09	14.78
51	2.94	204.55	46.6	-5.63	60.54	14.31
52	2.46	202.64	44.56	-5.71	60.02	13.69
53	7.74	197.71	41.79	-3.95	58.61	12.8
54	11.06	193.14	42.18	-2.8	57.22	12.88
55	12.91	186.22	42.18	-2.02	55.12	12.85
56	13.42	181.5	42.31	-1.71	53.68	12.88
57	11.23	180.24	42.62	-2.34	53.29	13
58	11.23	177.73	44.44	-2.26	52.47	13.55
59	12.47	173.13	45.28	-1.73	51.05	13.78
60	13.63	169.08	46.33	-1.25	49.79	14.09
61	14.66	163.98	47.28	-0.78	48.21	14.36
62	16.33	158.32	47.06	-0.09	46.5	14.27
63	16.71	152.86	48.42	0.2	44.8	14.67
64	17.12	149.94	49.43	0.41	43.89	14.97
65	9.18	149.8	47.89	-1.99	43.89	14.58
66	0	129.2	51.87	-4.12	37.52	15.86
67	5.02	124.84	47.39	-2.46	36.34	14.45
68	6.89	122.16	44.12	-1.8	35.63	13.43
69	9.9	120.21	40.77	-0.83	35.15	12.39
70	10.02	116.84	37.95	-0.68	34.22	11.53
71	11.09	113.89	34.69	-0.27	33.43	10.53
72	10.53	112.33	33.14	-0.39	33	10.06
73	10.11	109.72	31.3	-0.43	32.27	9.5
74	11.84	104.98	30.41	0.25	30.86	9.21
75	15.35	101.82	30.41	1.41	29.9	9.18
76	17.34	99.83	30.41	2.08	29.3	9.15
77	19.41	95.58	30.41	2.84	28.01	9.13
78	13.94	79.69	33.07	1.69	23.11	9.97
L.W.A	35.93	46.37	24.01	9.42	13.29	6.98
L.W.B	52.29	30.79	20.87	14.87	8.67	5.85
L.W.C.	51.95	12.27	11.85	15.36	3.34	3.1
L.W.D	49.59	4.94	10.83	14.88	1.15	2.81

Table 5-2) (X,Y,Z) and (X′,Y′,Z′) Coordinates

Station	X (m)	Y (m)	Z (m)	X′(m)	Y′(m)	Z′(m)
L.W.E	50.76	11.52	12.25	15.02	3.1	3.24
L.W.F	50.18	14.47	12.25	14.75	4	3.24
L.W.G	51.35	15.69	15.2	15.07	4.27	4.13
L.W.H	47.84	19.19	17.41	13.89	5.26	4.84
L.W.I	47.67	20.86	18.93	13.79	5.72	5.3
L.W.J	49.8	22.46	22.22	14.38	6.1	6.28
L.W.K	50.2	25.52	22.22	14.41	7.03	6.28
L.W.L	50.2	31.99	26.11	14.2	8.87	7.46
L.W.M	46.08	32.28	31.4	12.94	8.79	9.11
L.W.N	48.48	28.12	31.4	13.8	7.53	9.08
L.W.O	44.28	27.38	34.97	12.55	7.19	10.2
L.W.P	44.28	17.02	38.74	12.88	3.93	11.34
L.E.A	82.48	17.97	4.63	24.44	5.3	0.63
L.E.B	83.11	19.7	6.23	24.57	5.77	1.11
L.E.C	83.49	20.66	7.83	24.66	6.01	1.59
L.E.D	82.31	26.02	8	24.13	7.63	1.66
L.E.E	82.59	23.38	9.6	24.3	6.78	2.14
L.E.F	81.98	32.28	11.2	23.83	9.43	2.64
L.E.G.	81.56	35.1	11.2	23.61	10.29	2.64
L.E.H.	80.59	38.39	12.8	23.21	11.23	3.14
M.E.A	79.28	80.56	20.53	21.47	23.77	5.54
M.E.B	80.78	80.01	22.13	21.94	23.55	6.01
M.E.C	83.36	71.36	20.81	23	20.97	5.58
15A	76.95	92.38	22.13	20.39	27.3	6.06
15B	76.95	92.38	23.73	20.39	27.25	6.55
16A	77.04	100.66	23.73	20.15	29.76	6.55
16B	77.04	100.66	25.33	20.15	29.71	7.04
16C	77.04	95.17	25.33	20.33	28.05	7.03
16D	76.73	104.21	25.33	19.94	30.79	7.04
17A	72.39	110.05	23.73	18.44	32.61	6.61
17B	73.21	111.94	23.73	18.63	33.18	6.6
17C	71.79	118.62	25.33	17.99	35.16	7.11
18A	70.41	119.69	25.33	17.54	35.48	7.12
18B	70.38	121.72	26.93	17.46	36.05	7.61
20A	67.6	132.35	30.13	16.28	39.17	8.62
21A	66.74	134.3	31.73	15.96	39.71	9.11
22A	65.16	136.16	33.33	15.42	40.22	9.61

Table 5-3) Geologic Data from Control Stations

Station	S_0	S_1	S_2	L int.	Notes
L.E.A. (sample)	013 76E	015 25E	358 70E	358 10S	10' to S6E; 6.25' up
L.E.B	346 55W	017 24E			anastomosing cleavage
1.5' above H.L.	000 66E				At L.E.B
2' below H.L.	345 55W				" "
L.E.C	002 76E	022 24E			S_0 is perpendicular to S_1
L.E.D.	000 64E				5.25' up
L.E.D	341 47W				Vein set 10' up = 344 35E
L.E.E	000 64E				
L.E.F	345 69W	015 25E	010 66E	004 14S	Within 5" of H.L.
L.E.H (s. at L.E.G.)			011 26E	002 14S	
L.E.H +5.25'		004 28E			may be B.P.
L.W.A.	035 20E				
L.W.D (sample at L.W.C.)	004 72W	020 24E	334 29W	355 14S	2nd S_2 = 004 69E
L.W.E	339 34W	015 21E	350 84E	000 10S	at -6ft., S_2=010 81W
L.W.F	345 27W	000 27E		356 4S	
L.W.G				000 14S	2nd L = 030 5E
L.W.H (sample)	354 90	006 29E	000 90	000 6S	
3.5' below L.W.H	354 85W	002 25E	354 82E	356 1S	measured off same bed
L.W.I -3'5"	359 80E	006 27E			
L.W.I +6"	356 62E	008 28E	356 84E	002 0	
L.W.J	350 80W	004 20E	009 82E	000 12S	
L.W.K	348 71W	014 23E	354 84E	354 4S	S_2 = 350 66W
L.W.L		009 23E			
L.W.M		017 19E			B.M. on pipe
L.W.N	010 39E	008 30E		014 4S	
L.W.P (7' away-S38E)	006 38E	023 20E		004 6S	2nd L = 023 4S
M.E.B.		005 24E			
15a (sample)		002 29E		015 0	brown lenses
16B		354 19E			micro H.L. = 325 20E
16C		006 24 E			vein rich station
17B	009 56E	019 23E		014 6E	bedding is poorly defined
18A	352 55E	016 24E		002 0	and veins 000 85W
20A		007 26E			possible dolomitic lenses
21A		020 30E			micro H.L. = 351 15S
22A		024 22E			round dark markings (?)
23		020 17E		298 14E	
28B		026 22E	030 72W	356 5S	2nd l = 030 72W
28C		014 11E			2nd L = 025 0
M.G. / B.P. at 34					
35		029 27E			
37		024 20E			
38		029 27E			
40-41 (sample)	335 80W	029 20E	005 85E	357 13S	2nd S_2 = 006 39W

Table 5-3) Geologic Data from Control Stations

Station	S_0	S_1	S_2	L int.	Notes
41-42 (sample)				000 86E	2nd S_2 = 034 45W
44	020 73W	020 20SE		003 11S	2nd L-very faint
-3.5'	003 50W				
45	355 89E	015 27E	024 52W	356 9S	2nd L = 027 9N
48	344 58W	024 29E	353 86E		
48 +3'9" to N18E	350 61W				
48+6'10" to N18E	345 66W				
49 (5'4" towards 48)	351 52W				phosphate pebbles
50	325 21W				
51	306 16W	016 24E	000 61W		
52	330 20W	005 24E	000 69W		
55-4'	330 38W				
55+1'	336 44W				
56	329 42W				
57		005 24E			
58	332 50W		026 54W		
58 (7'5" towards 59)				000 55W	
59	345 74W				microH.L. = 325 shallow S
61-1'9"	338 66W				
61	341 70W	019 20E			
62	346 89W	000 29E			
63	345 64W				
64	353 53W				
66B	000 45E	000 31E		000 0	
66-67 (sample)	000 41E	010 19E			slickenlines down dip on S_1
70		330 68W	040 56W	024 20E	
71	334 39W	331 39E			
72		015 34E			
76	330 32W		004 61W		
77	332 40W		346 84E		
78	352 71E		359 85E	000 14S	fibrous veins

Table 5-4) Pitch of S_0 and S_2 in Projected Cross-section. (+) pitch is towards +X'.

Station	S_0'	S_2'
L.E.A.	-71.8	-69.6
L.E.B	-54.2	
1.5' above H.L.	65.3	
2' below H.L.	-54	
L.E.C	74.6	
L.E.D.	63.4	
L.E.D	45.5	
L.E.E	63.4	

Table 5-4) Pitch of S_0 and S_2 in Projected Cross-section. (+) pitch is towards +X'.

Station	S_0'	S_2'
L.E.F		62.9
L.E.H		
L.E.H +5.25'		
L.W.A.	16.5	
L.W.D	-70.2	-28.9
L.W.E	-32.7	84.9
L.W.F	-26.8	2nd = 67.3
L.W.G		2nd = -84.2
L.W.H	90	88.8
3.5' below L.W.H	-85.3	81.8
L.W.I -3'5"	81.1	
L.W.I +6"	62.2	83.7
L.W.J	81	78.8
L.W.K	70.1	84.1
L.W.L		2nd = -65.8
L.W.M		
L.W.N	39.8	
L.W.P (7' away-S38E)	37.1	
M.E.B.		
15a		
16B		
16C		
17B	53.6	
18A		
20A		
21A		
22A		
23		
28B		-76.4
28C		
M.G. / B.P. contact at 34		
35		
37		
38		
40-41	-83.7	82.7
41-42		2nd = -40.4
44	-77	2nd = 42.2
-3.5'	-51.6	
45	89.2	-52.7
48	-59.7	86.3
48 +3'9" to N18E	-60.9	
48+6'10" to N18E	-64.6	

Table 5-4) Pitch of S_0 and S_2 in Projected Cross-section. (+) pitch is towards +X′.

Station	S_0'	S_2'
49 (5'4" towards 48)	-52.9	
50	-18.3	
51	-10.6	-62.4
52	-18.2	-70.5
55-4'	-34.4	
55+1'	-41.4	
56	-37.7	
57		
58	-45.9	-54.6
58 (7'5" towards 59)		-56.3
59	-72.4	
61-1'9"	-62.9	
61	-67.6	
62	-87.3	
63	-62.7	
64	-54.5	
66B	46.1	
66-67	39.6	
70		-53.7
71		
72		
76	-29	-62.8
77	-36.7	85.8
78	-70.9	84.1

5.1.4. Additional Observations

The projected cross-section (**fig.5.7**) provides some additional observations. The lower limb in eastern sections of the quarry (to the right on the cross-section) seems to steepen in dip just above the base of the outcrop. This may be indicating that the Cedar Point Syncline has an adjacent anticlinal structure in the subsurface. This is in keeping with the syncline / anticline "fold train" which continues throughout the fold belt (**fig.5.2**).

There seems to be a mild change in the orientation of the axial plane (as defined by bedding measurements) from west to east (left to right on the cross-section). There are also bedding measurement at stations 64 and L.W.A. which are discordant to fold geometry defined by the bedding measurements from elsewhere in the quarry. The overall geometry of the fold does not change significantly, however, and there is no corresponding change in S_1.

The contact between the Middle Granville slates and the Brown's Pond formation is not perfectly conformable. This unconformable relationship is generally apparent only through detailed mapping. However, it can be recognized with first order observations, such as where the contact between the two formations dips shallowly against the quarry wall, while the bedding within the Middle Granville formation dips steeply, at the hinge of the fold (**fig.5.5**). Internal to the Brown's Pond formation are a variety of slumps and folds which have the characteristics of having been produced by soft-sediment deformation / deposition (**fig.5.4**). Large clasts within an otherwise fine grained matrix are a characteristic of this formation as well. Collectively, the above observations are field evidence to support the interpretation that the Brown's Pond formation was deposited as a debris flow or that post-depositional slumping occurred. Whatever the origin of the unconformity, it is likely due to an event which pre-dates tectonic transport. The clearest evidence for this unconformity is that the contact, present immediately above stations 34

and L.E.G., plots below station L.W.P. on the projected cross-section. L.W.P., however, is within the Middle Granville formation on the lower west side of the quarry.

There are two other field scale observations which are important to note. The first is that at station 66-67 there are well developed slickenlines on S_0 (**fig.5.9**). The slickenlines have developed upon layers of highly strained quartz and calcite grains. The slickensides may have developed in response to flexural slip, though there are no indications of the sense of shear on the slickensides. Pieces of float have the same slickenlines. Some of these pieces show a gradational change in S_2 orientation towards the slickenside (**fig.5.9**). This observation suggests that some amount of bedding parallel slip occurred after the formation of S_2. The slickenside seems to be isolated to one particular layer within the fold. There is little other field evidence for flexural slip, or post - S_2 formation bedding parallel slip, elsewhere in the quarry.

Another field scale observation worthy of note is that a layer in the region of L.E.A. has an anastomosing slaty cleavage as opposed to a planar slaty cleavage (**fig.5.10**). The layer extends into the outcrop no more than a few centimeters. Here too, there is a lineation on the bedding surface. The lineation is less well defined and does not clearly indicate a slickenside surface. Thin sections show that the anastomosing cleavage is in a hematitic layer, and large phyllosilicate grains lie oblique to slaty cleavage within the anastomosing sections. However, no grains are observed to "overprint" the surrounding foliation. The anastomosing cleavage and the lineation are here suggested to be earlier than the development of S_2 and synchronous with the development of S_1.

A last observation worthy of note is that there are isolated localities within the quarry with a large amount of vein material. This material is generally calcite and quartz though no extensive study has been conducted. These veins can be parallel to S_0, S_1, and S_2 (see also **Section 5.2**). Veins of both a fibrous type and granular type were observed.

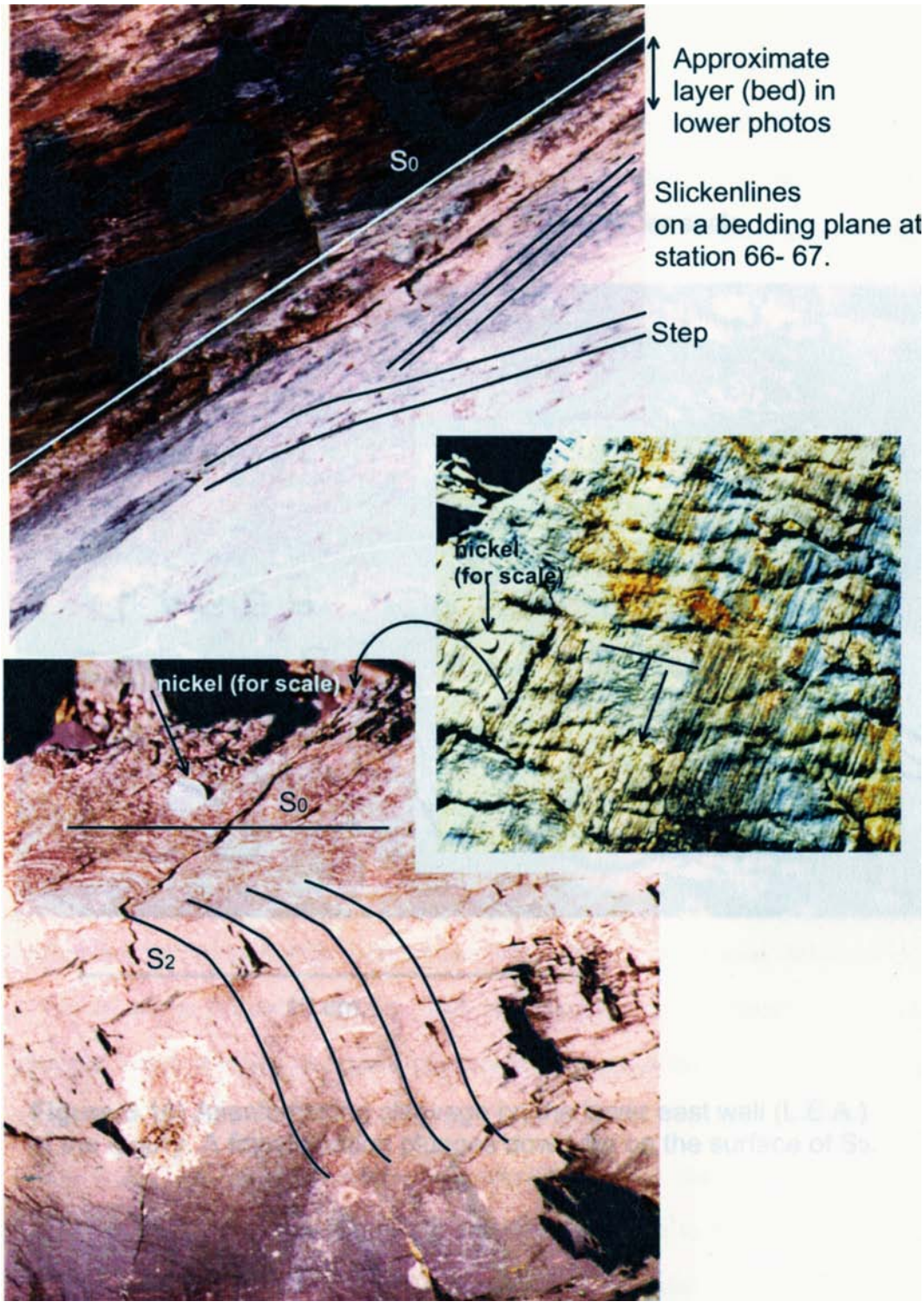

Figure 5.9) Slickenside on a bedding plane between stations 66 - 67 (top). The float in the middle and lower photographs comes from approximately the same bed, also on the upper limb of the fold. Well developed fibrous slickenlines are on a thick, vein quartz and calcite rich layer, parallel to bedding (middle). Immediately below this layer, S_2 is defelected, adjacent to the slickenside (bottom).

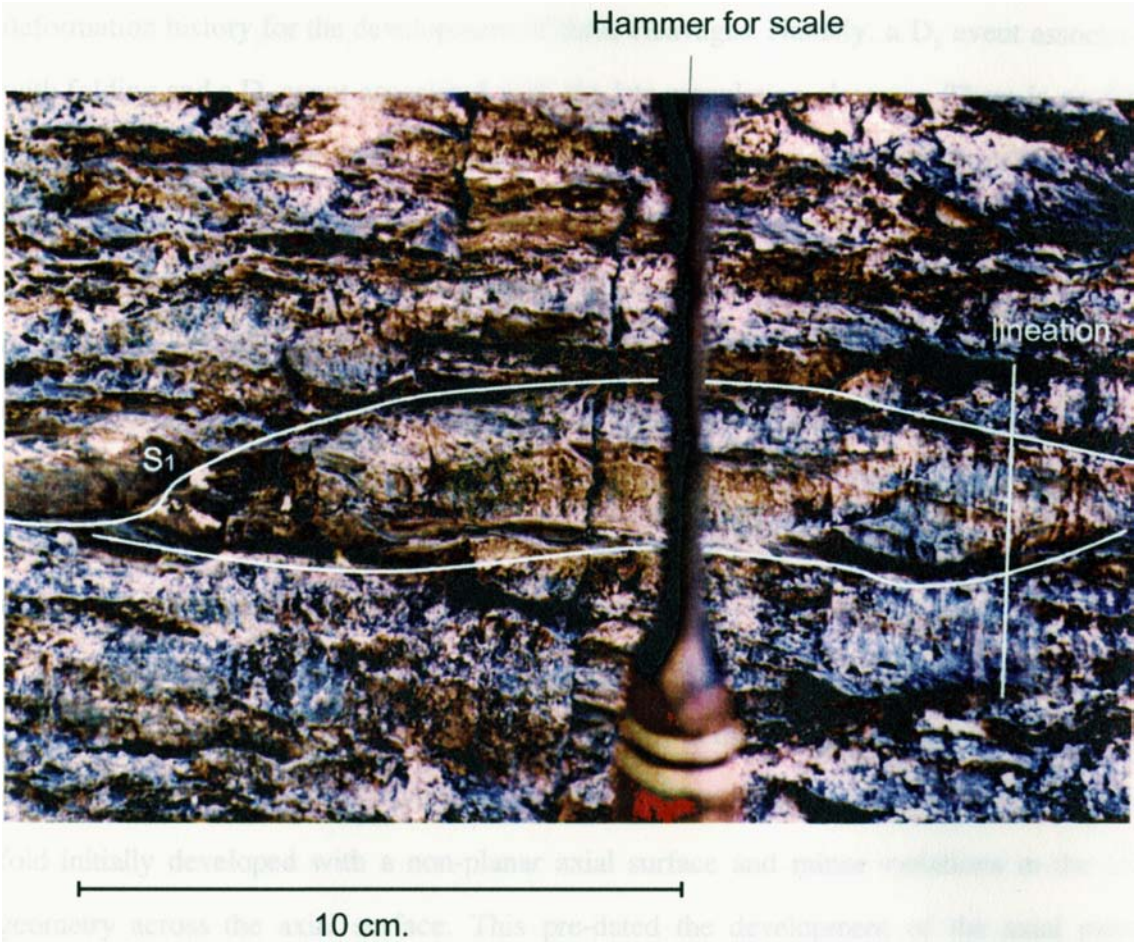

Figure 5.10) Anastomosing cleavage on the lower east wall (L.E.A.) of the quarry. A faint lineation plunges down dip on the surface of S_0.

5.1.5. Discussion - Deformation History

The initial description of the structure at the Cedar Point Quarry was that there is a fold, an axial planar cleavage, and late crenulation cleavages. One could ascribe a simple deformation history for the development of these cleavages. Namely, a D_1 event associated with folding and a D_2 event associated with the late crenulation cleavage. There is no field evidence presented here which warrants discounting such a simple history. There is, however, field evidence to warrant the use of caution when proposing such a history.

The depositional environment of the early Cambrian continental rise was not one of quiescence as shown by the sedimentary structures in the Brown's Pond formation. The unconformity between the two formations at Cedar Point represents a disturbance in bedding which pre-dates tectonic transport. The folding in the Middle Granville slate is certainly post-lithification, and likely initiated during the early stages of tectonic transport (Rowley and Kidd, 1982, 1982b; Chan and Crespi, 1997).

There is, as mentioned previously, a minor change in the orientation of the axial plane of the fold across the quarry. How, and when, did the change in the orientation of the axial plane of the fold in the Middle Granville formation occur? One possibility is that the fold initially developed with a non-planar axial surface and minor variations in the fold geometry across the axial surface. This pre-dated the development of the axial planar cleavage which does not change in orientation throughout the quarry. Such a proposal is consistent with the conclusions of Rowley and Kidd (1981), Rowley (1983), and Chan and Crespi (1997) that the regional S_1 developed after the initial stages of folding. Alternatively, S_1 development may not have been sensitive to the minor variations in the fold geometry and thus is not precisely parallel to the axial surface. Some of the data suggest that at least some of the variations in the fold geometry result from events which pre-date tectonic transport (e.g. the unconformity with the Brown's Pond formation). Such variations would not be reflected in the orientation of S1.

Another possibility for the variation in the axial plane's orientation across the quarry, is that the fold has a long deformation history which continues even after the development of S_2. If the slickensides at one locality in the quarry indicate tightening of the fold after S_2 developed (highly speculative), then such a hypothesis is supported by the deflection in S_2 orientation adjacent to these slickensides. Such macroscopic evidence for post - S_2 formation, bedding parallel slip is only observed at this locality. Thus, it is possible that changes in the fold geometry were localized to particular layers at particular locations throughout the quarry. As a result, no *pervasive* change in S_1 orientation occurred with the continuing, tightening of the fold. Regardless, the possibility that deformation continued after S_2 developed is worth note, especially considering that the microstructural focus of this study assumes that S_2 is the result of some of the latest deformation to have occurred at Cedar Point.

The other field data brings out one other important conclusion. The rocks at Cedar Point are not structurally homogeneous between stratigraphic horizons. In other words, one bedding horizon may have slickensides while another has anastomosing cleavage. Though slickensides and anastomosing cleavage likely developed during different periods in the folds history, neither is associated with a pervasive deformation fabric. Furthermore, veins, the product of solution processes, are heterogeneously distributed between different localities within the quarry. The implication of these observations is that the geochemistry and microstructure of the slate can be expected to vary depending upon what part of the quarry was sampled. Furthermore, this variation may be due to events which could have occurred prior to tectonic transport, during the formation of S_1, or after the formation of S_2.

5.2. Petrographic Observations

All of the thin sections discussed here are cut normal to S_1 and S_2. A few thin sections were cut parallel to either S_1 or S_2, but did not yield views of clearly defined micro-kink band boundaries and thus were not used for an investigation of cross-micas. One thin section cut parallel to S_1 showed a weak mineral lineation in the dip direction of slaty cleavage (roughly normal to the S_1 / S_2 intersection lineation).

5.2.1. Mineralogy and Microstructure of the Cedar Point Slates

The Cedar Point Slates are very fine grained with phyllosilicate grain sizes on the order of 20 - 30 microns long and 2 - 5 microns wide (i.e. a length to width ratio between 10:1 and 5:1). The phyllosilicate minerals are white micas with chlorite interstitially surrounding the grains of white mica and surrounding coarser grains. It is impossible to determine exactly how much chlorite is present optically. It is also impossible to differentiate between different types of white mica optically. Phyllosilicates and quartz make up roughly 90% of the rock with phyllosilicates being the dominant phase. The opaque minerals are inferred to be a mixture of hematite, pyrite, and magnetite, collectively constituting roughly 5% of the rock's mineralogy. This was confirmed by analyses using the electron microprobe. The concentration of opaque minerals, however, is extremely variable throughout the quarry. The remaining 5% of the mineralogy consists of carbonate minerals as well as accessory minerals which are not identifiable optically (though microprobe analysis determined that apatite and dolomite are major constituents of the accessory and carbonate minerals, respectively). Some stratigraphic horizons have carbonate minerals constituting more than 5% of the mineralogy while others have less than 1% carbonate minerals.

The microstructure of the Cedar Point Slate is defined principally by the alignment of phyllosilicates with S_1, and S_2 which forms a complex branching network throughout a

typical thin section (**fig.5.11**). S_0 is not observed in typical thin sections. Occasionally there are quartz rich regions which trend obliquely to either S_1 or S_2 (**fig.5.12**). These are interpreted to be bedding, though they never continue for more than a centimeter. S_1 is regularly spaced at all scales, with principal cleavage planes spaced < 1cm. apart at the field scale, and several microns apart at the microscopic scale. Below 25X magnification, at the grain scale, S_1 is poorly defined.

Opaque minerals either coat S_1 in "micro-deposits" or are distributed randomly along S_1 as single grains (**fig.5.13**). The amount of quartz varies in directions normal to S_1. There are often micro-lentils of quartz (**fig.5.12**) and the margins of these micro-lentils are cut by S_2.

S_2 can be described as two types. The first type is enriched with opaque minerals giving S_2 a stylolitic appearance (**fig.5.11, 5.13b,c**). The second is not enriched with opaques and is more transparent than the surrounding rock. The change in color within the second type of micro-kink is suggestive of a mineral enrichment, either of quartz or some other light colored mineral. Grain scale observations, acquired optically, do not clearly reinforce the suggestion that S_2 is enriched with a particular mineral, though backscatter S.E.M. images show an enrichment in phyllosilicates (a quartz deficiency) in some micro-kinks (**fig.5.22a**).

5.2.2. Micro-Kink Geometries

All of the thin sections discussed here are cut normal to both S_1 and S_2 (unless otherwise stated). Thus, the micro-kink geometries are not artifacts of view, as would result if S_1 and S_2 intersected the plane of the thin section at a low angle. Very few of the types of micro-kinks observed have a well defined and planar micro-kink band boundary. Any interpretation of a cross-mica must be made in the context of the surrounding micro-kink geometry.

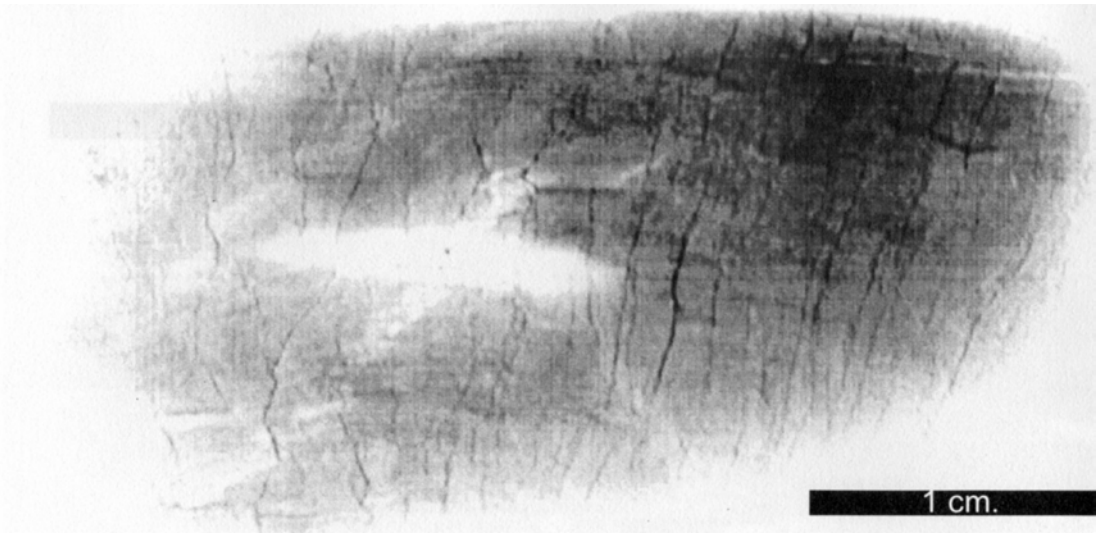

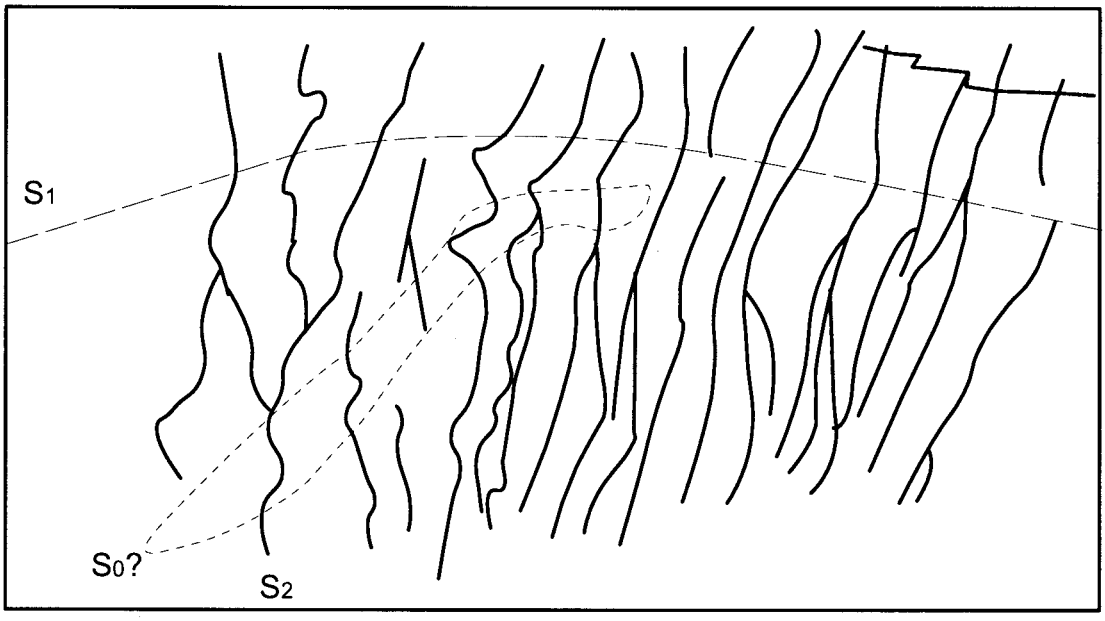

Figure 5.11) A thin section and line drawing from a float sample - a quartz rich layer has an orientation oblique to both S_1 and S_2. This layer could be bedding. A complex network of micro-kinks (S_2) lie at a high angle to S_1. The micro-kinks are lined with opaque minerals, giving them their dark appearance. S_1 is deflected across each of these micro-kinks resulting in moderate folding of S_1 across the sample. Note how S_2 branches into splays, many of which "pinch out".

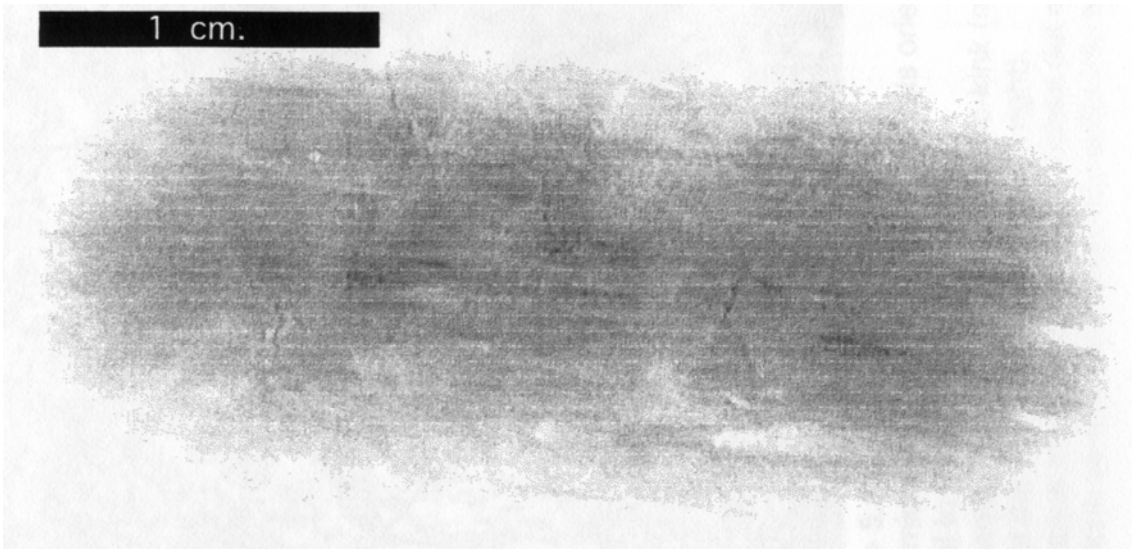

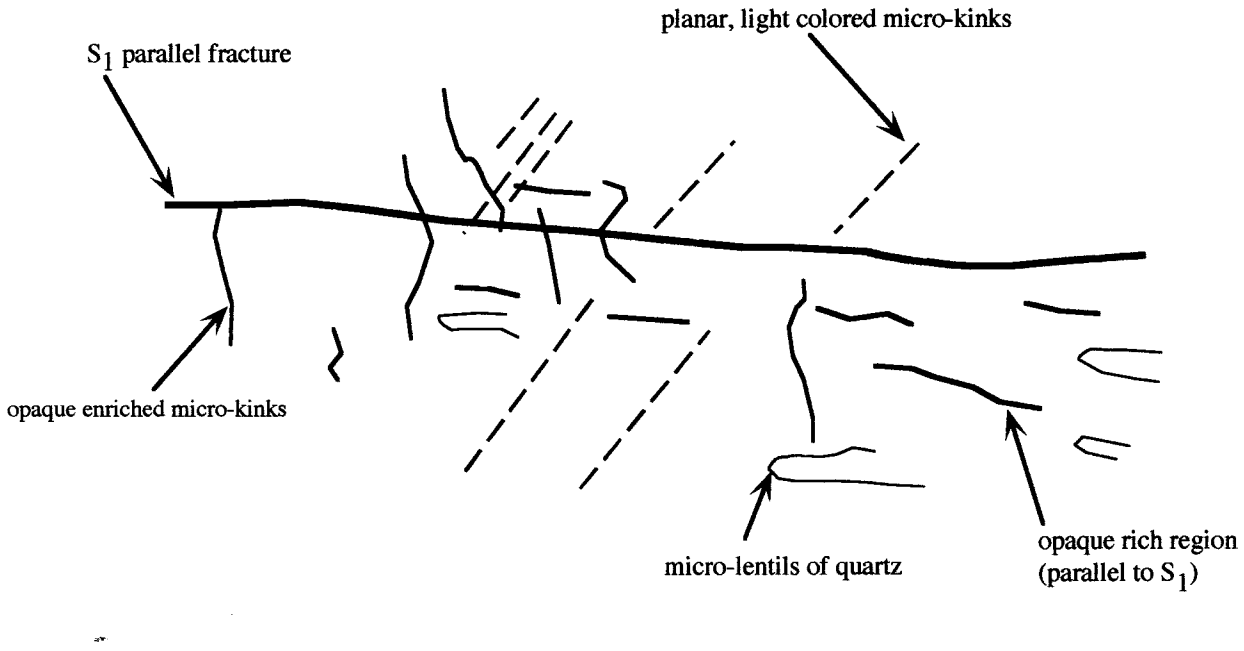

Fig.5.12) Thin section and line drawing from station 45.

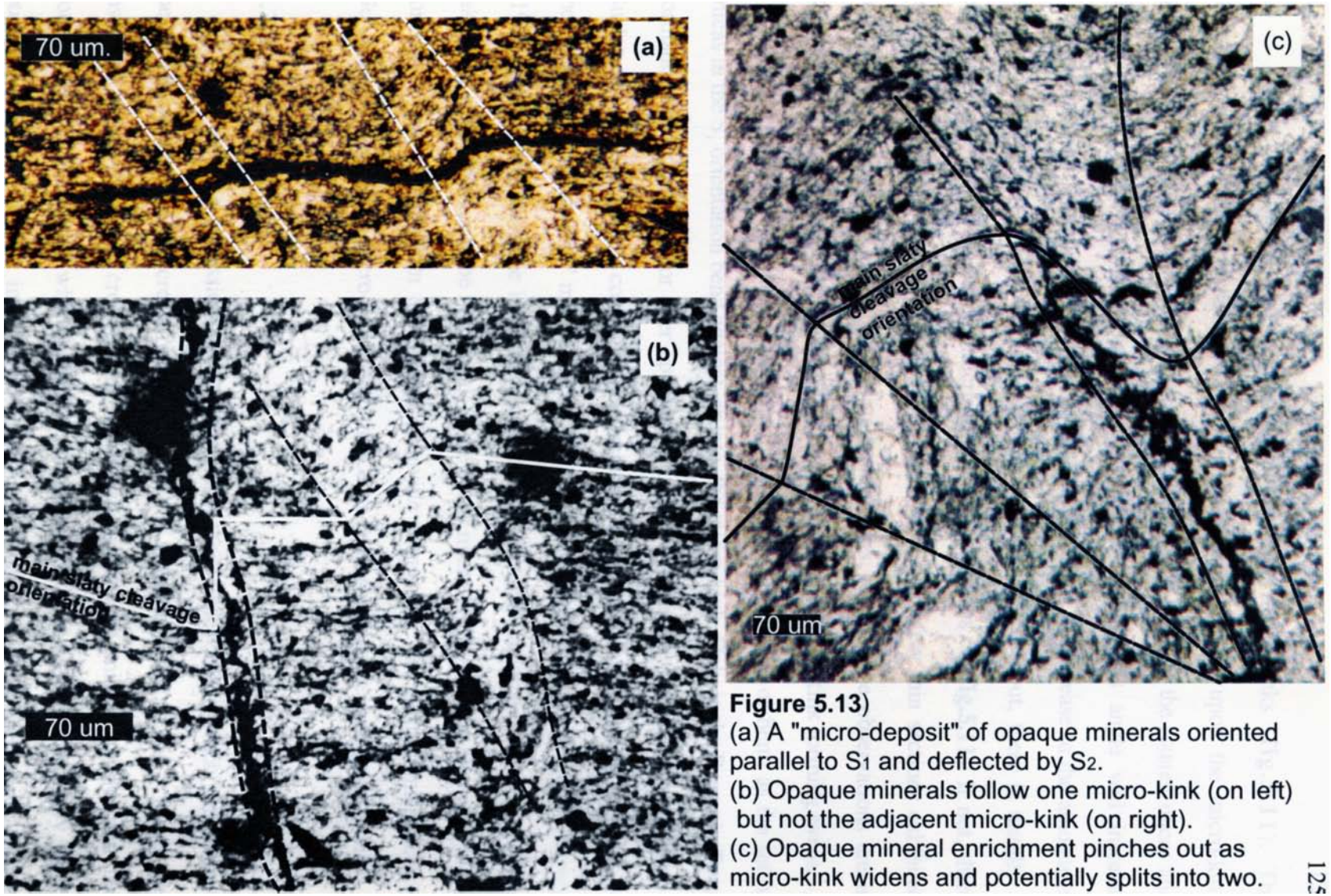

Figure 5.13)
(a) A "micro-deposit" of opaque minerals oriented parallel to S_1 and deflected by S_2.
(b) Opaque minerals follow one micro-kink (on left) but not the adjacent micro-kink (on right).
(c) Opaque mineral enrichment pinches out as micro-kink widens and potentially splits into two.

Micro-kinks taper, widen, and branch into new micro-kinks (**fig.5.11**). The degree of rotation that occurred within a micro-kink is dependent upon the micro-kink geometry. For example, as a micro-kink widens, the angle between the rotated micas and the main slaty cleavage decreases. As a micro-kink tapers, this angle will increase (**fig.5.14**). Alternatively, the micro-kink may taper without an increase in the amount of rotation and "pinch out" (**fig.5.15a**). After a micro-kink pinches out, there is usually a conjugate or branch of the "dead" micro-kink which continues on (**fig.5.11**). If not, there is an immediately adjacent tip of a different micro-kink. Very few thin sections exhibited micro-kinks which were planar, parallel and continuous. All of these observations are in keeping with somewhat brittle behavior of the slate during the micro-kink forming event.

Mica grains are occasionally observed to be internally kinked, or bent, as the set of micas in the S_1 orientation bend against, or into, the micro-kink. Only in the Brown's Pond formation does this behavior ever approach a classic crenulation cleavage (**fig.5.15b**). Such a crenulation cleavage could also be considered a "normal" micro-kink as opposed to the more common "reverse" micro-kinks. This terminology was first proposed by Dewey (1965) and follows the same logic as discussions of "normal" faults and "reverse" faults, taking the slaty cleavage to be horizontal. Some of the micro-kinks from the Brown's Pond formation, and locally from the Middle Granville formation, are normal micro-kinks. Generally, however, the micro-kinks from the Cedar Point slates are reverse micro-kinks.

5.2.3. Cross-Micas

The following discussions are descriptions of those observations which supplement the initial observation of cross-micas by Prof. W.D.Means (**fig.5.16**). These are instances where there are cross-cutting relationships between mineral grains and the boundaries of a micro-kink which cannot be explained by the micro-kink geometry. Such examples can be separated into "type" cross-micas, with a well defined cross-cutting

Figure 5.14) A micro-kink from station 41 tapers and widens with increases and decreases in the amount of rotation within the micro-kink. Lines are added to highlight the preferred orientation of micas within the micro-kinks, and within the main slaty cleavage. At this scale it is difficult to be certain about cross- cutting relationships, though the boxed region (right) shows a set of micas which seem to cross-cut the micro-kink band boundaries.

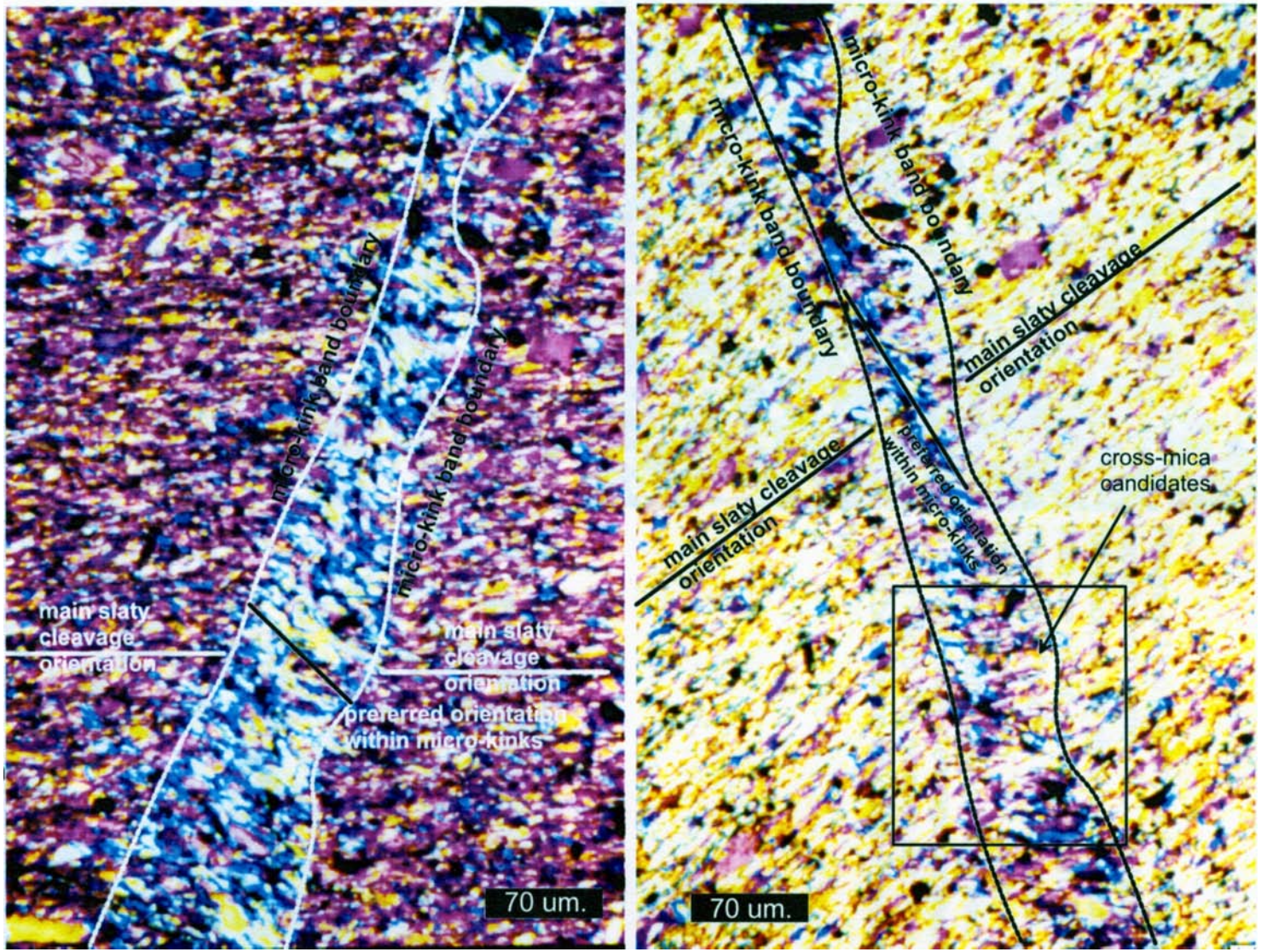

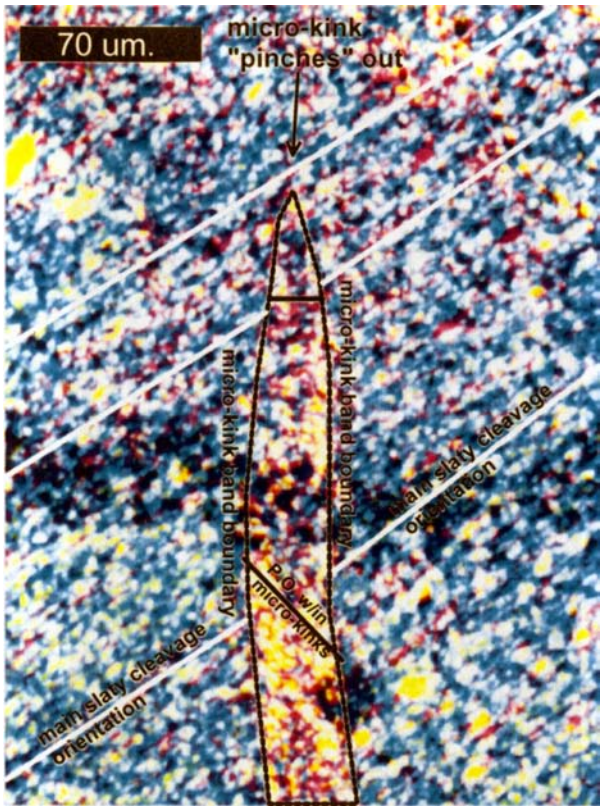

Figure 5.15a) A micro-kink in a thin section from station 41. The black mark across the slide is a scratch from the silicon carbide polish. The micro-kink "pinches out" towards the top of the photo. The angle between rotated grains and grains in the main slaty cleavage decreases as the micro-kink pinches out. This would be a micro-kink of the reverse type.

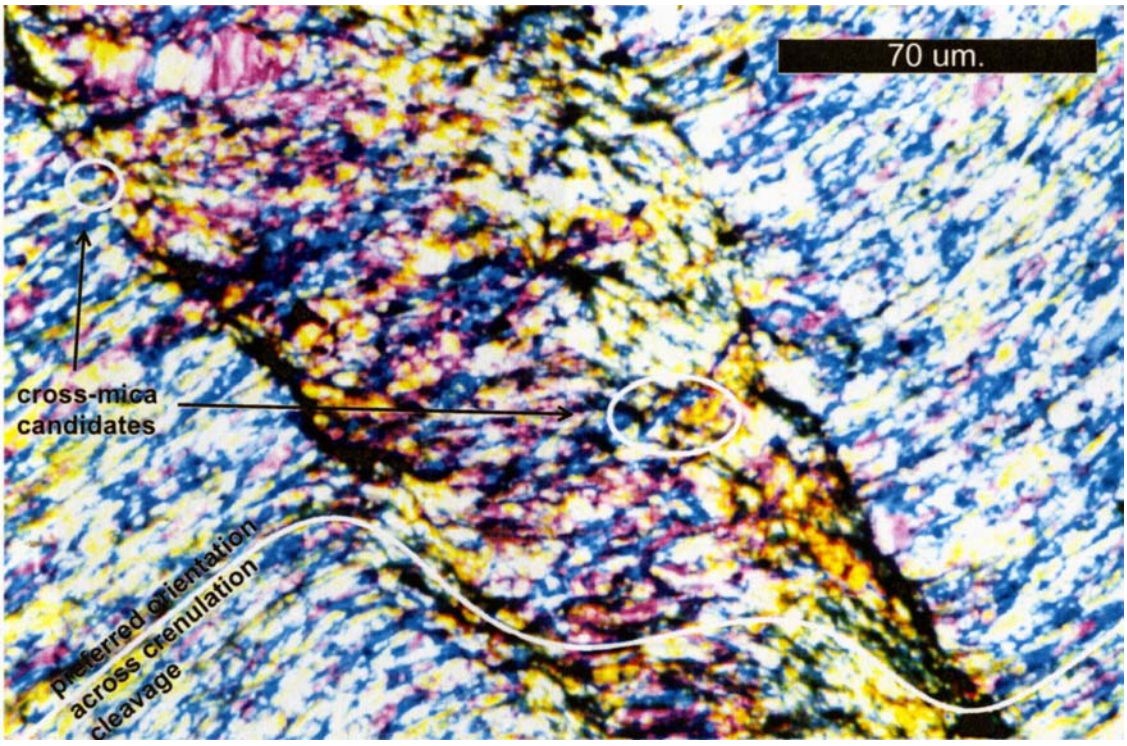

Figure 5.15b) S_2 in the Brown's Pond Formation is more like a crenulation cleavage, rather than a micro-kink, as found in the Middle Granville Formation. This would be a normal micro-kink. Here micas "bend" into the crenulation. Some of the birefringent mineral grains (circled) are candidates for cross-micas

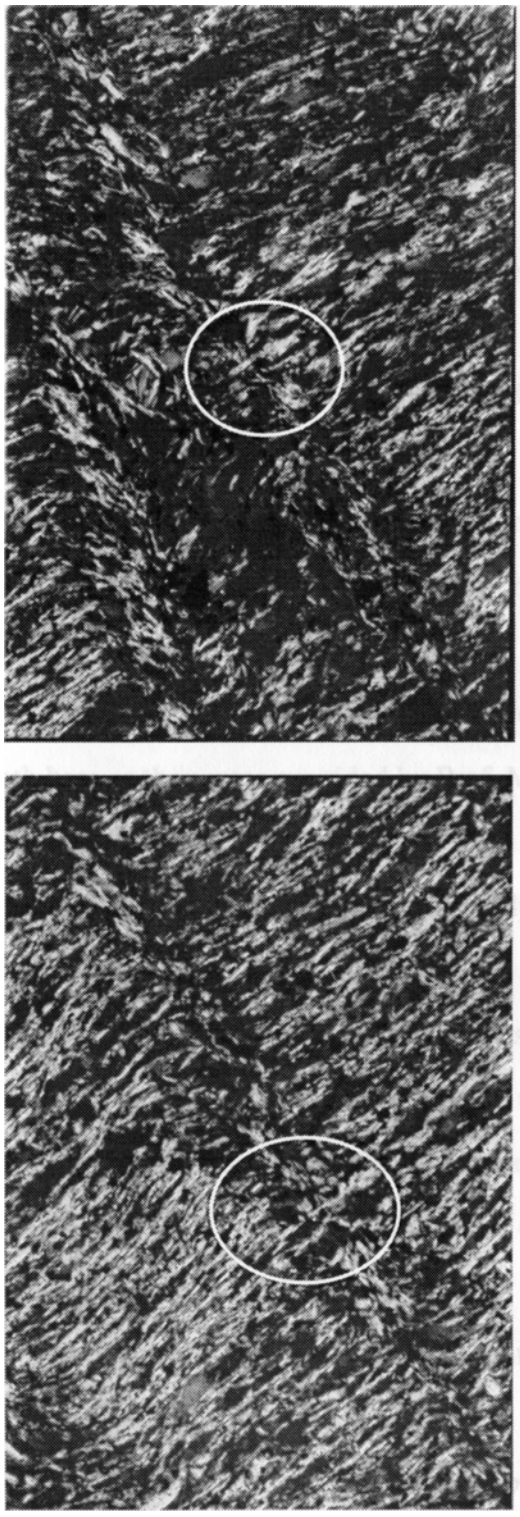

Figure 5.16) Photomicrographs of cross-micas, courtesy of W.D. Means. These were some of the first cross-micas observed in the Cedar Point Slates. In the top photomicrograph a mica in the main slaty cleavage orientation cross-cuts the right micro-kink band boundary. In the lower photomicrograph a cross-mica cross-cuts the entire micro-kink.

relationship, and cross-mica "candidates", those micas which have a cross-cutting relationship with surrounding structures (or are in a different orientation than the local preferred orientation) but where the cross-cutting relationship may be apparent (i.e. an artifact of view)

Cross-micas are best observed using polarized light and a gypsum plate. The gypsum plate helps to increase the contrast between the set of micas in the main foliation orientation and the set of micas in the rotated orientation. By first aligning the main foliation to the horizontal axis of the field of view (such that micas in the main slaty cleavage orientation reach extinction) and then rotating the stage 45 degrees, the micro-kink band boundaries can be defined and any grains cross-cutting the micro-kink band boundary can be observed (**fig.5.14**).

The cross-micas in **figure 5.16** are "type" cross-micas, but are not discussed at length here as they were provided by Prof. Means while this thesis was in preparation, and the thin sections and sample localities were not studied by this author. The "type" cross-micas, collected over the course of this study are from station L.E.C. (**fig.5.17, 5.18**). A micro-kink is well defined though it tapers towards the lower part of the photomicrograph. Two large micro-deposits of opaque minerals serve as a marker from one view to the next. It is readily apparent that several of the grains, and in particular the large grain in the middle of the photomicrograph, cut the micro-kink band boundary without being deflected. There is no optical difference between the micas in the main slaty cleavage orientation and the rotated micas.

In **figure 5.19** there is an excellent view of a micro-kink tapering and widening. The grains in the tapered sections (yellow) are birefringent with an orientation at a high angle to the main slaty cleavage orientation. Against the rightmost boundary, a set of birefringent micas (blue) remain in the slaty cleavage orientation through this portion of the micro-kink. There is roughly a twenty degree difference between these grains (in blue) and

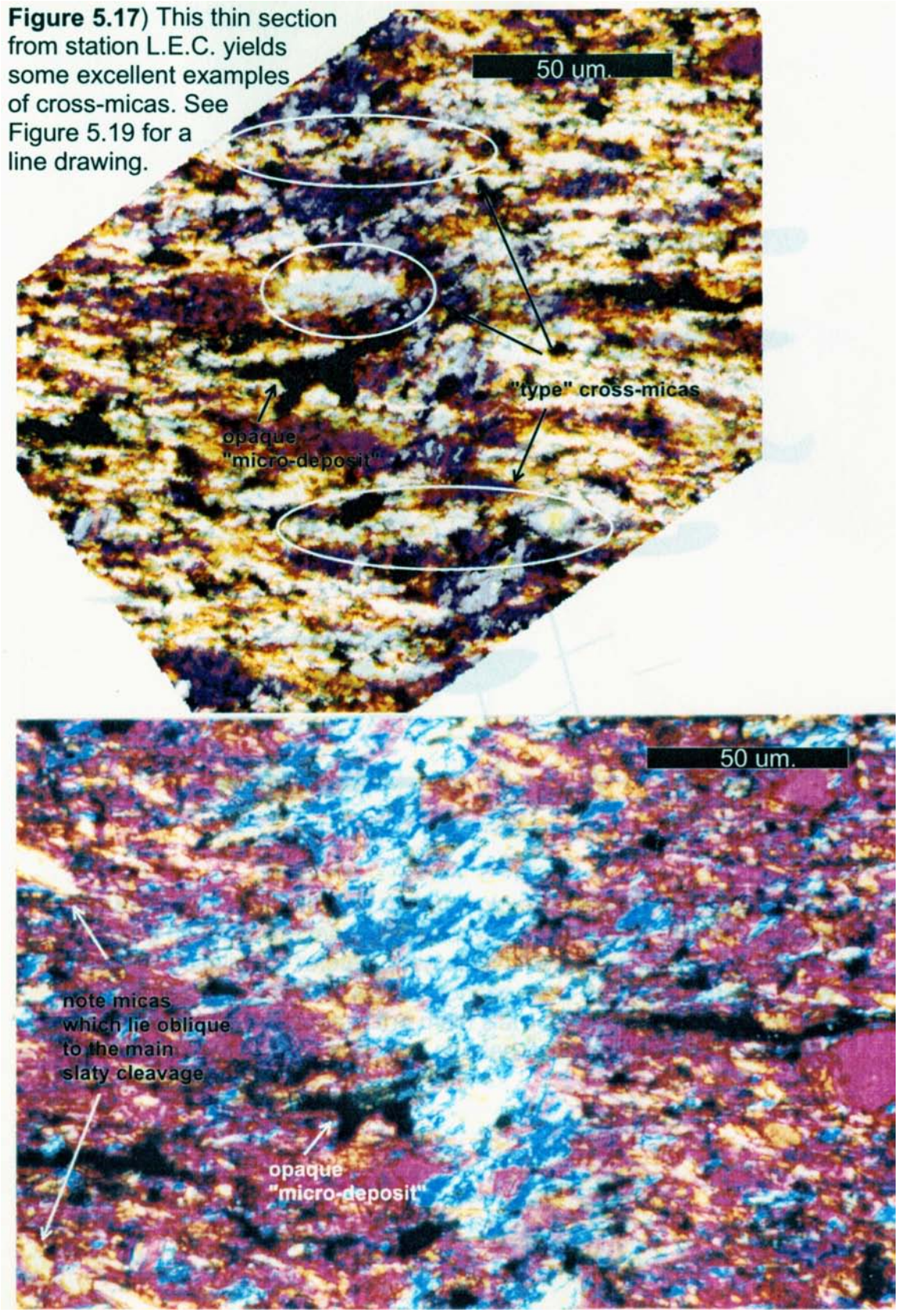

Figure 5.17) This thin section from station L.E.C. yields some excellent examples of cross-micas. See Figure 5.19 for a line drawing.

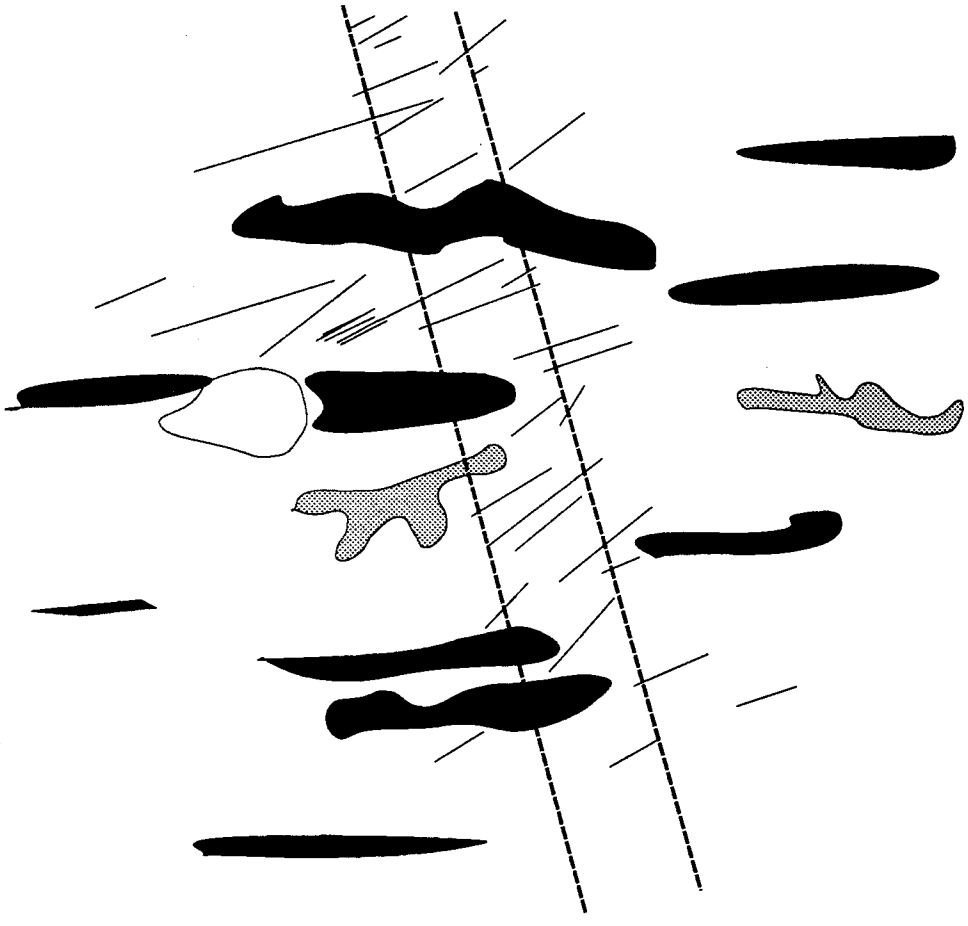

Figure 5.18) A line drawing of the photomicrographs in Figure 5.18 showing micas in the main slaty cleavage orientation (black) juxtaposed against micas in the rotated orientation (lines). The micro-kink band boundaries are drawn as a most conservative estimate of width. Note how several of the micas in the main slaty cleavage orienation cross the boundaries undeflected. The shaded grains are the large deposits of opaque minerals.

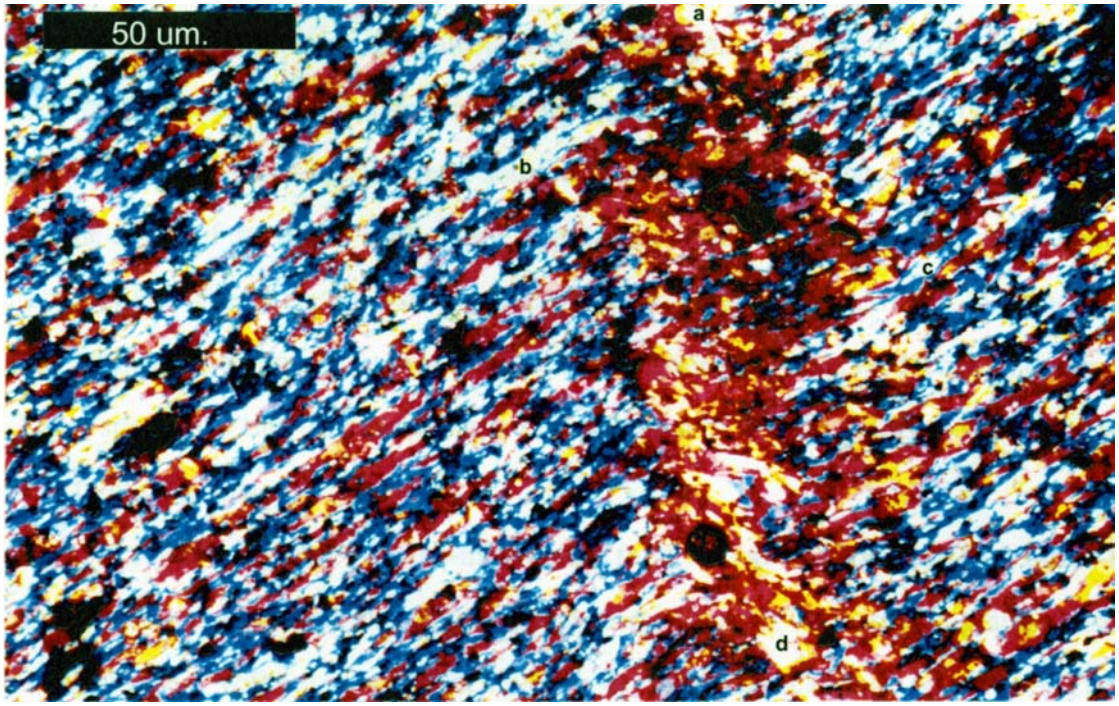

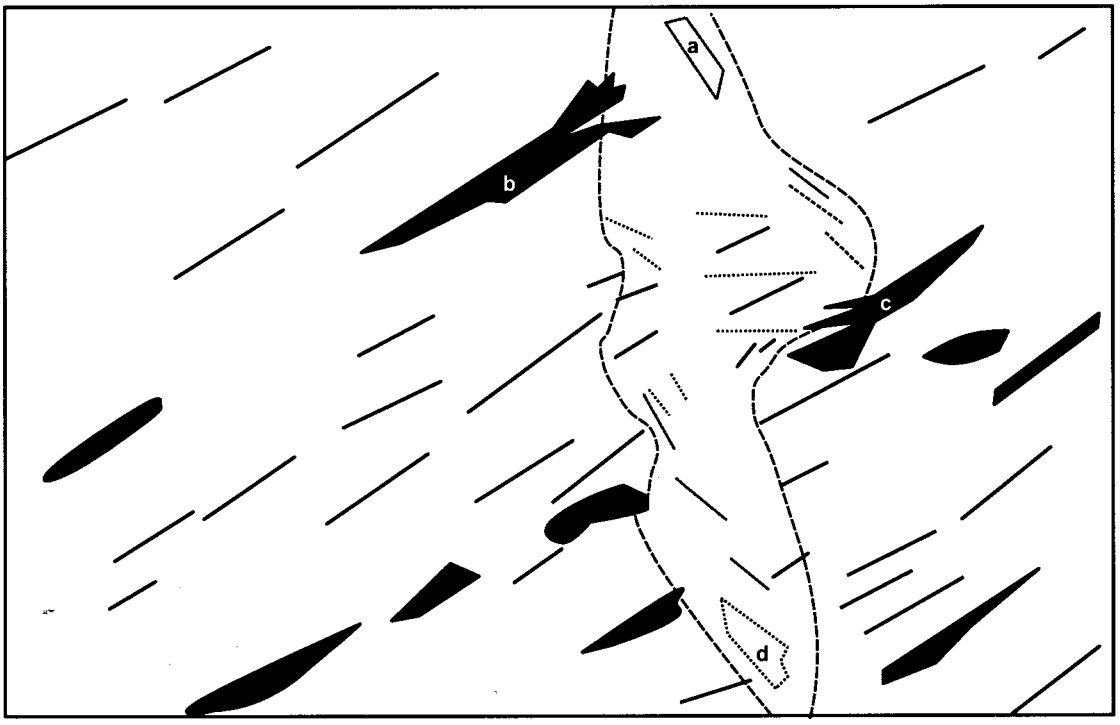

Figure 5.19) This section (from L.E.G.) shows the tapering and widening of a micro-kink accompanied by changes in the amount of rotation of micas (dashed). Within one of the wider regions of the micro-kinks, many grains lie in the main slaty cleavage orientation, undeflected (solid). Larger grains also have ends which cross the micro-kink band boundaries. Some grains are labeled to help orient the sketch to the photomicrograph.

the preferred orientation of the surrounding grains (either extinct or in yellow). Though some of these may have an *apparent* cross-cutting relationship related to the tapering and widening of the micro-kink, at least some of them extend from the slaty cleavage directly into the center of the micro-kink. These approach a "type" cross-mica though the complex micro-kink geometry creates a setting where a "type" cross-mica is difficult to demonstrate. It is interesting to note how some of the larger grains have splayed ends and irregular shapes suggesting that they are perhaps a combination of several grains too fine to resolve as individual grains.

Another example of a cross-mica comes from station 41 (**fig.5.20**). A micro-kink bends, widens, and tapers throughout the photomicrograph. At least two grains cross the entire boundary without being deflected from the main slaty cleavage orientation. Though not the best examples of cross-micas because of the poorly defined micro-kink, this slide shows how the micas in the slates often have different habits. These grains have asymmetric ends or "caps" which splay off of the main grain, or packages of grains. This is in contrast to the habit of the mica grains in **figure 5.17**.

From the same thin section, the two photomicrographs in **figure 5.14** show a micro-kink with well defined micro-kink band boundaries. The micro-kink tapers and widens and a large section of the rightmost boundary bends into the micro-kink. A best estimate for a micro-kink band boundary was drawn on the photomicrograph where the micas in the main slaty cleavage orientation are extinct, and the rotated micas are birefringent. This boundary was transferred to the photomicrograph where the slaty cleavage micas are birefringent and rotated micas are extinct. There is no clear example of a single cross-mica here. Rather, there is a lower apparent thickness for the micro-kink in the photomicrograph where the main slaty cleavage is birefringent. In the lower portion of the micro-kink, some slaty cleavage micas (in yellow) seem to cross the entire micro-kink,

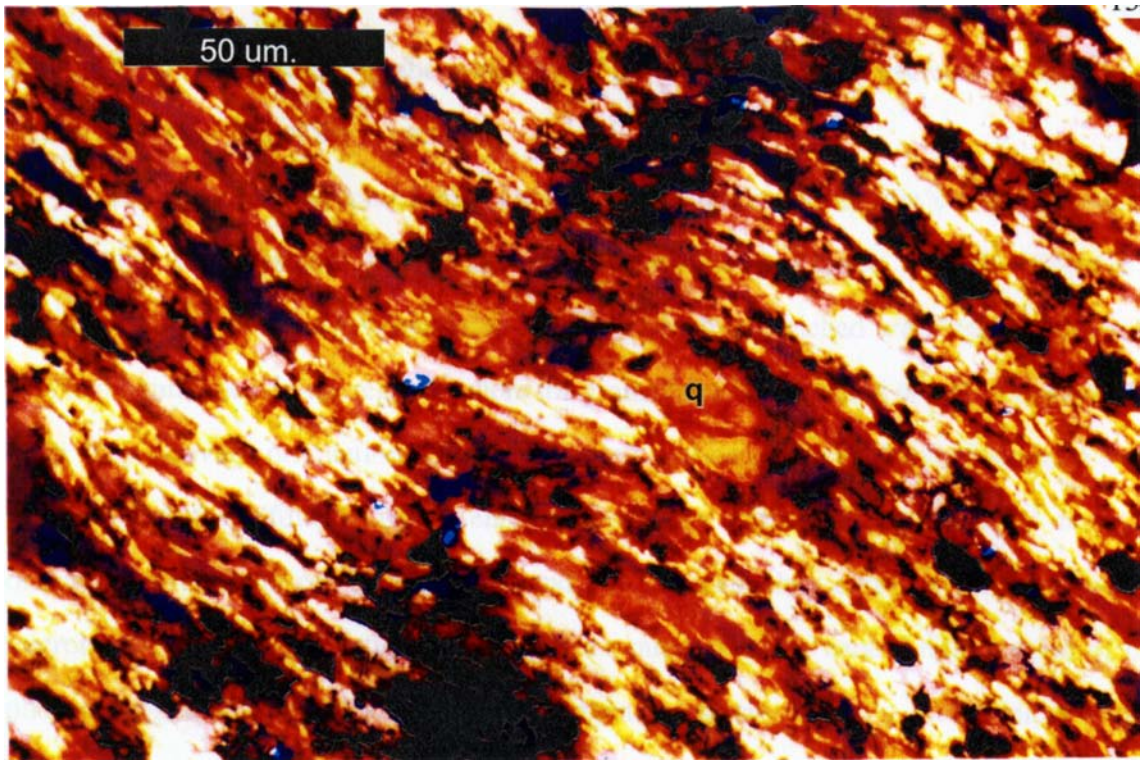

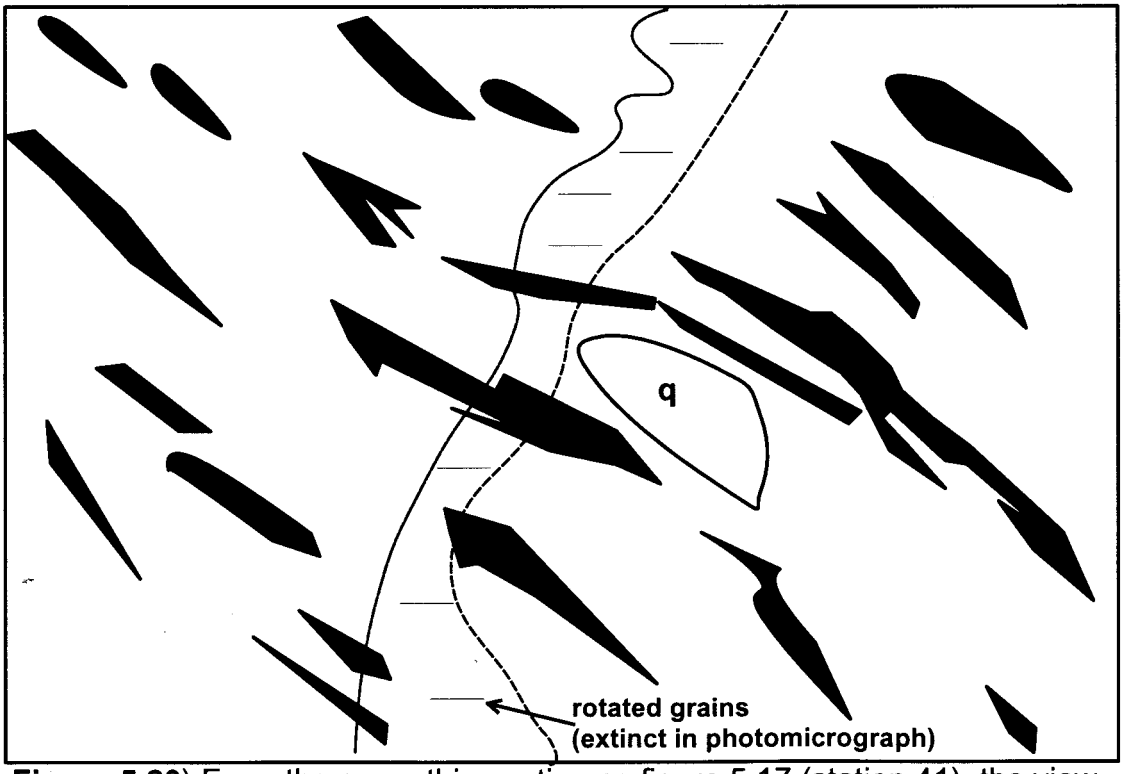

Figure 5.20) From the same thin section as figure 5.17 (station 41), the view of the micro-kink boundaries reveals large grains cutting across them, undeflected. Note the wide, aesymmetric ends on some of the larger grains. The large grain of quartz is marked **q** to orient the sketch to the photo-micrograph.

though this is complicated by the widening of the micro-kink, and decrease in rotation of micas, at that section of the micro-kink.

The photomicrograph of the crenulation cleavage in the Brown's Pond formation also yields some examples of cross-mica "candidates". **Figure 5.15b** displays a crenulation with two distinct boundaries, each of which is enriched with opaque minerals. The two boundaries define regions where the grains have been rotated to a high angle to the main slaty cleavage orientation. On the upper left portion of the photomicrograph, a large grain crosses the leftmost opaque enriched boundary without being deflected from its orientation. The grain can be seen to extend into the main slaty cleavage for over twenty microns and into the crenulation for less then ten microns. In the central right portion of the photomicrograph, a mica, with blue birefringence, crosses across a set of micas which have a preferred orientation at a high angle to the main slaty cleavage. This mica is in the main slaty cleavage orientation though it does not cross into the main slaty cleavage; a cross-cutting relationship with the crenulation boundaries is not observed. Because of the complex crenulation geometry surrounding these micas, they are both considered "candidates" for cross-micas, and not "type" examples.

The latter observations of cross-micas presented above could have resulted from complex micro-kink geometries and not from an actual cross-cutting relationship. Clearly, the best examples are found at higher magnifications where there are simpler micro-kink geometries, such as in **figure 5.17**. The last example of a cross-mica is in **figure 5.21a**. Viewed at high magnification, a thin and long grain of mica is cutting a micro-kink band boundary. The bright yellow grains in the center of the photo define the micro-kink and the host of dark blue grains define the main slaty cleavage. This mica crosses the boundary, and its end shares the micro-kink with rotated grains. Unfortunately, at this magnification, the larger scale micro-kink morphology is not clearly defined. At lower magnifications, this cross-mica is barely visible. One conclusion which can be drawn from

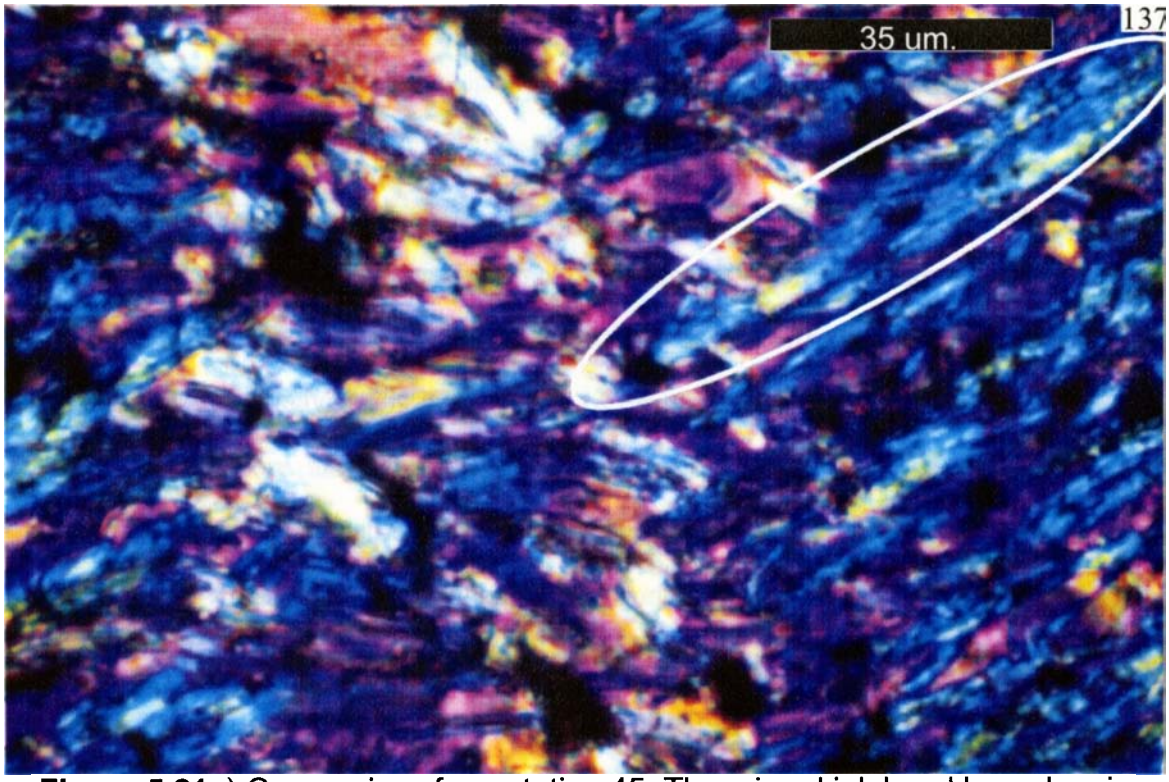

Figure 5.21a) Cross-micas from station 45. The micro-kink band boundary is poorly defined at this scale. However, many of the blue grains are present in regions dominated by yellow or extinct grains. Note the phyllosilicate material on the end of the circled cross-mica.

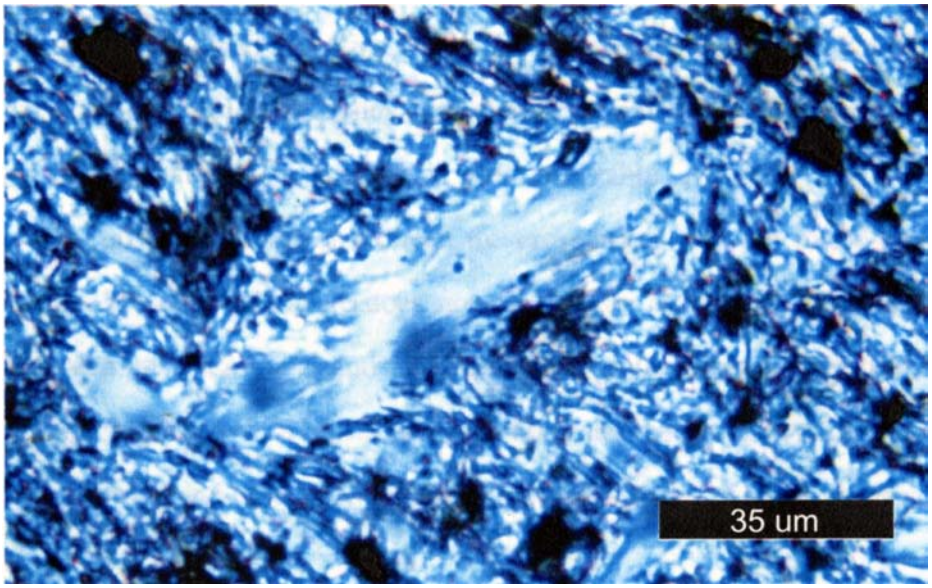

Figure 5.21b) This is a cross-mica of a different kind. This grain has its 001 face oriented sub-normal to the preferred orientation of the surrounding micas. Note the blue to green phyllosilicate (chloritic) material which seems to wrap around both this mica, and the surrounding minerals.

the observations presented in this section is that because of the contrasting scales of the micro-kinks and the micas, cross-micas are difficult to document.

It is interesting to note the "wispy" ends coming off the cross-mica in **figure 5.21a**. Difficult to see in polarized light, this mineral habit is commonly seen in plane light. The best example is in **figure 5.21b**. This mica, with its 001 face normal to the surrounding slaty cleavage, is not the type of cross mica discussed in this thesis. Rather, this would be more akin to the type of mica observed by Beutner (1978) which he interpreted to represent detrital grains. Whatever the origin of this grain, it exhibits an example of phyllosilicate overgrowths on the boundaries of the larger grain of mica. This is common on many of the examples of cross-micas observed. This includes the figures presented here, though with the exceptions of **figure 5.21** and **figure 5.17** the overgrowths are too fine grained to observed in the photomicrograph.

The overall observation presented in this discussion of cross-micas is that cross-micas can be observed optically, both as grains which cross-cut one micro-kink band boundary, and also as grains which cut across the entire micro-kink. Cross-micas can be observed at a variety of scales, although at extremely high magnifications the morphology of the surrounding micro-kink is not observable. At lower magnifications the detailed cross-cutting relationship between the cross-micas and the micro-kink band boundaries cannot be observed. There does not seem to be an optically distinguishing characteristic between the cross-micas and the surrounding grains. However, between samples there is a change in the overall mica habit in the slate, with some mica grains having chloritic overgrowths and others being chlorite free. This is discussed at greater lengths in **section 5.3**.

2.5.4. Discussion - Products of Solution Processes

Having documented that there are micas which cross-cut the micro-kink band boundaries, there is a need to ask the following question: is there any other petrographic evidence to support mineral growth which post-dates the deformation which produced S_2? The field scale evidence supports the notion that deformation may have continued after the formation of S_2. However, this deformation was likely to have been bedding parallel slip, localized to particular bedding horizons, and may have been continuous throughout the evolution of the Cedar Mountain Syncline.

There is also field evidence for solution processes, in the form of veins which are distributed throughout the slates. Solution processes are not a requirement for mineral growth as phase changes can occur without the presence of free aqueous solution. However, the presence of veins, and the distribution of the products of solution transfer throughout the slate, suggests an environment amenable to mineral growth. This is especially true for low grade shales and slates (Lee et. al., 1984). If there were evidence for the dissolution and reprecipitation of mineral phases after the formation of S_2, this would also be evidence to support the hypothesis of either late, or post- deformation mineral growth.

The "micro deposits" of opaque minerals in the S_1 orientation are deformed by the same rotation which created S_2 (**figure 5.13a**). This can be interpreted two ways. There may have been an enrichment of opaque minerals prior to the episode of deformation which produced S_2, and this micro-deposit was later deformed by the micro-kinking event. Alternatively, these micro-deposits may represent a consolidation of opaque minerals after S_2 developed, during solution transfer along S_1. This set of micro-deposits may have developed mimetically, following the deflection in the main slaty cleavage orientation. This latter possibility is more likely, as a period of post- S_2 formation solution transfer is interpreted to have occurred and to have been localized along micro-kinks. Therefore a pre-

existing cross-cutting micro-deposit of opaques would likely have been "destroyed" during this later solution event.

There is further evidence for free solution transport occurring after the formation of S_2. In **figure 5.13b**, one micro-kink is enriched with opaque grains and an adjacent micro-kink, which is a branch of the other, is not. If it is assumed that these two micro-kinks formed at the same time, why would one accumulate opaque minerals while the other remained free of opaque minerals? This preferential coating of one micro-kink over the other suggests that the origin of these opaque "streams" was a solution process. The micro-kink network acted as a plumbing system for a modest, but pervasive micro-hydrologic system.

Backscatter imagery reveals that some micro-kinks are enriched with phyllosilicates (**fig.5.22a**). Other micro-kinks are enriched with opaque minerals. It seems reasonable to believe that there was mass transfer along these micro-kinks which removed phyllosilicates from some micro-kinks (and perhaps quartz as well) and left the opaque minerals as residue. The alternative, not mutually exclusive, is that opaque minerals dissolved and re-precipitated along micro-kinks. This latter suggestion is supported by the petrographic observations. In order to relate the dissolution and reprecipitation of micas to the opqaque minerals would require extensive (and complex) modeling of the mica system. Nonetheless, free solution was likely present during a late to post- S_2 period and thus a transport mechanism for necessary ions for a mica growth event was present.

This study does not go any further than to suggest that the necessary data is present in the slates to model any changes in the mica system after the formation of S_2. Such a petrological / geochemical model involving oxide, sulfide, and phyllosilicate phases would be an important step in the argument for, or against, cross-micas representing widespread late growth in the Cedar Point slates. Such a study would also be relevant to paleo-

magnetic studies of slates, such as those done by Housen et. al. (1993), which suggest that oxide dissolution and neo-crystallization can produce a late magnetization event.

5.3. Geochemical Observations

This investigation of the cross-micas at Cedar Point relies heavily on data attained with field and optical techniques. As the cross-micas are optically indistinguishable from the surrounding micas, other data must be attained in order to address outstanding problems. The most pertinent problem is whether the cross-micas represent "localized" post- S_2 growth, "widespread" post- S_2 growth, or "no" post- S_2 growth. The last possibility would be the case if the cross-micas are the result of purely rotational processes. An example of this could be if some number of micas were at an angle to the slaty cleavage prior to micro-kink formation and were rotated into their cross-cutting orientation by the same deformation which produced the micro-kinks. If this is the case, an electron microprobe analysis of a cross-mica would show similar chemical characteristics on both sides of the micro-kink band boundaries. If the cross-micas represent widespread mica growth throughout the rock, electron microprobe analyses would also show that cross-micas have similar chemical characteristics across the entire grain. If the localized mica growth hypothesis is the case, then the cross-micas would have different chemical characteristics on each side of the micro-kink band boundary (**fig.4.6**). Thus, theoretically, it should be possible to either confirm or reject the localized growth hypothesis. Additional observations would then be needed to confirm a "widespread" mica growth event.

Unfortunately, this study was only able to attain a small chemical database from the electron microprobe, and little of the data helped shed any light on the above mentioned problems. If anything, the microprobe data provided a picture far more complex than the

(already complicated) petrographic and field data. Nonetheless, this data is presented here and yields some useful and interesting results.

5.3.1. Chemical Composition of the Phyllosilicate Minerals

A total of twelve thin sections were studied using S.E.M. backscatter imagery at the electron microprobe. Full analyses were done on four thin sections using an acceleration voltage of 15kV and a probe diameter of <1um.. The culmination of this data is presented in **Table 5-5** and **Table 5-6**. The standard deviation of the measurements was calculated on the S.U.N.Y. Binghamton laboratory standards and on 39 of the measurements (calculated by the system software using the peak width). The average of these 39 measured standard deviations, as well as the standard deviation of measurements of the laboratory standards are reported at the end of **Table 5-5**. This gives a good indication of the uncertainty (precision) associated with each measurement.

An indication of how well the tabulated chemical data describes the mineral chemistry is the totals of the oxide weight percents which are generally above 90% and most near 100% (including H_2O). Measurements with total oxide weight percents less than 90% are included in **Table 5-5**. These measurements usually represent the presence of chlorite or interlayered muscovite and chlorite. To accurately record the mineralogy of chlorite these measurements would need to be recalculated (chlorite composition requires 36 H_2O and muscovite 24 H_2O). However, this is not done in this thesis as there is a gradation in the amount of chlorite - muscovite interlayering, and no "pure" muscovites or chlorites exist in the slate (as discussed in the next section). In addition, the data tables (**Table 5-5, 5-6**) represent successive traverses across micro-kinks, and this format is desired for future reference. For these reasons the chlorite and muscovite minerals on **Tables 5-5** and **5-6** are kept on the same table and not calculated with separate amounts of H_2O.

The phyllosilicate mineralogy could be considered to be dominantly illite ($K_{1.5-1.0}Al_4[Si_{6.5-7}Al_{1.5-1.0}O_{20}](OH)_4$) because of the relatively high SiO_2 and low K_2O, relative to a true muscovite ($K_2Al_4[Si_6Al_2O_{20}](OH)_4$), in most of the micas analyzed (**Table 5-6**, **Fig.5.26**). However, the term illite implies a grain size <2 um. (Srodon and Eberl, 1984) and thus these phyllosilicates are considered part of the muscovite series. Ca (not shown in the above tables), when measured, was virtually absent (CaO<.02 wt.%). The common mica is therefore considered to be a muscovite and perhaps a phengitic muscovite due to the relatively high SiO_2 and FeO values, and the low K_2O values (relative to true muscovite). Lee et. al. (1984) remark that phengitic values from muscovites can be the result of contamination from adjacent and intergrown chlorite (at the angstrom scale). Despite this, their study concluded that some component of the phengitic values do represent a solid solution trend towards phengite. This study considers the major phyllosilicate component to be a phengitic muscovite and discusses this topic further in the next two sections. The other major constituent of the mineralogy of the rock is chlorite. Chlorite too is discussed in the next two sections.

Table 5-5) Oxide Weight Percent - Electron Microprobe Analyses

Sample L.W.C.

Analysis No.	Na2O (wt.%)	K2O (wt.%)	MgO (wt.%)	Al2O3 (wt.%)	SiO2 (wt.%)	FeO (wt.%)	Total (wt.%)
1	0.057	7.975	3.497	26.569	54.41	4.407	96.916
2	0.242	7.753	3.243	26.625	54.83	3.709	96.406
3	0.047	7.758	3.467	26.338	55.174	3.693	96.488
4	0.447	8.19	3.523	25.703	56.37	4.041	98.275
5	0.212	8.431	3.289	26.478	54.34	4.376	97.126
6	0.037	5.924	9.913	25.106	46.11	8.55	95.645
7	0.055	7.922	3.228	25.609	55.014	3.986	95.825
8	0.074	7.788	3.445	27.399	53.896	3.848	96.46
9	0.015	4.097	13.341	22.552	40.162	11.329	91.519
10	0.01	7.816	2.951	27.448	54.248	4.163	96.646
11	0.034	8.426	3.458	25.662	53.77	4.098	95.456
12	0.178	7.532	4.036	26.471	53.861	4.176	96.266
13	0.052	8.403	3.096	26.925	53.928	3.739	96.152
14	0.117	4.484	11.906	25.137	42.098	10.136	93.896
15	0.051	7.618	3.808	26.919	53.351	5.022	96.778
16	0.069	7.923	3.213	26.751	52.095	3.88	93.949
17	0.127	5.115	2.636	26.018	60.234	2.678	96.82

Sample L.E.G.

Analysis No.	Na2O (wt.%)	K2O (wt.%)	MgO (wt.%)	Al2O3 (wt.%)	SiO2 (wt.%)	FeO (wt.%)	Total (wt.%)
1	0.11	9.717	3.248	25.441	52.783	8.611	99.91
2	0.015	0.305	17.495	19.255	30.485	20.848	88.4
3	0.081	9.728	3.427	25.698	54.077	4.647	97.66
4	0.12	9.467	3.017	23.203	61.002	4.446	101.3
5	0.329	9.405	3.665	25.772	54.943	5.096	99.21
6	0.055	0.04	17.958	20.363	27.723	21.825	87.96
7	0.02	0.045	17.43	19.937	27.294	21.286	86.01
8	0.043	1.741	12.907	21.131	32.939	17.619	86.38
9	0.067	10.063	3.35	26.102	53.672	4.592	97.85
10	0.194	9.038	3.48	24.618	52.192	9.913	99.44
11	0.054	0.365	18.447	20.254	29.762	20.114	89
12	0.113	9.691	2.816	27.794	54.324	3.912	98.65
13	0.055	8.052	5.449	25.463	49.895	8.351	97.27
14	0.178	9.638	3.461	26.835	51.214	5.738	97.06

Table 5-5) Oxide Weight Percent - Electron Microprobe Analyses

Sample 41

Analysis No.	Na2O (wt.%)	K2O (wt.%)	MgO (wt.%)	Al2O3 (wt.%)	SiO2 (wt.%)	FeO (wt.%)	Total (wt.%)
1	0.115	0.488	19.034	21.087	28.886	18.197	87.819
2	0.149	8.048	0.893	30.286	49.768	3.929	93.073
3	0.09	8.148	2.539	28.36	54.361	2.876	96.374
4	0.028	0.606	17.458	20.129	29.744	19.699	87.682
5	0.034	8.046	3.354	27.613	54.696	3.521	97.264
6	0.059	7.098	4.556	25.681	48.999	7.333	93.726
7	0.014	0.12	18.495	19.751	28.29	19.752	86.422
8	0.069	7.737	3.041	25.891	56.863	4.24	97.841
9	0.036	8.061	3.565	27.263	53.409	4.711	97.045
10	0.075	7.69	3.387	28.443	53.031	4.308	97.002

Sample 45a

Analysis No.	Na2O (wt.%)	K2O (wt.%)	MgO (wt.%)	Al2O3 (wt.%)	SiO2 (wt.%)	FeO (wt.%)	Total (wt.%)
1	0.074	10.213	3.52	25.472	56.015	3.97	99.313
2	0.134	10.015	3.634	27.08	54.449	3.889	99.327
3	0.113	9.942	3.626	26.944	54.766	3.988	99.51
4	0.152	10.167	3.573	26.069	54.147	4.678	98.917
5	0.915	9.792	3.726	24.408	51.416	4.557	94.964
6	0.14	9.936	4.263	26.221	53.919	3.522	98.121
7	0.131	3.633	16.306	23.253	38.903	11.703	94.048
8	0.138	10.435	3.881	26.061	54.954	3.631	99.239
9	0.174	9.796	4.294	26.318	53.015	3.719	97.431
10	0.144	10.185	4.425	25.856	54.769	4.423	99.907
11	0.225	10.143	3.609	27.119	54.912	3.349	99.477
12	0.115	7.229	8.958	24.601	47.551	7.856	96.44
13	0.22	10.736	3.011	26.759	51.777	4.229	96.856
14	0.243	10.124	3.542	25.132	52.433	4.133	95.748
15	0.21	10.3	3.877	27.437	56.558	3.288	101.797
16	0.142	10.031	3.928	26.539	54.544	3.613	98.916
17	0.159	10.04	3.887	26.813	54.242	3.374	98.624
18	0.275	7.013	8.047	23.919	47.821	8.922	96.178
19	0.181	7.95	8.237	25.133	49.413	6.057	97.111
20	0.14	9.652	3.79	26.505	54.16	3.622	98.003
21	0.244	10.027	3.713	25.852	54.249	3.573	97.793
22	0.304	9.852	3.612	25.049	53.787	3.557	96.298
23	0.217	10.158	3.473	26.038	53.397	3.681	97.106
24	0.228	9.732	3.129	25.725	50.989	3.531	93.468
25	0.227	9.782	3.528	26.993	51.416	3.589	95.667

Table 5-5) Oxide Weight Percent - Electron Microprobe Analyses

Standard Deviation (%) associated with each measurement as calculated from laboratory standards.

Na2O	K2O	MgO	Al2O3	SiO2	FeO
0.76	0.46	0.13	0.14	0.11	0.28

Standard Deviation (%) associated with each measurement. Calculated as the mean of the standard deviation of standard deviation of 39 separate analyses, each calculated by the system software using the analysis peak width and the analysis counting time.

Na2O	K2O	MgO	Al2O3	SiO2	FeO
11.6	2.17	0.59	0.23	0.24	2.37

Table 5-6) Cation Totals - Electron Microprobe Analyses calculated for 24 Oxygens (i.e. calculated for muscovite composition)

Sample L.W.C.

No.	Na	K	Mg	Al	Si	Fe	Total	Comment
1	0.0156	1.4378	0.7367	4.4254	7.6888	0.5208	14.8252	
2	0.0663	1.3976	0.6831	4.4343	7.7473	0.4383	14.7675	
3	0.0129	1.3959	0.7289	4.3782	7.7811	0.4356	14.7341	
4	0.1206	1.454	0.7308	4.2157	7.844	0.4703	14.8355	high Na
5	0.0582	1.5217	0.6936	4.4154	7.6878	0.5178	14.8945	
6	0.0106	1.1172	2.1844	4.3744	6.8161	1.057	15.5606	chlorite
7	0.0152	1.439	0.6851	4.2976	7.8326	0.4746	14.7457	
8	0.0203	1.4057	0.7265	4.569	7.6251	0.4553	14.8034	
9	0.0046	0.8242	3.1357	4.1913	6.3325	1.4939	15.9862	chlorite
10	0.0027	1.4085	0.6214	4.5698	7.6625	0.4918	14.7582	low Na
11	0.0095	1.5457	0.7412	4.3493	7.7316	0.4928	14.8714	low Na
12	0.049	1.3644	0.8543	4.4304	7.6479	0.4959	14.8437	
13	0.0144	1.5258	0.6569	4.517	7.6755	0.4451	14.8361	
14	0.0345	0.8697	2.6984	4.5047	6.4004	1.2888	15.7994	chlorite
15	0.014	1.3795	0.8057	4.5035	7.5724	0.5961	14.8726	
16	0.0195	1.4733	0.6981	4.5958	7.593	0.473	14.8555	
17	0.0336	0.8897	0.5357	4.181	8.212	0.3053	14.1591	low K / high Si

Table 5-6) Cation Totals - Electron Microprobe Analyses calculated for 24 Oxygens (i.e. calculated for muscovite composition)

Sample L.E.G.

No.	Na	K	Mg	Al	Si	Fe	Total	Comment
1	0.0303	1.7616	0.688	4.2612	7.5005	1.0233	15.26	
2	0.005	0.0673	4.5115	3.9261	5.2735	3.0162	16.8	Chlorite
3	0.0223	1.7639	0.7261	4.3049	7.6856	0.5523	15.06	
4	0.0315	1.634	0.6084	3.7	8.2529	0.503	14.73	
5	0.0893	1.6792	0.7646	4.2512	7.689	0.5964	15.07	in kink
6	0.0187	0.009	4.7051	4.2185	4.8726	3.2081	17.03	in kink / chlorite
7	0.007	0.0103	4.6651	4.2193	4.9005	3.1963	17	in kink / chlorite
8	0.0145	0.3853	3.3373	4.3202	5.7133	2.5559	16.33	in kink / chlorite
9	0.0185	1.8252	0.71	4.3741	7.6306	0.546	15.1	in kink
10	0.0539	1.6537	0.744	4.1616	7.4853	1.189	15.29	
11	0.018	0.0799	4.7161	4.0943	5.1042	2.885	16.9	chlorite
12	0.0307	1.7297	0.5873	4.5833	7.6	0.4577	14.99	
13	0.0155	1.4932	1.1807	4.3627	7.2528	1.0152	15.32	high Mg
14	0.0499	1.7761	0.7452	4.5689	7.3976	0.6932	15.23	

Sample 41

No.	Na	K	Mg	Al	Si	Fe	Total	Comment
1	0.0385	0.1074	4.8962	4.289	4.9845	2.6261	16.9439	Chlorite
2	0.0425	1.512	0.196	5.2568	7.3288	0.4839	14.8201	
3	0.0246	1.4646	0.5333	4.7098	7.6592	0.3389	14.7305	
4	0.0094	0.1344	4.5257	4.126	5.1725	2.865	16.8364	Chlorite
5	0.0092	1.438	0.7004	4.5594	7.6622	0.4125	14.7817	
6	0.0171	1.3506	1.013	4.5148	7.3082	0.9147	15.1183	
7	0.0048	0.0271	4.8768	4.118	5.0041	2.922	16.9528	Chlorite
8	0.0186	1.3727	0.6304	4.2439	7.9075	0.4931	14.6662	
9	0.0099	1.4566	0.7527	4.5514	7.5645	0.558	14.8931	
10	0.0205	1.3846	0.7126	4.7316	7.4844	0.5085	14.8524	

Table 5-6) Cation Totals - Electron Microprobe Analyses calculated for 24 Oxygens (i.e. calculated for muscovite composition)

Sample 45a

No.	Na	K	Mg	Al	Si	Fe	Total	
1	0.02	1.8152	0.731	4.1827	7.8037	0.4626	15.0225	
2	0.0362	1.7818	0.7554	4.4512	7.5931	0.4536	15.0903	
3	0.0305	1.7647	0.752	4.4186	7.6195	0.464	15.0688	
4	0.0415	1.8269	0.7502	4.3279	7.6265	0.551	15.1438	
5	0.2618	1.8434	0.8196	4.2452	7.5869	0.5624	15.3431	high Na
6	0.0383	1.7885	0.8966	4.3607	7.6076	0.4156	15.1255	
7	0.0392	0.715	3.7496	4.2279	6.001	1.5098	16.2621	chlorite
8	0.0374	1.8604	0.8085	4.2926	7.6793	0.4244	15.1233	
9	0.048	1.7789	0.9111	4.4154	7.546	0.4427	15.1597	
10	0.0389	1.81	0.9188	4.2452	7.629	0.5153	15.1728	
11	0.0606	1.7976	0.7473	4.4404	7.628	0.3891	15.0809	
12	0.0328	1.3548	1.9616	4.2595	6.9849	0.9651	15.5791	low K / high Mg
13	0.0616	1.9793	0.6486	4.5578	7.482	0.5111	15.2596	
14	0.0686	1.8801	0.7686	4.3119	7.6321	0.5031	15.1863	
15	0.0552	1.7811	0.7834	4.3835	7.6661	0.3727	15.0604	
16	0.0385	1.7904	0.8192	4.3763	7.6307	0.4227	15.0956	
17	0.0432	1.7958	0.8124	4.431	7.6048	0.3956	15.0992	
18	0.0788	1.3229	1.7736	4.1685	7.0705	1.1032	15.5461	low K / high Mg
19	0.0507	1.4664	1.7752	4.2829	7.1439	0.7324	15.4732	low K / high Mg
20	0.0383	1.7354	0.7962	4.4028	7.6328	0.4269	15.0526	
21	0.067	1.8112	0.7837	4.3144	7.681	0.4231	15.1009	
22	0.0847	1.8069	0.7741	4.2445	7.7323	0.4277	15.0913	
23	0.0601	1.8522	0.7399	4.3863	7.6314	0.44	15.1316	
24	0.0656	1.8434	0.6925	4.5018	7.5702	0.4384	15.1334	
25	0.0639	1.8107	0.763	4.6161	7.4597	0.4355	15.1694	

5.3.2. Backscatter Electron Imagery

An important result from the sessions at the electron microprobe laboratory were the few backscatter S.E.M. images that were attained (**fig.5.22 - 5.25**). Those photomicrographs presented in the previous section cannot be analyzed because the surface of those particular thin sections are not polished, and the thin sections are already too thin

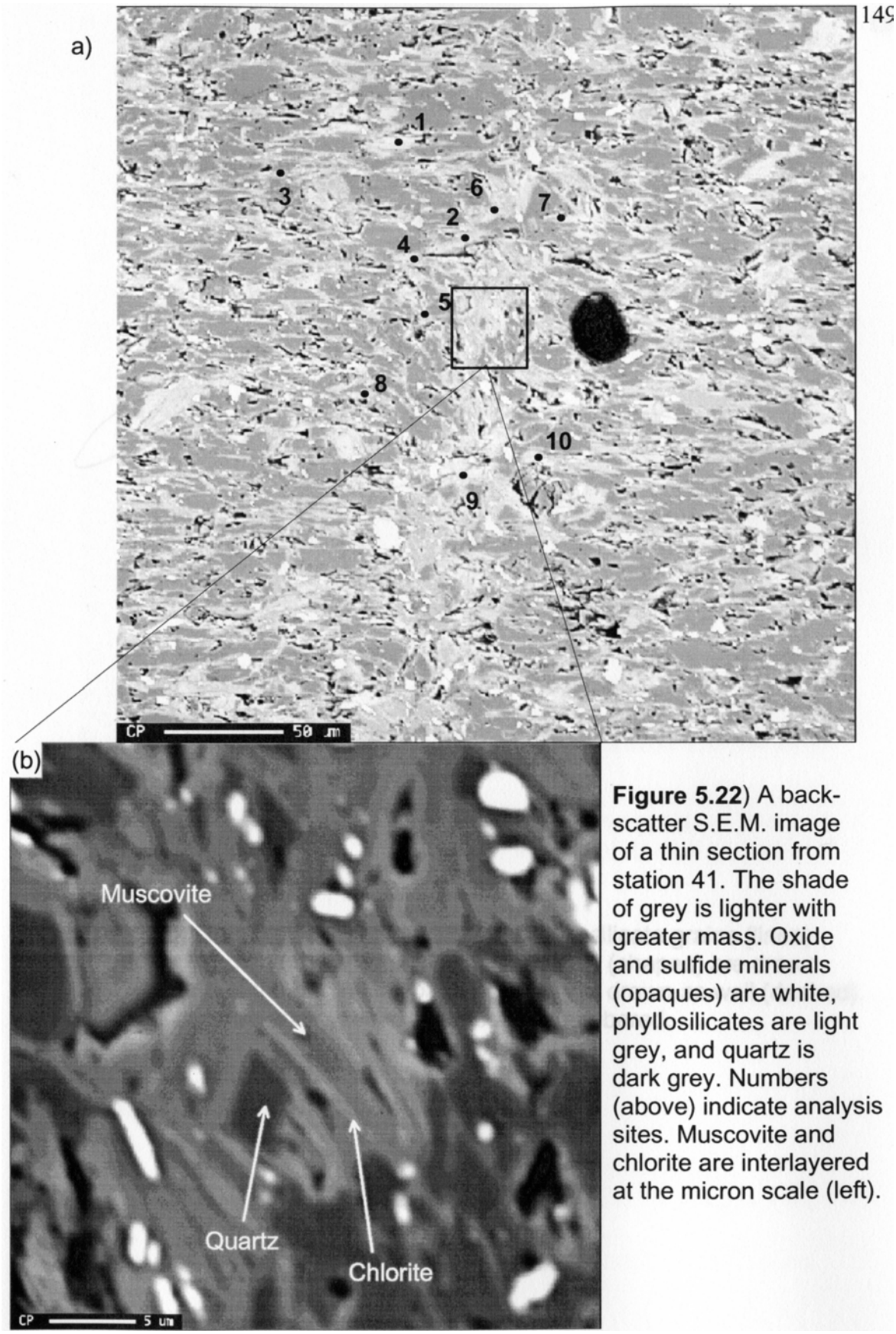

Figure 5.22) A back-scatter S.E.M. image of a thin section from station 41. The shade of grey is lighter with greater mass. Oxide and sulfide minerals (opaques) are white, phyllosilicates are light grey, and quartz is dark grey. Numbers (above) indicate analysis sites. Muscovite and chlorite are interlayered at the micron scale (left).

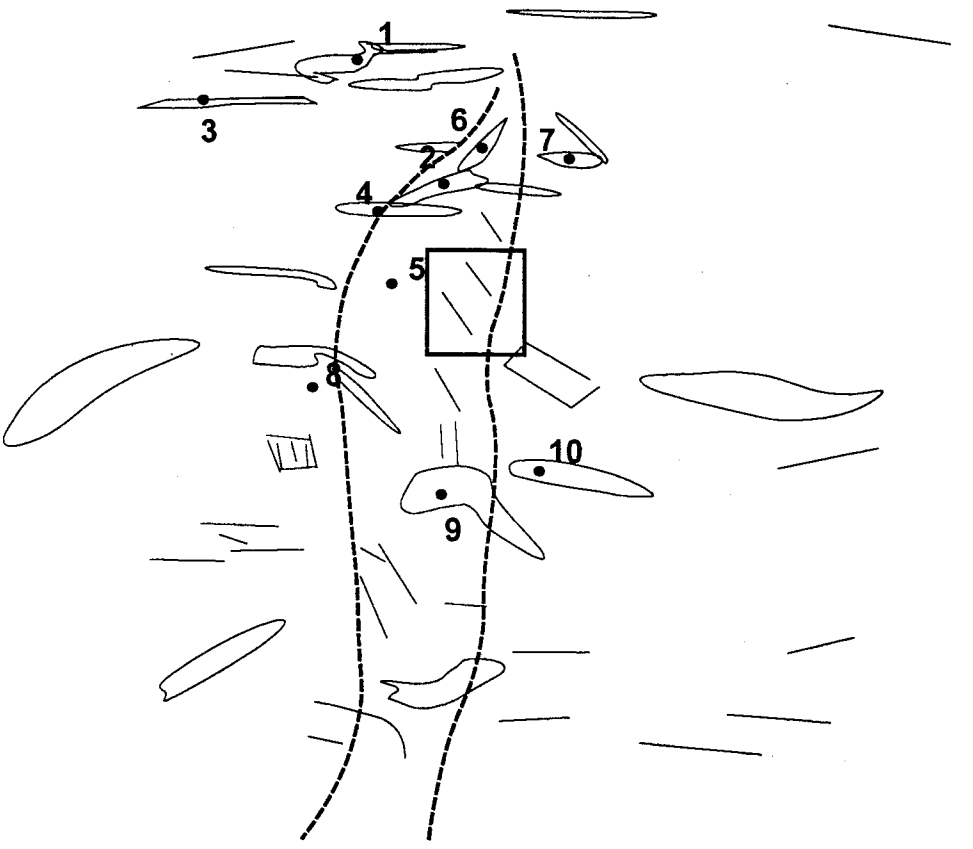

Figure 5.23) Line Drawing of Figure 5.24a. Phyllosilicate grains (lines) and "packages" of interlayered phyllosilicate grains (shapes) are drawn. A best estimate of the micro-kink band boundary is drawn as well (dashed). Sites of microprobe analayses are plotted and numbered.

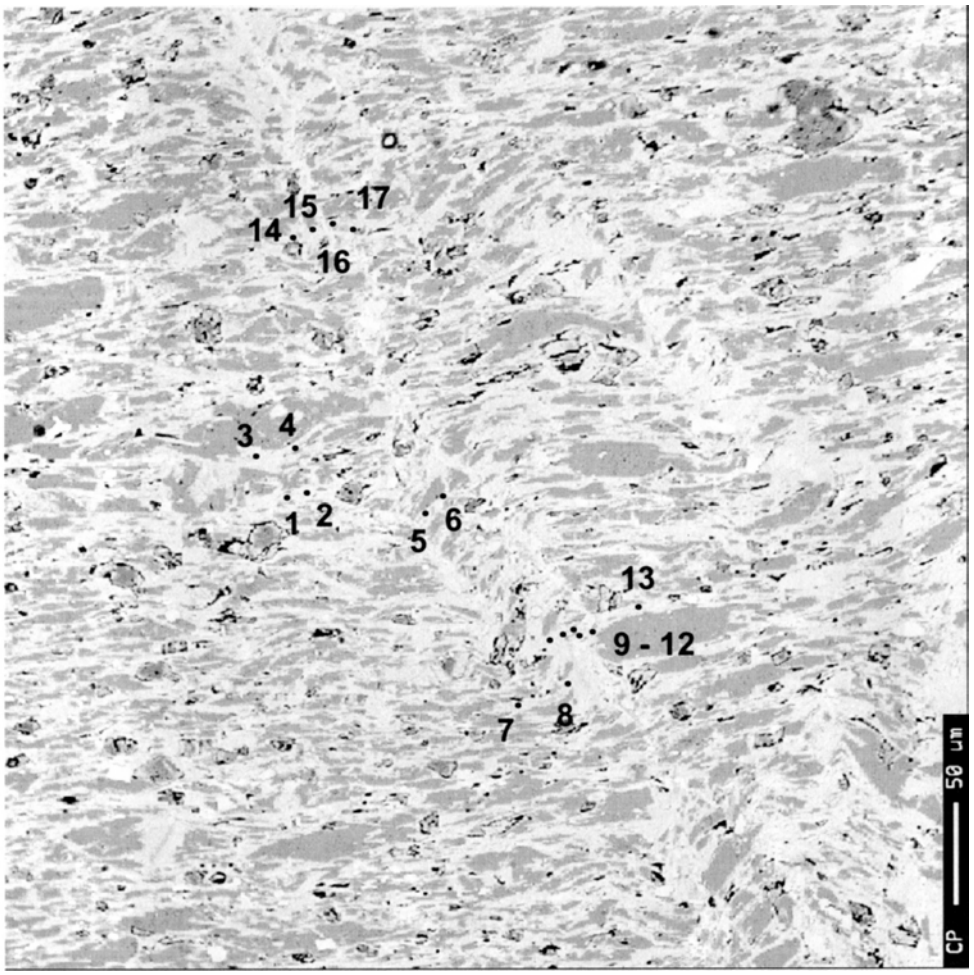

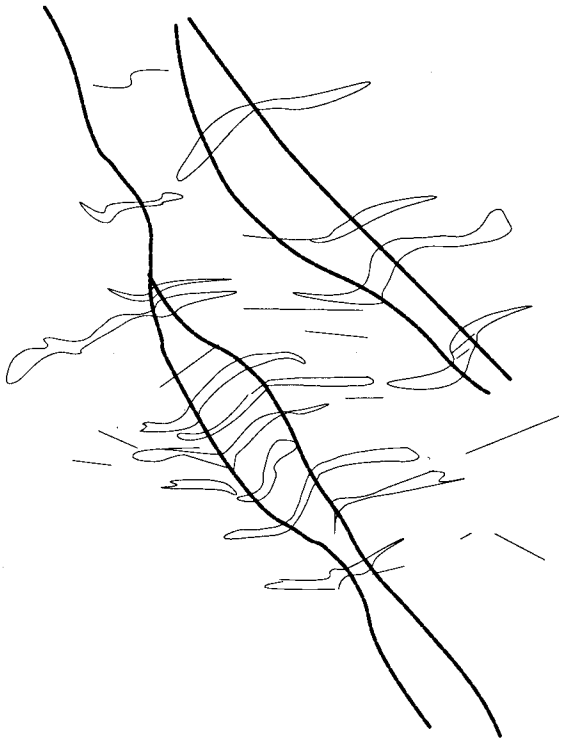

Figure 5.24) S.E.M. Image and line drawing of a micro-kink from station L.W.C.

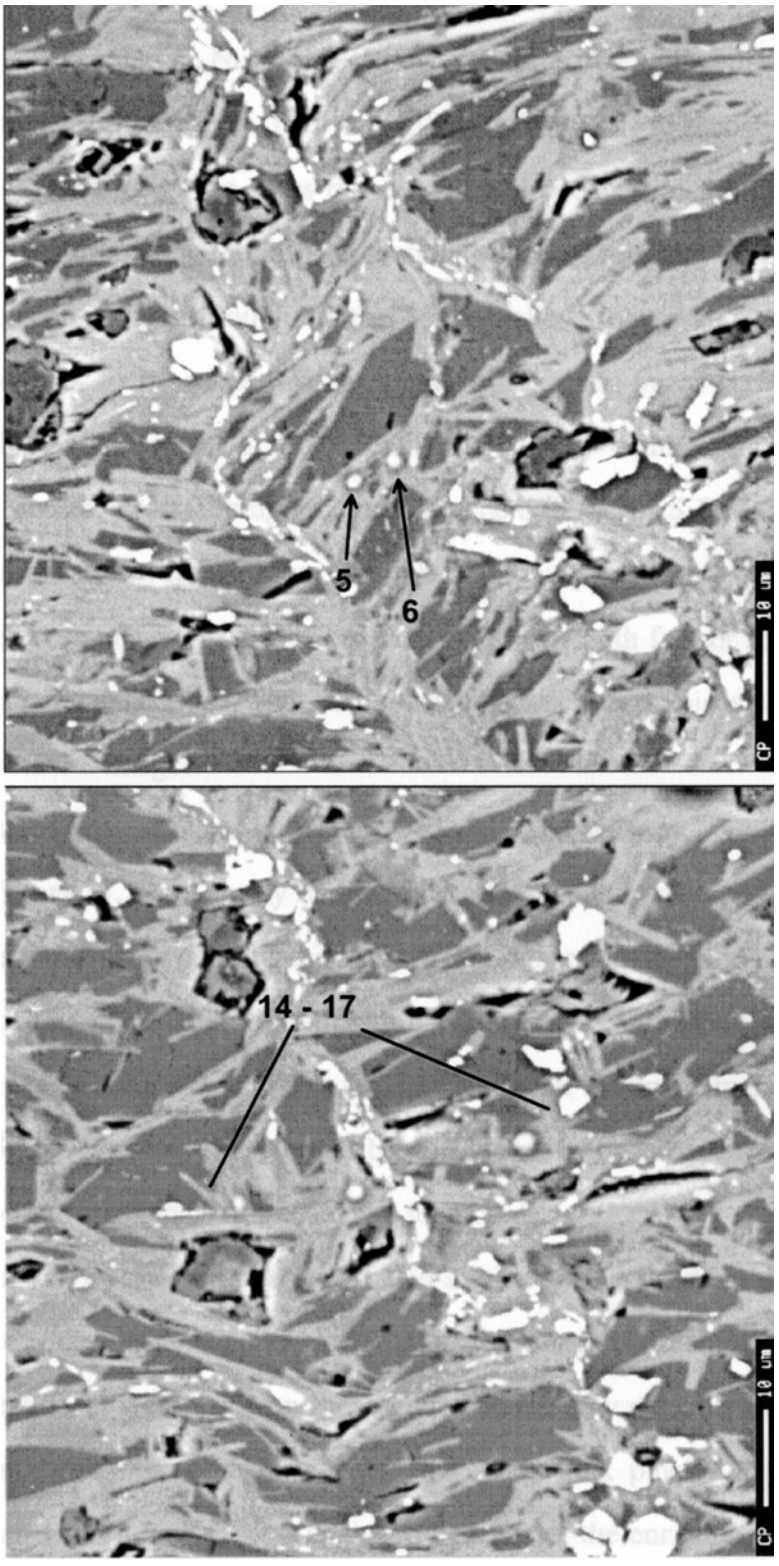

Figure 5.25) Micro-kinks from Figure 5.26 at high magnifications.

to undergo further preparation. New thin sections were prepared and studied both optically and in backscatter S.E.M. imagery. It is very difficult, however, to recognize cross-micas with the electron technique. The cross-micas observed optically in the previous section "over-printed" the surrounding fabric. Thin sections are cut to roughly 30 um. in thickness and the transmission of light through the thin section allows observations of these over-printing relationships to be made. For example, many cross-micas have been defined optically by bringing one set of grains to extinction thereby highlighting the micro-kink band boundary and the cross-cutting relationship. The backscatter S.E.M. technique does not allow transmission of electrons through the sample. Thus, micro-kink band boundaries, and cross-micas, are difficult to define. Perhaps with further future work, and the author's increased experience using this technique, "type" cross-micas will be identified in back-scatter S.E.M. images.

The vast majority of micro-kinks observed with the backscatter S.E.M. are like the micro-kink in **figure 5.22a**. Poorly defined micro-kink band boundaries, an enrichment of phyllosilicates, and quartz defining the micro-kink - rather than the phyllosilicates, are all characteristics of this micro-kink viewed with backscatter S.E.M.. There are some micas within micro-kinks that retain the preferred orientation found within the main slaty cleavage (**fig.5.22a, 5.23, 5.24**). These could be considered to be cross-mica "candidates", though no individual cross-mica candidate was identified.

Fourteen analyses were made across thin section L.E.G. to get a first view of the mineralogy inside and outside a micro-kink (backscatter image is not shown). Analyses of grains in thin section 41 were made on those grains which may optically have been cross-mica candidates and on those regions where the micro-kink pinches out (**fig.5.22a, 5.23, 5.24**). Thin section L.W.C. was analyzed because of the enrichment of oxides and sulfides, and because it has a well defined micro-kink (despite the fact that it is extremely short, pinching out over roughly 50 um.) (**fig.5.24, 5.25**).

The backscatter imagery provides some additional data. When viewed at high magnifications the muscovite in sample 41 can be seen to be interlayered with chlorite (**fig.5.22b**). Chlorite creates a sheath around all of the muscovite grains in this sample. When muscovite is adjacent to quartz, there is always an enrichment in chlorite between the two grains. This growth of chlorite around muscovite grain boundaries has long been recognized in slates and is similar to the phenomena of chlorite -muscovite "stacks" (Knipe, 1981; Lee et. al., 1984; Clark and Fisher, 1994). Thus, in the analyses above, those analyses referred to as "chlorite" or low K / high Mg, may be analyses where chlorite was partly or completely analyzed rather than the muscovite between the chlorite. The presence of interstitial chlorite was already recognized optically (previous section) and thus was no surprise. Yet, the backscatter image of **figure 5.22b** is better evidence of the relationship of chlorite to the surrounding grains than any previously presented image. What is interesting is that, despite the presence of chlorite in sample L.W.C., the backscatter imagery does not reveal the same chlorite / muscovite interlayering. Is it possible that some stratigraphic or structural levels have interlayered chlorite and muscovite while others do not? Is it possible that well defined micro-kinks only developed in regions where there was little chlorite / muscovite interlayering? How does this relate to the cross-micas observed?

5.3.3. Discussion - K2O / Na2O

The study of Knipe and White (White and Knipe, 1978; Knipe, 1981) mapped a mineralogical change from paragonitic illite (K) to phengitic muscovite (Na) to chlorite (generally deficient in the lighter cations) which corresponded to interpreted older (illites) to younger (phengites and chlorites) grains. Lee et. al. (1984) took this one step further by showing that well crystallized grains tend to be free of lattice defects and have well ordered interlayering of mica and chlorite whereas less well crystallized grains tend to have complex interlayering and a high density of lattice defects. The study of Lee et. al. (1984) puts forth

a general warning that electron microprobe data of phyllosilicates in slates should be interpreted with caution as angstrom-scale intergrowths of phyllosilicates of a solution series (i.e. paragonite - phengite), or intergrowths of different phases (i.e. phengite - chlorite) can affect the larger scale chemical analyses (e.g. chlorite intergrowths could skew a measurement towards a phengitic composition from a paragonitic composition). Nonetheless, both of the aforementioned studies show that K and Na can be indicative elements for the amount of interlayering, and the degree of neo-crystallization and re-crystallization.

Na_2O and K_2O weight percents demonstrate that there are two distinct muscovites present in the slate. There is a high K muscovite (K_2O clusters around 10 wt. %) and a low K muscovite (K_2O clusters around 8 wt.%). Na concentrations also change between the two groups of muscovite. The high K muscovites have Na_2O values around 0.2 wt% and low K muscovites have Na_2O values around 0.05 wt.%, at, or below, the detection limit of the electron microprobe) (**figure 5.26b**). There are also the occasional grains with high Na_2O values and others with low Na_2O values, relative to the two main groups of muscovite (**figure 5.26a**). What is most interesting is that the two types of muscovite seem to be roughly split between control stations in the Cedar Point Quarry. The high K group is found at stations L.E.G. and 45 while the low K group is found at stations L.W.C. and 41, with some mixing between the two groups. L.W.C. and 41 are stations on the lower limb of the fold while L.E.G. and 45 are stations on the upper limb of the fold.

There are four possibilities for the muscovite grouping. One is that there is a change in muscovite composition in directions normal to the slaty cleavage. The other is that the location of the muscovite groups preferentially on one limb or the other is coincidental and it is the bulk rock composition (as a function of stratigraphic position) which determines the type of muscovite. This would mean that assemblages of high K and low K muscovites are distributed unevenly throughout the stratigraphic section. The third possibility is that it was

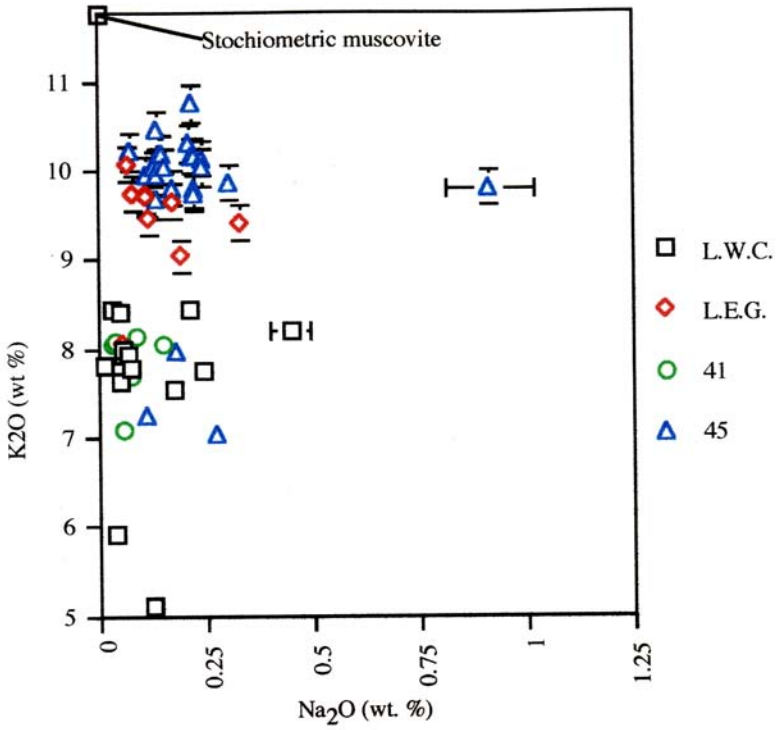

Figure 5.26a) Na_2O vs. K_2O for muscovite

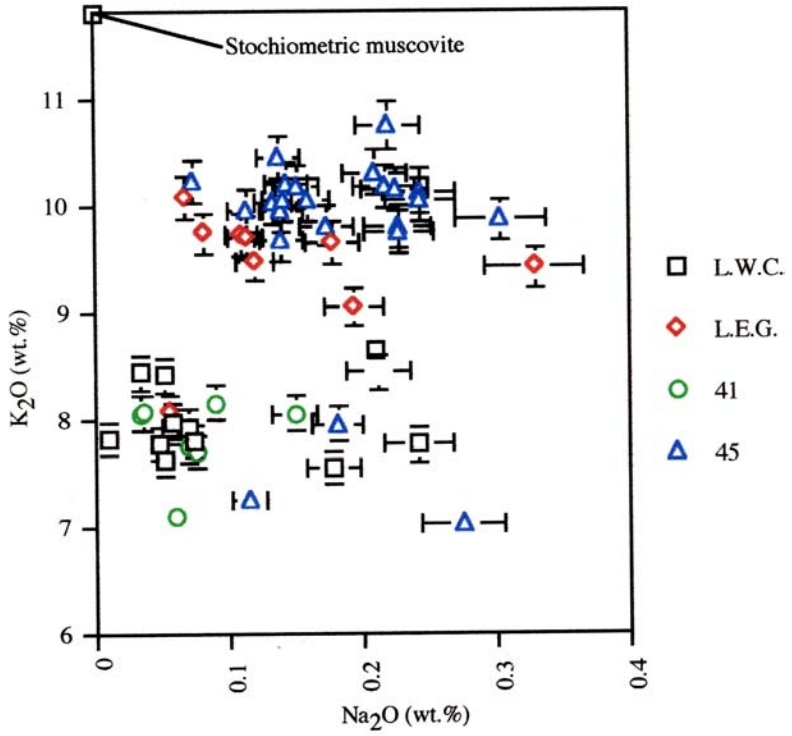

Figure 5.26b) Na_2O vs. K_2O for muscovite, same as in (a) without low-K and Na-rich grains

the location of the analysis relative to a micro-kink which yielded the different values for muscovite. All of the analyses were taken across a micro-kink. Some micro-kinks may provide a high K muscovite while others provide a low K muscovite. With only four micro-kinks analyzed it is difficult to make a conclusion regarding this last proposal. The fourth possibility is that the differing values are a reflection of different sample preparation procedures between thin sections (some were polished with a diamond paste and others with a corundum grit - each likely left differing amounts of topography on the thin section surface which could have, in turn, affected analyses). This last idea is not meant as a preferred proposal. It is simply suggested to underscore the fact that with only four samples analyzed, it seems pre-mature to claim that there is a predictable enrichment in light cations across the Cedar Mountain Syncline.

Related to the observation of two muscovite compositions is that Al_2O_3 and MgO values, when plotted against SiO_2 show that, while there are two fields for chlorite and muscovite, several grains lie between the two fields (**fig.5.27**). The muscovite - chlorite series is discontinuous chemically, but the amount of interlayering of the two minerals can certainly be gradational from dominantly muscovite to dominantly chlorite. Thus, within the entire population of the grains analyzed there is a chemical division between cation rich and cation poor muscovites and a trend from dominantly muscovite to dominantly chlorite grains. The latter trend shows no correlation to the field scale structural setting.

The above observations are interesting but not surprising considering it is already established that the Cedar Point Slates are a low grade metamorphic slate (as shown by the presence of chlorite). It is interesting that muscovite alteration, be it chemical, (a solution trend towards phengite) or structural (a gradation in the amount of chlorite interlayering), can be shown to exist with backscatter S.E.M. imagery and microprobe analyses. However, without a definable cross-mica, and a "proof", so to speak, that the cross-micas represents some definable stage in this progressive chemical / structural history of the

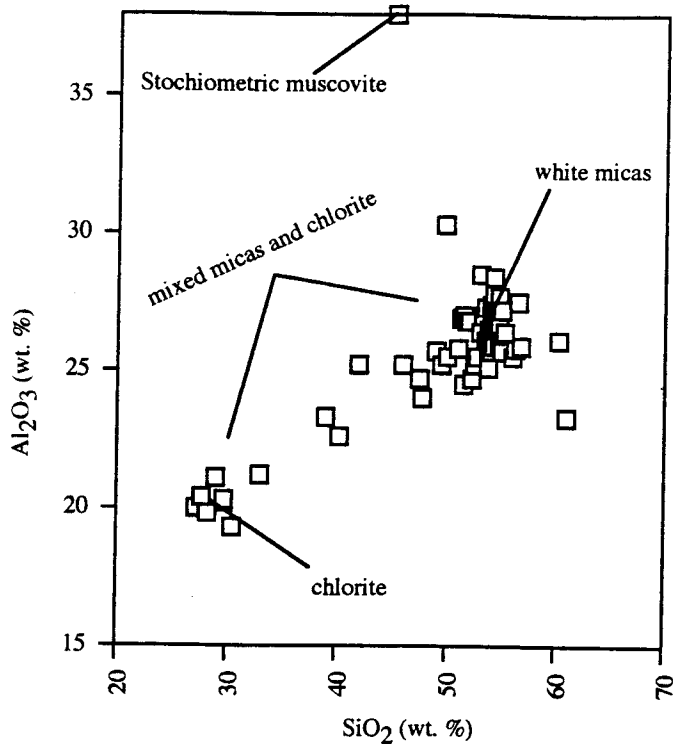

Figure 5.27a) Chlorite - Muscovite for all analyses.

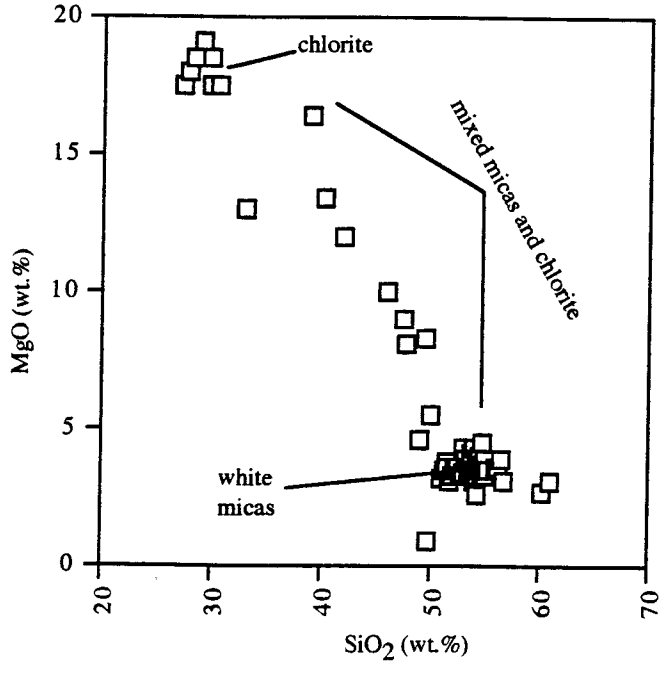

Figure 5.27b) Chlorite - Muscovite for all analyses.

phyllosilicates, then the above outlined relationships have little relevance to the main thesis of this study. As it stands, there is evidence for mica growth, in the form of varying muscovite composition and changes in the amount of chlorite interlayering. However, there is no indication of when this mica growth occurred. To add to this uncertainty, the two well constrained traverses across micro-kinks (**fig.5.22 - 5.25**) yielded no predictable chemical signature whatsoever (**fig. 5.28**). Some of the analyses hit chlorite and some hit various muscovites, and some hit a combination of the two. Clearly, more data must be attained before anything definitive can be said about the geochemistry of the Cedar Point slates.

5.4. Discussion

Despite the strengths of the proposal of this investigation, as outlined in **Chapter 4**, there are many shortcomings. For one thing, investigating the cross-micas optically and with the electron microprobe could never prove or disprove the presence of a "widespread" mica growth which post-dated all deformation. Transmission Electron Microscopy (T.E.M.) could potentially confirm the presence of a widespread late growth event by studying varying amounts of dislocations in the micas, but such an approach is beyond the scope of this study. By the time the initial field data had been collected, and a general understanding of the regional geology had been attained, it became apparent that proving that S_2 represented the final phase of deformation could be difficult and would likely rely on other regional studies. Furthermore, if cross-micas could be identified under the S.E.M. and shown to be part of a chemically distinct group of muscovites prevalent throughout the slate, how could one rule out the possibility that the cross-micas represent grains rotated into the cross-cutting orientation? Clearly methods other than optical microscopy and electron microprobe analyses would be needed to verify that there was a post-tectonic mineral growth event.

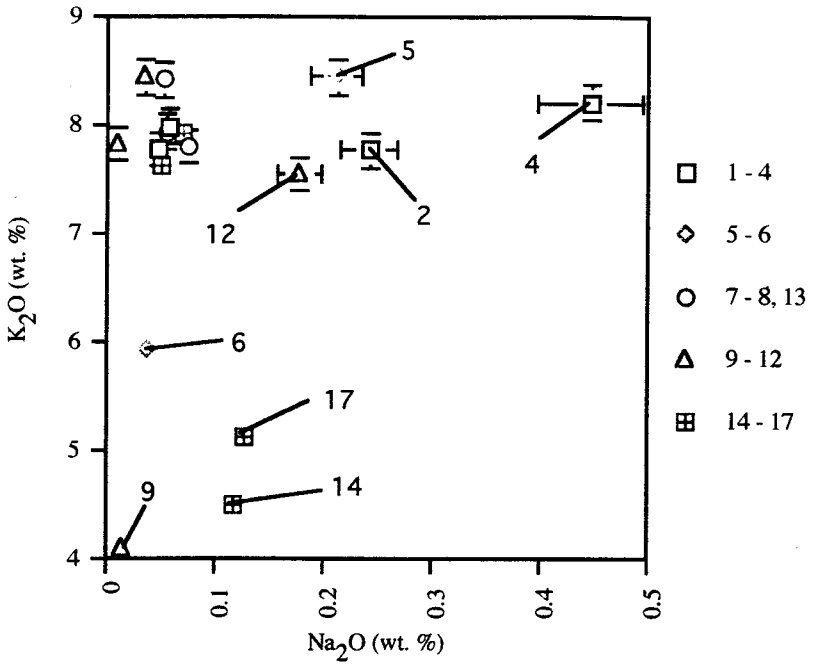

Figure 5.28a) Analyses from L.W.C.

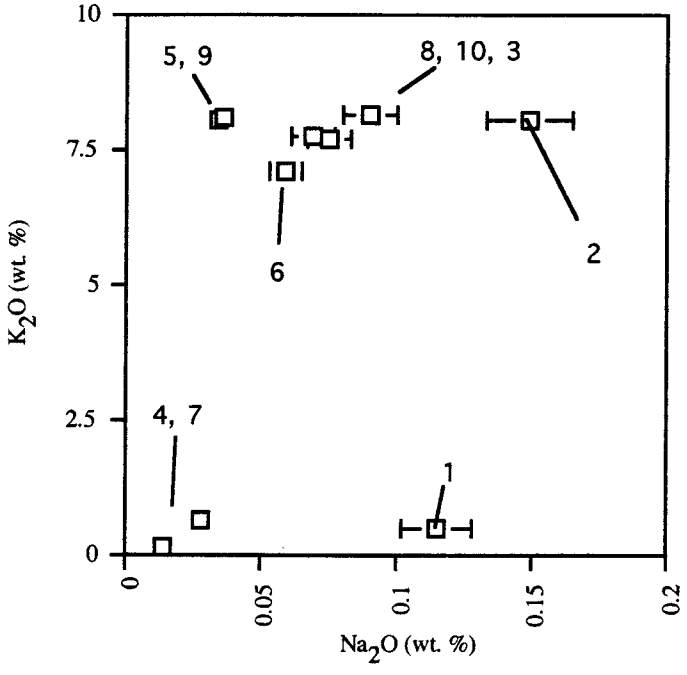

Figure 5.28b) Analyses from 41

Proof ("the truth") is always impossible to come by in any deductive process (Feynman, 1965). Thus, this study limited itself to (**a**) doing a multi-scale analysis of the Cedar Point Quarry, to produce results which could be useful for future work (i.e. the control station and sample locality map), (**b**) optically characterizing the microstructure of the slates, and (**c**) attaining some reconnaissance level data of the chemistry of the micas in regions surrounding and inside micro-kinks. The results, contrary to the last discussion, are rather exciting. Via this study, there is a better understanding of the structural geology and deformation history at the Cedar Point Quarry. Petrographic observations confirm the initial observation of Prof. W.D. Means, and observations of the microstructure may provide data for future discussions regarding slaty cleavage and late crenulation cleavages. Perhaps most importantly, is the realization that within the micas are different chemical characteristics, consistent with previous studies of metamorphic micas and phyllosilicates.

Future work on this topic could focus on three data sets. Bulk sample X.R.D. data could reveal whether the pattern of K enriched muscovites is a real property of the slate and if it represents a bulk rock property, or is a local property around micro-kinks. Ultimately, this could provide the mineralogical data necessary to interpret cross-micas in the context of late mica growth. More electron microprobe data could then be used to relate the "base-line" mineralogical data to the micro-structure. Ultimately, however, T.E.M. is needed to verify whether there are multiple generations of micas in the slates and how these relate to the surrounding microstructure and, in particular, S_2. This is because only T.E.M. is capable of revealing the amount of strain and the amount of interlayering of minerals with any degree of certainty. At a more fundamental level, T.E.M. is capable of resolving micron and sub-micron scales while still attaining observations of "over-printing" relationships. These types of information, supplied by T.E.M., are requirements for anything approaching the "truth" when it comes to relative timing of mineral growth and deformation in fine grained slates.

Should such a data-set provide the evidence necessary to make a conclusion about the timing of the growth of cross-micas, the conclusion would ultimately be a disproof of either the "localized", "widespread", or "no", post- S_2 growth hypotheses. If the localized growth hypothesis were to remain a valid explanation for the cross-micas, then this would mean that post- S_2 growth occurred mimetically from pre-existing grains, without actually completely changing the pre-existing mineral grain. This would imply that mineral growth occurred (**a**) without the entire rock being brought into a state of disequilibrium for the mica phase (i.e. there was not a significant regional metamorphic, or re-heating, event), and (**b**) mineral growth occurred with a very slow cation diffusion rate within mica grains, as mineral growth occurred mimetically from a pre-existing grain without completely re-setting the pre-existing mineral chemistry. However, the localized hypothesis is mutually exclusive of the "widespread" growth hypothesis, which predicts that isotopic ages attained from micas in the rock greatly underestimate the age of slaty cleavage. If, after further study, the "no" growth hypothesis is the most plausible, than this reveals more information about the deformation which produced S_1 and S_2, as opposed to information about a metamorphic or mineral growth processes. Regardless, future work on this topic would undoubtedly increase our understanding of the behavior, and the geologic history, of slates and their phyllosilicate mineral constituents.

Chapter 6. Conclusion

This thesis discusses two separate projects conducted in the Taconic range of the Lower Champlain Valley, west - central Vermont. I have tried to discuss both projects in the general context of the Ordovician tectonic events which occurred in the Taconic foreland. However, the two projects are different in methodology of investigation and scientific approach. One project is a regional mapping project, with conclusions derived via a largely inductive approach. The other project is a study of a single locality, and the micro-structure and micro-chemistry of the rocks at that locality were studied via a largely deductive approach. The conclusions reached for each study are discussed separately in the following two sections.

6.1. Geologic Maps of the Shoreham to Benson Region

New geologic maps show that the Champlain Thrust System traces continuously between Shoreham and Benson, Vermont, where it was previously unrecognized as a regional thrust belt. In conjunction with the maps of Hashke (1994), Granducci (1995), Steinhardt (1983), and Kidd et. al. (1995), the Champlain Thrust System has been traced through the Vermont Taconics from southern Quebec, to Washington Co., New York.

Between Shoreham and Orwell, the Champlain Thrust System consists of at least three major thrust slices, each internally imbricated. The thrust slices in this area are thickened by thrust duplexing and the presence of a nearly complete stratigraphic section, from the basal Potsdam Quartzite to the Middlebury / Orwell limestones. South of Orwell, the thrusts have climbed in stratigraphic section, thereby eliminating the Potsdam Quartzite from the thrust slices. There is also an absence of large thrust duplexes south of Orwell. South of Benson, there is an autochthonous section of carbonates below the basal Champlain Thrust, in contrast to the north (Shoreham area) where such a section is absent.

Thus, there is an overall thinning of the Champlain Thrust System from north to south, and an overall climbing in stratigraphic level by the thrusts.

Stratigraphic variations between thrust slices suggest that the Providence Island formation, a thick dolostone unit, was originally deposited in a distal shelf setting, and has been tectonically transported large distances. Two separate sequences of limestones and siltstones in the stratigraphic section beneath the Providence Island formation were likely deposited in a proximal shelf setting, the lowermost siltstone / limestone units being only present in autochthonous or nearly autochthonous sections. This interpretation of the stratigraphic section is consistent with the conclusions regarding the relative amounts of transport upon the various thrusts. For example, the Shoreham thrust, which transported Providence Island dolostone, is interpreted to be a far traveled thrust whereas the southernmost extent of the Champlain Thrust, which transports units immediately above the Whitehall dolostone, is interpreted to have less displacement upon it.

The Mettawee River Fault, an east-side-down normal fault, juxtaposes an intermixed belt of Middle Ordovician shelf facies shale, Pre-Cambrian continental rise facies slates and arenites, and Middle Ordovician flysch and melange against the Champlain Thrust System. This fault has been previously recognized to the north and south (Fisher, 1984; Hashke, 1994; Granducci, 1995) but has never been traced through the Shoreham - Benson region. This normal fault is now recognized to extend from the Vermont / New York border, through the hinge of the "Middlebury Synclinorium", the classic interpretation for the overall structure of the Lower Champlain Valley (Cady, 1945; Doll et. al., 1961), and as far north as Quebec. This structure could be late Taconic (orogenic) to post- Taconic in age, and have amounts of throw equal to the thickness of the Middlebury through Glens Falls stratigraphic section.

East of the intermixed black shales and slates is the westernmost Taconic allochthon, the Sunset Lake Slice. This is a belt of slates with lenses of continental rise

facies quartzites in a roughly north - south trending belt. A small belt of Hatch Hill formation of shales and quartz arenites, is structurally separate from the larger Sunset Lake Slice, and is folded about a north - south axial plane. The Sunset Lake Slice is bound to the east by the Taconic Frontal Thrust, a late, out of sequence thrust, which transports an eastern belt of intermixed Ordovician and Taconic shales and melange, as well as an eastern thrust belt of shelf facies carbonates and shales. This belt of carbonates and shales is lithologically identical to the rocks found in the Champlain Thrust System.

Within the Champlain Thrust System are a set of across-strike structures which create offsets in the thrusts and the surrounding lithic map unit boundaries. These structures function as lateral ramps in the thrust system geometry and bound thrust duplexes. Often there are changes in the stratigraphic level across these offsets which cannot be explained by the thrust geometry (classic lateral ramps, for example). These are therefore interpreted to be pre-thrust offsets, and furthermore, are interpreted to be pre-thrust normal faults. These faults are proposed to be a subsidiary set to the normal faults predicted by the model of Bradley and Kidd (1991), a model wherein faults occur in the continental crust in response to lithospheric flexure with the onset of collision. The set of roughly north-south striking, trench parallel faults in the model of Bradley and Kidd (1991) are thought to be largely concealed beneath the Champlain and Taconic thrust sheets. Locally, however, these trench parallel normal faults bound grabens containing shales, and horsts of carbonate rocks. With subsequent tectonic transport by the major thrusts the basins are preserved in duplex structures, such as occurs along the Shoreham Thrust near Orwell. The horsts are preserved as relatively flat-lying bedrock between lateral ramps in the thrust system, such as occurs in the Benson region. The eastern belt of carbonates and shales is also interpreted to be a large horst on the distal paleo- shelf. This particular horst was incorporated into the thrust belt in a separate location from the Champlain thrust System, with a different "style" of thrust system development.

To this author's knowledge, this study contains some of the first evidence for pre-thrust normal faults exerting basic structural control in tectonically transported rocks. With further study of the interaction between pre-thrust normal faults and thrust faults could provide insight into whether flexural extension is the dominant mechanism for pre-thrust normal faults on the outer shelf (i.e. east of the Mohawk Valley), or if thrust loading is the dominant mechanism. In addition, the evidence provided by this study, in conjunction with the mapping of Hermann (1994) and Washington (1992), suggests that the concept of the Middlebury Synclinorium (Cady, 1945) should be dismissed in light of the evidence that both limbs of the Synclinorium are east dipping thrust belts, and that the Mettawee River fault projects through the Synclinorium's hinge.

6.2. Investigation of the Cedar Point Slates

The concept that mineral grains which define a foliation are the same age as, or older than, that foliation could be argued to be within the realm of "common sense". One implication of this assumption is that the mineral grains which define a foliation are generally interpreted to be the same age as, or older than the deformation which produced that foliation. Observations made at the Cedar Point Quarry, W. Castleton, Vt., could provide evidence to the contrary.

"Cross-micas" are observed mica grains which cross-cut the boundaries of a late crenulation cleavage, or micro-kinks. This cross-cutting relationship suggests that these grains grew later than the deformation which produced the micro-kinks, and therefore later than the deformation which produced the slaty cleavage. If this is the case, then perhaps many, or all of the mica grains in the slate grew at this later time. This growth may have occurred due to a late thermal event, a solution event in the absence of re-heating, or some combination of solution transfer and temperature increase.

There are three competing hypotheses for the origin of the Cedar Point cross-micas, the "localized" post- S_2 growth hypothesis, the "widespread" post- S_2 growth hypothesis, and the "no" post- S_2 growth hypothesis. Should future work reveal that the "localized" growth hypothesis is the preferred one, then it is implied that there was a mineral growth event in the absence of a whole-rock metamorphic event. Should future work reveal that the "widespread" growth hypothesis is the preferred one, than this would imply that the micas which define the slaty cleavage are of an age younger than the deformation which produced the slaty cleavage. Should the "no" growth hypothesis be the preferred one, than this would imply that the deformation, and not the mineral growth history of the rock, gave rise to this microstructural anomaly (cross-micas), at odds with the overall texture produced by the deformation history.

The investigation to gain insight into timing of the development of the cross-micas included producing a structural map and cross-section of the Cedar Point Quarry, W. Castleton, Vermont. This structural map and cross-section may be useful for future studies of the Cedar Point slates. Several new observations come from the structural mapping. The contact between the Brown's Pond calcareous shales, and the Middle Granville purple and green slates, is not perfectly conformable. Slickensides, and deflections in the late crenulation cleavage adjacent to these slickensides, are evidence that bedding - parallel slip occurred locally until fairly late in the deformation history of the Cedar Mountain Syncline. There is a subtle change in the Cedar Mountain Syncline's axial plane orientation across the quarry. There is, however, no corresponding change in the axial planar cleavage orientation. This may be evidence to support the proposal that folding began before the initiation of slaty cleavage development. It should be noted that there are other possible interpretations for the field scale observations made at Cedar Point which are not discussed in this thesis.

The cross-micas and the surrounding micro-structure of the slate are documented with photomicrographs. The observation that some micro-kinks are enriched with opaque minerals (oxides and sulfides), whereas other adjacent micro-kinks are enriched with phyllosilicates, is evidence that there was some amount of mass transfer, presumably due to solution processes, after the formation of the micro-kinks. This, in turn, supports the hypothesis that there was mineral growth after the later stages of deformation of the slate.

Electron Microprobe data was attained from the slates in the hopes of confirming whether the cross-micas represent mica growth which was localized along the micro-kinks (and thus in the absence of a widespread metamorphic / mica growth event), or mica growth which was widespread throughout the slates. Confirming whether or not the latter case represented mica growth after the formation of the micro-kinks would undoubtedly require T.E.M. analysis, which is beyond the scope of this study.

The results of the electron microprobe analyses were inconclusive. However, it was found that there are two groups of muscovite in the slate, a high K and a low K muscovite. There is also a group of interlayered muscovite and chlorite. There is no obvious relationship between structural setting (i.e. cross-micas) and the mineralogical variation. With future work, a relationship between these mineral groups and the cross-micas, or other microstructures, may be established.

References

Apirisi, M., 1984. Stratigraphy and Structure of the Ganson Hill Area: Northern Taconic Allochthon: M.S. thesis, University at Albany, 128p.

Beutner, E.C., 1978. Slaty Cleavage and related strain in the Martinsburg Slate, Delaware Water Gap, New Jersey, American Journal of Science, v.278, p.1-23.

Bierbrauer, K., 1990.Geology of Taconic Thrust Sheets and Surrounding Carbonates of the West Central Vermont Marble Belt, North of Rutland Vermont: M.S. thesis, University at Albany, 105 p.

Bird, J.M., 1969. Middle Ordovician Gravity Sliding; taconic region, Memoir - American Association of Petroleum Geologists, p.670 - 686.

Bird, J.M. and Dewey, J.F., 1970. Lithosphere Plate-Continental Margin Tectonics and the Evolution of the Appalachian Orogen, Geologic Society of America Bulletin, v.81, p.1031-1060.

Bosworth, William P., 1980. Structural Geology of the Fort Miller, Schuylerville and portions of the Schaghitoke 7.5' Quadrangles, Eastern New York, and its implications in Taconic Geology: Ph.D. thesis, University at Albany, 237 p.

Bradley, D.C. and Kusky, T.M., 1986. Geologic Evidence for the Rate of Plate Convergence During the Taconic Arc - Continent Collision, Journal of Geology, v. 94, p.667 - 681.

Bradley, D.C.and Kidd, W.S.F., 1991. Flexural Extension of the Upper Continental Crust in Collisional Foredeeps, Geological Society of America Bulletin, v.103,p.1416-1438.

Brainard and Seeley, 1890. The Calciferous formation in the Champlain Valley: American Museum of Natural History Bulletin, v.3, p.1-23.

Cady, W.M., 1945. Stratigraphy and Structure of West-Central Vermont, Geological Society of America Bulletin, v.56, p.515-587.

Cady, W.M. and Zen, E-An, 1960. Stratigraphic Relationships of the Lower Ordovician Chipman Formation in West-Central Vermont, American Journal of Science, v.258, p.728-739.

Chan and Crespi, 1997. Geological Society of America Bulletin, in press.

Clark, M. Brooks, and Fisher, D.M., 1995. Strain Partitioning and Crack-Seal Growth of Chlorite-Muscovite Aggregates During Progressive Noncoaxial Strain: an example from the slate belt of Taiwan, Journal of Structural Geology, V.17, p.461-474.

Clark, T.H., 1934. Structure and Stratigraphy of Southern Quebec, Geological Society of America Bulletin, v. 45, p.1 - 20.

Coney, P.J. et.al. , 1972. The Champlain Thrust and Related Features Near Middlebury, Vermont: in New England InterCollegiate Field Conference, 1972 guidebook, p.97-115.

Cushing, H.P and Ruedemann, R., 1914. Geology of Saratoga Springs and Vicinity: New York State Museum Bulletin, no.169, 177p.

Dale, T.N., 1899. The Slate Belt of Eastern New York and Western Vermont: U.S.G.S. Annual Report, no.19, p.153-300.

Dale, T.N. and others, 1914. Slate in the United States, U.S.G.S. Bulletin 586, 220 p.

Dana, J.D., 1877. An Account of the Discoveries in Vermont Geology of the Rev. Augustus Wing: American Journal of Science, 3rd ser., v.13, p.332-347, 405-419.

Delano, J.W. and others, 1990. Petrology and Geochemistry of Ordovician K-Bentonites in New York State: Constraints on the Nature of a Volcanic Arc, Journal of Geology, v.98, p.157-170.

Dewey, J.F., 1965. Nature and Origin of Kink-Bands, Tectonophysics v.1, p.459-494.

Doll, C.G. and others, 1961. Centennial Geologic Map of Vermont, Vermont Geologic Survey.

Dong, H., Hall, C.M, Peacor, D.R., Halliday, A.N., 1995. Mechanisms of Argon Retention in Clays Revealed by Laser 40Ar/39Ar Dating, Science, v.267, p.355.

Drake, A.A., Jr., Davis, R.E., and Alvord, D.C., 1960. Taconic and Post-Taconic Folds in eastern Pennsylvania and western New Jersey: U.S.G.S. Prof. Paper 400-B, p.180 - 181.

Emmons, E., 1838. New York Geologic Survey Annual Report, no.2.

Epstein, J.B., and Epstein, A.G., 1969. Geology of the Valley and Ridge Province Between Delaware Water Gap and Lehigh Gap, Pennsylvania: Geology of Selected Areas in New Jersey and Eastern Pennsylvania and Guidebook of Excursions: New Brunswick, New Jersey, Rutgers University Press. p. 132 - 205.

Feynman, Richard, 1965, The Character of Physical Law, MIT Press, Cambridge, Mass. 173p.

Fisher, D.W., 1977. Correlation of the Hadrynian Cambrian and Ordovician Rocks in New York State, NY State Museum Map and Chart Series no. 33, 46 p..

Fisher, D.W., 1984. Bedrock Geology of the Glens Falls-Whitehall Region, New York, New York State Museum Map and Chart Series no. 35.

Flower, R.H., 1964. The Foreland Sequences of the Fort Ann Region, New York:, NM Bulletin, Mines and Mine Resources, Mem.12, p.153-161.

Friedman, G.M., 1997. Gas Reservoir Potential of the Lower Ordovician Beekmantown Group, Quebec Lowlands, Canada: Discussion, A.A.P.G. Bulletin, v.80, p.1674

Goldstein, A. and others, 1996. Geochemical Evidence for Volume Loss in the Taconic Slates, Journal of Structural Geology

Goldstein, A., and others, 1996. Finite Strain Heterogeneity and Volume Loss in Slates of the Taconic Allochthon, Vermont, U.S.A., Journal of Structural Geology

Goldstein, A., 1996. Structural and Tectonic History of the Taconic Slate Belt, Geological Society of America, Abstracts with Program : Northeastern Section.

Granducci, J.L., 1995. Stratigraphy and Structure at the Southern End of Lake Champlain in Benson, Vermont: M.S. thesis, University at Albany, 99p.

Greensmith, J.T., 1989. Petrology of the Sedimentary Rocks - 7th ed., Unwyn Hyman Ltd, London. 262p.

Harper, C.T., 1968. Isotopic Ages from the Appalachians and Their Tectonic Significance, Canadian Journal of Earth Science, v.5, p.49-59.

Harris, A.G., Harris, L.D., Epstein, J.B., 1978. Oild and gas data from Paleozoic rocks in the Appalachian basin: Maps for assessing hydrocarbon potential and thermal maturity (conodont color alteration isograds and overburden isopachs): U.S.G.S. Miscellaneous Investigations Map I-917-E, scale 1:2,500,000.

Haschke, M.R., 1994. The Champlain Thrust System In Northwestern Vermont - Structure and Lithology of the Taconic Foreland Sequence in the Highgate Center Quadrangle: M.S. thesis, University at Albany, 110p.

Hayman, N.W., Kidd, W.S.F., Granducci, J., 1996. The Champlain Thrust System in the Shoreham - West Haven - Whitehall Region, West - Central Vermont, Eastern New York, G.S.A. Abstracts with Program: Northeastern Section.

Hermann, R., 1992. The Geology of the Vermont Valley and the Western Flank of the Green Mountains between Dorset Mountain and Wallingford, Vermont: M.S. thesis, University at Albany, 101p.

Hess, H.H., 1955. Serpentine, orogeny, and epeirogeny: Geological Society of America Spec. Paper 62, p.391 - 408.

Hitchcock et. al. , 1861. Report on the Geology of Vermont: 2 vol., Claremont, New Hampshire.

Ho, Nei-Che, Peacor, D.R., Van Der Pluijm, B., 1995. Contrasting Roles of Detrital and Authigenic Phyllosilicates During Slaty Cleavage Development, Journal of Structural Geology.

Holleywell, R.C., Tullis, T.E., 1975. Mineral Reorientation and Slaty Cleavage in the Martinsburg Formation, Lehigh Gap, Pennsylvania, Geological Society of America Bulletin, v.86, p.1296-1304.

Housen, B.A., Van Der Pluijm, Ben A., Van Der Voo, R., 1993. Magnetite Dissolution and Neocrystallization during cleavage formation: Paleomagnetic study of the Martinsburg Formation, Lehigh Gap, Pennsylvania, Journal of Geophysical Research, v. 98, No. B8, p. 13,799 - 13,813.

Ishi, Kazuhiko, 1988. Grain Growth and re-orientation of phyllosilicate minerals during the development of slaty cleavage in the south Kitakami Mountains, northeast Japan, Journal of Structural Geology, v.10, p. 145 - 154.

Jacobi, L.D., 1977. Stratigraphy, Depositional Environment and Structure of the Taconic Allochthon, Central Washington County, New York: M.S. thesis, University at Albany, 191p.

Keith, A., 1932. Stratigraphy and Structure of Northwestern Vermont, Journal of the Washington Academy of Sciences, v.22, no.13, p.357-379.

Kidd W.S.F., Plesch, A., Vollmer, F., 1995. Lithofacies and Structure of the Taconic Flysch, Melange and Allochthon in the New York Capital District, in Field Trip Guide for the 67th Annual Meeting of the N.Y.S.G.A., p.57 - 80.

Knopf, E.F.B. and Ingerson, F.E., 1938. Structural Petrology: Memoir - Geological Society of America, p.270.

Knipe, R.J., 1981. The Interaction of Deformation and Metamorphism in Slates, Tectonophysics, v.78, p.249-272.

Lee, J.H., Peacor, D.R., Lewis, D.D., Wintsch, R.P., 1984. Chlorite -Illite Interlayered and Interstratified Crystals: A TEM/STEM Study, Contributions to Mineralogy and Petrology, v.88, p.372-385.

Maxwell, J.C., 1962. Origin of Slaty and Fracture Cleavage in the Delaware Water Gap area, New Jersey and Pennsylvania, in Geol. Soc. America, Petrologic Studies: a volume in honor of A.F. Buddington, p.281 - 311.

McDougall, I., Harrison, T.M., 1988. Geochronology and Thermochronology by the 40Ar/39Ar Method, Oxford Monographs on Geology and Geophysics, No.9, Oxford University Press.

Mehrtens, C., Dorsey, RJ, 1987. Stratigraphy and bedrock geology of the Northwest Portion of the St. Albans Quadrangle and the Adjacent Highgate Center Quadrangle, Special Bulletin - Vermont State Geologist 9.

Ramsay, J.G., Huber, M.I., 1987. The Techniques of Modern Structural Geology, Vol.2: Academic Press Inc., London, 700p.

Rodgers, John, 1937. Stratigraphy and Structure in the Upper Champlain Valley, Geological Society of America Bulletin, v.48, p.1573-1588.

Rodgers, John, and Fisher, D.W., 1969. Paleozoic Rocks in Washington County , New York, west of the Taconic Klippe: in J.M. Bird (ed.), N.E.I.G.C. Guidebook no.61, p. 6-1 to 6 - 12.

Rodgers, John, 1968. The Eastern Edge of the North American Continent During the Cambrian and Early Ordovician: in Studies of Appalachian Geology: northern and maritime, p.141-149.

Rodgers, John, 1971. The Taconic Orogeny, Geological Society of America Bulletin, v.82, p.1141-1178.

Rowley, D.B., Delano, L.L., Kidd, W.S.F., 1979. Detailed Stratigraphic and Structural Features of the Giddings Brook Slice in the Taconic Allochthon in the Granville Area, p. 1860242 in Friedman, G.M. (ed.), N.Y. State Geol. Assoc. and N.E.I.G.C. Guidebook, 457 p..

Rowley, D.B. and Kidd, W.S.F., 1981. Stratigraphic Relationships and Detrital Composition of the Medial Ordovician Flysch of Western New England: Implications for the Tectonic Evolution of the Taconic Orogeny, Journal of Geology, v.89, p.199-218.

Rowley, D.B. and Kidd, W.S.F., 1982a, Stratigraphic Relationships and Detrital Composition of the Medial Ordovician Flysch of Western New England: implications for the Tectonic Evolution of the Taconic Orogeny : a reply to Rodgers, Journal of Geology, v. 90, p. 230 - 233.

Rowley, D.B., 1982. New Methods for Estimating Displacements of Thrust Faults Affecting Atlantic Type Shelf Sequences: With an Application to the Champlain Thrust, Vermont, Tectonics, v.1, no.4, p.369-388.

Rowley, D.B., 1983. Operation of the Wilson Cycle in Western New England During the Early Paleozoic: With Emphasis on the Stratigraphy, Structure and Emplacement of the Taconic Allochthon: Ph.D. thesis, University at Albany, 602p.

Ratcliffe, N.M.; Hatch, N.L., Jr., 1979. A Traverse Across the Taconide Zone in the Area of the Berkshire Massif, Western Massachusettes, in Skehan, J.W., and Osber, P.H., eds., The Caledonides in the U.S.A., Geological Excursions in the Northeast Appalachians: Weston, Mass., Weston Observatory, p. 175 - 224.

Ruedemann, R., 1909. Types of Inliers observed in New York, N.Y.S. Mus. Bull 133, p.164 - 193.

Ruedemann, R., 1912. The Lower Siluric Shales of the Mohawk Valley, New York State Museum Bulletin, no.162.

Ruedemann, 1942. Geology of the Catskill and Kaaterskill Quadrangles, Pt.I Cambrian and Ordovician Geology of the Catskill Quadrangle, N.Y.S. Mus. Bull 331, 188p.

Sedgwick, 1835. ?

Sorby, H.C., 1856. On slaty cleavage as exhibited in the Devonian Limestones of Devonshire, Philosophical Magazine, v.11, p.20-23.

Sorby, H.C., 1856. On the Theory of the Origins of Slaty Cleavage, Philosophical Magazine, v.12, p.127-129 +discussion w/ Tyndall, J..

Steinhardt, C.T., 1983. Structure and Stratigraphy of West Haven, Vt.: M.S. thesis, University at Albany, 167 p.

Srodon, Jan, Eberl, Dennis S., 1984. Illite, in Micas, Reviews in Mineralogy, Vol. 13 p.495 - 535.

Stanley and Ratcliffe, 1985. Tectonic Synthesis of the Taconian Orogeny in Western New England, Geological Society of America Bulletin, v.96, p.1227-1250.

Swinnerton, A.C., 1922. Geology of a Portion of the Castleton, Vermont Quadrangle, Harvard University Thesis, 262 p.

Theokritoff, G., 1964. Taconic Stratigraphy in Northern Washington County, New York, Geological Society of America Bulletin, v.75, p.171-190.

Thompson, J.B., 1967. Bedrock Geology of the Pawlet Quadrangle, Vermont; Part 2 Eastern Portion Bulletin - Vermont Geological Survey, p. 61 - 98

Turner, F.J., Weiss L.E., 1963. Structural Analysis of Metamorphic Tectonites: McGraw Hill, N.Y..

Ulrich, E.O., Cooper, G.A., 1938. Ozarkian and Canadian Brachiopada, Geological Society of America Special Paper 13.

Voight, B., 1965. Structural Studies in west - central Vermont: Ph.D. thesis, Columbia University, 1965; (microfilm): University of Michigan , Ann Arbor.

Washington, P.A., 1985a. Roof Penetration and Lock-Up on the Leading Imbricate of the Shoreham, Vermont Duplex, Geological Society of America Abstracts with Programs, v.17, p.68.

Washington, P.A., 1992. Geology of the Taconic Orogen: A Sesquicential Field Conference-Guidebook, Field Conference of Taconic Geologists, 79p..

Welby, C.W., 1961. Bedrock Geology of the Central Champlain Valley of Vermont, Vermont Geologic Survey Bulletin, no. 14, 296p..

White, S.H., Knipe, R.J., 1978. Microstructure and Cleavage Development in Selected Slates, Contrib. Min. Petrol., v. 66: p.165 - 174.

Whitfield, 1890. Observations on the faunas of the rocks at Fort Cassin, Vermont with descriptions of a new species, Amer. Mus. Nat. Hist. Bull 9(11), p174-184

Williams, P.F., 1976. Relationships Between Axial Plane Foliations and Finite Strain, Tectonophysics, v. 30, p.181 - 196.

Wintsch, R.P. Kunk, M.J., 1992. 40/Ar/39Ar Evidence for an Alleghanian Age of the Slaty Cleavage in the Martinsburg Formation, Lehigh Gap Area, Eastern Pennsylvania, G.S.A. Abstracts with Program: northeastern section.

Wood, D.S., 1974. Current Views of the Development of Slaty Cleavage, Annual Reviews of Earth Sciences, v.2, p.1-36.

Zen, E-An, 1961. Stratigraphy and Structure at the North End of the Taconic Range in West-Central Vermont, Geological Society of America Bulletin, v. 72, p.293-338.

Zen, E-An, 1964. Taconic Stratigraphic Names: Definitions and Synonymies, U.S.G.S. Bulletin no.1174, 95p.

Zen, E-An, 1967. Time and Space Relationships of the Taconic Allochthon and Autochthon, Geological Society of America Special Paper 97, 107p.

Zen, E-An, 1972. Some Revisions in the Interpretation of the Taconic Allochthon in West-Central Vermont, Geological Society of America Bulletin, v.83, p.2573 - 2588.